A PHYSICALLY-BASED NUMERICAL MODEL OF RIVER CHANNEL WIDENING

by

Stephen E. Darby

Thesis submitted to the University of Nottingham for the degree of Doctor of Philosophy, May, 1994

CONTENTS

ABSTRACT

The application of many existing numerical models of river channel morphology is limited by their inability to account for bank erosion and changing channel width through time. In this research, a physically-based numerical model which simulates the evolution of channel morphology, including channel width, through time has been developed and tested. Predictions of channel evolution are obtained by solving deterministically the governing equations of flow resistance, flow, sediment transport, bank stability and conservation of sediment mass. The model is applicable to relatively straight, sand-bed streams with cohesive bank materials.

In the channel evolution model, a method is used to solve the shallow water flow equations, and to account for lateral shear stresses which significantly influence the flow in the near bank zone. The predicted distribution of flow is then used to predict the sediment transport over the full width of straight river channels. Deformation of the bed is calculated from solution of the sediment continuity equation. Predictions obtained in the near bank zone allow the variation in bank geometry to be simulated through time. Since bank stability is determined by the constraints of the geometry of the bank and the geotechnical properties of the bank material, channel widening can, therefore, be simulated by combining a suitable bank stability algorithm with flow and sediment transport algorithms.

In combining bank stability algorithms with flow and sediment transport algorithms, there are two paramount considerations. First, the longitudinal extent of mass failures within modelled reaches must be accounted for. Second, it is necessary to maintain the continuity of both the bed and the bank material mixture in the time steps following mass failure, when the bed material consists of mixtures of bed and bank materials with widely varying physical properties. In this model, a probabilistic approach to prediction of factor of safety is used to estimate the fraction of the banks in the modelled reaches that fail in any time step. Mixed layer theory is then used to model the transport of the resulting bed and bank material mixture away from the near bank zone.

Comparisons of model predictions with observations of channel geometry over a 24 year period indicate that the new model is capable of simulating temporal trends of channel morphology with a high degree of accuracy. The model has been used successfully to replicate the form of empirically-derived hydraulic geometry equations, indicating that the model is also able to predict stable channel geometries accurately.

The numerical model has also been used to investigate the influence of varying the independent variables and boundary conditions on channel adjustment dynamics.

ACKNOWLEDGEMENTS

I would like to thank the Natural Environment Research Council for funding and supporting this project as a CASE studentship with Hydraulics Research Ltd., Wallingford. I am also grateful to the U. S. Army Corps of Engineers for supplying flow data and to the U. S. Geological Survey for supplying data and logistical support for fieldwork undertaken in the United States. Plates 3.4 and 3.5 were kindly provided by the Rijkswaterstaat.

Several individuals deserve special thanks for help provided during the course of this project. First and foremost I am indebted to my supervisor, mentor and friend, Professor Colin Thorne. This thesis would truly not have been possible without him, for it was his eager lectures that, as an undergraduate student, first enthused me with an interest in fluvial geomorphology. In my postgraduate career, Colin has been no less willing to offer technical advice, moral support and even hospitality when needed. For all of these things I am truly grateful.

I am also grateful to my co-supervisor, Dr. Roger Bettess, for freely providing thought provoking suggestions and comments throughout the course of my research, as well as technical and logistical assistance during my visits to Wallingford.

Two colleagues and friends within the Department of Geography have also helped me immensely at various times during the course of my career at the University of Nottingham. During my first two years in Nottingham, Richard Masterman was always ready to give me the benefit of his experience as a research student, provide help with computing, or just sit and talk about the problems of research in general or rivers in particular. More recently, Dr. Andrew Simon, a visiting scientist on leave of absence from the United States Geological Survey, provided immense enthusiasm, encouragement and support to keep me going in the latter stages of this project.

I would also like to thank Professor Paul Mather and the Natural Environment Research Council for giving me permission to place my studentship into abeyance to enable me to work as a visiting scientist at the U. S. Army Corps of Engineers Waterways Experiment Station, Vicksburg, Mississippi.

Finally, throughout the course of my University education, my parents have never failed to support me at every possible level. This thesis is dedicated to them.

LIST OF FIGURES

CHAPTER 1

CHAPTER 2

CHAPTER 3

CHAPTER 4

CHAPTER 5

LIST OF PLATES

CHAPTER 1

CHAPTER 3

LIST OF TABLES

CHAPTER 2

CHAPTER 3

CHAPTER 4

CHAPTER 5

CHAPTER ONE

INTRODUCTION

1.1 THE NEED AND JUSTIFICATION FOR A WIDTH ADJUSTMENT MODEL

In alluvial streams, the size and geometry of the channel is controlled by the interaction of the independent variables describing the hydrologic, hydraulic and sediment regime with the boundary conditions that depend on the properties of the sediments through which the stream flows. Since the physics of open channel flow with a deformable bed and banks is complicated, quantities of water and sediment input to the stream vary through time and space, and the nature of the channel boundary sediments is frequently diverse, these interactions are complex and are not easily explained.

Fluvial geomorphologists have traditionally striven to understand the morphological characteristics of river channels including both the smaller scale morphological features (such as bedforms) within channels, and the larger scale features (such as deltas, gorges and flood plains) that river channels either construct or modify over long time spans. But, what is perhaps surprising in the study of process-form interactions in alluvial streams at intermediate time and space scales (Schumm & Lichty, 1965) is the relative neglect of adjustment in width compared to studies of depth, slope and planform pattern. The concentration of effort on aspects such as depth prediction, bed material transport, bed scour and fill, and channel aggradation and degradation is understandable in that such aspects are fundamental to both the theory and practical engineering of rivers. But, in terms of channel change that occurs in response to a change in the hydrologic or sediment regime over intermediate ("graded" or "engineering") time and space scales, the width adjustment is often the most marked dimension of channel response. Hamlin & Thornes (1974) suggested that in evaluating responses to processes at these time scales, channel width is likely to be a particularly interesting and sensitive variable in so far as it may have greater flexibility for adjustment than slope (see also Mackin, 1948). Smith & Smith (1984), Burkham (1972) and Schumm *et al.* (1984) have all documented examples of spectacular width adjustments. Width may also exert considerable control on other morphological variables, such as meander geometry (Hey, 1976), through its influence on the flow hydraulics and sediment transport (Yalin, 1971). In all these senses, the prediction of channel width adjustments at this scale can be considered to be a problem of particular scientific interest at the very core of fluvial geomorphology.

It is important to recognise that channel width is just one of the interdependent variables which define the form of the channel. Hey (1978) has argued that the width dimension is just one of nine degrees of freedom available for adjustment of the fluvial system. While it is possible to question the precise number of degrees of freedom for adjustment that river channels possess, as well as the status of Hey's "independent" variables over a wider range of time scales (Schumm & Lichty, 1965), two important points remain. First, a governing equation for each individual degree of freedom is required in order that a solution for the fluvial system be determinate. Hence, the development of a suitable width equation based on the dynamic processes and mechanisms involved (Hey, 1982) would be a significant advance towards this goal. But second, width adjustments must be recognised as just one facet of the morphological adjustment of stream channels, both being influenced by and influencing the adjustment of other degrees of freedom. Mutual adjustments of gradient, planform and cross-section properties characterize the true response of alluvial streams to environmental controls (Richards, 1982). The study and understanding of width adjustment can also, therefore, be justified through the improved prediction of other facets of river channel behaviour that such an understanding would undoubtedly bring.

There are also practical reasons for modelling width adjustments in stream channels. The applied need and justification for modelling width adjustments in stream channels is twofold. First, width adjustments directly impact flood plain dwellers and users, and such adjustments can seriously threaten structures both in and adjacent to the channel (Plate 1.1). For example, bank erosion and channel widening lead to loss of flood plain land and inputs of significant amounts of sediment to the fluvial system, which can cause economic, environmental and social problems in such diverse geographical locations as the Nile in northern Sudan (Osman, 1985) and the Red River in Louisiana (Thorne, 1989). Bird (1980) has suggested that widening and deepening of incised channels is a major cause of bridge failure in Victoria, Australia. Second, the application of many existing numerical models of river channel morphology, which are frequently used as standard tools for prediction of bed level changes in the vertical dimension, is limited by their inability to account for bank erosion and changing channel width. It is clear that the development of a morphological model, that takes into account transient adjustments of channel width, would greatly improve the ability of practising engineers and scientists facing real world problems to predict the impact of engineering schemes, as well as allowing the identification of stable and unstable reaches and diagnosis of the process-response mechanisms involved in adjusting river channels.

Throughout this discussion, the word "adjustment" has been used to imply that it is not enough to be able to predict the change in equilibrium morphology consequent upon a change in the control variables or boundary materials, but it is also necessary to predict the dynamic, transient response of the system between equilibrium, or stable, states. Figure 1.1 schematically illustrates possible responses, through time, of the channel width to an imposed disturbance. Both fluvial geomorphologists and river engineers have traditionally dealt only with the values of the width observed at the equilibrium states. They have addressed primarily the *magnitude* of the channel changes, but have been less able to explain and predict the *rate* at which this change is achieved, or the sequence of events that occur during adjustment. However, Figure 1.1 shows that both of these latter aspects are just as interesting from both a scientific and engineering perspective as determining the overall magnitude of change. Indeed, by narrowly focussing on the steady state, rather than the dynamic, characteristics of the morphology of river channels, geomorphologists and engineers may have ignored a potentially rich and varied category of channel behaviour characteristics (Figure 1.1). Moreover, there is a growing body of evidence, described in Chapter 2, that suggests that in fact analysis of the dynamic characteristics of channel adjustment may improve our understanding of, and ability to predict, the establishment of stable or equilibrium channel morphologies.

Plate 1.1 Power Pylon Under Threat From Bank Retreat, Nonconnah Creek, Memphis, Tennessee

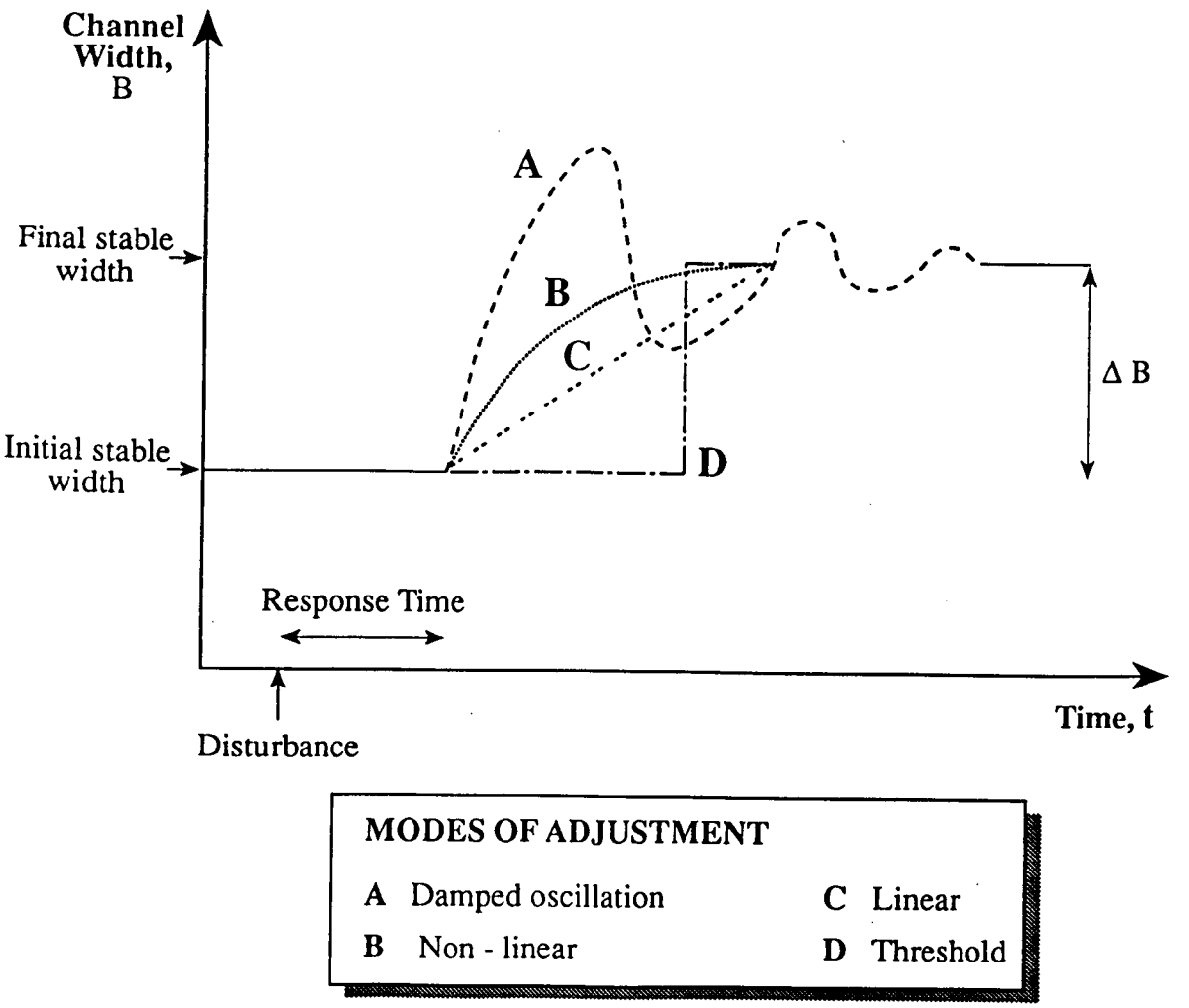

Figure 1.1 Possible Modes of Width Adjustment in a Disturbed Alluvial Channel

1.2 OBJECTIVES

The primary objective of this research is to develop and test a rational, physically-based, method of predicting width adjustment in natural river channels in response to changes in boundary material characteristics and/or the hydrological, hydraulic and sediment regimes, in order to improve on the explanatory and predictive ability of existing methods of determining channel morphology. The method should be capable of simulating morphological response through time and space, as well as accurately predicting the ultimate, equilibrium values of channel morphology. A second objective is to apply the developed model in order to gain insight into the processes and dynamics of morphological response to changes in control variables. The model is intended to be applicable to intermediate to large scale natural river channels with cohesive bank materials and non-cohesive bed materials.

1.3 APPROACH

In general there are two broad groups of approaches to modelling natural phenomena: experimental and theoretical. The experimental approach involves direct measurement and subsequent analysis of the processes, mechanisms and responses of a stream channel to measured changes in control variables, either in the laboratory or in the field. The theoretical approach usually involves construction of some kind of mathematical model of the system of interest, based on a set of governing rules concerning the system behaviour. The mathematical model may then be applied to analyse the behaviour of the system to changes in control variables specified by the user of the model.

There are advantages and disadvantages associated with each of these approaches. The great advantage of the experimental approach is that, within the limitations of measurement errors, the data obtained describe the real, not assumed or modelled, response of the river system to a real disturbance. However, there are several practical difficulties with this approach, especially if the aim is to analyse transient responses of channel morphology. A large number of measurements have to be made to document all processes and responses occuring during adjustment. These measurements are inevitably subject to error and uncertainty, even if considerable care is taken. To continue to repeat the measurements through time is a very costly exercise, both in terms of time and money. In the field, work is subject to the vagaries of climate, so that it is usually difficult to exert control over the independent variables of interest. This

latter problem may be overcome by conducting experiments in a laboratory channel, but such facilities are costly and time consuming to design and build. Moreover, scale effects also must be taken into consideration, and these may even divorce the laboratory experiment too far from flow conditions in real river channels. Finally, unless the data collection programme is repeated for a variety of sites, the results obtained are site specific and it is not usually possible to judge their validity beyond the limitations of the particular environment in which the data were collected.

The numerical modelling approach has the disadvantage that *a priori* assumptions about the system behaviour have to be made in order to construct the model. But, by basing the formulation of the model on physical principles, where possible using tested algorithms, and by calibrating and validating the model, it is possible to be reasonably confident that the system described by the mathematical model is a reasonable model of the natural phenomenon of interest. Once this step is achieved, the numerical modelling approach has many advantages over the experimental approach. These lie in the ability of numerical models to simulate long periods of prototype behaviour in much shorter periods of real time. It is, therefore, possible to conduct many more analyses than the experimental approach given the same time constraints. Moreover, the numerical model user can simply change input data files to exert total control over changes in control variables to assess the response of the system to such changes. Similarly, input data can be varied to simulate a much wider range of channel types and environments than is practically possible with an experimental approach. Another advantage is that the model output can be viewed for any number of user specified time increments during the simulation.

It is clear that the numerical modelling approach is not only cheaper in terms of time and resources than an experimental approach, but once set up and carefully calibrated and validated, the modelling approach offers much greater flexibility in terms of the range of responses that can be simulated over a variety of boundary and control conditions and the number of observations that can be made when compared to the experimental approach. There is also the added advantage that a numerical model of width adjustment would be of great use as an engineering tool, as explained in section 1.1. For these reasons, the numerical modelling approach is adopted in this research.

The format of this thesis is as follows. Chapter 2 is a critical literature review which establishes the conceptual framework adopted in this research and which places this framework in the context of previous attempts to model channel adjustments. Chapter 3 details the physically-based numerical model of channel widening developed in the

course of this work. The predictive ability of the new model was established by comparing model predictions with observed data. The results of these model validations are presented in Chapter 4. A variety of simulations and geomorphological analyses using the numerical model were undertaken in order to analyse various aspects of channel adjustment dynamics. The results of these simulations are reported in Chapter 5. Finally, a summary of conclusions and recommendations for future research is presented in Chapter 6.

CHAPTER TWO

APPROACHES TO PREDICTING THE MORPHOLOGY OF ALLUVIAL CHANNELS

2.1 INTRODUCTION

The aim of this chapter is to establish the most appropriate conceptual framework within which a physically-based model of width adjustment in natural river channels may be developed and applied to achieve the goal of an improved understanding of the dynamics of processes and mechanisms of morphological adjustment. Establishing the conceptual framework is an important step, since the entire approach to a problem is, necessarily, dictated by the conceptual basis of the research. Conducting a critical literature review of previous approaches to predicting the width of natural river channels is one way of allowing the strengths and weaknesses of individual techniques to be identified. By building upon the strengths of these methods, a suitable conceptual framework that meets the criteria set by the aims of this thesis, as outlined in the previous chapter, can be constructed. Previous approaches to predicting the width of natural river channels are now, therefore, reviewed and a conceptual framework that meets the criteria for this research outlined in chapter 1, is proposed.

2.2 EMPIRICAL APPROACHES TO PREDICTING THE MORPHOLOGY OF ALLUVIAL CHANNELS

Early attempts to predict the "stable" or "equilibrium" morphology of river channels for a given set of boundary conditions were empirical. Historically, two main groups of contributors can be recognised. Engineers developed a variety of empirical relationships known as "regime theory" to aid in the design of stable drainage, irrigation or navigation channels to reduce the costs associated with maintenance of such channels, while geomorphologists and geographers have proposed a variety of "hydraulic geometry" relationships which have largely been used as analytical tools in both describing and explaining channel form. While both the results and the approaches of these two groups of workers have been largely similar in substance, for the purposes of this review this traditional dichotomy is maintained.

2.2.1 Regime Theory

British engineers working on the design of Indian irrigation canals towards the end of the last century commonly found that the constructed canals were extremely expensive to maintain since they often very quickly filled with sediment. This problem

stimulated research aimed at designing alluvial canal geometries which would neither silt nor scour, leading to maintenance savings. Such stable canals were termed "regime" channels. Blench (1952) has suggested that the term regime implies obeyance of laws, yet freedom to adjust; so that in the same way that "climate" is distinct from the term "weather", the term "regime" implies an overall stability with an ability to adjust over a certain time scale. In the case of regime theory this time scale is the "engineering" time span (Blench, 1952) of about 10 to 100 years. Regime theory provides the basic design criteria for stable, sediment bearing, artificial channels. A canal "in regime" has a sediment transport capacity which matches the input sediment transport rate, so that although local, temporary scour and fill occur, over a period of years the morphology is, on average, constant (Richards, 1982).

Regime studies attempted to rationalize the design procedure of canals by regarding the morphology of the canal (width, depth, slope, velocity) as dependent on the imposed discharge and sediment discharge. Planform and bedform degrees of freedom are, therefore, ignored which is a major simplification. Consequently, regime relations strictly apply only to straight channels with plane beds.

Kennedy (1895) was the first to attempt to rationalize the design of canals. By gathering data from the stable Bari-Doab canal system, Kennedy noted that the data from a stable canal would provide the means of discerning how the width, depth, velocity and slope are varied among themselves to ensure no bed sedimentation will take place. He used this stable canal data to derive a relationship for the critical velocity, V_o (fts^{-1}) required to just avoid sedimentation at a given depth, D (ft):

$$V_o = 0.84\, D^{0.64} \qquad (2.1)$$

However, although he used a resistance equation (the Kutter equation) to derive this relationship, the lack of a width equation meant that both wide, shallow and narrow, deep canals were wrongly deemed equally stable under the imposed conditions of sediment load and discharge (Richards, 1982).

Lindley (1919) recognized the need for 3 independent relations, to characterize the 3 assumed degrees of freedom of adjustment, with the critical velocity being a function of both width and depth. He was also the first to introduce the term "regime". Using data from the Lower Cenab canal system he derived the relationships:

$$V_d = 0.95\, D^{0.57} \qquad (2.2)$$

$$V_b = 0.59\ D^{0.355} \qquad (2.3)$$

where the subscripts d and b identify the critical velocities with respect to stable depth and width, respectively. By eliminating the velocities, Lindley was able to calculate the widths, depths and slopes necessary to carry any specified discharge. He constructed nomograms to allow the easy calculation of these design values. It may be noted, though, that both the exponents and coefficients in the Lindley equations differ from those in the Kennedy equation. This highlights the fact that these approaches are highly empirical. It is not surprising that the relations do not agree since they were derived from separate data sets.

Lacey (1930) was the first person to take explicit account of the variations in sedimentologic criteria, the omission of which had previously been a major deficiency. He realised that the critical velocity for stability in regime canals is a function not only of depth, but also an erosion resistance factor which he termed the silt factor. Note that "silt" was used as a general term for sediment by British engineers, so that the term does not have sediment size implications in this context. Lacey reasoned that in channels of infinite width and having uniform flow, the critical velocity for the regime condition is a function of the depth and the silt factor (*i.e.* in essence a balance between erosive and resisting forces). In deriving his silt factor, Lacey argued that it was essentially the ratio of the critical velocity for stable channels predicted by Lacey to the critical velocity for stable channels calculated by Kennedy. Thus, Lacey in effect proposed that the variation in results of regime type equations was due to the variability of the sedimentological conditions between the locations from which the data sets were compiled. Lacey's contribution represented an interesting attempt to overcome one of the inherent limitations of the empirical approach, that of inapplicability beyond the limits of the data set used to develop the equations, by taking empirical account of the channel boundary material properties. It is, therefore, perhaps the first multivariate approach to empirical regime theory.

Lacey (1930) defined the silt factor as equal to unity for the "reference silt" of Kennedy's (1895) Bari-Doab data. He then showed that:

$$V_o = 1.17 \sqrt{f_s R} \qquad (2.4)$$

where f_s = silt factor and R = hydraulic radius (ft). Realising that this equation alone was insufficient to determine a solution to the problem of sediment transportation, he

used data which he had compiled from a variety of Indian irrigation canals to present the relation:

$$A f_s^2 = 3.8 V_o^5 \tag{2.5}$$

where A = cross-sectional area of the channel (ft^2). By combination:

$$Q f_s^2 = 3.8 V_o^6 \tag{2.6}$$

where Q = the discharge (ft^3s^{-1}). Lacey rearranged equation (2.4) to give:

$$R = 0.7305 \frac{V_o^2}{f_s} \tag{2.7}$$

while from (2.5) it can be shown that:

$$A = 3.8 \frac{V_o^5}{f_s^2} \tag{2.8}$$

From these equations it is a simple step to calculate the wetted perimeter, P (ft), (a coarse measure of width) to give Lacey's (1930) regime width equation:

$$P = 2.668 Q^{0.5} \tag{2.9}$$

In the words of Lacey (1930) this is "a somewhat remarkable formula" as it implies that the regime width depends only on discharge and is independent of the amount of sediment transported. Lacey (1930) believed that the silt merely controlled the shape, rather than the size of the channel. Despite the unrealistic basis to this formula, when tested against observed stable widths there was an impressive amount of agreement (Lacey, 1930). Lacey also compared his regime width formula with a similar formula derived from Lindley's (1919) data such that:

$$P = 1.984 Q^{0.506} \tag{2.10}$$

These two equations have almost identical power exponents but the coefficients are different. This reinforces the functional form of the width - discharge relationship but also highlights the deficiencies of equations based solely on empirical data.

The final problem that Lacey considered was the relationship between the size of the silt particles and the value of the silt factor, enabling the silt factor to be derived by simple measurement. For the reference, or Kennedy, silt of the Bari-Doab canal, Lacey used the data to derive the empirical relation:

$$d_{50} = \frac{f_s^2}{64} \qquad (2.11)$$

where d_{50} = the median particle size of the sediment (inches). It should be noted that the units for all of the above equations are the units of the Imperial system. Although these relationships were regarded at the time as a significant advance, there are a number of problems. Firstly, the equations suggest that width is dependent solely on the discharge. Secondly, the reliance of these empirical regime relations on site specific data limits their predictive ability outside of the areas from which the data set was derived. To compound this problem, the data used to derive the Lacey equations covers only an extremely narrow range of sediment sizes and takes no account of the processes of sediment transport (Henderson, 1961). Finally, the data were derived from canals with near constant discharges. This is a disadvantage if the aim is to apply the regime relations to natural river channels with more variable hydrographs. Post war work has attempted to remedy some of these deficiencies.

Inglis (1949) addressed the problem of the effects of varying flows in an attempt to extend regime work on artificial channel morphology (canals) to natural river channels. He argued that the effects of the entire range of the flows experienced by the river channel could be accounted for by a single representative flow which he termed the *dominant discharge*. Inglis defined this term as "the integrated effect of all (the) varying (flow) conditions over a long period of time". At this discharge the channel morphology is adjusted so that there is, on average, a year to year stability. This advance paved the way forward for a great deal of work that extended the techniques of canal regime theory to natural river channels. The concept of a dominant discharge for natural river channels has also stimulated a large number of controversial attempts to equate this discharge with identifiable natural flows such as the bankfull discharge. But Pickup and Warner (1976), Pickup & Rieger (1979), Yu & Wolman (1987) and Rhoads & Miller (1991) have all argued that it is impossible to apply such a concept to natural river channels, and that the morphology of a river adjusted to some single "dominant" discharge can not be the same as the morphology resulting from the response of the channel to a wide range of flows of varying magnitude and frequency. If this is true then this must undermine, at least to some extent, the conceptual framework of the studies reviewed below.

In fact the application of regime theory to natural river channels has been the major thrust of the post war work in this field. Prominent amongst the post war regime theorists has been Blench (1952, 1969). Blench has consistently maintained that regime theory provides a "dynamical framework for morphological prediction of alluvial channels" (Blench, 1952). He regarded the observed, overall consistency of river behaviour as evidence that regime theory could successfully be extended to natural channels. Blench's regime equations (1952, 1969) recognised that channel form reflects the intensity of bed load transport. His width equation (2.12) explicitly incorporates two sedimentological parameters, one for the bed (F_b) and one for the banks (F_s), which attempt to measure the distinct influences of non-cohesive bed and cohesive bank materials:

$$B = \sqrt{\frac{F_b}{F_s}}\, Q^{0.5} \qquad (2.12)$$

where B = width (m) and Q = discharge (m^3s^{-1}). The equation is similar in form to the traditional regime equations, with good agreement between the discharge exponents. In effect Blench's (1952) equation predicts that the coefficient of the Lacey equation can actually be determined by the sedimentological constraints of the bed and banks. In this respect the Blench equation is a better approach than had previously existed, since the multivariate approach potentially reduces uncertainty in the derived relations by incorporating more than one statistically significant variable in the regression.

The sedimentological parameters were initially estimated from:

$$F_b = \frac{V^2}{D} \qquad (2.13a)$$

and

$$F_s = \frac{V^3}{B} \qquad (2.13b)$$

where V = mean stream velocity (ms^{-1}), D = depth (m) and B = width (m). These equations give calculated values that do not correlate well with specific sedimentological properties (Charlton *et al.*, 1978). It appears that the bed factor is essentially the Froude number and the bank factor is a measure of the shear stress exerted on a hydrodynamically smooth bank (Blench, 1969). However, the bed factor may also be

defined in terms of grain size and bed load concentration (Richards, 1982). In fact limiting values for both factors have been specified for a variety of bed and bank materials so that the method involves a classificatory, rather than rational, approach to channel design. Blench's work is also highly empirical and in fact does not offer a suitable predictive model outside of the areas from which the data were gathered. Further, the method fails to explain the processes of morphological adjustment. However, at least some attempt was made to account for the sedimentologic factors involved. Another advantage of Blench's work is that the form of his equations was determined by dimensional analysis (Davies, 1987).

Other workers also realised the need for incorporation of further terms to describe the external sedimentological constraints and sediment transport processes in order to extend the traditional bivariate form of the regime equations. Inglis (1949) modified Lacey's equations into a form more suitable for design purposes. The equations in this form show that each dependent variable is a function of the discharge and the silt factor. Inglis further generalized these equations by introducing a parameter for the bed load transport (Richards, 1982). Chien (1957) has discussed the effect of the incorporation of a bed load transport factor over the Lacey silt factor. He showed that the product $f_s VR$ is strongly related to the bed load concentration, while $f_s VS$ (where S = channel gradient), which is derived from a resistance relation, is correlated to a measure of the bed material grain size. Despite these more realistic incorporations, the modified Lacey approach remains strongly empirical in nature, and furthermore the relations are dimensionally inconsistent.

A classificatory approach was also adopted by Simons and Albertson (1963). They classified data from a number of North American and Indian channels from differing environments into four sedimentological groups (sand-bed and banks, sand-bed and cohesive banks, cohesive bed and banks, and coarse, non-cohesive materials). Simons & Albertson derived regime relationships for each of these classifications. This approach actually also considered gravel-sized bed material (see below), representing the first tentative extension of regime theory to this environment.

Schumm (1968) stressed that natural rivers are two phase flows, so that ignorance of the sedimentological constraints and sediment transport processes cannot support understanding of morphological channel adjustments. Working on the Murrumbidgee River in New South Wales, he documented a number of cases where changes in the sediment load alone led to significant channel changes, which in some cases were actually the opposite of what previous regime relationships would predict. Importantly,

Schumm (1968) also noted that the type of sediment transported was important in affecting the shape, as well as the gross dimensions, of the channel. Schumm (1968) derived an empirical relationship between the width, B (m), mean annual discharge, Q_m (m^3s^{-1}), mean annual flood, Q_{ma} (m^3s^{-1}) and the channel silt-clay ratio, M, such that:

$$B = 37 \frac{Q_m^{0.38}}{M^{0.39}} \tag{2.14}$$

and

$$B = 2.3 \frac{Q_{ma}^{0.58}}{M^{0.37}} \tag{2.15}$$

Using these equations Schumm found a large measure of agreement between measured and calculated channel widths and indicated that the family of curves relating channel width to discharge can be reduced to one curve by the introduction of a parameter expressing the type of sediment load moved through the channel.

Alvarez and Villanueva (1973) have also stressed the requirement of incorporating the sediment transport process into regime equations. They used empirical data from sand-bed channels to establish a set of three equations to define the regime geometry of a stream as a function of its discharge, sediment transport and the type of channel boundary material. Osterkamp (1980) has also highlighted the role of sediment entrainment in determining the regime width. He presented a Shields like graph of sediment size versus channel width, such that width is maximised when the basal sediments consist of very easily entrained fine to medium sands.

Mahmood & Shen (1979) and Mahmood (1974) have provided useful reviews of the status of regime theory. In particular, Mahmood & Shen (1979) consider the requirements for a successful regime width equation. They note that the mechanisms of width adjustment are different for cohesive and non-cohesive banks. Regime width equations must, therefore, include: the fine suspended load, due to its potential role in berm building; seepage effects on bank and berm stability; and the role of side berms. They also note that the dominant discharge must be correctly specified (if possible). Clearly, the regime equations reviewed above are deficient in all of these aspects. Mahmood (1974) has also considered the physical interpretation of regime coefficients. He notes that the aim of the width coefficient is to incorporate all the factors affecting bank erosion or deposition into a single numeric value. The width coefficient is, in

effect, a measure of the likely resistance of the bank to erosion, but factors such as seepage, berm building and so on are rarely incorporated. It is, therefore, considered unlikely that regime equations will provide adequate prediction or explanation of either the mechanism of width adjustment or the value of the stable channel width.

The regime equations considered so far have another major problem in common, which limits their applicability still further; they apply only to sand-bed streams. More recently, work has been directed at formulating regime equations for gravel-bed rivers. Kellerhals (1967) was one of the first to develop regime type formulae for gravel-bed streams, by analyzing field data from a number of Canadian rivers together with data from flume experiments. A discharge range of 0.0283 to 2831 m^3s^{-1} and a bed material size range from 0.0127 to 0.457m were covered in this data set. The regime equations derived included a term to incorporate the bed material and were otherwise essentially similar to the traditional regime equations, with similar discharge exponents, but differing coefficients. However, a major limitation of this data set is that the natural channels studied were all deliberately sited downstream of lakes in order to enable an assumption of negligible bed load transport. This limits the applicability of this study in environments of high bed load, such as the braided streams of New Zealand (Carson & Griffiths, 1987). Further work by Bray (1982) in Canada and Hey & Thorne (1986) in Great Britain have made significant contributions to the gravel-bed river data set and confirmed the general form of the regime relations. Bray (1982) also regarded the earlier data set of Kellerhals (1967) as unrepresentative, with smaller than expected values of channel width, suggesting that increasing the bed load transport capacity would necessitate an increase in channel width. However, the work of Bray should also be treated with caution with respect to streams in New Zealand (Carson & Griffiths, 1987). They argue that Bray failed to define adequately the term "regime" and that the data set applies only to stable channels that are relatively inactive with respect to bed load transport. These problems emphasize the problems of geographical applicability in regime theory (Chalov, 1972).

In addition, the work of Andrews (1984) and Hey & Thorne (1986) has provided empirical evidence that vegetation effects can be a significant factor in determining the width of natural channels. Julien (1988) has noted the importance of incorporating terms to account for radial mobility of sediment in channel bends when deriving regime relations for meandering channels. Lewin *et al.* (1988) have even questioned whether the assumption that regime channels are in some form of dynamic equilibrium can possibly apply. They argue that regime assumptions need setting in a more dynamic framework.

It is apparent that the regime approach, with its empirical basis and emphasis on stable, steady state behaviour, is limited in terms both of predictive ability beyond the limitations of the range of data used to derive the regime equations, and in providing insight into the processes and mechanisms of channel adjustment. Conversely, the various regime researchers have underlined the general ubiquity of river channel morphology as well as establishing, through the use of multivariate approaches, the significance of various factors, which in addition to the discharge, exert control on the equilibrium morphology of river channels. In particular, the importance of sediment transport processes and the geotechnical properties of the channel boundary materials have been established.

2.2.2 Hydraulic Geometry

Hydraulic geometry studies are closely related to regime theory in that they have attempted to identify functional relationships between the dependent morphological variables and the independent variables of sediment load and discharge. The hydraulic geometry approach was first used by Leopold and Maddock (1953) who, like Inglis, attempted to apply regime type equations to natural river channels with varying flows. This seminal paper led to the domination by hydraulic geometry of studies in fluvial geomorphology and this work highlighted the essential uniformity of river cross-sections, planforms and profiles across a wide range of environments (Thornes, 1977). The applications of hydraulic geometry studies are many and varied, including identifying, estimating and verifying actual and suspected changes in environment, especially climate (Thornes, 1977). Above all, hydraulic geometry was seen in the 1950s and 1960s as providing a functional explanation for river channel form irrespective of regional setting and history (Ferguson, 1986).

Leopold and Maddock (1953) introduced logarithmic plots of river properties against discharge, with trends described by power laws of the form:

$$B = a\ Q^{b} \tag{2.16}$$

$$D = c\ Q^{f} \tag{2.17}$$

$$V = k\ Q^{m} \tag{2.18}$$

where Q = discharge (m^3s^{-1}), B = width (m), D = depth (m) and V = velocity (ms^{-1}). The continuity equation requires that $b + f + m = 1$ and also $ack = 1$ (Leopold *et al.*, 1964; Ferguson, 1986). Two broad groups of hydraulic geometry studies may be identified, "At-a-Station" hydraulic geometry and "Downstream" hydraulic geometry.

The size and shape of a channel at a point reflects the balance of erosive and resistive forces. In the medium term this balance is the subject of downstream hydraulic geometry relations (below). At-a-point hydraulic geometry is concerned instead with variations in flow geometry due to the short term rise and fall of the river within its channel as discharge varies (Ferguson, 1986). Such studies are of no benefit in understanding morphological adjustment processes, since the channel boundary is assumed fixed in these studies.

The large set of observations taken from many downstream hydraulic geometry studies have shown that, on the whole, channel width and depth are related in a regular way to bankfull discharge as it varies over the billionfold range from laboratory channels to the worlds largest rivers (Ferguson, 1986). This suggests that transient changes in channel dimensions at a point are minor compared to systematic, downstream trends, and that discharge is the dominant control, but much scatter still remains and several factors other than discharge are intuitively relevant (Ferguson, 1986). In fact the best use for empirical studies of hydraulic geometry lies in the identification of factors relevant in the processes of morphological adjustment. Hey (1978, 1982) has argued that hydraulic geometry is complicated but determinate, and best quantified by multiple regression analysis using all the physically relevant predictors for each adjustable variable. However, this multivariate approach (Richards, 1977) was used only later in the history of hydraulic geometry studies. Early studies, following the work of Leopold & Maddock (1953), tended to be bivariate in approach. This approach defines average downstream trends in width, depth, velocity and so on by correlating these variables with a suitable discharge parameter (Richards, 1977). Examples of these early studies are numerous, and have been used in a variety of analyses of channel form (Williams, 1987).

A particular feature of the early studies was interest in the observed variation in exponents and coefficients in the Leopold-Maddock downstream hydraulic geometry equations. This led to considerable debate concerning the "true" nature of hydraulic geometry variations (Table 2.1). The studies of Chong (1969), Stall & Yang (1970), Hedman & Kastner (1977), Riley (1976), Sergutin & Turutin (1984) on channel geometry relations (width, depth, velocity and slope) can be added to the studies in

Table 2.1 and the studies on the geometry of meanders by Ackers & Charlton (1970) and Hey (1976). Whilst these studies showed considerable variation in the values of both coefficients and exponents derived in the relations, they all show systematic downstream variation in hydraulic geometry variables in response to increasing discharge in the downstream direction, over a wide range of environments. Further, despite considerable scatter the exponents appear to be at least similar on the whole both between each other and with the similar regime type equations. These studies, therefore, demonstrate the essential uniformity of river channel geometry and the dominance of discharge as an independent variable; they are also vital in that they represent a considerable data base of river channel behaviour.

Table 2.1 Hydraulic Geometry Exponents (after Richards, 1977)

Reference	Location	Discharge	*b*	*f*	*m*
Leopold & Maddock, 1953	Mid-West USA	Q_{ma}	0.76	0.44	0.15
"	"	"	0.50	0.40	0.10
"	"	"	0.46	0.09	0.06
Wolman, 1955	Brandywine Creek	$Q_{50\%}$	0.34	0.45	0.32
"	"	$Q_{15\%}$	0.38	0.42	0.32
"	"	$Q_{2\%}$	0.45	0.43	0.17
"	"	Q_b	0.42	0.45	0.05
Leopold & Miller, 1956	New Mexico	?	0.50	0.30	0.20
Miller, 1958	Rio Santa Barbara	$Q_{2.33}$	0.49	0.39	0.13
"	Pecos River	"	0.59	0.30	0.13
"	Rio Santa Cruz	"	0.23	0.22	0.56
"	Pojoaque River	"	0.17	0.09	0.75
Brush, 1961	Appalachian s	"	0.89	0.70	0.29
"	"	"	0.55	0.36	0.09
"	"	"	0.30	0.29	0.05
Lewis, 1969	Manati, Puerto Rico	$Q_{70\%}$	0.46	0.27	0.27
"	"	$Q_{50\%}$	0.44	0.30	0.35
"	"	$Q_{30\%}$	0.46	0.32	0.25
Carlston, 1969	Mid-West USA	Q_{ma}	0.46	0.38	0.16
Knighton, 1974	Bollin-Dean, Cheshire	$Q_{50\%}$	0.46	0.16	0.38
"	"	$Q_{15\%}$	0.54	0.23	0.23
"	"	$Q_{2\%}$	0.61	0.31	0.08
Leopold & Langbein, 1962	Theory		0.55	0.36	0.09
Langbein, 1965	Theory		0.50	0.37	0.13

The scatter of exponents and coefficients in these early studies led to the adoption of the multivariate approach, which attempted to reduce this scatter by the incorporation of additional independent variables into the hydraulic geometry analysis. These studies are useful in identifying other significant factors that have to be incorporated in models of morphological adjustment. Foremost in these studies was the work carried out by the US Geological Survey (USGS). Wolman & Brush (1961), Caddie (1969) and Maddock (1969) all carried out experiments which involved varying the type and concentration of sediment load as well as discharge. These studies not only stressed that morphological adjustments occur by mutual adjustment of the dependent variables but also highlighted the status of the "independent" variables of slope and sediment discharge. Wolman & Brush (1961) also showed that the detailed cross-sectional morphology is greatly influenced by the amount and type of sediment in transport, while the gross channel dimensions appeared to be more a function of the magnitude of the discharge.

Subsequent studies have also highlighted the fundamental importance of the amount and type of the sediment in transport. Wilcock (1971) attempted to relate hydraulic geometry characteristics of Pennine streams with that fraction of the coarse bed load which was capable of movement. He related different values of the hydraulic geometry exponents to varying rates of increasing and decreasing competence. In a series of papers Osterkamp (1976, 1979, 1980) first derived a hydraulic geometry relation between width and discharge. He then introduced silt-clay percentages of the bed and bank material into this standard relation. This showed that, at constant discharge, width varies inversely with both bed and bank silt-clay percentages. Osterkamp (1976) concluded that the ratio of suspended load to bed load appears to be a principal determinant of channel morphology, whereas sediment yield affects the rapidity with which channel healing can occur after flood induced widening. He later noted that the width exponent, b, appeared to vary with the tractive sediment load of the stream (Osterkamp, 1980). Using data collected from alluvial streams in the western United States, he showed that the lowest value of b (0.45) was associated with silt-clay bed channels in which essentially no sediment is moved by traction. The exponent value increased to about 1.0 for some braided stream channels in which large amounts of sediment are moved in traction. This result appears to be unusual, since it implies that the f and m exponents must both be equal to zero, indicating that the depth and velocity would both be independent of discharge. Schumm (1960) found that channel perimeter sediment characteristics exercise control over the shape (width-depth ratio) of alluvial channels. However, a re-analysis of Schumm's data using multiple regression techniques suggested that channel perimeter sediment characteristics play only a minor

role in the development of channel shape, discharge being the main factor controlling both size and shape of these streams (Miller & Onesti, 1979).

The effects of vegetation on channel morphology have also been identified. It appears that bank vegetation is a major control on channel width and flow velocity (Hey & Thorne, 1986). Zimmerman *et al.* (1967) found stream channels were narrower in forest reaches, but wider in meadow reaches. However, vegetation effects are complex and it remains difficult to predict the overall effect in a particular reach. This is a topic of current research.

Park (1977) and Rhodes (1987) independently collated available results by plotting the b, f, m exponents on a triangular diagram. Both found considerable scatter in the values of these exponents. Park (1977) tried to systematically explain the world wide variation in hydraulic geometry exponents, but found these cannot be explained using different curve fitting techniques. He also failed to find systematic variations according to climatic, or other, environmental controls. Rhodes (1987) found some separation of b, f, m envelopes according to channel pattern. He found that six lines representing thresholds of adjustment to downstream changes in discharge and sediment load delineated a set of river responses, within which rivers have similar modes of adjustment to changes in control variables. However, this illuminates nothing about the mechanisms of adjustment. Moreover, the success of such studies in contributing to the understanding of channel change is likely to be limited by problems associated with the technique.

Thornes (1977) has noted that hydraulic geometry has both technical and conceptual problems associated with it. Considering first the technical problems, Benson (1965) has shown that the use of a common variable on both sides of the regression equation (*e.g.* discharge, which is defined as the product of velocity, depth and width, as independent variable; and width, depth and velocity as dependent variables) can lead to spurious results in terms of the correlation coefficient. More scatter may be found if this effect were taken into account (Thornes, 1977). There is also no reason to assume that the regression equations should be monotonic power functions. Thornes (1970) observed sharp changes in the hydraulic geometry of small channels with increasing discharge in the downstream direction, which were thought to represent thresholds of bank resistance due to vegetation effects.

In terms of predicting channel change, technical problems are small compared to conceptual problems. The major difficulty is that channel changes are, by definition,

transient in nature, but hydraulic geometry defines steady state behaviour. Thornes (1977) states that a conceptual approach to transient behaviour in hydraulic geometry is now required, to build on empirical observations of the transient evolution of disturbed fluvial systems (*e.g.* Burkham, 1972; Schumm & Lichty, 1963). A second area of difficulty lies in the undoubted existence of thresholds and discontinuities in the relationships involved. Yet in using the standard power functions it is generally assumed that these relationships are smooth and continuous. It is evident that there must be doubt as to whether the conventional hydraulic geometry can assist further in understanding the response of fluvial systems to exogenous change (Thornes, 1977).

More recent hydraulic geometry analyses have attempted to address some of the *technical problems* through the much more rigorous application of more sophisticated statistical and analytical techniques (Miller, 1984; Rhoads, 1991a; 1991b; 1992). However, even while these studies undoubtedly are useful in improving the methodological basis of hydraulic geometry, conceptual limitations associated with the steady state, empirical nature of the approach remain, even if some advocates of the hydraulic geometry approach (*e.g.* Rhoads, 1992) claim to have established improved conceptual, as well as technical, foundations for their work.

In conclusion, it is apparent that traditional regime and hydraulic geometry studies are similar in their empirical approach to the problem of morphological adjustment. A number of serious problems with both approaches stemming from the lack of deductive reasoning and blind empiricism coupled with their applicability to steady state systems make these approaches unsuitable for the dynamic modelling of width adjustment. However, their usefulness in establishing the ubiquity of river behaviour should not be underestimated. Hydraulic geometry and regime studies provide a mutually complementary data base, and help to identify the important factors controlling the response of river channels. Any results from rational regime studies (see below) and, indeed, other more physically-based models in general must show some approximate agreement with the results in this data base.

2.3 RATIONAL APPROACHES TO PREDICTING THE MORPHOLOGY OF ALLUVIAL CHANNELS

The many problems with the traditional empirical approaches reviewed above have led scientists and engineers to attempts to develop regime-type, functional relationships based more on the fundamental processes involved. Engineers in particular have attempted to develop models with a more powerful predictive element than had

previously existed. These approaches have become known as *rational regime theory.* For the purposes of this review, it is possible to classify these approaches into studies using some form of extremal hypothesis, tractive force theory and the work inspired by Parker (1978ab).

2.3.1 Extremal Hypotheses

There is almost universal agreement that the processes of sediment transport and alluvial friction are significant and should be included in any rational approach to deriving regime relationships using descriptions of the fundamental processes involved (Bettess *et al.*, 1988). However, even when neglecting the planform and bedform degrees of freedom for river channel adjustment (Hey, 1978), these two relationships are, by themselves, insufficient to enable a determination of channel width, even assuming that the sediment transport and flow resistance relations presently available adequately describe these processes (White *et al.*, 1982). Extremal hypotheses have been proposed to provide the extra relationship necessary to close the system and enable the channel geometry to be determined. These hypotheses are based on the assumption that the regime width is that width which either maximises or minimises some variable. A number of such hypotheses have been proposed.

2.3.1.1 Minimum Energy Dissipation Rate (MEDR)

Yang *et al.* (1981) hypothesized that:

" A system is in equilibrium condition when its rate of energy dissipation is at a minimum value. This minimum value depends on the constraints applied to the system. When a system is not in an equilibrium condition, its rate of energy dissipation is not at its minimum value. However, the system will adjust in such a manner that the rate of energy dissipation can be reduced until it reaches the minimum and regains equilibrium."

Davies & Sutherland (1983) comprehensively reviewed the theoretical basis of this hypothesis. Originally, Yang (1971) proposed analogies between river elevation and temperature and between potential energy and thermal energy in order to deduce his "law of least time rate of energy expenditure" from the thermodynamic principle of minimum rate of energy production. However, such an analogy is unjustified as this principle is valid only in the range of linear thermodynamic processes (Davy & Davies, 1979), yet energy transformations in streams are often highly non-linear. Nicolis &

Prigogine (1977) have also found that the behaviour of systems in the strongly non-linear region does not correspond to any particular behaviour of energy production. More recently Yang & Song (1979) attempted a second theoretical justification of the MEDR hypothesis. However, Davies & Sutherland (1983) also strongly attack this attempt, on the grounds that the assumed analogy between laminar and turbulent flow used to derive the MEDR hypothesis is fundamentally unjustified. Lamberti (1988) has also noted the theory cannot be derived from the theory of mechanics. It is apparent that there is no theoretical or physical basis for the MEDR hypothesis.

Despite this, the method has enjoyed considerable predictive success. Yang & Song (1979) used the MEDR hypothesis to explain measured hydraulic data from flumes and the Rio Grande. The MEDR predictions and empirical observations were in reasonable agreement. Yang *et al.* (1981) used the MEDR hypothesis to obtain theoretical values of the exponents of the hydraulic geometry relations proposed by Leopold & Maddock (1953). Although the theoretical analysis was limited to channels which were approximately rectangular in shape, the agreement between predicted and observed exponents was impressive. The b, f and m exponents they derived were 9/22, 9/22 and -1/6 for width, depth and slope respectively, in reasonable agreement with empirical results. The best agreement, though, was with the depth exponent. Yang *et al.* (1981) suggested that it appears that the channel depth can readily be adjusted in accordance with the theory, while the width adjustment may depend on constraints other than discharge and sediment load. The MEDR hypothesis may not, therefore, be the best predictor for channel width.

2.3.1.2 Minimum Stream Power (MSP)

Chang (1980b) has stated the MSP hypothesis as:

"For an alluvial channel, the necessary and sufficient condition of equilibrium occurs when the stream power per unit length of channel is a minimum subject to given constraints. Hence, an alluvial channel with water discharge and sediment load as independent variables tends to establish its width, depth and slope so that the stream power is a minimum. Since the discharge is a given parameter, minimum stream power also means a minimum channel slope."

In a series of papers Chang (1979ab, 1980ab) used this hypothesis to derive regime type hydraulic geometry relations for both sand and gravel-bed rivers. The "analytical channel geometry" obtained was in general agreement with previous regime relations.

In particular, there was close agreement with the regime width equation, where width is proportional to the square root of the discharge. Chang also used the hypothesis to successfully "explain" the channel pattern of natural rivers, width-depth ratio of regime rivers and the form of delta streams (Chang & Hill, 1977). Thorne *et al.* (1988) have also applied the method to British rivers. Their results showed significant scatter, but they concluded that the predictions were reasonable. The incorporation of bank vegetation parameters reduced the scatter. The overall agreement with observations that this method shows is ample indication of the predictive power of this method.

Davies & Sutherland (1983) have shown that under normal flow and sediment conditions the MEDR and MSP hypotheses are equivalent, though they are not equivalent when the stream boundary is moving with appreciable velocity (Song & Yang, 1980): that is when sediment concentrations are high. The equivalence of the MEDR and MSP hypotheses suggests the hypotheses have similar theoretical limitations.

2.3.1.3 Minimum Unit Stream Power (MUSP)

This hypothesis has been defined by Yang & Song (1979) as:

"... for subcritical flow in an alluvial channel, the channel will adjust its velocity, slope, roughness and geometry in such a manner that a minimum amount of unit stream power is used to transport a given sediment and water discharge. The value of minimum unit stream power depends on the constraints... applied to the channel. If the flow deviates from its equilibrium condition, it will adjust its velocity, slope, roughness and channel geometry in such a manner that the unit stream power is minimised until the equilibrium condition can be regained."

Song & Yang (1980) note the similar nature of the MSP and MUSP hypotheses, and regard both as a special case of a more general hypothesis, that of the MEDR. Again, it is to be expected that this hypothesis has the theoretical limitations outlined above.

2.3.1.4 Maximum Friction Factor (MFF)

This extremal hypothesis was originally proposed by Davies & Sutherland (1980) as:

"If the flow of a fluid on an originally plane boundary is able to deform the boundary to a non planar shape, it will do so in such a way that the friction factor increases. The deformation will cease when the shape of the boundary is that which gives rise to a local maximum of friction factor. Thus the equilibrium shape of a non planar self-formed flow boundary or channel corresponds to a local maximum of friction factor."

Davies & Sutherland (1983) recognise that this hypothesis also has no fundamental theoretical explanation. However, they claim that the MFF hypothesis is compatible with the known behaviour of turbulent flows. They cite the observed tendency of friction factor to approach the limiting upper bounds in turbulent flows with a given discharge as strong independent support for the MFF hypothesis. Moreover, they argue that the hypothesis is also compatible with the known behaviour of non-linear processes. Experimental evidence provides conflicting results. Temporal trends of Darcy-Weisbach friction factor calculated using direct observations of channel geometries obtained from repeated surveys of the Toutle River system in Washington indicate that friction factor marginally decreases through time (Simon, personal communication, 1993). On the other hand, Abrahams (1993) conducted flume experiments which suggest that step-pool sequences in high gradient, mountain streams are spaced so as to maximise the friction factor. It appears that the true validity of the maximum friction factor hypothesis over a wide range of environments is, at best, uncertain. In fact, the environmental controls on channel adjustment processes may be the key to understanding the true validity of the hypothesis. In evolving towards equilibrium, channels may adjust each of the width, depth and slope, resulting in variation of friction factor (equation 2.19). Depending on the boundary materials and initial channel geometry, each of these components may be free to adjust to varying extents. The degree to which system change in response to a disturbance is absorbed by change in either of the slope, depth or width will control the direction of temporal change in friction factor and, therefore, the validity of the maximisation hypothesis.

2.3.1.5 Maximum Sediment Transport Rate (MSTR)

White *et al.* (1982) proposed the MSTR hypothesis:

"For a particular water discharge and slope the width of the channel adjusts to maximise the sediment transport rate."

They added:

"The writers can find no physical justification to support the principle of maximizing the sediment transporting capacity but regard it as a useful hypothesis which... leads to acceptable predictions over a large range of flow conditions."

Predictions obtained using this method appear to be in reasonable agreement with observations. White *et al.* (1982) calculated channel widths for both sand and gravel-bed rivers. In sand streams the agreement with observed data is reasonable, but this agreement declines as the width increases. In gravel-bed streams the MSTR method tends to underpredict for low discharges. The discrepancy increases with increasing particle size but decreases with increasing discharge. The poor results for gravel-bed rivers, compared to sand-bed streams, were attributed to the special features of gravel streams such as the widely graded sediment and the structural qualities of the bed.

Wang Shiqiang *et al.* (1986) have noted a number of other additional extremal hypotheses in a list that they note is not exhaustive. These are minimum Froude number, minimum total friction resistance, minimum friction factor and minimum discharge. These additional hypotheses are not commonly used.

On the face of it a number of these extremal hypotheses appear to be incompatible and it is not clear why one particular hypothesis should be chosen in preference to another one. In fact it has been suggested that the 5 major hypotheses are closely related, and that under certain conditions these hypotheses are essentially equivalent (Griffiths, 1984). It has already been shown that the MSP and MUSP hypotheses can be regarded as special cases of the MEDR hypothesis (Davies & Sutherland, 1983; Yang & Song, 1979; Song & Yang, 1980). Moreover, White *et al.* (1982) and Lamberti (1988) have demonstrated the equivalence of the maximum sediment transport hypothesis with the minimization hypotheses. Fixing the discharge and the slope and maximising the sediment transport rate is equivalent to fixing the discharge and the sediment transport rate and minimizing the slope (Figure 2.1). White *et al.* (1982) demonstrate this equivalence analytically for a large range of sediment transport theories and friction equations.

Wang Shiqiang *et al.* (1986) also note the equivalence of the minimum Froude number and maximum friction factor hypotheses. Since the definition of the friction factor is:

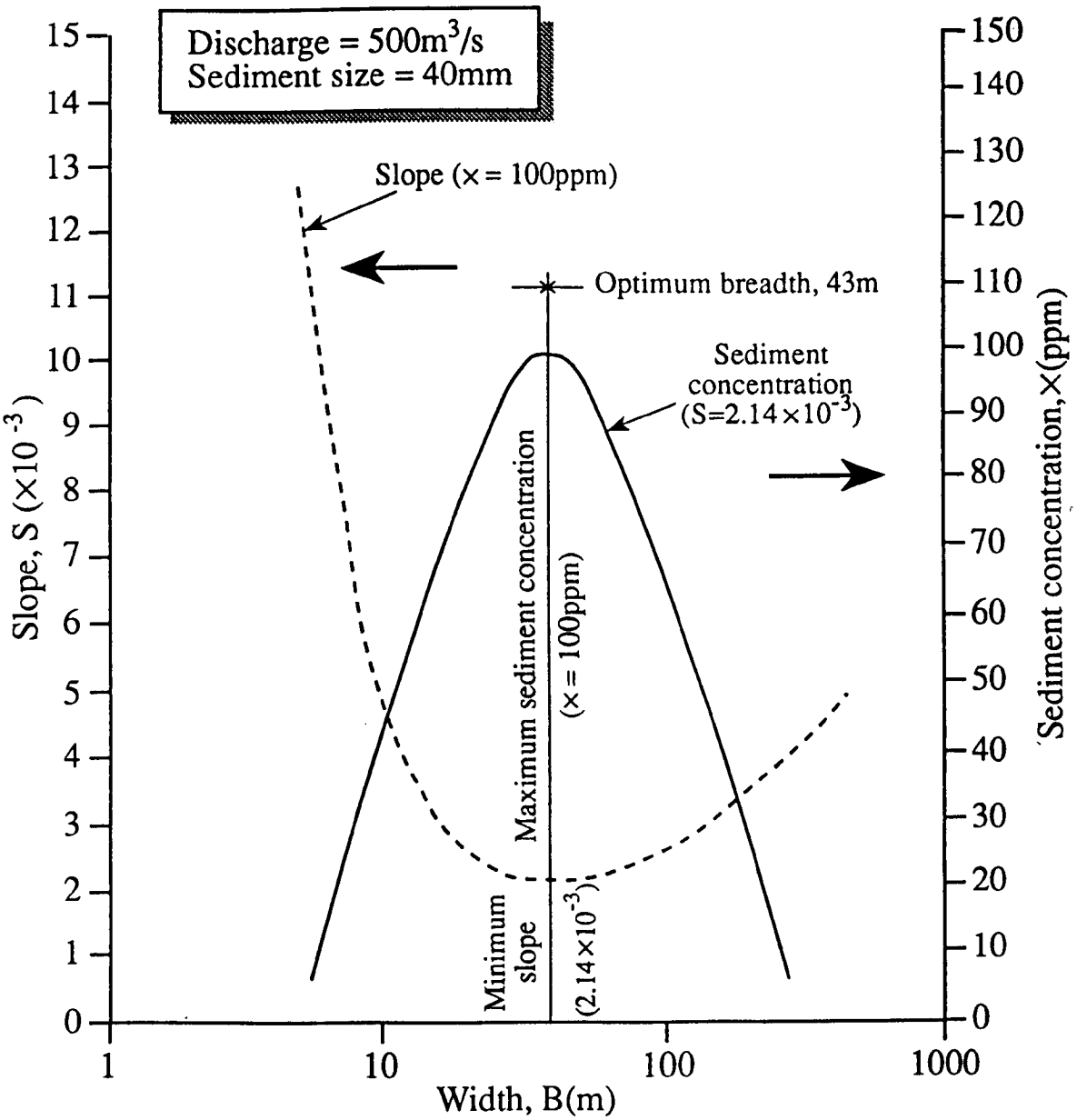

Figure 2.1 Equivalence of Maximisation of Sediment Transport and Minimisation of Energy Hypotheses (after White *et al.*, 1982)

$$f = \frac{8gDS_w}{V^2} \tag{2.19}$$

where V = flow velocity (ms^{-1}), f = dimensionless Darcy-Weisbach friction factor, g = acceleration due to gravity (ms^{-2}), D = flow depth (m), S_w = water surface slope and the Froude number is given by:

$$Fr = \frac{V}{\sqrt{gD}} \tag{2.20}$$

it follows that:

$$f = \frac{8S_w}{Fr^2} \tag{2.21}$$

so the friction factor is maximised when the Froude number is minimised.

Table 2.2 Summary of Implications of Extremal Hypotheses (after Davies & Sutherland, 1983)

Constraint (Independent Variables)	MUSP Hypothesis QS/D = Min	MSP Hypothesis QS = Min	MFF Hypothesis D^3SQ^2 = Max
Q, Qs	max D min S	max D min S	max D min S
Q, Qs	max D (slope fixed)	not applicable	max D (slope fixed)
Q, S	max D (max sediment transport rate)	not applicable	max D (max sediment transport rate)
Q, S	max D (sed. trans rate fixed)	not applicable	max D (sed. trans rate fixed)
Q, D	min S (min sediment transport rate)	min S (min sediment transport. rate)	max S (max sediment transport rate)

It has also been shown that the maximum friction factor hypothesis is related to the minimum energy hypotheses. Davies & Sutherland (1983) noted that the minimum energy hypotheses are special cases of the MFF hypothesis under certain specified conditions. Davies & Sutherland provide a table of the implications of the hypotheses (Table 2.2), these implications being calculated by working through the hypotheses under the constraints shown. It is seen that, except where Q and D are the independent variables, the hypotheses of MUSP and MFF predict the same extrema.

However, a crucial comparison occurs where Q and D are independent, so that the MSP hypotheses directly contradict the implications of the MFF hypothesis (Davies & Sutherland, 1983). Observations from flume experiments under these constraints show that, during the approach to equilibrium, the flow conditions pass through a series of states of lower stream power than the equilibrium value. This makes it impossible to accept the minimum energy hypotheses, but in the same experiments maximisation of friction factor does occur. This leads Davies & Sutherland to conclude that the MFF is more fundamental and more widely applicable over a range of conditions than the minimisation hypotheses. According to Davies & Sutherland, the empirical success of the minimisation hypotheses occurs exclusively in situations where they are equivalent to the MFF hypothesis. However, the condition in which both Q and D are independent is probably limited to flume, rather than natural, channels, suggesting Davies & Sutherland's conclusion may be misleading.

The predictive capabilities of the extremal hypotheses have been examined in two studies. Wang Shiqiang *et al.* (1986) compared empirical data, consisting of 203 sets of data from sand rivers and canals and 59 sets of data from gravel rivers. These observations were compared to various extremal hypothesis predictions calculated using the Ackers and White sediment transport relationship for sand streams and the Engelund and Hansen relation for gravel streams. The comparison was made in terms of the discrepancy ratio (Me), that is the ratio of predicted to observed values, and the value of standard deviation (SD) which indicates the scatter of individual predictions (Wang Shiqiang *et al.*, 1986). Their results indicate a considerable degree of success for the various extremal hypotheses, highlighting their usefulness for predicting regime conditions in alluvial channels. However, there are also differences between the predictions of different hypotheses. Of the tested hypotheses, the principles of minimum stream power or maximum sediment concentration gave the best agreement with field data.

An interesting contribution to the extremal hypothesis debate has recently been made by Simon (1992). In this study, energy variations through time were documented for two fluvial systems of a very diverse nature. The Toutle River system, Washington, represents a coarse-grained, high energy fluvial environment, with several valley constrictions, that has been catastrophically altered by deposition of a debris avalanche accompanying an explosive volcanic eruption. On the other hand, the Obion-Forked Deer River system, West Tennessee, represents a fine-grained, low energy environment with broad flood plains and no valley constrictions. This system has been disturbed by dredging, straightening, and the removal of riparian vegetation (Simon, 1992). Flow-energy variables from both sites were calculated using observed channel geometries obtained by direct repeated surveys of the channels. The data clearly show convergence towards a minimum energy dissipation rate with time (Figure 2.2), suggesting that "Study of the expenditure of kinetic and potential energy components of total mechanical energy provide an energy based rationale of the interdependency between processes and forms during channel evolution" (Simon, 1992). Simon's study is noteworthy for the clear evidence, from diverse environments, that it provides for validating the hypothesis that, following a disturbance, natural, field scale channels do indeed adjust such that the rate of energy dissipation is minimized. Moreover, the observations of Simon (1992) are set in a dynamical framework explicitly concerned with transient adjustment through time.

Both Bettess & White (1987a) and Wang Shiqiang *et al.* (1986) have compared the effects on the extremal hypothesis predictions of using different sediment transport equations. The results clearly show that the choice of sediment transport relation significantly affects the quality of the prediction. This fact is something of a double-edged sword. It shows either, on the one hand, that the hypotheses would give reasonable predictions but for the poor description of the sediment transport relations or, on the other, that the "fudging" of the predictions by use of a sediment transport calibration can be viewed as highlighting the poor physical basis of the extremal hypothesis.

2.3.1.6 Conclusion

Extremal hypotheses are similar to the regime theory approach in that it just presents a method of calculating channel width while not suggesting a mechanism by which this is achieved (Bettess *et al.*, 1988). This is the major drawback of the extremal hypothesis approach, these hypotheses offer a metaphysical method of steady state width calculation which offers no explanatory power (Ferguson, 1986). In this sense

extremal hypotheses are unhelpful, both in understanding processes of width adjustment (Ferguson, 1986) and, since the methods are like traditional regime theory steady state, in predicting the dynamics of width adjustment through time.

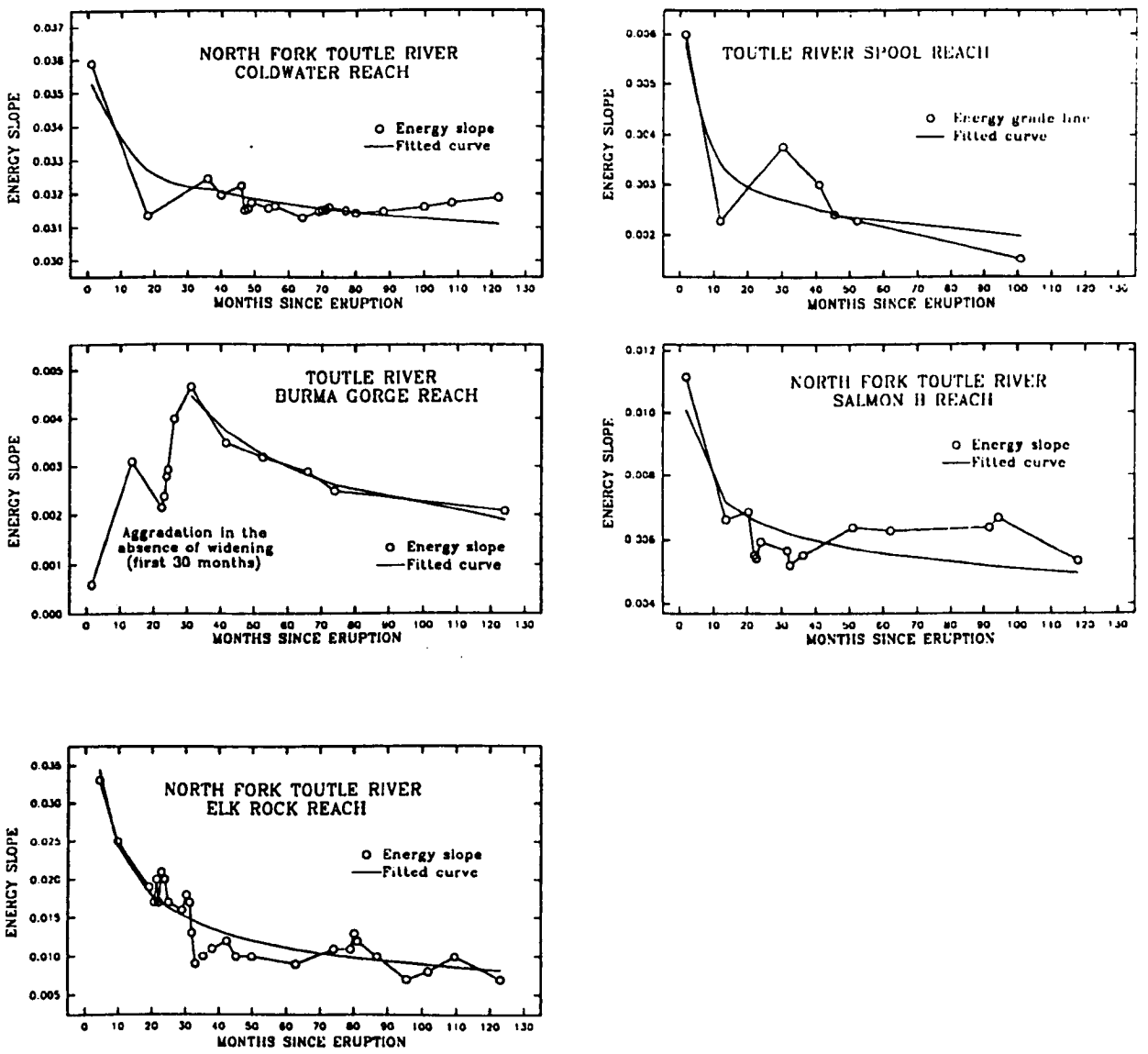

Figure 2.2 Minimisation of Total Mechanical Energy (Head) Loss with Time at Various Toutle River System Sites (after Simon, 1992)

Moreover, the arguments of Davies & Sutherland (1983) suggest that extremal hypotheses may not even be based on sound theoretical grounds and must therefore be regarded as unjustified (Ferguson, 1986). The work of Davies & Sutherland (1983), as well as more recent experimental work by Simon (1992) and Abrahams (1993) also

suggests that the proposed extremal hypotheses have not yet been properly tested under a full range of imposed constraints and conditions, so judgement must also be at least partially reserved on the apparent predictive success of the various methods.

Griffiths (1984) has suggested that despite their apparent predictive success, extremal hypotheses for river regime are an illusion of progress. This is because the hypotheses, when combined with conventional sediment transport and flow resistance equations, lead to conclusions incompatible with observations. For wide, straight, unconstrained alluvial reaches in equilibrium, these conclusions include that the Einstein sediment discharge and Shields entrainment function are nearly constant whereas empirical evidence suggests both expressions are highly variable in such streams. Constancy of the Einstein and Shields expressions provide a sufficient but unnecessary condition for channel stability. Griffiths (1984) argues that current formulations of extremal hypotheses thus require redefinition. Another major problem is that all extremal hypotheses still neglect plan form adjustments and strictly can only be applied to straight streams.

The apparent predictive success of extremal hypotheses is all the more remarkable given these serious problems. It could well be that these hypotheses are essentially correct, but the current limits of technology do not permit us to understand why this is so. It is concluded that extremal hypotheses cannot provide a complete understanding of the process of width adjustment. It is all the more remarkable that the method enjoys such apparent predictive success. Until more rational process based methods replace metaphysical speculation, engineers will continue to rely on the predictive ability of extremal hypotheses.

2.3.2 Tractive Force Theory - "Threshold" Channel Design

Another rational approach to stable channel design was presented by Lane (1955). This approach, termed tractive force theory, was based on considering the magnitude of the critical tractive stress for bank material entrainment, and then designing a "threshold" channel for the pre-specified slope (Carson & Griffiths, 1987) in which the boundary shear stress could not attain this value.

Mean tractive stress is controlled, however, by the depth-slope product, hence steeper channels can be maintained at the threshold state provided that the mean depth of flow is decreased, by increasing width, to counter the steeper gradient (Carson & Griffiths, 1987). In order to predict the stable channel geometry it is, therefore,

A

W' = Submerged weight

T' = Downslope component of W'

N' = Normal submerged weight component

F' = Frictional resistance

τ_c = Critical shear stress for entrainment on a flat bed

τ_{cs} = Critical fluid shear force for entrainment on a sloping bank

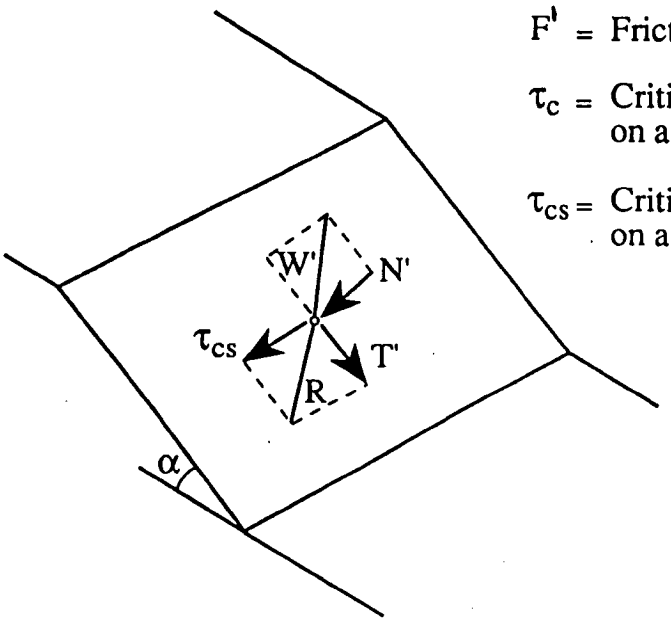

B

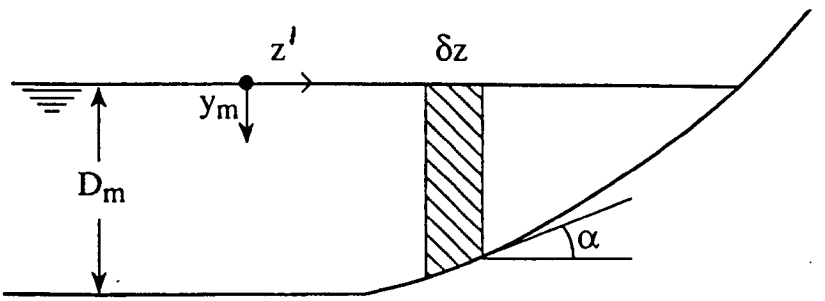

Figure 2.3 Definition Diagrams for Terms Used in Threshold Channel Design (A) Forces on a Bank Particle (B) Definition Diagram for the Threshold Channel Design Method (after Thorne, 1978)

necessary to solve the force balance on the sloping banks of the channel (Figure 2.3). For channels with low longstream slope and non-cohesive boundary materials, the critical fluid shear stress for entrainment, τ_c (Nm^{-2}), is proportional to the submerged weight and the apparent friction angle of the sediment particles:

$$\tau_c \propto W' \tan \phi \tag{2.22}$$

where ϕ = friction angle (degrees) and W' = submerged weight of the sediment particles (N). Provided the proportionality coefficient is constant for a material of uniform packing density and effective roughness height, then the ratio of critical shear stresses for material resting on the bed and the banks (Lane, 1955) is given by:

$$\frac{\tau_{cs}}{\tau_c} = \cos \alpha \sqrt{\left(1 - \frac{\tan^2 \alpha}{\tan^2 \phi}\right)} \tag{2.23}$$

where τ_{cs} and τ_c = critical fluid shear stresses for entrainment on a sloping bank and on a plane bed, respectively (Nm^{-2}), and α = side slope of the bank (degrees). This expression can be simplified to give:

$$\frac{\tau_{cs}}{\tau_c} = \sqrt{\left(1 - \frac{\sin^2 \alpha}{\sin^2 \phi}\right)} \tag{2.24}$$

The tractive force approach presented by Lane used a highly simplified version of the momentum balance equation to calculate the mean fluid shear stress so that:

$$\tau = \gamma_w y_m S_e \tag{2.25}$$

where τ = boundary shear stress (Nm^{-2}), γ_w = unit weight of water (Nm^{-3}), y_m = flow depth above a point on the bed (m) and S_e = energy slope, assumed equal to the bed slope for steady, uniform flow. From Figure 2.3 it can be shown that:

$$\frac{y_m}{D_m} = \cos\left(\frac{z' \tan \alpha}{D_m}\right) \tag{2.26}$$

where D_m = depth at the bank foot (m) and z' = lateral coordinate. This equation requires the bank to have the profile of a cosine curve in order to maintain the predicted fluid shear stress below the predicted critical value. This profile enables erosion to

begin simultaneously at all points on the bank when the fluid shear stress reaches the critical value (Thorne, 1978).

In order to determine the downstream hydraulic geometry, a flow resistance equation is required to solve the problem (Ferguson, 1986). Henderson (1966) used the Manning-Strickler equation to show that for boundary material of size d_s (mm), the width, B (m), is given by:

$$B = 1.1\, d_s^{-0.15}\, Q^{0.46} \tag{2.27}$$

Lane had previously shown that for a uniform boundary material:

$$B = 1.1\, d_s^{-0.15}\, Q^{0.46} \tag{2.28}$$

for $\phi = 30$ degrees, and

$$B = 0.91\, d_s^{-0.15}\, Q^{0.46} \tag{2.29}$$

for $\phi = 35$ degrees.

In theory the tractive force approach represents an important contribution, through its rational treatment of channel boundary erosion in terms of the explicit formulation of the applied fluid forces and the resisting forces influenced by the physical properties of the boundary material. But, in practice, there are problems with this type of approach. Ferguson (1986) notes that the coefficients in the equations depend on the assumed value of the friction angle, which may not be estimated accurately. Also, the exponents vary slightly according to the flow resistance law employed. Furthermore, in reality the boundary material of a channel is heterogeneous. A problem therefore lies in specifying the correct "representative" boundary material size, d_s. Most estimates of representative grain size are in the region d_{80} to d_{90} (Thorne, 1978), but Henderson (1966) used the d_{75}, while Carson & Griffiths (1987) argue the d_{50} should be used in natural channels which have a coarse cover layer.

Calculation of the critical shear stress for entrainment of the boundary material is also problematic and a likely source of error. The fluid lift force is neglected, though in practice the effect of the lift force is included in the empirical constants used to relate the critical stress to the flow required to produce it. These constants also attempt to account for the grain shape and packing density (Thorne, 1978), which is notoriously difficult.

The analysis also requires longitudinal flow parallel to the channel boundary, so secondary currents, which act to distort the primary isovels, are assumed to be small enough that they may be neglected. The determination of the applied fluid shear stress is also subject to uncertainty, since turbulent momentum exchange processes are also neglected. Indeed, the resulting error in the predicted distribution of boundary shear stress consequent upon the neglect of the process of turbulent momentum exchange leads directly to the most serious limitation of the threshold approach to channel design. In natural river channels stable widths are observed to be maintained even in channels with sediment transport active on the bed. But, under the threshold channel approach, bank erosion and widening is a necessary consequence of sediment transport on the bed, as there is a lateral component of bed load transport on a side slope due to the influence of gravity. Parker (1978b) termed this problem the "stable channel paradox". This problem is discussed in the review of Parker's contributions to rational regime theory (section 2.3.3), but the paradox is resolved through recognition of the fundamental importance of the inclusion of turbulent momentum exchange terms in models which attempt to predict the distribution of boundary shear stress.

Assessment of the validity of the equations presented above by comparison with natural channels believed to be in the threshold condition, or application of the width equation to width design faces another major hurdle: fluctuating discharge over time (Ferguson, 1986; Carson & Griffiths, 1987). The problems of specifying a dominant discharge have been discussed above in relation to the discussion of regime theory and hydraulic geometry.

Comparisons of the predictions of threshold channel theory with observed gravel-bed river data (*e.g.* Kellerhals, 1967) unsurprisingly show little close agreement, though general trends are apparent. More recently, advances have been made in attempts to rectify the deficiencies of the original approach. Lateral distributions of fluid shear stresses have been much more accurately predicted using more sophisticated solutions of the momentum equations which include most of the important momentum exchange terms (*e.g.* Lundgren & Jonsson, 1964; Parker, 1978b; Wark *et al.*, 1990; Pizzuto, 1991). Further advances have been made in predicting the critical threshold for transport of non-cohesive bed and bank materials, particularly in the presence of side slopes (*e.g.* Ikeda, 1982ab; Sekine & Kikkawa, 1992; Kovacs & Parker, in press) and also in the more realistic case of widely graded sediments (*e.g.* Wiberg & Smith, 1987; Carling *et al.*, 1992; Andrews & Smith, 1992). These advances have led to more sophisticated analyses (*e.g.* Ikeda et al., 1988; Ikeda & Izumi, 1990) of stable channel

forms using the same basic force balance approach outlined above, with only a little more predictive success than the previous studies had achieved.

However, in the context of width adjustment processes in natural channels, such comparisons of predictive ability are anyway rather meaningless, as present tractive force theory merely predicts stable channel widths. In any case the theory applies only to channels composed entirely of non-cohesive boundary materials. Such channels appear to be comparatively rare. The true value of the tractive force theory approach rests in its worthy emphasis on the rational prediction of channel form through an understanding of the mechanics of flow, sediment transport and bank stability processes in non-cohesive channels. The challenge lies in extending this type of rational, mechanistic approach into a more dynamical framework in order to develop a rational channel evolution model.

2.3.3 The Work of Parker

Parker's (1978ab) work on the determination of the regime width of alluvial channels stands out as an attempt explicitly to incorporate mechanisms for both bank erosion and deposition into the analysis of regime width. Parker (1978ab) considered channel formation in straight rivers with equilibrium banks and mobile beds. This was a major advance, incorporating the fact that sediment transport is possible in stable channels, the neglect of which had been the major problem of "threshold" channel design.

Parker first considered the case of self-formed sand-silt rivers. He noted that if bed load alone occurs across the perimeter of a wide channel, gravity will pull particles down the lateral slopes of the banks. Bank erosion is, therefore, a necessary consequence of bed load transport and the channel widens as a result. However, Parker noted that in order to maintain an equilibrium width, the export of material from the channel banks must be countered by an import of sediment from the centre of the channel, and postulated that the lateral diffusion of suspended sediment is the mechanism for this import. The import of this suspended sediment overloads the flow near the banks and drives deposition, so that a stable width is maintained.

Parker (1978a) analytically modelled this hypothesis. In making the problem tractable he considered only the simplest case, that of steady, uniform flow in a wide, laterally symmetrical, straight channel in uniform non-cohesive suspendable sand or silt carrying a constant discharge. He also neglected the effects of secondary currents.

Parker himself recognised the problems associated with these simplifications, but he only intended the theory to be a first step towards a more general model. By formulating the vertically integrated lateral diffusive flux of suspended sediment that was hypothesized to drive bank deposition and applying the sediment mass balance equation such that the lateral diffusive flux was balanced by a return lateral bed load flux, a steady state condition was maintained. Then, by relating the lateral bed load and suspended load fluxes to the downstream flow, Parker was able to obtain an approximate analytical solution with the use of a singular perturbation technique, such that for a stable channel:

$$R_c = 85.1 \sqrt{R_f}\, S^{-0.5} \tag{2.30}$$

This equation is a specification of the centre depth, D_c (m), as a function of the downstream slope, S, particle size, d_s (mm), and non-dimensional particle Reynolds number, R_f, where the non-dimensional centre depth, $R_c = \frac{D_c}{d_s}$. Bettess *et al.* (1988) present this equation in the form:

$$\frac{D}{d_s} = 85.1 \left(\frac{\omega}{(\rho_s/\rho - 1)\, g\, d_s} \right)^{0.5} S^{0.5} \tag{2.31}$$

where ρ_s and ρ = sediment and water densities, respectively (kgm^{-3}), D = flow depth (m), d_s = sediment size (mm) and ω = fall velocity of sediment (ms^{-1}).

As Bettess *et al.* (1988) note, although the theory developed by Parker in essence gives a complete regime theory, in practice the only parameter that can be easily determined is the channel depth. However, once the depth is known, the width may be determined by the continuity equation (Pizzuto, 1984), if a dominant discharge is specified and the velocity is estimated from a flow resistance relation. Thus, according to Parker, the depth is determined by the mechanics of erosion and deposition at the bank, and the width is adjusted to satisfy the necessity of conservation of mass (Pizzuto, 1984).

Parker (1978a) compared the depths predicted from his equation (2.30) with observed values (Figure 2.4). As Parker himself noted, insofar as the theory is approximate and the effective particle size has been chosen arbitrarily, one must be cautious in interpreting these results. At the very least, Parker argued, it indicates that the mechanism postulated for channel maintenance is a reasonable one that can predict broadly correct depths, although there is much scatter and the data set is somewhat

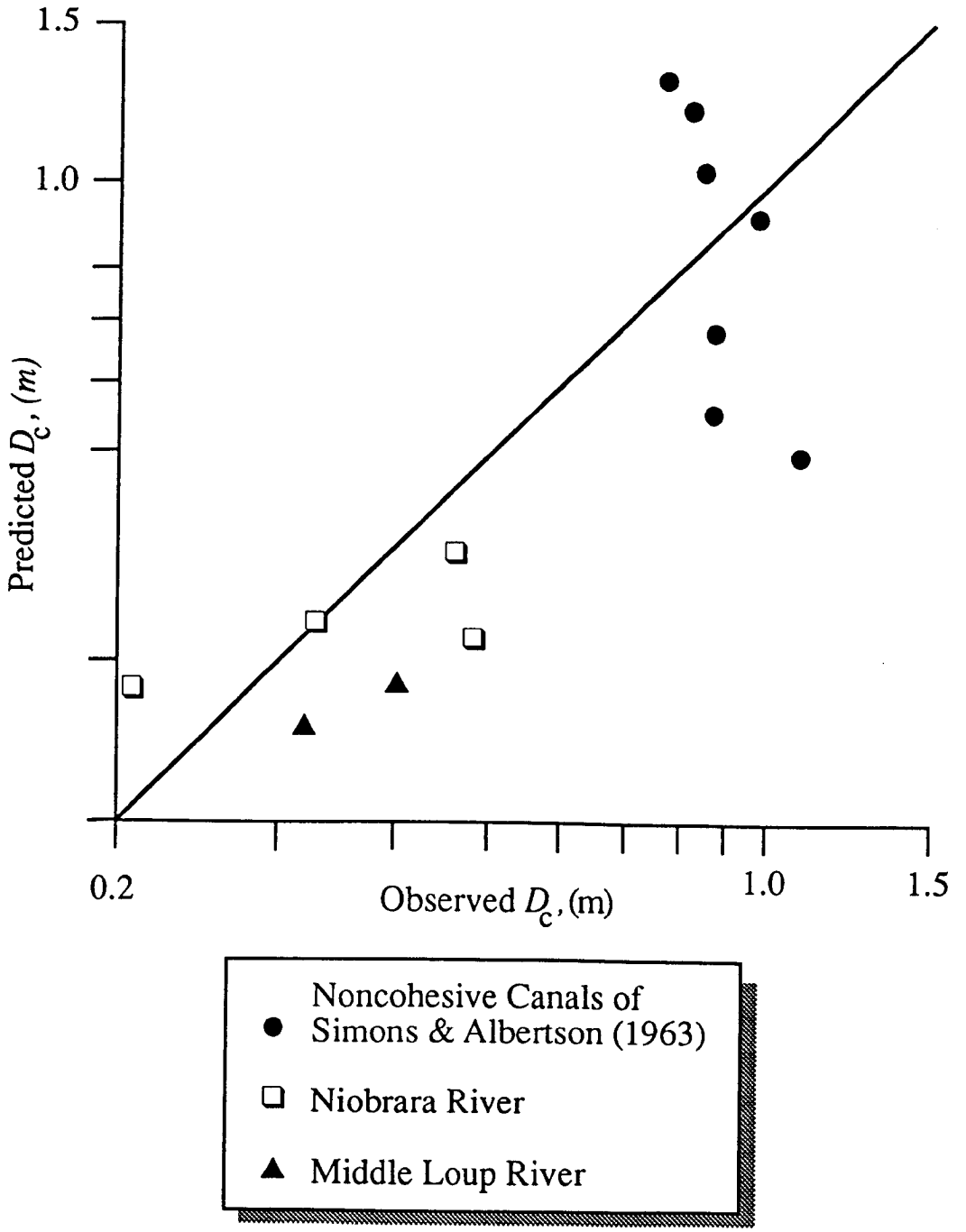

Figure 2.4 Comparison of Equation (2.30) with Data (after Parker, 1978a)

limited. Ikeda's (1982ab) flume experiments have also been used to provide support for Parker's model.

Bettess *et al.* (1988) note that equation (2.31) predicts that for a given sediment, depth is proportional to the square root of slope, which leads to depth being proportional to the square root of discharge when an empirical regime expression is used for slope. They note that this prediction contrasts with empirical regime theory in which the exponent on the discharge in the expression for channel depth is in the range 0.3 to 0.4. As the predictions for depth and width are closely related (by continuity) it is probable that a similar sort of discrepancy would arise on the prediction of channel width. However, this does not mean the basic approach is at fault. As Bettess *et al.* (1988) put it:

" The derivation of the theory relies on expressions for the suspended load and bed load in the area adjacent to the bank. It is in just such areas where the lateral bed slope and the spatial variation of flow are significant that there is, at present, most uncertainty as to the sediment mechanics involved."

Pizzuto (1984) used Parker's analysis explicitly to solve for the width of shallow sand-bed streams. Streams in Minnesota, Iowa and Nebraska were found to have sandy beds and upper banks consisting of cohesive materials. Bank erosion occurred when the upper cohesive unit block was undercut by scour of the lower sandy unit, leading to cantilever failure (Thorne & Tovey, 1981). Pizzuto argued that the cohesive unit has little influence on bank retreat and that Parker's model could, therefore, be applied to these channels, since the bank stability appeared to be controlled largely by erosion and deposition within the lower sandy unit. Pizzuto (1984) compared the predicted and measured widths and claimed that, although there is considerable scatter, the results are encouraging. He suggested that the scatter could be reduced by the inclusion of more detailed longitudinal sediment transport processes. Parker himself was of the opinion that proper inclusion of secondary currents in a two dimensional analysis would improve the model. It thus appears that the significance of the lateral transport process is as follows: The shape of the lower bank is adjusted until an equilibrium form is attained; this form determines the depth; the width is then adjusted to ensure the channel capacity is sufficient to transport the mean annual flow (Pizzuto, 1984).

Parker (1978b) also analyzed the geometry of "live" gravel-bed channels. He noted that extension of the threshold theory of Lane and Henderson to gravel-bed rivers leads

to what he termed the "stable channel paradox", that is to say the transport of bed material is incompatible with a stable width. This is because channel widening due to bed load transport and gravity cannot be balanced by the lateral diffusion of suspended sediment in gravel-bed streams, since bed material in such streams is, by definition, unsuspendable.

Parker noted that "paradoxes" such as the stable channel paradox are often resolved in terms of singular perturbation analyses, and he proposed a resolution based on the mechanism of turbulent momentum transfer. The downstream velocity, and thus momentum, is greater near the channel centre than near the banks. Parker postulated that turbulence can be expected to produce a net lateral flux of longitudinal momentum from regions of high momentum to regions of low momentum (*i.e.* from channel centre to the banks). This results in a deficit of bed stress near the channel centre and a surfeit near the banks. Thus, the lateral transfer of momentum is responsible for a redistribution of bed stress that allows mobile bed but immobile banks at the design discharge. In his analysis, Parker was aware that secondary currents also induce lateral transfer of longitudinal momentum, but ignored these effects, arguing they were small. By solving the problem formulated above, Parker (1978b) also devised rational regime relations for gravel-bed rivers. Again, Parker noted that his analysis did not provide a complete and accurate picture of gravel-bed rivers. However, a data set comprising observations of 41 gravel-bed river reaches was used to test these regime relations with some measure of success.

Parker's work is of great worth even if there is some controversy over the ability of his models to successfully predict the regime morphology of river channels. Firstly, his work is useful in stressing that the establishment of a regime width depends on both processes of bank erosion and bank deposition. Moreover, his analysis also demonstrates that the regime morphology is controlled by an interaction between the flow, sediment transport, boundary materials and the bank stability. However, a number of limitations remain. First and most importantly, Parker only solved his model analytically for the case of steady state channel behaviour. Hence, this work casts no light on transient morphological adjustments. Secondly, the influence of longitudinal flux divergences on the establishment of the regime morphology was also neglected by Parker. Thirdly, Parker's models were derived for channels with non-cohesive bank materials, so that the analysis is not valid in those channels with cohesive bank materials.

2.4 DYNAMIC MODEL OF CHANNEL EVOLUTION

A number of studies have documented observations of dynamic width adjustments over periods of a few years to tens of years at the scale of the river reach (Schumm & Lichty, 1963; Burkham, 1972; Leopold, 1973, Schumm *et al.*, 1984; Harvey & Watson, 1986; Simon, 1989). These studies highlight the fact that both the sediment supply and water discharges, together with the boundary material properties, control morphological channel response. Such studies are particularly useful since they document transient, dynamic adjustments of morphology in natural channels. These studies contrast with the approaches outlined above, be they empirical or rational in nature, which, even assuming that these approaches have reasonable predictive ability, can only provide insight into the *steady state* morphology of natural river channels. Such methods give no information on the time rate of adjustment between steady states, and no insight into the dynamics of processes of width adjustment in natural river channels. An understanding of the dynamical response of channel morphology in response to changes in the discharge and/or sediment load and boundary materials, or modifications to the morphology of the channel itself (*e.g.* to achieve engineering goals) can only be obtained if it is known how the channel boundary is deformed in response to the imposed water and sediment loads, given the constraints of the properties of the channel boundary itself. With respect to channel width, an understanding of the process of width adjustment can, therefore, only be obtained if it is known how the banks - the channel boundaries that define the channel width - retreat or advance in response to the water and sediment discharges conveyed through the channel.

In recent years a few studies have capitalised on the increasingly detailed knowledge of river bank erosion mechanisms and processes to synthesize current understanding into a conceptual model of channel widening. These are the studies of Schumm *et al.* (1984), also reported by Harvey & Watson (1986), and the study of Simon (1989). Both of these contributions based their models on geomorphic observations of actively degrading channels, in northern Mississippi in the case of Schumm and his associates, and in nearby West Tennessee in the case of Simon. In light of the similarity of the two approaches, this review concentrates on the work of Schumm and his co-workers. They found that imbalances in the sediment transport supply : capacity in the surveyed stream, Oaklimiter Creek, led to degradation of the bed of this stream. The degradation was characterised by headcutting as knickpoints migrated upstream, so that stream bank heights and angles were increased as the knickpoints migrated past a given point along the stream. Severe bank erosion and

channel widening occurred in response to the destabilisation of the channel banks with respect to mass failure under gravity due to the channel degradation.

Schumm *et al.* (1984) used observations of these processes to derive a conceptual model of channel evolution, based on space for time substitution of surveyed cross-sections along Oaklimiter Creek. Harvey & Watson (1986) point out that the model is based on the assumption that distance downstream of the knickpoint is equivalent to the increased passage of time. The assumption is justified since knickpoints are observed to migrate upstream with time. The response at any given location in the channel can then be predicted from the morphology of channel sections that are located downstream of that location (Harvey & Watson, 1986). Inherent in this approach is the assumption that the observed sequence reflects the passage of time exclusively. In Oaklimiter Creek this assumption is reasonable because the materials that form the valley fill along its length are on average uniform, and the bed material size lies within a very narrow range (Harvey & Watson, 1986). The 5 stage model proposed by Schumm *et al.* (1984) is shown in Figure 2.5.

Harvey & Watson (1986) summarize the significance of each of these stages. Type I reaches are characterized by little or no sediment storage in the stream bed and have U-shaped cross-sections. As a knickpoint migrates upstream, the Type I reach is destabilised by incision into a Type II reach, with variable sediment accumulation, steep vertical banks and increased channel depth. If the critical bank height for mass instability with respect to gravity is exceeded, rapid channel widening occurs (Type III reaches). Sediment from upstream degradation and bank erosion begins to accumulate on the bed of these reaches. In Type IV reaches active channel widening continues, but at a reduced rate, as the sediment supply from upstream Type III reaches restores the sediment supply : capacity imbalance, and transport capacity in the Type IV reach is reduced due to the channel widening. Type V reaches are those which have actually regained dynamic equilibrium. Very little bank erosion is observed. An increased sediment depth is expressed morphologically by the presence of berms which become vegetated and stabilised (Harvey & Watson, 1986), and these may even eventually reduce channel width.

The study by Simon (1989) lends support to the model proposed by Schumm *et al.* (1984). On the basis of geomorphic observations in degrading western Tennessee creeks, Simon (1989) presented a channel evolution model which, in general, is similar to that presented by Schumm and his colleagues. Importantly, though, Simon (1989) derived his model by monitoring individual sections repeatedly through time, rather

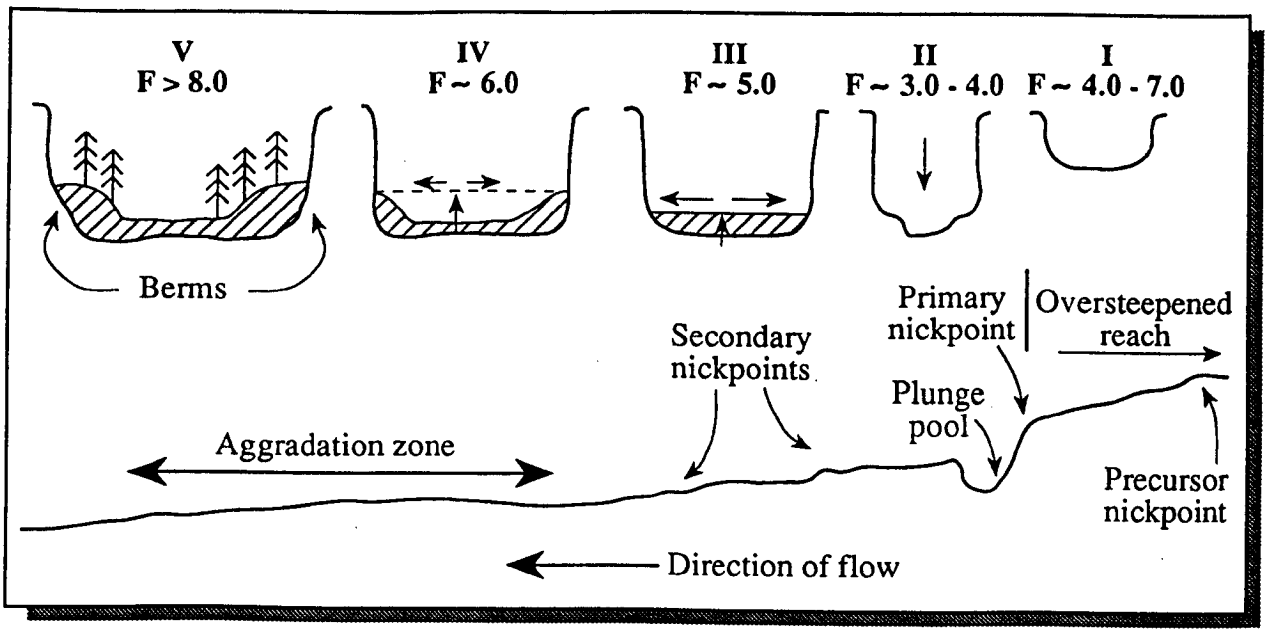

Figure 2.5 Schematic Diagram of Channel Evolution Model Developed by Schumm *et al.* (after Schumm *et al.*, 1984)

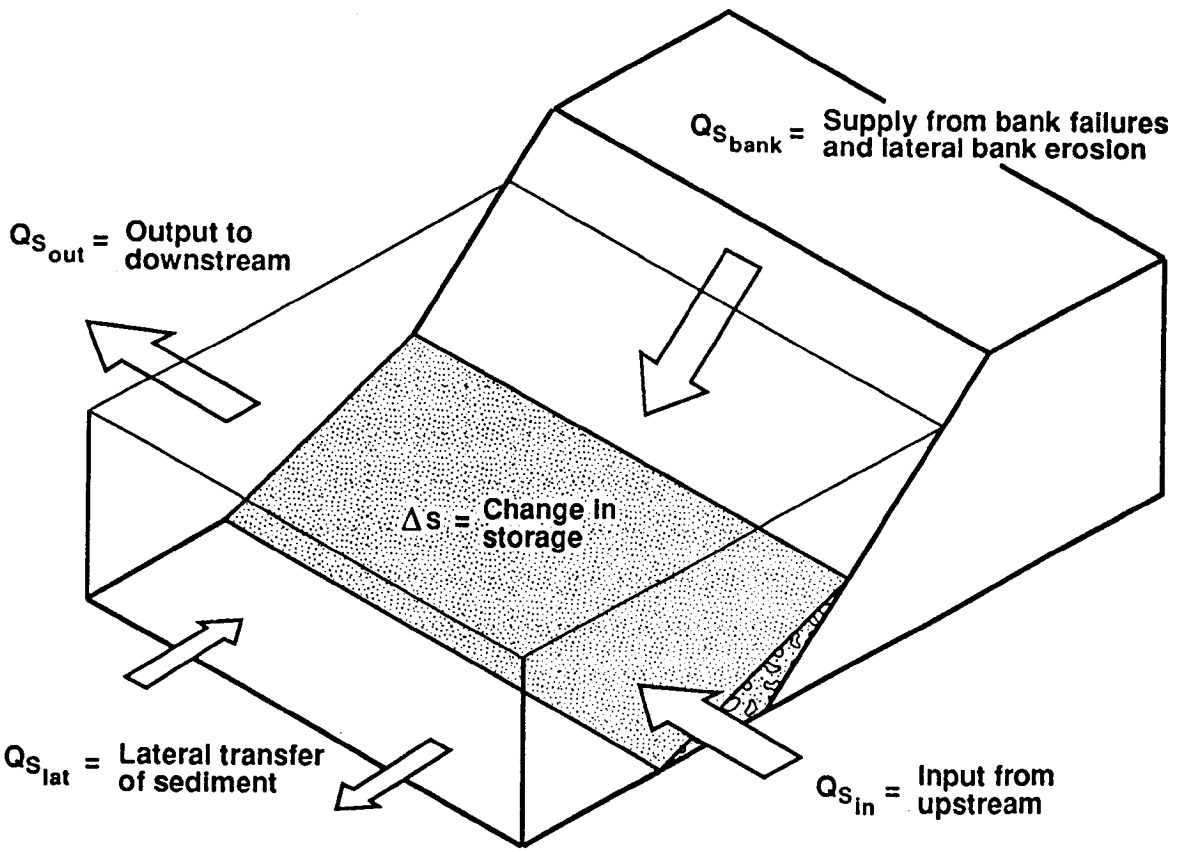

Figure 2.6 Sediment Fluxes in the Near Bank Zone (after Thorne & Osman, 1988a)

than by using a space for time substitution methodology. So, Simon's model of channel adjustment is particularly significant as it verifies the Schumm model using direct, rather than inferred, observations of channel response to imposed change.

The channel evolution models described above are significant in a number of ways. Firstly, they highlight the dynamic nature of the observed width adjustment and the characteristic mutual adjustment of morphological and sedimentological variables during channel change. Second, they also stress the importance of taking explicit account of the geomorphic processes and controls on the mechanics of bank stability (Schumm & Thorne, 1989). The importance of both of these points is emphasised by the possibility that the width adjustment process involves the crossing of a geomorphic threshold (Schumm, 1977). In some reaches, Schumm *et al.* (1984) noted "explosive" channel widening of hundreds of metres when the critical bank height for instability with respect to mass failure was exceeded due to degradation of the bed. It has been hypothesized that the critical bank height may be envisaged as a significant geomorphic threshold, perhaps as important as channel slope, in generating complex response (Thorne & Osman, 1988a). The important point is that there is every reason to expect morphological adjustments to occur in a complex, non-linear fashion. Such complex adjustments cannot be modelled using the approaches previously discussed, but are taken into account in the conceptual model outlined here. Furthermore, the model may provide a general framework for relating bank processes and adjustments of width to the hydraulic and sedimentological processes operating in the channel through the concept that the bank retreat rate (lateral instability) can be related to a stimulus in the vertical direction, caused by flow driven sediment transport flux divergences, through the application of bank stability theory. The fact that a similar model has been independently derived by Simon (1989) for the disturbed streams in a similar environment in West Tennessee and, moreover, that a similar sequence of events was observed on a small channelized gravel-bed river in Hertfordshire, England (Darby & Thorne, 1992a), suggests that the conceptual model may have a wide validity. Consequently, it may be argued that the conceptual model outlined above meets the necessary criteria for this study. Not only does the model allow for explicit account of the dynamic, rather than steady state, behaviour of river morphology, but the framework is rational, in the sense that in applying the model explicit account of both bank retreat and sediment transfer mechanisms, and the pivotal link between them - the bank stability with respect to mass failure - must be taken into account in order to predict the response of the channel morphology, including the width, to changes in discharge, sediment load or boundary materials.

In fact, the crucial contribution of the conceptual models of Schumm *et al.* (1984) and Simon (1989) is in the recognition of the role of the bank stability as the pivotal link between the determination of the sediment transfer processes and the rates of bank retreat or advance which define the channel width. The framework adopted as the conceptual model for this research may, therefore, be traced back to the concept of basal endpoint control (Carson & Kirkby, 1972). In essence, this concept applies the idea of the sediment transport supply : capacity balance (conservation of sediment mass) to the base of a hillslope. The basal endpoint status thus characterises the balance of supply and removal of sediment in the basal zone. Thorne (1978) identified three states of basal endpoint control for the case of an eroding river bank:

(i) Impeded removal. Here bank failure supplies material to the base of the bank at a higher rate than it is removed by the flow. Basal accumulation results, decreasing the bank angle and height. This stabilises the bank and the rate of supply decreases, tending towards the second state.

(ii) Unimpeded removal. Processes delivering material to the base and removing it from there are in balance. No change in basal elevation or slope occurs. The bank recedes by parallel retreat at a rate determined by the degree of fluvial activity at the base. In essence this is the state of dynamic equilibrium.

(iii) Excess basal capacity. Basal scour has excess capacity over the supply by bank erosion and mass failure. Basal lowering occurs, increasing bank angle and height, decreasing the bank stability and increasing the supply of sediment to the base by mass failure. The rate of supply thereby increases, so that the basal endpoint status tends towards the second state.

The balance of supply and removal results in a basal endpoint state which determines the stability of the bank with respect to mass failure so that feedback operates and the system tends towards dynamic equilibrium. The concept of basal endpoint control describes how the rate of bank retreat or advance (and hence width adjustment) is determined by the interaction between the flow, sediment transport and bank stability processes within the near bank zone. An important point is that, at equilibrium, the rate of fluvial activity at the base of the bank controls the time rate of retreat of the river bank. This concept provides a very powerful tool for predicting width adjustment by modelling the sediment fluxes which determine bank erosion or advance. The basal endpoint control framework used here in the development of a rational width adjustment model can be summarised in Figure 2.6. This conceptual framework allows width adjustment to be accounted for in terms of the mechanisms of bank advance or retreat in response to direct erosion of the bank by the flow and in

response to changes in bed level controlled by the changing hydraulic conditions and sediment fluxes at the base of the bank. In essence, the framework proposes that the problem of width adjustment can be solved using a sediment budgeting approach which takes into account all of the sediment fluxes entering and leaving the near bank zone. The difficulty in applying the approach lies in the difficulty of rationally specifying these fluxes (Thompson, 1990, personal communication) in the near bank zones where the driving flow structures are complex and difficult to predict.

A variety of empirical studies support the theoretical basis of the concept of basal endpoint control. That the long term rate of retreat or advance of river banks is controlled by the degree of fluvial activity at the base of the bank is apparent from the large number of statistical studies which have identified the degree of fluvial activity as the most important parameter controlling river bank erosion (Wolman, 1959; Twidale, 1964; Knighton, 1973; Hooke, 1979). Indeed, this may partially explain the apparent success of many regime type relations which relate channel morphology solely to the discharge. The rate of bank erosion has also been related to the properties of the sediment at the base of the bank (Nanson & Hickin, 1986), suggesting the importance of sedimentological controls on basal sediment fluxes in influencing the retreat of the river banks. Andrews (1982) related rates of width adjustment along reaches of the East Fork River, Wyoming to locations of scour and fill adjacent to the channel banks. Scour located adjacent to river banks was found to destabilise river banks and lead to increases in channel width.

Direct observations of slope development through time also support the theoretical basis of the concept of basal endpoint control. Brunsden & Kesel (1973) used the technique of space for time substitution to infer the development of slopes on a Mississippi River bluff through time, as the intensity of fluvial erosion at the base was decreased. They noted a progressive reduction in slope instability as the intensity of fluvial erosion was decreased. In the zone of least intense fluvial erosion, slope angles were lowest. This sequence of events is precisely that predicted by the concept of basal endpoint control. Given an increase in basal erosion it might be expected that this sequence of events could be reversed. However, Richards & Lorriman (1987) make the proviso that the mechanisms of slope steepening and failure during active undercutting are not necessarily those of slope decline in reverse, so that a sort of hysteresis effect may be introduced. If true, this could limit the application of the concept of basal endpoint control to situations where no fluctuations in stability occur. However, this view appears to be extreme. As Thorne (1982) puts it, the concept of basal endpoint control "....is of primary importance to the profile, form, stability and rate of retreat of

river banks of all sizes, structures and materials" and is, therefore, adopted here as the most suitable conceptual framework for the development of a numerical model of channel width adjustment.

CHAPTER THREE

A PHYSICALLY-BASED NUMERICAL MODEL OF CHANNEL EVOLUTION I: DEVELOPMENT

3.1 INTRODUCTION

In recent years a few attempts have been made to develop numerical models of river channel width adjustment, which are based on rigorous physical principles and are applicable to straight channels. These rigorous approaches are based on the numerical solution of the governing deterministic equations of flow resistance, hydraulics, sediment transport, bank stability and conservation of sediment mass. Two broad categories of models can be distinguished; first, those applicable to channels with non-cohesive bank material; second, those applicable to channels with cohesive bank materials. For non-cohesive bank materials, Pizzuto (1990) proposed a model in which widening was simulated using a simple planar grain flow of bank sediments at the angle of repose. This model has recently been improved by Kovacs & Parker (in press). They use an improved model of lateral bed load transport, applicable even at relatively steep side slope angles that are close to the angle of repose of the non-cohesive bank materials, in order to simulate widening and the lateral inflow of the bank grains. The advantage of the Kovacs-Parker model is, therefore, that the physics of the entrainment of the bank grains and, therefore, the widening process are correctly accounted for, rather than by using the heuristic bank failure model proposed by Pizzuto (1990) to simulate widening.

The few models of width adjustment applicable to channels with cohesive bank materials (Osman, 1985; Alonso & Combs, 1986; Borah & Bordoloi, 1989) are broadly similar in their approach. These approaches are characterised by attempts to directly couple a bank erosion/mass-wasting algorithm with various forms of simple one-dimensional aggradation-degradation models. This is done in order to simulate variations in bank morphology and stability with respect to mass failure in response to changes in flow hydraulics and sediment load. Channel widening is simulated by determining the width of the failure block once the banks become unstable. However, while these pioneering approaches are of great worth in correctly emphasising the importance of modelling the impact of bed level changes on bank stability and channel widening, as required by the concept of basal endpoint control, the application of the concept of basal endpoint control using these (albeit essentially developmental) models is, in practice, severely limited by a number of major problems.

The first of these problems is associated with the use of one-dimensional aggradation-degradation models to simulate bed level and bank morphology fluctuations in response to imposed water and sediment loads (Darby & Thorne, 1992b). One-dimensional sediment movement models are limited because only one computational point is used to characterise the bed level response at each cross-section. Hence, when using a one-dimensional approach, it is necessary to make an assumption about how the increments of aggradation and degradation are distributed over the bed of the cross-section. It is usually assumed that aggradation and degradation increments are distributed uniformly over the entire cross-section, even though in natural river channels the magnitude of aggradation and/or degradation varies across the width of the channel in response to the lateral distribution of the flow and sediment transport. But, the concept of basal endpoint control shows that the rates of retreat and advance of the river banks, and thus width adjustment, is controlled by the sediment budget in the *near bank* zone (Andrews, 1982) so that it is of critical importance to simulate the distribution of the flow, sediment transport and consequent increments of aggradation and degradation, across the full width of the channel (Darby & Thorne, 1992b). The importance of simulating the lateral distribution of flow and sediment transport has also been recognised by Simon *et al.* (1991), who attempted to use a quasi two-dimensional approach to overcome this limitation and so obtain more realistic predictions of near bank aggradation and degradation for their channel widening model.

A second, somewhat related, problem is that one-dimensional approaches also necessarily neglect lateral sediment transport fluxes. Figure 2.6 suggests that lateral sediment transport mechanisms may exert an influence on the supply and removal of sediment to and from the near bank zone and may, therefore, partially control observed rates of width adjustment. The work of Parker and others, reviewed in section 2.3.3 and above has heavily emphasised (even to the extent that longitudinal sediment flux divergences have been excluded from these analyses) the potential importance of mechanisms of lateral sediment transfer in controlling channel morphology. The relative importance of lateral versus longitudinal fluxes in controlling width adjustment processes is presently unclear. In light of the potential importance of lateral sediment transport processes, these processes should be included in the analysis, and they are included here.

The essential limitation of most of the previous approaches to modelling width adjustment numerically in straight reaches of river channel with cohesive bank materials is the failure to adequately address the problem of predicting the hydraulics and sediment transport within the near bank zones, as the concept of basal endpoint control

suggests is necessary if the influence of the interactions between in-channel and bank processes on channel width adjustment is to be correctly accounted for. The importance of modelling these interactions within the near bank zone has also been recognised by Simon *et al.* (1991). They presented a channel widening model which not only accounted for the lateral distribution of the flow and sediment transport across the full width of the channel, but also recognised the importance of modelling the impact of the inflow of bank materials following mass failure on the transport of sediments in the pivotally important near bank zones. Furthermore, they also presented a considerably more detailed and realistic bank stability algorithm which accounted for the influence of pore and confining pressures as well as relaxing the previous assumption that the failure plane is constrained to pass through the toe of the bank.

However, while the approach suggested by Simon *et al.* (1991) represents an important conceptual step from the earlier approaches by Osman (1985), Alonso & Combs (1986) and Borah & Bordoloi (1989), in practice the Simon *et al.* model is also limited by a number of problems, though it should be noted that it was the intention of Simon *et al.* to draw attention to the conceptual issues, rather than produce a definitive width adjustment code. First, it is shown below (section 3.2) that the approach they used to predict the lateral distribution of the flow hydraulics, while an improvement over the previous, strictly one-dimensional approaches, is inadequate within the near bank zones. Second, they did not attempt to account for lateral sediment transport processes. Third, explicit account was not taken of the impact on the mechanics of the sediment transport process of the delivery of bank sediments to the near bank zone following mass failure of the bank materials, though their model did correctly emphasise the importance of maintaining the continuity of the bank sediments in the time steps following mass failure of the bank materials. Finally, like the earlier approaches, it will be argued later (section 3.4) that the 2-dimensional bank stability algorithms used by Simon *et al.* are inappropriate when used to model bank stability in a numerical modelling framework.

The numerical model presented in the following sections attempts to overcome the limitations of these previous attempts at modelling width adjustment. The thesis that the concept of basal endpoint control is an adequate model of the interactions between the flow, sediment transport and bank stability processes that control the rate of width adjustment requires that emphasis must be placed firmly on modelling these process interactions within the near bank zone. The remainder of this chapter is divided into a number of sections which describe the selection and development of rational, physically-based, hydraulics, sediment transport and bank stability algorithms that are

valid within the near bank zone and are, therefore, much more appropriate for the task of modelling width adjustment in straight reaches of natural river channels with non-cohesive bed and cohesive bank materials, using the framework concept of basal endpoint control. The application and numerical solution strategy for combining the improved algorithms together into a much more sophisticated numerical model of channel widening is also discussed.

3.2 HYDRAULICS ALGORITHM

The concept of basal endpoint control emphasises the importance of predicting the sediment transport and, therefore, the hydraulics in the near bank zone. Accurate predictions of shear stress distributions in the near bank zone are also required in width adjustment modelling in order to predict the direct fluvial erosion of bank materials accurately (see section 3.4.1). However, most methods of predicting near bank flows are presently not very satisfactory. Flows in the near bank zone are particularly complex, due to the interactions between bed and side wall roughness, secondary flows and lateral momentum exchange processes. The full governing equation (Newton's second law of motion) for the mean streamwise velocity, u, may be written for a straight channel:

$$g S - \frac{\partial p}{\partial x} + \varepsilon\left(\frac{\partial^2 u}{\partial x^2} + \frac{\partial^2 u}{\partial y^2} + \frac{\partial^2 u}{\partial z^2}\right) = \rho\left(\frac{\partial u}{\partial t} + u\,\frac{\partial u}{\partial x} + v\,\frac{\partial u}{\partial y} + w\,\frac{\partial u}{\partial z}\right) \qquad (3.1)$$

where u = mean longitudinal velocity component (ms^{-1}), v = mean transverse velocity component (ms^{-1}), w = mean vertical velocity component (ms^{-1}), t = time coordinate (s), x = longitudinal coordinate (m), y = lateral coordinate (m), z = vertical coordinate (m), p = pressure (Pa), ρ = fluid density (kgm^{-3}), S = channel gradient, ε = eddy viscosity (m^2s^{-1}) and g = acceleration due to gravity (9.81 ms^{-2}). In this equation, the eddy viscosity model represents the influence of momentum exchange caused by velocity fluctuations superimposed on the mean flow field due to random turbulent fluctuations.

Although equation (3.1) describes the exact details of the flow field, the difficulty of representing the effects of turbulent flow through the eddy viscosity concept means that it is presently only possible to obtain an approximate solution, even when all the terms in (3.1) are included in the analysis. The fully three-dimensional nature of flows near side walls means that it is not possible to specify the turbulent momentum fluxes in the near bank zone. Rigorous solution of equation (3.1) is, therefore, one of the most

difficult problems facing physically-based approaches to width adjustment based on the concept of basal endpoint control (S. Thompson, personal communication, 1991).

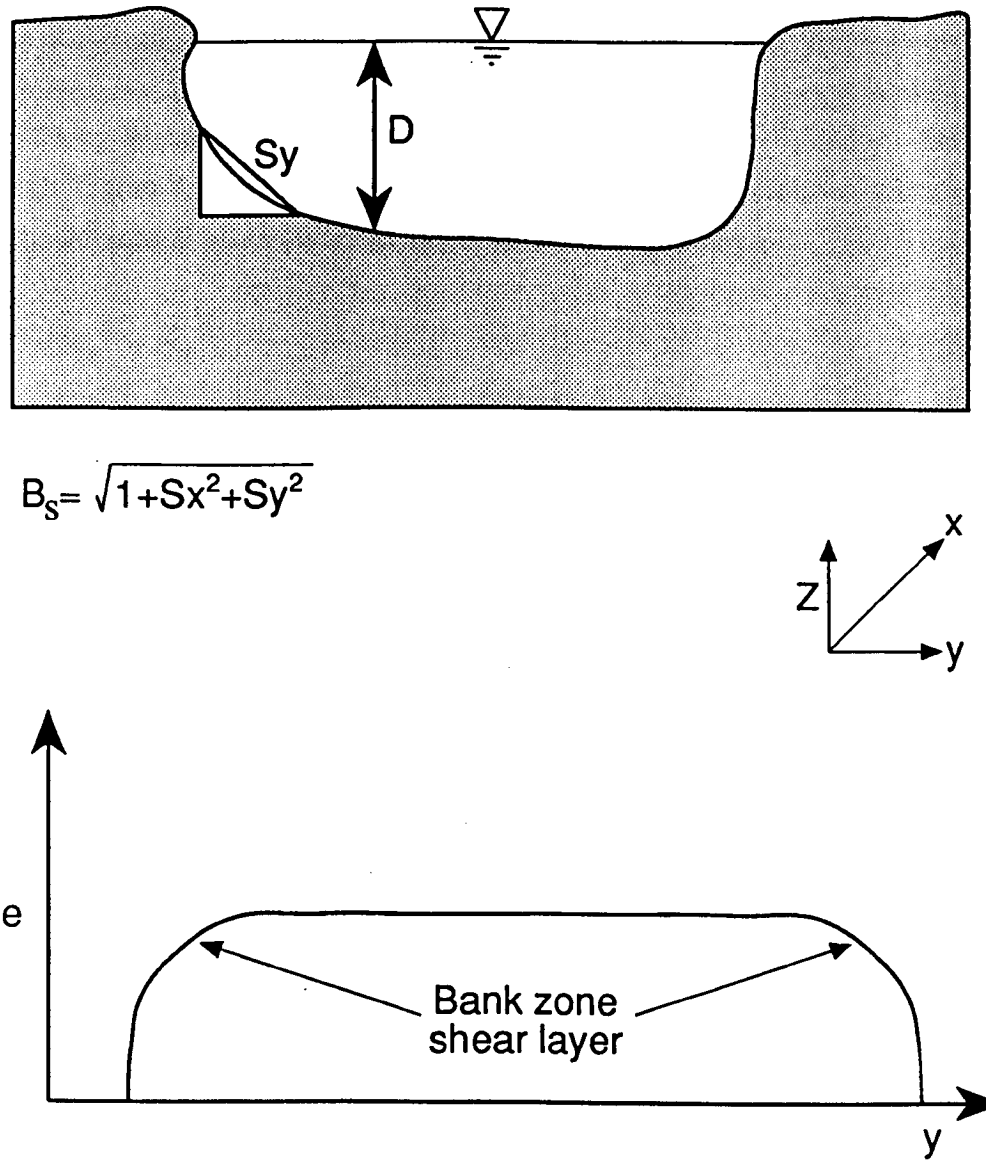

Figure 3.1 Definition Diagram for Hydraulics Algorithm

In order to predict the flow hydraulics in the near bank zone for the purposes of this research, an approach based on the Lateral Distribution Method (LDM) developed by Wark *et al.* (1990) was used to simplify and solve equation (3.1). First, by using the commonly adopted assumption of steady, uniform flow, quantities with derivatives in the streamwise direction can be neglected. Similarly, by assuming that secondary flows are negligible in straight channels, terms with secondary velocity components can also be equated to zero ($v = w = 0$). Finally, by depth-integrating the simplified equation, Wark *et al.* were able to obtain an expression for the lateral distribution of unit discharge, q (m^2s^{-1}):

$$gDS - \frac{B_s f q^2}{8D^2} + \frac{\partial}{\partial y}\left(\varepsilon \frac{\partial q}{\partial y}\right) = 0 \qquad (3.2)$$

where g = acceleration due to gravity (ms^{-2}), D = local flow depth (m), S = channel gradient , f = Darcy-Weisbach friction factor, ε = eddy viscosity (m^2s^{-1}) and y = lateral coordinate (m) (Figure 3.1). The factor B_s relates the stress on an inclined surface to the stress in the horizontal plane (Wark *et al.*, 1990), and is given by:

$$B_s = \sqrt{1 + S_x^2 + S_y^2} \qquad (3.3)$$

where, S_x = longitudinal bed slope and S_y = lateral bed slope (side slope).

In equation (3.2), the downstream component of the weight of a unit volume of water (term 1) is assumed to be balanced by frictional bed shear (term 2) and lateral shear (term 3) only. The lateral shear stresses are modelled using the eddy viscosity concept in order to represent the effects of the turbulent velocity fluctuations in the governing equations of motion. The eddy viscosity model was introduced by Boussinesq (1877) on the assumption that, by analogy with the viscous stresses in laminar flow, the turbulent stresses are proportional to the mean velocity gradients:

$$\tau = \varepsilon \frac{\partial u}{\partial x} = (\upsilon + \varepsilon) \frac{\partial u}{\partial x} \qquad (3.4)$$

where τ = turbulent fluid stress (Nm^{-2}) ε = (turbulent) eddy viscosity (m^2s^{-1}) and υ = molecular viscosity (m^2s^{-1}). The eddy viscosity is, therefore, assumed to have both viscous and turbulent components. Over most of the flow field the viscous component may safely be neglected because it is very much smaller than the turbulent component, except in the very thin viscous sub-layer near the boundary. This region is normally ignored or accounted for using appropriate semi-empirical bridging boundary conditions (ASCE Task Committee, 1988).

Equation (3.4) shows that, in contrast to the molecular viscosity, the eddy viscosity is not a fluid property, but a dynamical property of fluid motion. The close analogy between laminar and turbulent stresses that is the basis of the eddy viscosity concept has, therefore, often been criticized as physically unsound. However, in spite of these conceptual objections, the eddy viscosity concept has been found to work well in practice because it may be determined to good approximation in many flows (ASCE

Task Committee, 1988). Difficulties in applying the eddy viscosity concept in practice arise first, due to the difficulty in relating the turbulent stresses to mean flow properties and second, due to the difficulty in determining the distribution of these parameters over the flow field.

For dimensional reasons, the eddy viscosity may be related to a velocity scale, V' (ms^{-1}), and a length scale, l (m), characterizing the turbulent motion:

$$\varepsilon \propto V' l \tag{3.5}$$

This is an important assumption because it is actually the distribution of these scales that can be approximated reasonably well in many flows (ASCE Task Committee, 1988). A simple but reliable eddy viscosity model for use in equation (3.2), therefore, appears to be one based on the bed roughness turbulence (J. B. Wark, personal communication, 1991), in which:

$$\varepsilon = NEV\ U* D \tag{3.6}$$

where $U* = \sqrt{g D S}$ = shear velocity (ms^{-1}) and NEV = non-dimensional eddy viscosity coefficient, usually taken as approximately 0.16. In this model, ε is related directly to the mean flow field, so that it is assumed implicitly that the turbulence is dissipated by viscous action at the point where it is generated by shear. This means that the transport of turbulence is neglected, both through space and time; however, these effects can be important in shear layers (ASCE Task Committee, 1988).

More complicated eddy viscosity models have been formulated in order to account for these transport effects (see ASCE Task Committee, 1988). So-called Two-Equation models attempt to determine both the velocity and length scales independently. Pizzuto (1991) used a k-l turbulence model in order to solve a form of (3.2), for the distributions of velocity and boundary shear stress in straight channels with irregular geometry. This model determines the kinetic energy of the turbulent motion from the transport equation, while the length scale is derived using a simple ramp function to characterize the shear and non-shear layers. The use of this much more sophisticated eddy viscosity model should, in theory, result in improved predictions of velocity and boundary shear distributions in the shear layers near side walls (ASCE Task Committee, 1988). Indeed, comparisons of predicted and observed velocity and boundary shear stress distributions presented by Pizzuto (1991) suggest that his model is capable of predicting accurately the important near bank flows. However, the

computational time required to achieve convergence of the equations using the k-l model is prohibitively high when the model is required to generate data for use as input to the remainder of a much larger width adjustment model. In any case, the much simpler, yet physically sensible, eddy viscosity model (3.6) used by Wark *et al.* (1990) has also been found to give adequate predictions of velocity distributions in natural river channels. The use of the simple eddy viscosity model is also consistent with its common usage in many other numerical models. The final, compelling argument is that uncertainty associated with prescribing the boundary roughness distribution (see below) is anyway so great as to not warrant a more complex approach. Equation (3.6) is, therefore, used here, with the NEV coefficient used as a calibration coefficient. As Shiono & Knight (1990) have explained:

"*Use of the eddy-viscosity model may be criticized on the grounds of its simplicity. However..... the topographically complex geometry, the heterogeneous nature of the boundary roughness and the uncertainty in being able to prescribe boundary roughness coefficients sufficiently accurately for natural river channels....makes a more refined calculation method not only inappropriate but also difficult to calibrate successfully for natural flows.*"

Although the commonly used assumption of steady, uniform flow is reasonable in deriving equation (3.2), the effects of lateral momentum exchange by secondary flows are also neglected (*i.e.* the right hand side of equation 3.2 is assumed to be equal to zero). This assumption is required in order to reduce the shallow water equations to a relatively simple balance between weight, bed frictional resistance and lateral shear associated with the sidewall friction. The validity of equation (3.2), therefore, depends primarily on the relative magnitudes of the lateral momentum exchange by secondary flows and by lateral shear in straight channels, especially within the near bank zone.

Observations of secondary flows in straight channels have been made in a variety of studies (*e.g.* Brundett & Baines, 1964; Perkins, 1970; Gulliver & Halverson, 1987; Markham, 1990), but these have rarely focussed on the crucial near bank zone. The uncertainty in generalising secondary flow distributions in straight channels is underlined by the variable nature of secondary flow magnitudes and directions in straight channels. The only general comment is that secondary flows in straight channels are perceived to be much less significant than secondary circulations in curved channels (Prandtl, 1952; Markham, 1990). This has resulted in the neglect of secondary flows as a common means of simplifying the solution in a variety of applications. More recently, detailed laboratory measurements of flows in straight

channels with over-bank flow have become available as a result of work conducted at the Science and Engineering Research Council Flood Channel Facility (SERC-FCF) located at Hydraulics Research, Wallingford, UK (*e.g.* Knight & Sellin, 1987; Elliott & Sellin, 1990; Knight & Shiono, 1990; Myers & Brennan, 1990; Wormleaton & Merrett, 1990). Shiono & Knight (1990) have unequivocally demonstrated the significance of the secondary flow in the lateral shear layer in over-bank flows in the SERC-FCF. The secondary flow is driven by boundary generated turbulence, free shear layer turbulence and velocity fluctuations associated with perturbations in the longitudinal secondary flow cells. The impact of the secondary flow is, therefore, greatest when the free shear layer turbulence is at a maximum, which is at the point when the flow is just over bankfull (Shiono & Knight, 1990). At such "worst-case" stages, the SERC-FCF data suggest that the magnitude of the lateral shear and secondary flow terms are broadly similar (Shiono & Knight, 1990). It is, therefore, probably safe to assume that momentum exchange by secondary flow is less important than momentum exchange by lateral shear at stages below bankfull. It would seem that lateral shear terms probably dominate the secondary flow terms at these stages, though it is recognised that for over-bank flows the laboratory evidence demonstrates clearly that secondary flows are as important as lateral shear in influencing the distributions of flow and boundary shear stress. The case for neglecting secondary flows at in-bank discharges is strengthened by practical issues associated with the increased complexity and computational effort that would be required to solve the equations if these terms were included in the governing equations.

While the LDM derived by Wark *et al.* (1990) is a considerable simplification of the governing equations, it appears that the assumptions used to neglect some of the more complex terms are reasonable. The careful application of the method within the constraints set by these simplifying assumptions should mean that the powerful predictive ability associated with a rigorous, physically-based method is retained. The use of equation (3.2) is, therefore, perceived as a major advance over methods which do not take into account the lateral shear stresses when calculating the lateral distribution of the flow, such as stream tubes (Molinas *et al.*, 1986; Orvis & Randle, 1986) or Keulegan type splits (Hey, 1979). Indeed the neglect of lateral shear stresses is a well recognised problem of compound approaches to flow resistance, which consequently result in significant over predictions of discharge capacity if no correction is made (Myers, 1978; Wormleaton *et al.*, 1982; Wormleaton & Merrett, 1990). This advance is of fundamental significance in this study, where the aim is to better predict the hydraulics and sediment transport in the near bank zone, because it is in the near bank zone that the lateral velocity gradient and, therefore, the lateral shear stresses are

greatest. For steady, uniform flows at or below bankfull discharge, the lateral shear stresses are probably the most significant factor controlling the lateral distribution of the flow within the near bank zone. Overall, the LDM method represents a relatively simple, yet physically-based method of predicting the distribution of flow in straight river channels at steady, uniform discharges below bankfull stage. It should also be noted that varying discharges through time may still be accounted for using a stepped hydrograph, in which discharges are assumed to be constant in each discrete computational time step.

At each cross-section in the modelled reach, the slope and water surface elevation are required as input data for equation (3.2). These are obtained by using the LDM in conjunction with a simple backwater routine based on the standard step method (Chow, 1973). The total discharge obtained using the LDM is usually not identical to that used to generate the backwater curve, but these differences have been found to be minor. The primary reason for this discrepancy is that the LDM developed by Wark *et al.* (1990) assumes uniform flow and, therefore, uses the longitudinal bed slope as input to equation (3.2). However, the backwater routine solves the water surface profile for gradually varied flow. In these circumstances the longitudinal water surface slope (energy slope) determined from the backwater calculations is used as input to equation (3.2), though the bed slope must still be used to calculate the B_s factor (J. B. Wark, personal communication, 1991).

A major problem in applying the hydraulics algorithm presented above lies in the need to predict the distribution of the Darcy-Weisbach friction factor over the entire channel cross-section. Predictions of the flow distribution are sensitive to the prediction of the boundary roughness. The problem of the predicted distribution of the flow being overly sensitive to the roughness distribution is exacerbated by the tendency of the roughness distributions to be influenced by both the skin friction of the boundary material roughness elements as well as complex form roughness components caused by the flow deforming the boundary, both on the non-cohesive bed (bedforms) and by fluvial erosion of cohesive bank materials (*e.g.* Grissinger, 1982). However, although such dynamic roughness components are expected to be a major feature of the process-form interactions in the near bank zone, present understanding has not yet advanced to the stage where these roughness effects can be accounted for. The Darcy-Weisbach friction factor is, therefore, here simply related to the size of the boundary material roughness elements using an empirical roughness law (Strickler, 1923):

$$n = 0.0151\, d_s^{1/6} \qquad (3.7)$$

where d_s = boundary sediment diameter (mm) and n = Manning roughness coefficient ($f = 8gn^2R^{-1/3}$). Although it is recognised that this formulation is inadequate, it is argued that the form of equation (3.7) does retain the primary process coupling between the boundary material properties and the hydraulic roughness and, therefore, the flow and sediment transport processes. In turn, these may interact to influence the boundary material properties through sediment sorting processes. Form roughness components may be accounted for by varying the coefficient in (3.7).

3.3 SEDIMENT TRANSPORT ALGORITHM

The evolution of the bed topography within the near bank zones, and hence the stability of the bank materials with respect to mass failure and channel widening (section 3.4), may be modelled using the principle of conservation of sediment mass, which is formally written as the sediment continuity equation:

$$\frac{\partial Z}{\partial t} + \frac{1}{1-\lambda}\left(\frac{\partial q_x}{\partial x} + \frac{\partial q_y}{\partial y}\right) = 0 \qquad (3.8)$$

where Z = elevation of the bed (m), t = time (s), x = longitudinal coordinate (m), y = lateral coordinate (m) (Cartesian coordinate system), λ = porosity of the sediment, q_x = total streamwise volumetric sediment transport flux per unit channel width (m^2s^{-1}) and q_y = total transverse volumetric sediment transport flux per unit channel width (m^2s^{-1}). It is, therefore, necessary to relate the unknown spatial distribution of the longitudinal and lateral sediment transport fluxes to the known properties of the bed materials (specified as input data) and the known distribution of the flow (calculated using the hydraulics algorithm detailed above) and near bank geometry.

3.3.1 Streamwise Transport Flux

While many sediment transport theories are available which claim to be able to predict the streamwise transport of sediment in sand-bed streams, it is beyond the scope of this thesis to review the advantages and limitations of individual theories. In any case, such reviews have been made previously by, amongst others, White *et al.*. (1975), Stevens & Yang (1989) and Yang & Wan (1991). In fact, even physically-based sediment transport theories invariably contain some empirical elements in their derivation, so that the predictive ability of any individual transport function varies according to the type of constraints associated with the environment in which it is

applied (Yang & Wan, 1991). The selection of a streamwise sediment transport theory will, therefore, ultimately depend on the type of channel for which the model simulation is to be conducted. In this study, the Engelund & Hansen (1967) sediment transport equation was selected, where:

$$q_x = \frac{q^2 S_e^{1.5}}{20\, g^{0.5} D^{0.5} (SG-1)^2 d_{50}} \tag{3.9}$$

where q_x = total sediment transport rate per unit width (m^2s^{-1}), q = unit discharge (m^2s^{-1}), S_e = energy slope, g = acceleration due to gravity = 9.81 ms^{-2}, SG = specific gravity of sediment, d_{50} = median sediment diameter (mm) and D = flow depth (m). The Engelund-Hansen transport equation was selected for use in this study because it is physically-based, being derived from Bagnold's (1956) energy approach using similarity principles. It is dimensionally consistent and has also been shown to have reasonable predictive ability in natural sand-bed rivers. As well as being a relatively simple sediment transport equation, the Engelund-Hansen equation also uses the unit discharge to represent the flow conditions and is, therefore, consistent with the data generated by the hydraulics algorithm.

3.3.2 Lateral Suspended Load Flux

Einstein (1972) noted that it is not commonly appreciated that suspended load is continuously being deposited against the banks of alluvial channels which transport suspended load. Parker (1978a) suggested that the suspended load is driven towards the near bank zone from the central region by a turbulent diffusive flux caused by a lateral concentration gradient of suspended sediment. That is, a flux of suspended sediment is supposed to be driven down the lateral concentration gradient by the mechanism of turbulent diffusion. Since the concentration of suspended sediment at any point in the channel is a function of turbulent intensity, which is itself dependent primarily on flow depth, a continuous lateral variation of suspended sediment concentration is expected to be the norm in river channels, due to the variation in flow depth across the channel section.

Following Parker (1978a), the magnitude of the lateral diffusive flux of sediment can be written:

$$F_l = \varepsilon_y \frac{\partial \varsigma}{\partial y} \tag{3.10}$$

where, F_l = depth-integrated lateral volumetric flux of suspended sediment per unit width (m^2s^{-1}), ε_y = the lateral turbulent diffusivity coefficient (m^2s^{-1}) and $\frac{\partial \varsigma}{\partial y}$ = depth-integrated lateral concentration gradient of suspended sediment. It is, therefore, necessary to formulate expressions for the lateral eddy diffusivity coefficient and the depth-integrated lateral concentration gradient.

The lateral eddy diffusion coefficient can be considered to be analogous to the coefficient of diffusion of fluid momentum (eddy viscosity), so it is appropriate to seek solutions for ε_y and ε which have a similar form. Parker (1978a) suggested that the simplest justifiable procedure is to set the coefficients equal to constants based on averages of empirically determined data. Using canal data compiled by Simons & Albertson (1963), Parker adopted the expression:

$$\varepsilon_y = 0.13\, U* D \tag{3.11}$$

which is similar to that proposed by van Rijn (1984) where:

$$\varepsilon_y = 0.25\, k\, U* D \tag{3.12}$$

$U*$ = shear velocity (ms^{-1}), D = flow depth (m) and k = non-dimensional Von-Karman constant, here set equal to 0.40. This type of formulation is adopted here because it is simple, yet physically reasonable and different authors appear to give consistent results for the calibration coefficient. To be consistent with the the formulation of the eddy viscosity model employed in the hydraulics algorithm, the value of the coefficients used in equations (3.6) and (3.10) are both set equal to the NEV calibration factor (see section 3.2).

The depth-integrated concentration of suspended sediment is defined by:

$$\varsigma = \int_0^D c\,(z)\,\frac{1}{D}\,dz \tag{3.13}$$

where c (z) = concentration of suspended sediment (ppm) at vertical coordinate, z, and D = flow depth (m). Raudkivi (1989) has presented a detailed discussion of the problems of calculating the vertical suspended sediment concentration profile. Models of sediment suspension such as (3.13) assume that the steady-state, uniform concentration is a function of elevation z only, and independent of the streamwise and

transverse coordinates. Furthermore, continuity of solid and fluid phases must be satisfied and a steady state balance is usually assumed. This implies that at any elevation within the flow the downward convective movement at the fall velocity determined between the weight of the sediment particle and drag of the fluid is balanced by the upward convective velocity due to vertical diffusion of turbulence (Raudkivi, 1989). The concentration can, therefore, be expressed in the form:

$$c(z) = E \exp - \int_0^z \frac{\omega}{\varepsilon_z} \, dz \qquad (3.14)$$

where ω = sediment fall velocity (ms^{-1}), ε_z = vertical eddy diffusivity of the sediment (m^2s^{-1}) (*i.e.* the upward convective velocity) and E = coefficient to represent the entrainment, or reference, boundary condition for the suspended sediment, given by the near bed concentration of suspended sediment. Even assuming that the assumptions used to derive the steady state concentration equation (3.14) are valid, practical problems arise due to difficulties in calculating the fall velocity, vertical eddy diffusivity and threshold concentration boundary condition. The problems associated with specification of the eddy diffusivity values have been discussed previously; to maintain consistency the vertical eddy diffusivity is calculated here using the approximation (Engelund, 1970):

$$\varepsilon_z = 0.077 \, U* \, D \qquad (3.15)$$

The fall velocity is calculated using Stoke's law which assumes that the settling velocity of a single sphere is determined by the balance between submerged weight of the particle and the opposing forces of viscous fluid resistance and inertia effects (Richards, 1982):

$$\omega = \frac{1}{18} d_s^2 (\rho_s - \rho) \frac{g}{\mu_w} \qquad (3.16)$$

where ω = particle fall velocity (ms^{-1}), d_s = particle size (mm), ρ_s and ρ = densities of the sediment and water, respectively (kgm^{-3}) and μ_w = fluid viscosity ($kgm^{-1}s^{-1}$). In reality, the application of equation (3.16) is limited by a number of factors. The fluid viscosity is not a physical constant, but varies according to fluid temperature and is also influenced by the presence of sediment in suspension.

A significant problem with the evaluation of the suspended sediment concentration is in specifying a value of the reference concentration, E, at the boundary. In essence, this boundary condition describes the exchange of sediment between the bed and the suspension. Predictions of the concentration are directly proportional to E, yet E is determined close to the bed, where the rate of change in concentration with elevation is greatest (Raudkivi, 1989). The calculation of E is, therefore, prone to large errors. The reference concentration should be some function of turbulence and pressure fluctuations near the bed, but the details of this process are still ill-defined (Raudkivi, 1989). The approach used most frequently, therefore, is to relate E to mean flow and sediment properties (Garcia & Parker, 1991) in order to use empirical data to fit functional relationships of the type:

$$E = a\left(\frac{U*}{\omega}\right)^3 \tag{3.17}$$

where a = an empirical coefficient determined from a suitable data set. This formulation has been used by a variety of authors (Engelund, 1970; Parker, 1978a) and was adopted in this study because it is dimensionless, physically plausible, yet relatively simple. In view of the well known difficulties associated with the determination of the reference concentration (Raudkivi, 1989) and the empirical nature of all of the formulations available presently, the adoption of a more complicated expression (*e.g.* Smith & McLean, 1977; Itakura & Kishi, 1980; Celik & Rodi, 1984; Van Rijn, 1984) is not justified in the context of this study. A recent data set, compiled from a variety of sources (Ashida & Michiue, 1964; Ashida & Okabe, 1982; Barton & Lin, 1955; Brooks, 1954; Coleman, 1969, 1981; Ismail, 1951; Kalinske & Pien, 1943; Lyn, 1986; Straub *et al.*, 1958; Vanoni & Nomicos, 1960) and published by Garcia and Parker (1991), enabled the coefficient, a, in equation (3.17) to be estimated. Best fit against this data set was achieved with a = 0.0003274.

3.3.3 Lateral Bed Load Flux

It has long been recognised that a lateral bed load component is generated by the gravitational drag on bed load moving in a longitudinal direction along a channel with a side slope (Hirano, 1973; Smith, 1974; Ikeda, 1982ab). The gravitational bed load can be related to the longitudinal bed load using:

$$q_{yb} = \frac{q_{xb}}{\mu} \tan S_y \tag{3.18}$$

where q_{yb} = lateral gravitational bed load flux per unit width (m^2s^{-1}), q_{xb} = longitudinal bed load flux per unit width (m^2s^{-1}), μ = dimensionless, dynamic coefficient of Coulomb friction and S_y = side slope angle (degrees). Equation (3.18) is adopted here for its simplicity, physical plausibility and dimensional consistency. The longitudinal bed load flux is determined from the relation:

$$q_{xb} = q_x - q_{xs} \tag{3.19}$$

where q_{xs} = longitudinal suspended sediment transport flux per unit width (m^2s^{-1}), given by:

$$q_{xs} = q\varsigma \tag{3.20}$$

where q = unit discharge (m^2s^{-1}) and ς = depth-integrated concentration of suspended sediment, determined previously from equations (3.13).

There appears to be some confusion in the literature regarding the physical interpretation of the dynamic friction coefficient, μ, which represents a parameter describing energy loss due to intermittent grain to grain contact which occurs during the transport of sediment over a sediment bed by saltation (Bagnold, 1966, 1973). However, there is some debate over the physical meaning of such a parameter when bed load transport occurs through saltation, when individual particles are rarely in contact with the bed (Sekine & Parker, 1992; Sekine & Kikkawa, 1992). Bagnold (1973) argued, however, that:

"*.....although the energy dissipation during saltation may in part take place directly by fluid friction, both the saltation and accompanying energy dissipation result from the fact of momentary solid to solid contact* ".

In effect, this interpretation replaces the details of motion of individual saltating grains with a bulk formulation based on the average grain velocity tangential to the bed surface, so that the effect of collision of saltating grains with the bed is replaced by a bulk dynamic coefficient of Coulomb friction (Kovacs & Parker, in press). Moreover, the conceptual importance of this interpretation of the dynamic friction coefficient is as follows. The use of transverse bed load relations of the form of equation (3.18) has been criticized by Dietrich & Smith (1984) and Dietrich & Whiting (1989). They argue that in order for a bed load particle to feel the downslope effect of gravity, it must be in

continuous contact with the bed and such relations cannot, therefore, be applied to saltating sediment grains. However, equation (3.18) may be applied approximately to saltating grains when a bulk dynamic Coulomb coefficient is evaluated, based on the mean collisional momentum transfer from saltating grains to the bed, because an individual saltating grain is replaced conceptually by one moving at the mean bed load velocity at some characteristic height above the bed surface (Sekine & Parker, 1992).

Bridge (1983) stresses that this friction coefficient must be interpreted as a dynamic, rather than static, friction coefficient. This emphasis highlights an apparent controversy over the relationship between the dynamic friction coefficient and sediment properties, especially particle grain size. Experiment (Bagnold, 1954; Francis, 1973) and theory (Bagnold, 1954, 1966, 1973) suggest that this dynamic coefficient may be assumed equal to the tangent of the static friction angle of the sediment. Many authors have used the approximation that the dynamic friction coefficient is approximately equal to the tangent of the (static) internal angle of friction, ϕ, of the sediment, which is readily measurable, based on Bagnold's work. However, Bagnold (1973) went on to suggest that typical sand grains have been found to have a friction angle with tangent of about 0.63 (Bagnold, 1973). Although the approximation that the dynamic friction angle equals the tangent of the internal friction angle appears justified, the specification of a *constant* value of μ appears to be untenable. Bagnold (1966) himself, as well as Bridge (1983), noted that μ varies by as much as a factor of 2 with grain size. It is clear that $\mu = \tan \phi$ should be calculated for the bed material under consideration. However, if data for the internal friction angle of the bed material are unavailable, it is recommended that $\mu = 0.65$ is a reasonable approximate starting point for calibration of this variable.

The side slope angle is found by dividing the difference in bed elevations between adjacent flow segments by the width of the near bank flow segment when the flux is directed from the bank zone towards the central flow zone; and when the flux is directed from the central flow segment towards the banks, by dividing the difference in bed elevations between adjacent flow segments by half the width of the central flow segment.

It should be noted that equation (3.18) predicts that the lateral bed load flux is a linear function of the side slope. However, in reality the lateral bed load is a non-linear function of side slope. This non-linearity arises due to the reduction of the threshold of entrainment for sediment grains resting on a slope under the influence of gravity. More recent studies, concerned with applications in channels where there are steep side

slopes (*e.g.* analyses of bank erosion in channels with non-cohesive boundary materials) have attempted to take this effect into account for the cases of both steep side slopes only (Ikeda, 1982ab; Parker, 1984; Parker & Andrews, 1985) and both steep side and bed slopes (Kovacs & Parker, in press). However, this shortcoming does not impose severe limitations on the application of equation (3.18) for the purposes of this study. This is because the linear approximation holds well in cases of low bed and side slopes. In this study side slopes are expected to be low, even in the near bank zones. This is because the sediment transport equations are applied only to the non-cohesive part of the channel boundary, which is the (relatively flat) bed of the channel, even in the near bank zones (Figure 3.2).

3.3.4 Net Lateral Sediment Transport

The net lateral bed material transport flux, q_y, is found by summing each of the lateral sediment fluxes, so that:

$$q_y = q_{yb} + F_l \tag{3.21}$$

In this expression, the lateral sediment transport flux has only two components; the gravitational bed load and the suspended sediment transported by turbulent diffusion. Convective mechanisms of lateral sediment transport are, therefore, neglected.

The neglect of the convective transport of bed load and suspended load by secondary currents can be justified at a variety of levels. First, the magnitude of secondary flow velocities at stages less than bankfull are probably quite small in straight river channels, as discussed previously in section 3.2. Indeed, Parker (1978a) has used this assumption to justify the neglect of secondary flow transport mechanisms in his analysis of lateral sediment transfer processes. Moreover, it is extremely difficult to predict the secondary flow velocity distribution within the pivotal near bank zone (*e.g.* Rais, 1985; Jin *et al.*, 1990; Hicks *et al.*, 1990; Shiono & Knight, 1990; Darby & Thorne, 1993). No attempt to do so was made in the hydraulics algorithm, as discussed in section 3.2. Hence, any attempt to account for the direct influence of the secondary flows on the lateral transport of bed material would, therefore, have to be made through sensitivity analyses by arbitrarily specifying secondary flow velocities and directions on the basis of limited field and laboratory observations (*e.g.* Brundett & Baines, 1964; Perkins, 1970; Gulliver & Halverson, 1987; Markham, 1990). Such an approach was adopted by Darby & Thorne (1992b). Their results indicate that secondary flows have a significant direct impact on the transport of lateral suspended load, with the convective

suspended load flux an order of magnitude larger than the diffusive flux. But lateral gravitational bed load dominates the lateral bed load flux. These results indicate that secondary flows may have a significant impact on the lateral transfer of suspended sediments, but little effect on the lateral transport of bed load.

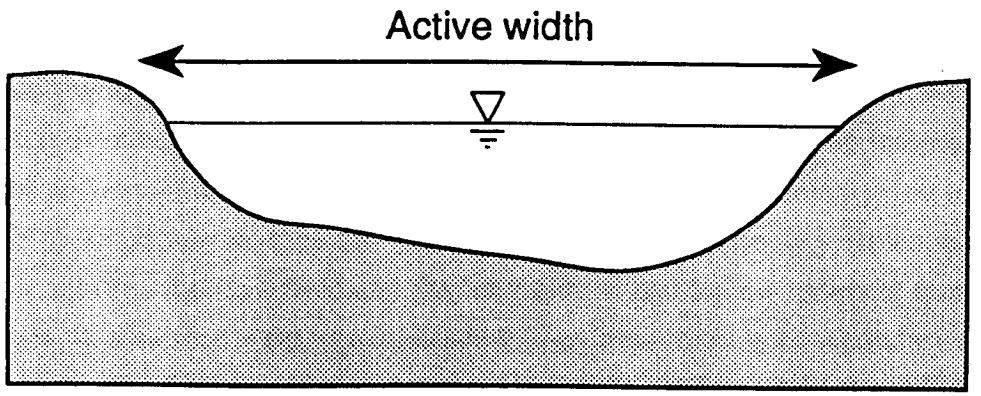

(A) Non-cohesive channel
Active width extends to water margins, where banks are steep (at high flow)

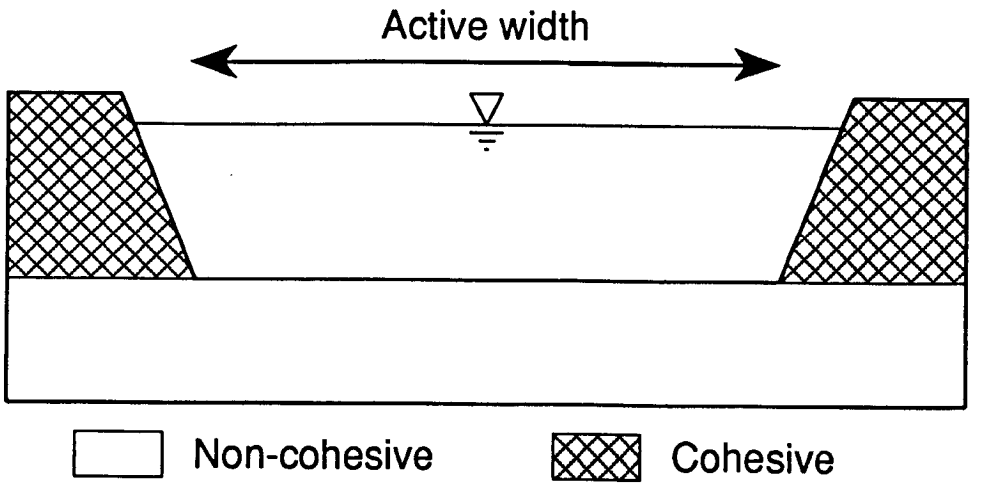

(B) Cohesive banks, non-cohesive bed
Active width extends to base of banks, relatively flat active width zone at all stages

Figure 3.2 Diagram Showing Low Side-Slope Angle on Channel Bed

However, approaches such as these are in fact limited in the insight they shed on the impacts of the secondary flow on dynamic near bank process-form interactions. This is because both the lateral bed load and suspended load sediment transport fluxes

are also strongly coupled to the longitudinal sediment transport fluxes, which in turn are controlled by the flow field. Lateral bed load is directly related to the magnitude of the longitudinal bed load flux, and also the suspended sediment concentration via equations (3.19) and (3.20). The lateral suspended transport flux is also directly coupled to the suspended sediment concentration field via equations (3.10) and (3.13), and these are also a function of the primary flow field. However, the secondary flow field interacts with the primary flow field as described by equation (3.1), influencing the predicted distributions of flow and boundary shear stress. Since the longitudinal transport of sediments responds to the flow field in a highly non-linear fashion, it is reasonable to hypothesize that the indirect impacts of secondary flows on the interactions between the flow field and the longitudinal and lateral sediment transport fluxes may be of a similar order of magnitude to the direct impacts of secondary flows on lateral transport. In these circumstances, sensitivity analyses which exclude the impacts of the secondary flow on the flow hydraulics and longitudinal transport flux field shed little real insight on the sediment transport process-form interactions in the near bank zone. Consequently, it is preferable to maintain consistency between individual algorithms and retain the neglect of the secondary flow effects in both the hydraulics and the sediment transport algorithms.

Nevertheless, it is recognised that the neglect of secondary flow effects is a potentially significant omission from this model and incorporation of these effects is recommended as a topic for future research. Attempts should not only be made to include secondary flow effects in hydraulic models applicable within the near bank zone (Darby & Thorne, 1993), but empirical studies are also required in order to establish the significance of secondary flow effects on flow distributions and both longitudinal and lateral transport processes in natural channels *within the near bank boundary layer.* Meanwhile, for the purposes of this study, it is considered reasonable to assume that the main features of the interactions between the near bank flow and longitudinal and lateral sediment transport fluxes are adequately represented by the hydraulic and sediment transport algorithms developed here, for straight channels with flows at or below bankfull stage with negligible secondary flows.

3.4 BANK STABILITY ALGORITHM

An important component of the near bank sediment balance (Figure 2.6) is the delivery of bank material by direct fluvial erosion of the bank materials together with mass wasting of the bank materials under gravity. Indeed, in situations where the bank materials are rapidly eroding or mass wasting, the bank material flux may dominate the

near bank sediment balance. It is, therefore, important to predict accurately the bank material inflow flux for the given constraints of bank geometry and geotechnical properties observed at any point in time. It is also necessary to update the bank geometry following mass failure accurately, since the bank geometry exerts a considerable control on the distributions of depth and roughness in the near bank zone, which in turn significantly influence the hydraulics and sediment transport process-form interactions in the basal region.

3.4.1 Lateral Fluvial Erosion of Cohesive Bank Materials

The prediction of the lateral erosion of the bank material is important in width adjustment modelling for a variety of reasons. Firstly, lateral erosion exerts an obvious control on the rate of widening at the base of the bank (bed widening), and the associated entrainment of bank materials may contribute directly to the near bank sediment balance, which indirectly influences the stability of the bank with respect to mass failure through its role in influencing the geometry of the bank profile in the basal region. But lateral erosion of bank materials also exerts a strong direct influence on the stability of the bank with respect to mass failure, because lateral erosion results in direct changes in the geometry of the bank profile. Unfortunately, the erosion of cohesive bank materials is a difficult problem (*e.g.* Grissinger, 1982), which has received relatively little attention, compared to the erosion of non-cohesive bank materials.

However, a promising method of calculating the rate and amount of lateral erosion of cohesive bank materials has been developed during laboratory work at the U. S. Army Engineers Waterways Experiment Station (WES) by Arulanandan *et al.* (1980). They found that, once the critical entrainment threshold is exceeded, the rate of lateral erosion (m min^{-1}), LE, is given by a linear surplus shear stress formulation, where:

$$LE = \frac{r}{\gamma}\left(\frac{\tau - \tau_c}{\tau_c}\right) \qquad (3.22)$$

where τ and τ_c = applied fluid and critical entrainment shear stresses (dynes cm^{-2}), respectively, γ = unit weight of the soil (kNm^{-3}) and r = initial rate of soil erosion (gm cm^{-2} min^{-1}), which Arulanandan *et al.* (1980) derived empirically as:

$$r = 0.0223\ \tau_c \exp(-0.13\tau_c) \qquad (3.23)$$

While equations (3.22 and 3.23) are both highly empirical and are not applicable beyond the range of data used in their derivation, the form of these equations appears to be realistic physically. These equations are, therefore, adopted here as the method used to calculate the lateral erosion rate. Indeed, the uncertainty associated with the empirical approach can be perceived as an advantage, allowing for flexibility in the calibration of the channel widening model. However, practical problems in using the method also arise; first, due to uncertainties in predicting the applied fluid shear stress *at the wall*, stressing the importance of modelling the near bank flow accurately; and second, due to uncertainty in predicting the entrainment threshold for cohesive bank material, a notoriously difficult problem (Partheniades, 1965; Grissinger, 1982). The rate of lateral erosion is most sensitive to uncertainty in the two shear stress values when the magnitude of the applied fluid shear is close to the critical entrainment threshold (small values of surplus shear).

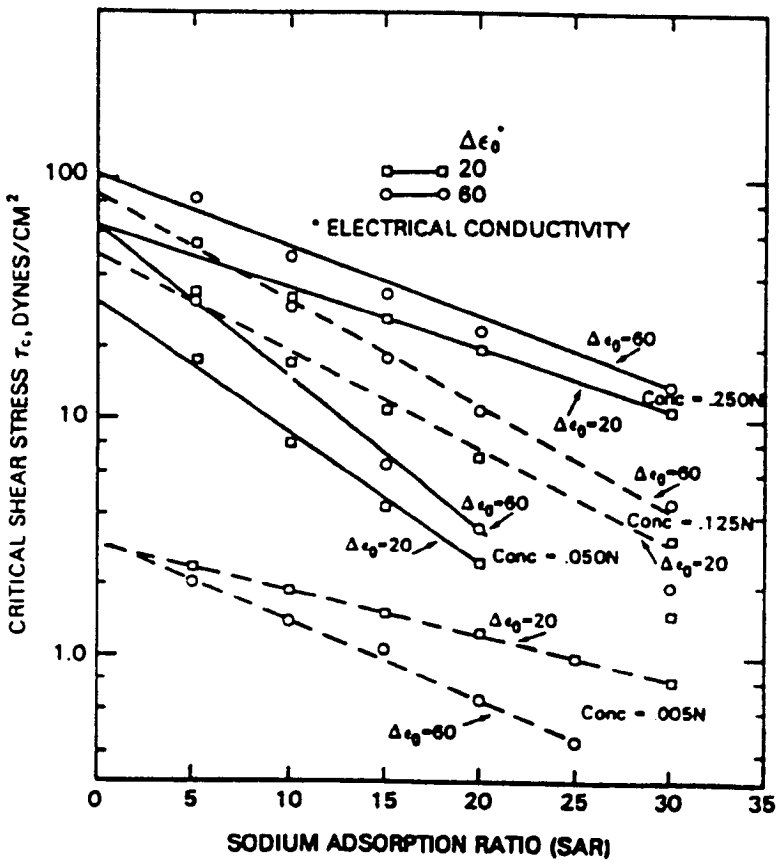

Figure 3.3 Cohesive Bank Material Entrainment Threshold as a Function of Soil Properties (after Arulanandan *et al.*, 1980)

Arulanandan *et al.* (1980) presented an empirical method to estimate the critical stress as a function of sodium adsorption ratio (SAR), pore fluid salt concentration

(CONC), and the dielectric dispersion ($\Delta\varepsilon$) (Figure 3.3). Although this approach makes physical sense, since the resistance of cohesive soils to fluid shear has been shown to depend largely upon the physical and chemical makeup of the soil, and the types and amounts of salts in the pore and eroding fluids (Christensen & Das, 1973; Arulanandan *et al.*, 1980; Grissinger, 1982), the high data requirements and intrinsic uncertainty associated with this empirical approach combine to suggest that a direct measurement of the critical shear stress (*e.g.* using erosion pin monitoring) may be both more convenient and more accurate than the "predictive" method outlined above. The critical shear stress for entrainment of the bank material is, therefore, specified as an input variable, helping to reduce the model data requirements as well as allowing for greater flexibility in model calibration.

The fluid shear stress at the wall may be predicted using the value of the boundary shear stress (term 2 in equation 3.2) at the base of the banks, previously calculated in the hydraulics algorithm. The difficulties associated with accurately predicting the distribution of flow and boundary shear have been discussed in section 3.2.

3.4.2 Erosion of Cohesive Bank Materials by Mass Wasting Mechanisms

Prediction of the volumetric inflow due to mass failure under gravity involves:

(i) Calculating the gross stability (factor of safety) of the river bank, in order to predict when the bank will fail; and
(ii) Predicting the geometry, magnitude and longitudinal extent of the failure block.

Depending on the bank geometry and soil properties, river banks fail by a variety of mechanisms, with a separate analysis required for each mechanism. Various failure mechanisms can be identified, such as rotational, wedge (planar), cantilever, piping or sapping failures and so on.

On large-scale rivers, although cantilever failure mechanisms (*e.g.* Thorne & Tovey, 1981) are very common, they may be assumed to be relatively small and tertiary in nature and can, therefore, be neglected. Piping and sapping type failures (*e.g.* Ullrich *et al.*, 1986; Hagerty, 1991) are also excluded from consideration. Although such water-driven failures are common, they are problematic to analyse and in any case the continued instability of banks subject to piping and sapping processes will also be constrained by the interaction between mass-wasting and fluvial processes. In this

study, only rotational and wedge (Culmann) type failure mechanisms are considered, but this is not a significant limitation for many natural river channels.

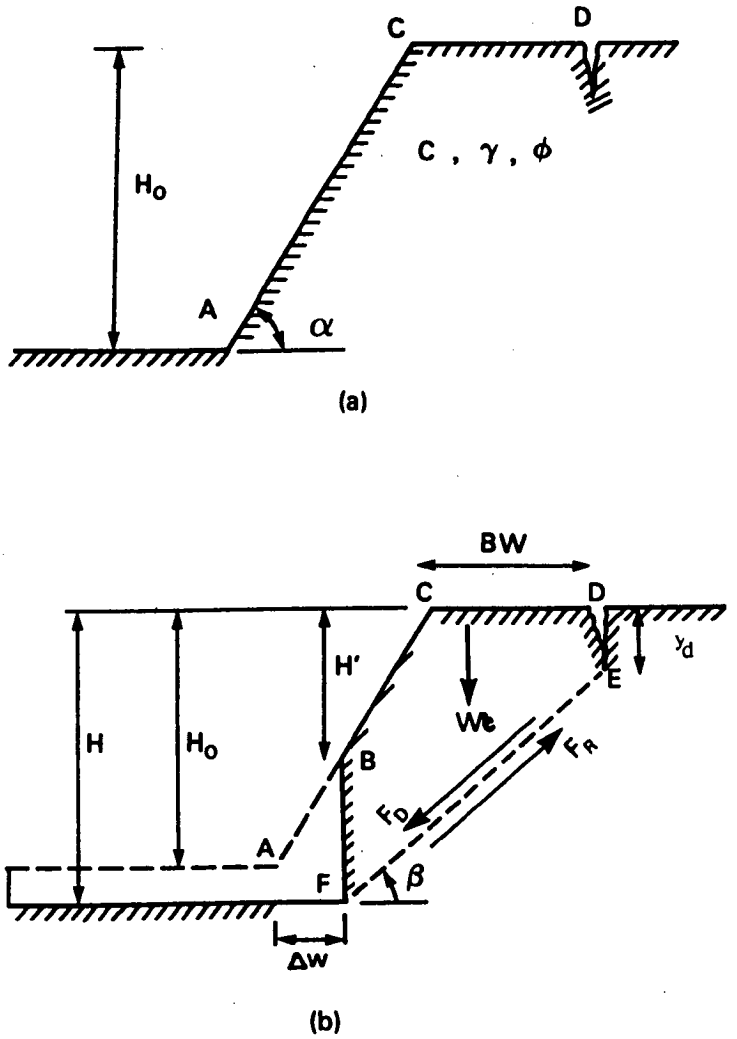

Figure 3.4 (A) Simple Geometry of Planar Failures (B) Geometry of Planar Failures in Osman-Thorne Analysis (after Osman & Thorne, 1988)

For each of the failure mechanisms of interest there are a large number of published stability analyses available to choose from (*e.g.* Taylor (1948), Morgenstern (1963), Lohnes & Handy (1968), Spangler & Handy (1982), Ponce (1978), Siegel (1975), Thorne *et al.* (1981), Ullrich *et al.* (1986), Simon *et al.* (1991)). Most of these studies apply soil mechanics theory to slopes with the simple geometry shown in Figure (3.4a). However, such approaches are limited because they fail to take into account the influence of both toe scour and direct lateral erosion on the geometry and stability of a natural, eroding river bank (Figure 3.4b). Osman (1985) and Osman & Thorne (1988) presented analyses for the stability of rotational slip and wedge type failures,

Plate 3.1 Geometry of Rotational Slip Failure on the Red River, Louisiana

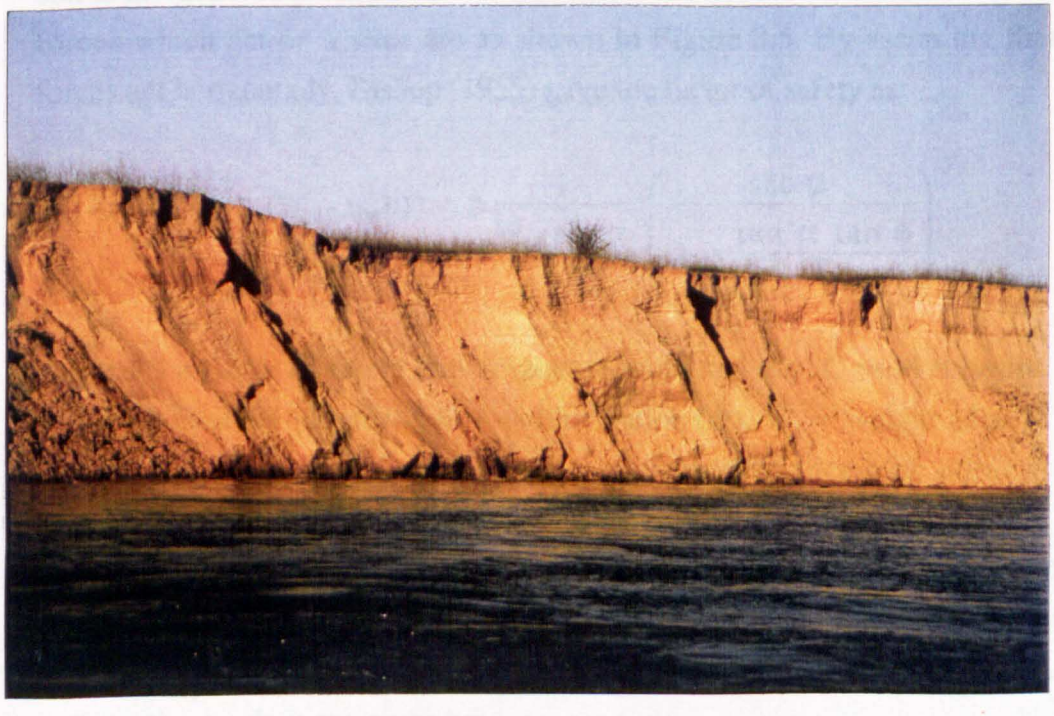

Plate 3.2 Geometry of Planar Slip Failure on the Red River, Louisiana

respectively, which do take explicit account of combinations of toe scour and lateral erosion on the geometry of eroding river banks. These analyses are, therefore, used here as a more realistic framework for predicting bank stability for the purposes of river channel width adjustment modelling.

3.4.2.1 Rotational Slip

Bishop's method of slices (Bishop, 1955) may be applied in order to calculate the factor of safety with respect to failure under gravity by the rotational slip mechanism to the case where eroding river banks have the type of geometry shown in Figure 3.5 and Plate 3.1. In order to simplify the calculations, it is necessary to make certain assumptions about the shape of the failure surface. Here, the failure surface is assumed circular, and is constrained to pass through the toe of the bank. Taylor (1948) has shown that the slices approach yields quite similar results when applied to circular arc and log-spiral failure surfaces, so that it is in any case reasonable to consider only the simpler circular failure surface here.

The factor of safety with respect to mass failure is defined by the ratio of restoring to disturbing moments about the centre of the failure circle. In the method of slices, the soil is divided into a number of vertical slices. If there are no forces along the slope, the forces which act on a slice are as shown in Figure 3.5. By assuming that interslice forces act horizontally, Bishop (1955) gave the factor of safety as:

$$FS = \Sigma Cb + (W_s - u_w b) \tan \phi \frac{1}{W_s \sin \alpha} \left(\frac{\sec \alpha}{1 + \frac{\tan \alpha \tan \phi}{FS}} \right) \qquad (3.24)$$

where FS = factor of safety with respect to rotational slip, C =soil cohesion (kPa), ϕ = soil friction angle (degrees), b = width of slice (m), W_s = weight of slice (kN), α = bank angle (degrees) and u_w = pore water pressure at slice base (kPa). An iterative procedure is required to solve equation (3.24). The shape of the failure surface is important, since it not only determines the factor of safety but, together with the bank profile, the volume of the failure block, V_f ($m^3 m^{-1}$), and the increment of bank top widening, BW* (m) are also set by the failure surface geometry. For a circular failure surface, these values are given by:

$$BW^* = H - \frac{H'}{\tan \alpha} \qquad (3.25)$$

$$V_f = \pi H^2 - \frac{H'^2}{2 \tan \alpha} \qquad (3.26)$$

where H = overall height of the bank (m), H' = height of the uneroded bank face (m) and α = bank angle (degrees).

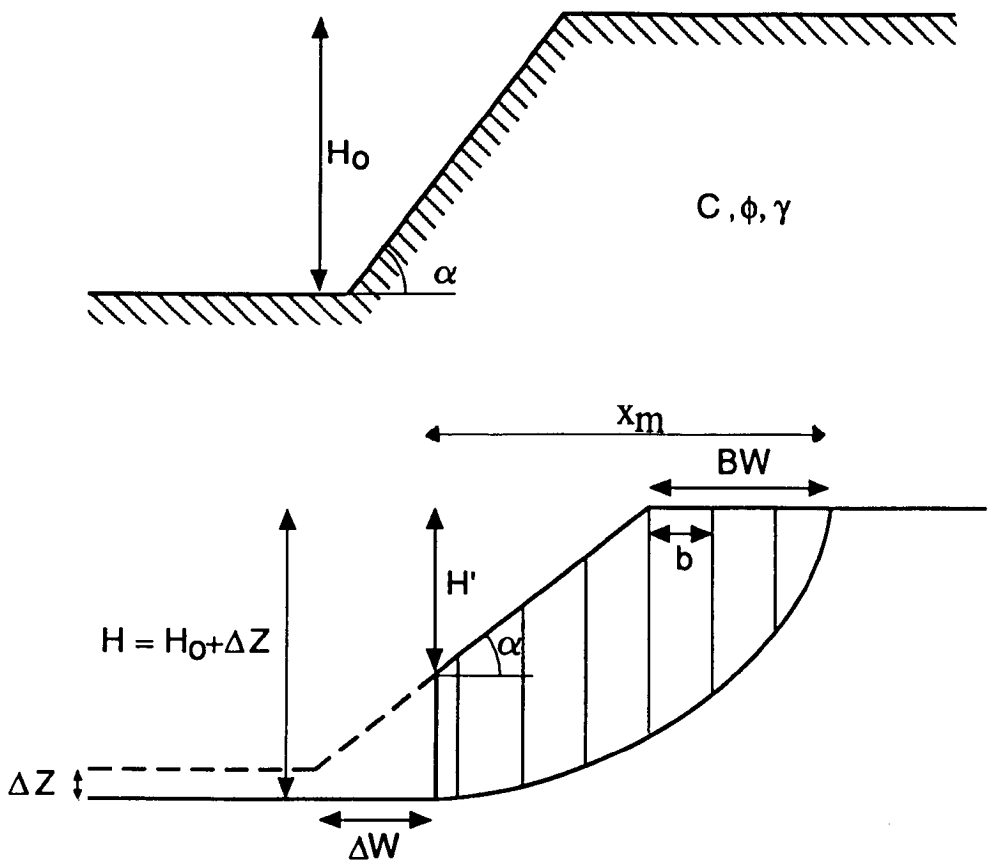

Figure 3.5 Stability Analysis for Rotational Slip Failures

Non-circular slips are associated with heavily fissured materials, the presence of a soft layer low in the bank, multi-layered banks and cases of unusual drainage. These are conditions often encountered in river banks and so it should be expected that methods for non-circular failure surfaces should be more generally applicable than those for circular slip failures (Thorne, 1982). Morgenstern & Price (1965) developed an analysis applicable to non-circular failure surfaces of unknown geometry. Comparisons of the Morgenstern-Price solutions with solutions obtained using Bishop's method show that the two methods produce similar results for circular toe

failures. Similar results are also obtained for non-circular failure surfaces, but the results using the Morgenstern-Price method are more reliable (Thorne, 1982). It seems that approaches which are more complicated than Bishop's simplified solution do yield slightly more reliable solutions, but at the cost of greatly increased complexity and computational effort. The Bishop method is adopted here because it is rationally derived from first principles, adequately describes the mechanism of rotational failure and is reasonably reliable.

3.4.2.2 Planar Failures

Figure 3.4b and Plate 3.2 show the geometry of an eroding river bank, and the forces acting along a potential planar, wedge-type failure surface. In order to predict the stability of the river bank, it is necessary to define a factor of safety (FS) as the ratio of the resisting forces and driving forces acting on the block. Failure is predicted to occur when the factor of safety falls below unity. The driving, F_D, and resisting, F_R, forces are functions of the failure block geometry and soil properties (Osman & Thorne, 1988) so that:

$$F_D = Wt \sin\beta = \frac{\gamma}{2}\left(\frac{H^2 - y_d^2}{\tan\beta} - \frac{H'^2}{\tan\alpha}\right)\sin\beta \qquad (3.27)$$

$$F_R = \frac{(H - y_d)\,C}{\sin\beta} + \frac{\gamma}{2}\left(\frac{H^2 - y_d^2}{\tan\beta} - \frac{H'^2}{\tan\alpha}\right)\cos\beta\tan\phi \qquad (3.28)$$

where Wt = weight of the failure block (kN), H = overall bank height (m), H' = uneroded bank height (m), y_d = depth of the tension crack (m), α = bank angle (degrees), β = failure plane angle (degrees) and C, ϕ and γ are the soil cohesion (kPa), friction angle (degrees) and unit weight (kNm^{-3}), respectively. Osman & Thorne's (1988) contribution was to formulate the above equations for the more realistic geometry associated with natural, eroding river banks depicted in Figure 3.4b. Since the soil properties and bank profile are given as input data, in order to predict the failure block geometry it is necessary to predict the location of the tension crack and the failure plane angle. Taylor (1948) and Spangler & Handy (1982) showed that the failure plane angle corresponds to the plane of fully developed cohesion, on which the stability number is a maximum. In this case the failure plane angle can be found by equating the first derivative of C with respect to β in equation (3.28), to zero (Osman & Thorne, 1988). This leads to:

$$\beta = \frac{1}{2}\{\tan^{-1}[\frac{H}{H'}(1 - K^2)\tan\alpha] + \phi\} \quad (3.29)$$

where K = tension crack index, the ratio of tension crack depth to bank height. Osman & Thorne (1988) suggest the tension crack index may be given as user specified input data and this approach is also adopted here.

Once failure is predicted, the magnitude of the failure block is determined by the failure block geometry, so that:

$$BW^* = \left(\frac{H - y_d}{\tan\beta} - \frac{H'}{\tan\alpha}\right) \quad (3.30)$$

$$V_f = \frac{1}{2}\left(\frac{H^2 - y_d^2}{\tan\beta} - \frac{H'^2}{\tan\alpha}\right) \quad (3.31)$$

where BW^* = width of flood plain bank retreat (m) and V_f = volume of failed bank material per unit channel length (m^3m^{-1}) (Figure 3.4b).

A number of assumptions are needed in order to derive equations (3.27) through (3.31). First, the failure plane is constrained to pass through the toe of the bank. Osman & Thorne (1988) state that other failures were not considered because toe failures are most commonly observed. Simon (personal communication, 1992) and Simon *et al.* (1991), however, stress that this may not be realistic for many types of failure. They have developed a procedure which allows this constraint to be relaxed (Simon *et al.*, 1991). Such an approach is not incorporated into this study, however, due to extra computational effort required, which is particularly problematic when implemented within the probabilistic framework developed below (section 3.4.2.4). Factors such as vegetation, water table, surface runoff and seepage are also not considered directly, though they may be accounted for by calibrating the soil property values. Overall, although there are clearly deficiencies with the Osman-Thorne stability analysis, it is selected for use because it incorporates a more realistic bank geometry, it is physically-based and appears to give reasonable predictions for a range of natural river banks (*e.g.* Thorne, 1989; Darby & Thorne, 1992a). Perhaps the most significant limitation is the failure to account explicitly for the influence of river bank hydrology on stability with respect to mass failure. This is discussed in the following section.

3.4.2.3 Hydrological Impacts on Bank Stability

Several investigators have emphasised the importance of interactions between the hydrology of the riparian zone, soil properties and the stability of the bank with respect to mass failure. Various researchers have reported the impacts of piping and sapping on mass instability (Ullrich *et al.*, 1986; Hagerty, 1991), but mass failures are also frequently observed to occur during or after the recessional limb of storm hydrographs when the bank is saturated, positive pore pressures have been generated and the confining pressure of the water in the stream has been removed (Thorne, 1982; Simon *et al.*, 1991). In such cases, although fluvial processes are responsible for the erosion of the bank close to the critical conditions, the trigger for the mass failure is the abrupt change in driving and resisting forces as a consequence of the rapid change in flow stage and hydrological status of the river bank. Such water driven "worst-case" scenarios are a particularly significant control on mass instability along streams in West Tennessee (Simon, 1989; Simon & Hupp, 1992, Simon, personal communication, 1992). One of these streams is used later in this research in an attempt to validate the model developed here (see Chapter 4). It is clear that some attempt must be made to account for the interaction between the flow, hydrological conditions of the bank, bank material properties and stability with respect to mass failure. This is particularly important with respect to the analysis of the impact of flow variability on channel adjustment.

To account for the combined impacts of rapid drawdown on reduction in bank material shear strength through positive pore pressures together with removal of the confining pressure of the flow on the bank, an attempt was made to formulate a "drawdown" parameter and relate this parameter to the bank material properties. The worst case scenario is a very rapid reduction in flow stage from a saturated bank condition. Rapid reductions in flow stage are required to generate worst case conditions because there is a time lag between rate of reduction of flow stage and de-saturation of the banks. In these circumstances, the removal of the confining pressure of the water in the channel coincides with saturated banks with positive pore water pressures. In such cases, the frictional component of the soil shear strength will tend to zero. Since a significant component of the shear strength of many alluvial soils is the frictional component, failure is likely under such conditions (Simon & Hupp, 1992). It is, therefore, physically plausible to relate the drawdown parameter to the internal friction angle of the soil, in order to account for the impact of changes in flow stage (controlled by the catchment hydrology) on fluctuations in the distribution of the pore water and confining pressures acting on the incipient failure block. In effect this approach

represents the influence of the variation in these forces on the factor of safety and the stability of the bank by calculating variation in soil shear strength.

It may be hypothesized that the important factors influencing bank hydrology-induced changes in soil shear strength and bank stability with respect to mass failure are the rate and amount of drawdown (influences incidence of positive pore water pressures) and the fraction of the bank height supported by the flow (directly proportional to the confining pressure exerted by the water on the bank). Using daily stage and discharge records, it is not necessary to explicitly account for the rate of drawdown, since this is determined implicitly by the daily change in stage. Using such data, a drawdown parameter may be formulated, such that an increase in the numerical value of the drawdown parameter represents a decrease in the stability of the bank:

$$\varphi = \frac{\Delta E}{h_f} \tag{3.32}$$

where φ = daily drawdown parameter (m), ΔE = daily reduction in flow stage elevation (m) and h_f = dimensionless ratio of flow depth to bank height. Thus, high values of φ correspond to cases where large and rapid drawdown rates (generation of positive pore pressures) are combined with low flow depths (low confining pressure). In instances where a value of less than zero is predicted (when flow stage rises), the procedure is to set φ to zero, reflecting the decrease in positive pore pressures and increase in confining pressures, independent of the absolute magnitude of the stage. This formulation of the drawdown parameter assumes that the hydrological status of the bank is coupled only with the flow stage. This is discussed below. The daily drawdown parameter may be calculated for each day of the model simulation using daily stage-discharge records. The daily drawdown parameter may then be non-dimensionalized by dividing by the maximum daily drawdown parameter, φ_{max}, for the period of record, so that:

$$\varphi^* = \frac{\varphi}{\varphi_{max}} \tag{3.33}$$

where φ^* = dimensionless drawdown parameter. It is necessary to non-dimensionalize the drawdown parameter in order to ensure dimensional consistency in equation (3.34), below. To account for the impact of changing hydrological conditions on the soil shear strength and bank stability, the friction angle of the soil (degrees) is modified by relating the "average" friction angle to the drawdown parameter using:

$$\phi = \phi_o \, a_1 \, (b_1 - \exp(-c_1 \varphi^*)) \tag{3.34}$$

where ϕ_0 = "average" soil friction angle for dry bank material (degrees) and a_1, b_1 and c_1 are constants. Thus, the soil friction angle is reduced from its average value as an exponential function of the dimensionless drawdown parameter. A friction angle equal to zero may be assumed to correspond to the worst case dimensionless drawdown parameter ($\varphi^* = 1.0$) and the best case dimensionless drawdown parameter ($\varphi^* = 0$) corresponds to the dry soil, average friction angle ϕ_0. These conditions, together with the choice of the constant c_1, determine the shape of the exponential curve and allow the constants a_1 and b_1 to be determined. A value of $c_1 = 1$ gives rise to a relatively long exponential tail. This may lead to an overly sensitive relationship between friction angle and dimensionless drawdown parameter when there is an extreme value of the maximum drawdown parameter, φ_{max}, used to non-dimensionalize the drawdown parameter. To avoid this problem a value of $c_1 = 0.25$ was chosen arbitrarily for this study. This leads to the adoption of the following expression relating the drawdown parameter to the soil friction angle:

$$\phi = \phi_0 - 4.52081\,(0.7788007 - \exp(-0.25\varphi^*)) \qquad (3.35)$$

Although there are no data available either to lend support to, or refute, equation (3.35) it is thought that this equation reasonably accounts for the influence of hydrologically controlled bank instability mechanisms. It is also recognised that the flow stage is the sole variable representing the influence of all the various factors controlling bank hydrology driven failures at a site in this formulation. This is despite the fact that critical instability conditions may be generated by positive pore pressures in bank materials saturated by localised incidences of heavy rainfall, rather than flow stage fluctuations. However, flow stage is a good surrogate variable, since stage is well correlated with rainfall on all but the largest scale river catchments and the use of equation (3.35) is, therefore, justified in the context of this study. Overall, the use of equations (3.32) through (3.35) represents a physically reasonable method of accounting for the influence of stage fluctuations on the hydrological status of the bank and bank material strength as well as accounting for the confining pressure of the water acting on the bank. Incorporating these effects into the numerical channel widening model in this way allows the significance of these interactions on channel adjustment to be established using sensitivity analyses and numerical experiments, even though the detailed physics of the these processes are not explicitly accounted for.

3.4.2.4 Probabilistic Approach to Mass-Wasting Computations

In addition to inevitable concerns over the ability of individual bank stability algorithms to predict reliably the stability of the bank and the geometry of mass failures, much more serious and fundamental problems arise when using the Osman-Thorne bank stability equations, or any similar 2-dimensional analysis, for the purpose of morphological modelling. In a numerical model of width adjustment that uses the concept of basal endpoint control, the aim is to predict all of the sediment fluxes shown in Figure 2.6 and then use these fluxes to solve the sediment continuity equation through time in order to predict the evolution of channel morphology. Unfortunately, the bank stability theory reviewed above becomes difficult to apply when the requirement is to estimate a bank material inflow *flux* within a numerical modelling framework, for two closely related reasons.

The first problem is that such bank stability models are threshold models. Mass failure is predicted to occur instantaneously when the factor of safety falls below some critical value. Hence, the delivery of bank material to the reach by mass failure is conceptually viewed as a discrete, rather than continuous, process. It is, therefore, impossible to calculate a meaningful time-averaged rate for the delivery of failed bank material. In theory, the time rate of delivery of failed bank material is infinite if the failure is instantaneous. Consequently, it is impossible to solve the sediment continuity equation numerically. In practice, previous width adjustment models have circumvented this problem by simply averaging the volumetric inflow of bank material over a computational time step in order to obtain the bank material flux, with the constraint that the chosen time step be relatively small, in order to allow short period changes in bank stability (threshold responses) to be "caught" by the model (Osman, 1985). The problem is that the predicted bank material flux is entirely dependent upon the length of the arbitrarily chosen computational time step. This is to some extent an unavoidable problem associated with this type of numerical modelling. But since the volume of bank material associated with an individual mass failure is anyway quite large, the use of a short time step results in the prediction of a bank material flux perhaps orders of magnitude larger than the remaining fluxes contributing to the near bank sediment balance (Figure 2.6). Such a large flux may still result in problems with the numerical solution of the sediment continuity equation. Discussions with Osman's PhD supervisor revealed that that the overly-large predicted bank material flux dominated the response of the near bank zone to the extent that, after initial failure was predicted, the modelled flows were unable to transport the bank sediment away so that Osman was unable to simulate sequences of bank failures with his channel widening model.

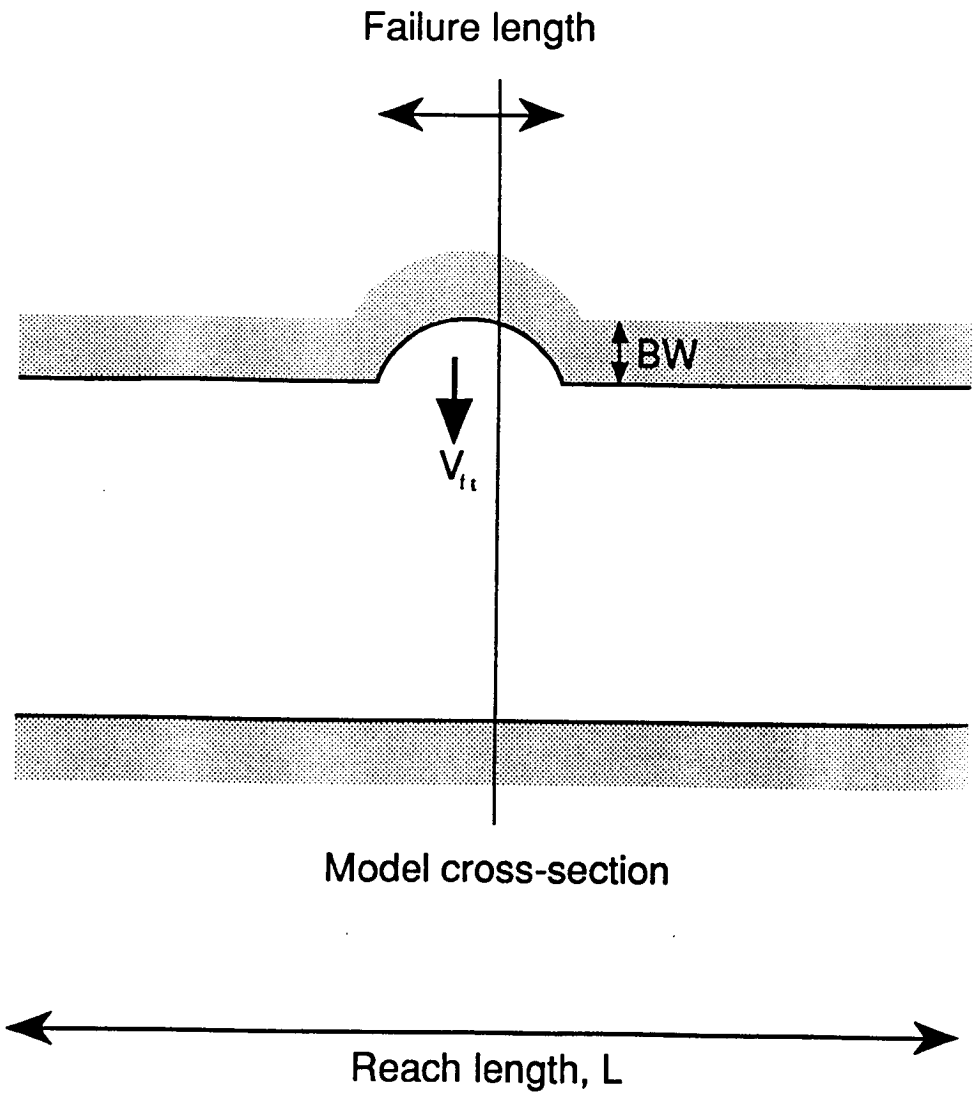

Figure 3.6 Diagram Showing Relative Scales of River Reach and Mass Failure

The second, somewhat related, problem is that within the domain of a discretized numerical model, the bank stability is necessarily calculated at only a finite number of computational nodes (model cross-sections). The bank stability predicted at that *point* is assumed to be representative of the *reach* that the cross-section is supposed to represent (Figure 3.6). The consequence of this assumption is that, in order to calculate a volumetric influx rate due to mass failure along the length of a reach, it is necessary to integrate the unit failure volume obtained from the 2-dimensional bank stability calculations described previously along the length of the model reach, so that:

$$V_{ft} = \frac{V_f L}{\Delta T} \tag{3.36}$$

where V_{ft} = total potential volumetric bank material inflow flux due to mass failure (m^3s^{-1}), L = length of the reach (m), V_f = unit volume of failed bank material (m^3m^{-1}), as defined by equation (3.31) and ΔT = chosen time step over which the total volumetric inflow of mass failure products is time averaged (s). So, when failure is predicted at a computational point, a uniform failure along the entire reach is assumed to occur instantaneously, resulting in a sudden and large sediment input to the reach which may not only shock the sediment continuity computations and cause numerical instability, but is in any case unrealistically large.

Plate 3.3 Discontinuous Banklines Along Eroding Creek, northern Mississippi

The predicted volumetric inflow is overly large because in reality the frequency, or probability, of individual *localized* river bank failures within the reach is observed to progressively increase as the banks along the reach are destabilized by fluvial erosion. Rarely, if ever, are single mass failures observed over bank lengths of more than a few metres or tens of metres, even along the world's largest rivers. Yet numerical models of river morphology commonly use grids where the nodes are spaced at intervals of hundreds or thousands of metres. It is clear that the scale of the river reach will usually be at least an order of magnitude larger than the scale of an individual mass failure. Consequently, the bank material inflow rate determined using equation (3.36) will represent an unrealistically large maximum possible value which may be termed the "potential" bank material flux. Similarly, since not all of the banks along the reach will

fail, the flood plain widening increment determined using equation (3.30) also represents a maximum "potential" value, BW*. Moreover, it is apparent that mass failure under gravity cannot be viewed as a threshold phenomenon at the scale of the river reach. Rather, it may be hypothesized that the inflow of bank material in response to mass failure under gravity is analogous to the entrainment of sediment in the process of bed material transport, in which it is now recognised that local variations in turbulent stresses and sedimentological parameters make it impossible to identify a single entrainment "threshold" (Einstein, 1950; Begin & Schumm, 1984; Naden, 1987; Richards, 1990). Indeed, observations of bed load transport in flumes and natural river channels confirm that the entrainment of bed material occurs over a band of flow conditions, rather than at a single, critical, flow (Cheetham, 1979). The typically discontinuous nature of banklines when viewed in plan (Plate 3.3) at the scale of the reach may be analogous geomorphological evidence of micro-scale variations in the controls on bank retreat observed within reaches.

Table 3.1 River Bank Soil and Geometry Characteristics at Varying Scales

SCALE	LENGTH (km)	SOILS	GEOMETRY
Micro (Single Failure)	< 0.05	Homogeneous (Low Variability)	Uniform
Meso (River Reach)	0.1 - 10	Heterogeneous	Uniform (Low Variability)
Macro (River Basin)	> 10	Heterogeneous	Non-Uniform

The problems associated with this type of scale dependent causality are well recognised by geomorphologists (Schumm & Lichty, 1965) and in a variety of fields where a primary concern of numerical modellers has been to account adequately for the influence of micro-scale process mechanisms which "fall through" the computational mesh used to analyse meso or macro-scale system response. Examples include the well known difficulties associated with turbulence modelling in hydraulics and the failure to account for clouds in Global Climate Models (GCMs) in meteorology (Jones & Henderson-Sellers, 1990; Henderson-Sellers, 1991). It is clear that controls on bank retreat operating at the micro-scale must be taken into account if the influence of these controls on the response at the larger, reach-scale is to be adequately represented in the

channel widening model. Some kind of modifying function is required in order to represent the influence of micro-scale controls on meso-scale response so that the overly large and sudden predictions of the onset of mass instability obtained by mis-applying "at-a-site" 2-dimensional, threshold bank stability theory at the scale of the river reach may be reduced. This will enable the reach-scale time-averaged bank sediment volumetric inflow rate and failure block widths to be better predicted, in order to reflect more realistically the sequence of events observed in nature at the scale of the river reach.

In order to achieve this aim it is first necessary to identify the dominant controls on mass wasting at both the scale of the computational grid (the river reach) and at sub-grid scales. The bank stability theory detailed in the preceding sections indicates that the stability of a river bank with respect to mass failure under gravity is determined by the constraints of the bank geometry and the geotechnical properties of the bank materials, which together determine the driving and resisting forces acting upon the incipient failure block. Table 3.1 illustrates the ways in which these variables are hypothesized to influence the application of bank stability theory as the spatial scale increases. At the micro-scale, or the scale of an individual mass failure, the bank geometry can be considered uniform along the length of the failure. Similarly, although some small degree of local statistical variation in soil properties is to be expected, the bank materials can also be considered homogeneous at this scale. However, at the meso-scale, that is the scale of the river reach, the geometry of the bank is observed to be somewhat more variable over the length of the bank line, though it can still be considered to be near uniform. In contrast, observed variation in geotechnical properties at the scale of the river reach is commonly so great that the bank materials must be characterised as heterogeneous, as evidenced by Figure 3.7. This diagram illustrates the observed variation in bank materials along reaches of largely similar streams in western Tennessee. It is seen that the geotechnical properties at this scale can be characterised using frequency distributions determined by measurement. At the macro-scale it may be hypothesized that both the bank geometry and the geotechnical properties of the bank materials are essentially heterogeneous.

It is clear that the fundamental problem lies in mis-application of the 2-dimensional bank stability theory, which was designed to predict the stability of the bank over a relatively small length of bank over which the geometrical and geotechnical properties controlling the stability of the bank can reasonably be considered uniform. The numerical modelling approach requires application of the bank stability theory over a much larger spatial extent - the model reach - in which the geotechnical, if not the

geometrical, properties cannot be expected to be uniform. Indeed, the heterogeneity of natural alluvial soils, even at relatively small spatial scales, is well recognised. Table 3.1 shows that at the scale of interest - the river reach - variability in soil properties is so much greater relative to variability in the geometry of the bank that it can be hypothesized that the observed variation in stability with respect to mass failure under gravity along a river reach is due entirely to the statistical variation in the properties of the soils within that reach.

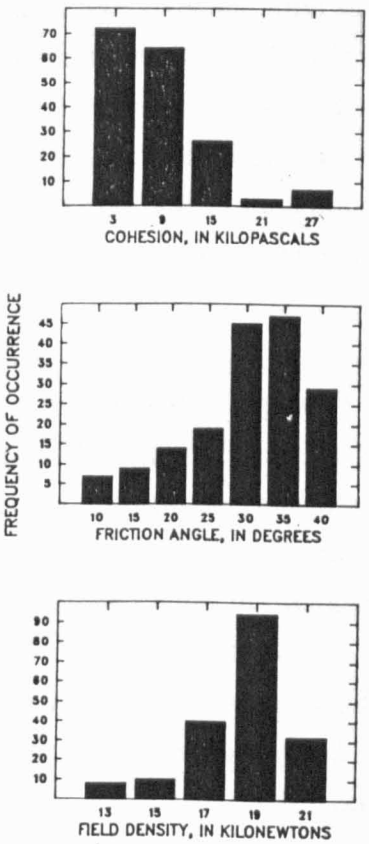

Figure 3.7 Geotechnical Soil Property Frequency Distributions (after Simon, 1989)

It follows that it is possible to obtain more realistic predictions of reach-scale stability with respect to mass failure by putting the deterministic bank stability theory reviewed in the preceding sections into a more probabilistic framework, so that the influence of the observed statistical variations in the soil properties along the reach on the factor of safety can be taken into account. In this way the new approach allows the variability in geotechnical properties, which are assumed to control the micro-scale

variation of stability along the reach, to be coupled with the meso-scale geometry in order to more realistically model the influence of sub-grid scale controls on river bank stability and the response of the reach as a whole. Physically, this integration up to a larger space scale also allows the discrete inflow of bank materials traditionally associated with at-a-site scale "threshold" instability to be smoothed out so that the new method can be used to define a true influx rate for bank material which fails by mass wasting mechanisms. This is because the probabilistic framework does not allow prediction of where an individual failure within the reach will occur, except at a statistical level, so that the total predicted volume of bank material products for the reach as a whole may be averaged over the time step to give the total time averaged inflow rate. The hypothesis that the observed variation in bank stability along a river reach is due entirely to spatial variation in the geotechnical characteristics of the bank materials implies that it is reasonable to assume that the reach-scale geometry is uniform. This is anyway required within the conceptual framework of a numerical model in which cross-sections are chosen to characterize the morphology of individual reaches.

The development of a probabilistic approach is also consistent with previous attempts to characterise the risk of mass failure by producing curves of bank stability for "worst case" and "average" soil property values which change in response to soil moisture variation (Thorne *et al.*, 1981; Thorne, 1988) (Figure 3.8). Under the probabilistic framework developed here, the stability of the bank is characterised by defining a probability of failure for the bank along a reach, with this probability defined as being equal to the probability that the factor of safety with respect to mass failure is less than unity. This latter value can be calculated by computing all factors of safety possible for the given constraints of the reach bank geometry, and the soil property frequency distributions within that reach.

The procedure for calculating the overall probability of failure for both rotational slip and slab type failure mechanisms is as follows. The first step is to determine the frequency distributions for each of the soil properties: cohesion, friction angle and unit weight. By dividing each continuous frequency distribution into discrete classes, it is possible to define a finite number of combinations of soil properties, with representative values of each of the soil properties for each class. Each of these combinations, together with the reach-scale geometry, may be directly applied in the bank stability theories detailed in sections (3.4.2.1 and 3.4.2.2) to determine the factor of safety for that individual combination of soil properties. However, in the analysis of slab type failures, this does require some minor modification, since it is necessary to

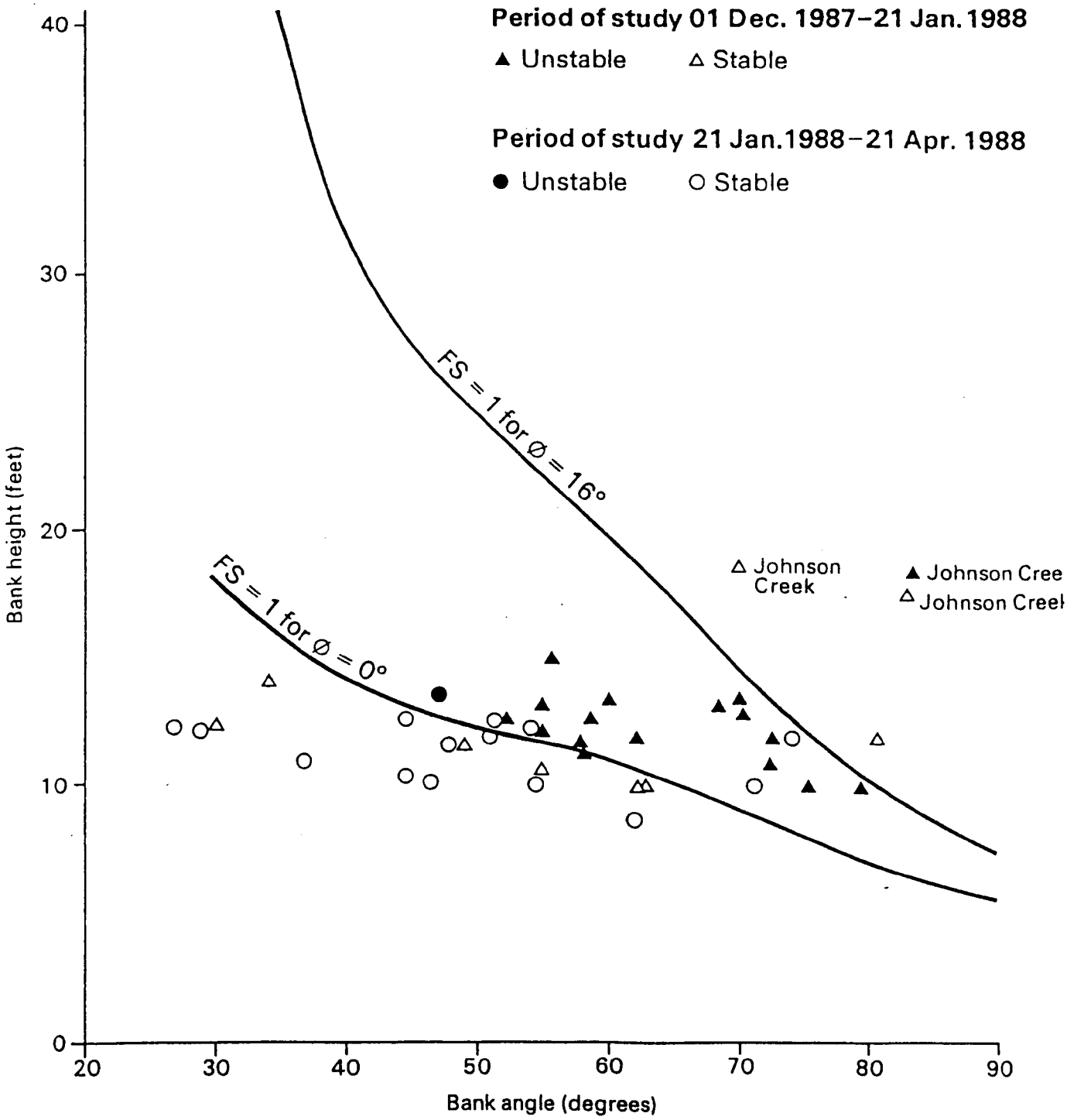

Figure 3.8 Diagram Showing Predicted Factor of Safety for Worst Case and Average Soil Conditions (after Thorne, 1989)

predict the failure plane angle as a function of the bank geometry and friction angle (equation 3.29). In order to simplify the prediction of the failure plane angle and retain a uniform reach-scale failure block geometry, the influence of statistical variation in friction angle on the predicted failure plane angle is ignored herein. Instead, the modal friction angle is used in equation (3.29) to determine the failure plane angle.

The probability of occurrence of an individual factor of safety, P(FS) can be equated to the probability of occurrence of the soil property combination that gives rise to that particular factor of safety given the constraints of the specified bank geometry. Thus:

$$P(FS) = P(C) * P(\phi) * P(\gamma) \tag{3.37}$$

where P(FS) = probability of the predicted factor of safety for an individual soil property combination, P(C) = probability of the cohesion being in the class represented by the value, C, and $P(\phi)$ and $P(\gamma)$ = probabilities of the friction angle and soil unit weight being represented by the values ϕ and γ, respectively. The probability of occurrence of an individual soil property class is calculated from the frequency distributions for each soil property. If the individual factor of safety calculated using equation (3.37) is less than unity, then failure is predicted for that combination of soil properties. If failure is predicted, this probability is stored while computations proceed through all the other possible combinations of soil properties. Finally, the overall probability of the reach-scale factor of safety being less than unity is found from the sum of all the previously calculated probabilities corresponding to individual factors of safety of less than unity, so that:

$$RP(FS<1) = \sum_{i=1}^{i=i} P(FS<1) \tag{3.38}$$

where RP(FS<1) = reach-scale probability of failure, and P(FS<1) = probability of an individual factor of safety being less than unity. The probability of failure may be calculated for both rotational slip and slab type failure mechanisms, using the algorithms detailed in sections 3.4.2.1 and 3.4.2.2, respectively.

Banks along an individual reach are constrained to fail by a single failure mechanism, so that in the event of a non-zero probability of failure being predicted it becomes necessary to choose the appropriate mechanism of failure prior to updating the

bank geometry. The criterion used in the bank stability algorithm developed here is to select the failure mechanism with the highest probability of failure.

The probabilistic method may then be used to obtain more realistic predictions of the flood plain widening increment and volumetric inflow of bank material associated with mass wasting in the following way. The probability of failure occurring along the reach may be assumed equal to the fraction of the reach that actually fails, so that the "potential" bank flux and flood plain retreat increments determined from equations (3.30), (3.31) and (3.36) (slab failure) and equations (3.25), (3.26) and (3.36) (rotational failure) can now be modified to give the more realistic values:

$$V_m = RP(FS<1)\ V_f \tag{3.39}$$

and

$$BW = RP(FS<1)\ BW* \tag{3.40}$$

where V_m = total mass failure bank material influx per unit length of reach (m^2s^{-1}) and BW = reach-averaged flood plain widening increment (m).

Following failure, the bank geometry must be updated using a reach-averaged updating scheme, so that the uniform reach-scale geometry is maintained. In the case of rotational slip, the reach-scale geometry is updated using:

$$H = H \tag{3.41}$$

$$H' = (H' (1-RP(FS<1)) + (H\ RP(FS<1)) \tag{3.42}$$

$$\alpha = \tan^{-1}\left(\frac{H}{x_m + BW}\right) \tag{3.43}$$

where x_m = distance defined in Figure 3.5 (m). For planar failures, the bank geometry is updated using:

$$H = H \tag{3.44}$$

$$H' = (H' (1-RP(FS<1)) + (H\ RP(FS<1)) \tag{3.45}$$

$$y_d = (y_d (1-RP(FS<1)) \tag{3.46}$$

$$d_t = (d_t\ (1\text{-}RP(FS<1)) \quad (3.47)$$

$$\alpha = (\alpha\ (1\text{-}RP(FS<1)) + (\beta\ RP(FS<1)) \quad (3.48)$$

The computational procedure used to calculate the probability of failure and update the bank geometry is summarised in Figure 3.9.

It is noteworthy that this probabilistic approach does not require any assumptions to be made concerning the frequency distributions of the alluvial soils properties. In fact, these distributions may be determined by repeated measurements of soil properties in the field over the scale of the river reach. This was actually precisely the procedure used to construct Figure 3.7. In effect, the new approach takes account of the observed variations in soil properties deterministically, emphasising that the method is not a stochastic method of predicting the stability of river banks. However, construction of the soil property frequency distributions does require an intensive data collection programme. An interesting topic for future research might be to establish more general rules governing the frequency distributions of soil properties in order to reduce the high data collection requirements. However, no attempt to do so was made in the course of this research because, for the purposes of this research, it was only considered necessary to investigate the effects of varying *specified* soil frequency distributions on the response of the model using sensitivity analyses. This enables their significance to be assessed without introducing the inevitable uncertainty associated with assumptions that would be needed to generate "theoretical" soil frequency distributions into the analysis.

3.5 MODELLING THE BASAL ENDPOINT STATUS: DYNAMIC INTERACTIONS BETWEEN BANK MATERIAL SUPPLY AND BED MATERIAL TRANSPORT IN THE NEAR BANK ZONE

Following mass wasting or fluvial erosion, quantities of bank materials are delivered to the channel in the basal region of the near bank zone. Basal endpoint control, outlined in section 2.4 emphasises the importance of the interaction between the rate of supply of bed and bank sediments to the near bank zone and their transport away from the basal region. This balance controls the geomorphic response of the near bank basal region and, consequently, the bank geometry, stability and migration rate of the river bank (Figure 2.6). Although methods of calculating the bed and bank material sediment fluxes which determine the status of the basal sediment budget within this

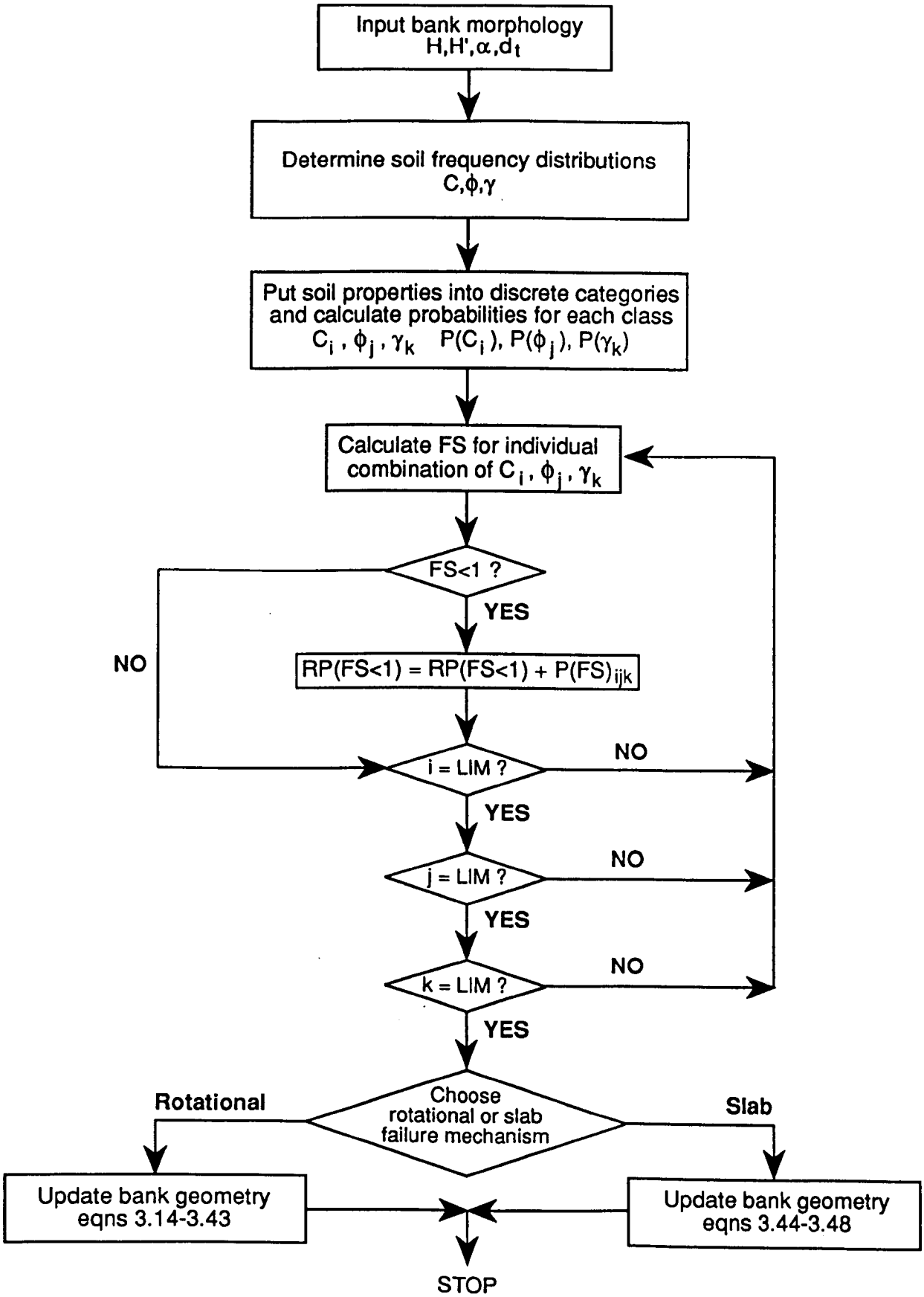

Figure 3.9 Algorithm for Calculating Probability of Mass Failure and Updating Bank Geometry

near bank zone have been presented in the preceding sections, these methods take no account of the impact of the changing hydrological, hydraulic and sedimentological conditions on the near bank sediment fluxes as bank material is supplied to the near bank zone and as the channel morphology adjusts through time according to the governing constraint of the conservation of sediment mass.

In general, previous morphological models have accounted for these interactions by solving the sediment continuity equation (3.8) numerically, and integrating through time by updating the morphology and sedimentological characteristics, boundary roughness and flow and sediment transport characteristics at the end of each discrete time step. However, most previous morphological models have not accounted for the inflow of bank materials and changing channel width through time. Even the few available width adjustment models have made only crude attempts to address the continuity of the failed bank materials. Usually, it is assumed that once bank material is entrained, it is directly transferred to wash-load (Osman, 1985; Alonso & Combs, 1986; Borah & Bordoloi, 1989). It is apparent that if the dynamics of the process-form interactions in the near bank zone are to be modelled successfully, continuity of the bank materials must be maintained as rigorously as the continuity of the bed materials. Simon *et al.* (1991) also stress that maintaining the continuity of the bank materials is a paramount consideration in the development of a physically-based, deterministic channel widening model which simulates widening by coupling bed evolution and bank stability algorithms. This is because following mass failure, it is necessary to transfer the failed bank materials between the mass-wasting algorithms and the sediment transport equations. By allowing a given volume of failed bank material to be updated conceptually as one of either bank material, bed material, bed material load or wash load in any given time step, the continuity of sediment is maintained. However, the transfer of the bank material into the various transport modes is governed by complex interactions between the flow, bed material transport and changing sedimentological constraints, as bank materials are supplied to the near bank zone through mass failures and lateral erosion, to form a heterogeneous mixture of bed and bank material.

Simon *et al.* (1991) argue that the transfer of the failed bank material between the various transport or deposition modes is determined by the interactions between the physical properties of the failed bank materials and the hydraulic and sedimentological characteristics of the basal region of the near bank zone. They used a conceptual model to discriminate between the various transport modes of failed bank material in time steps j and j+1 (Figure 3.10) based on simple sedimentological and hydraulic criteria. The conceptual model of Simon *et al.* (1991) is correct to stress the importance of

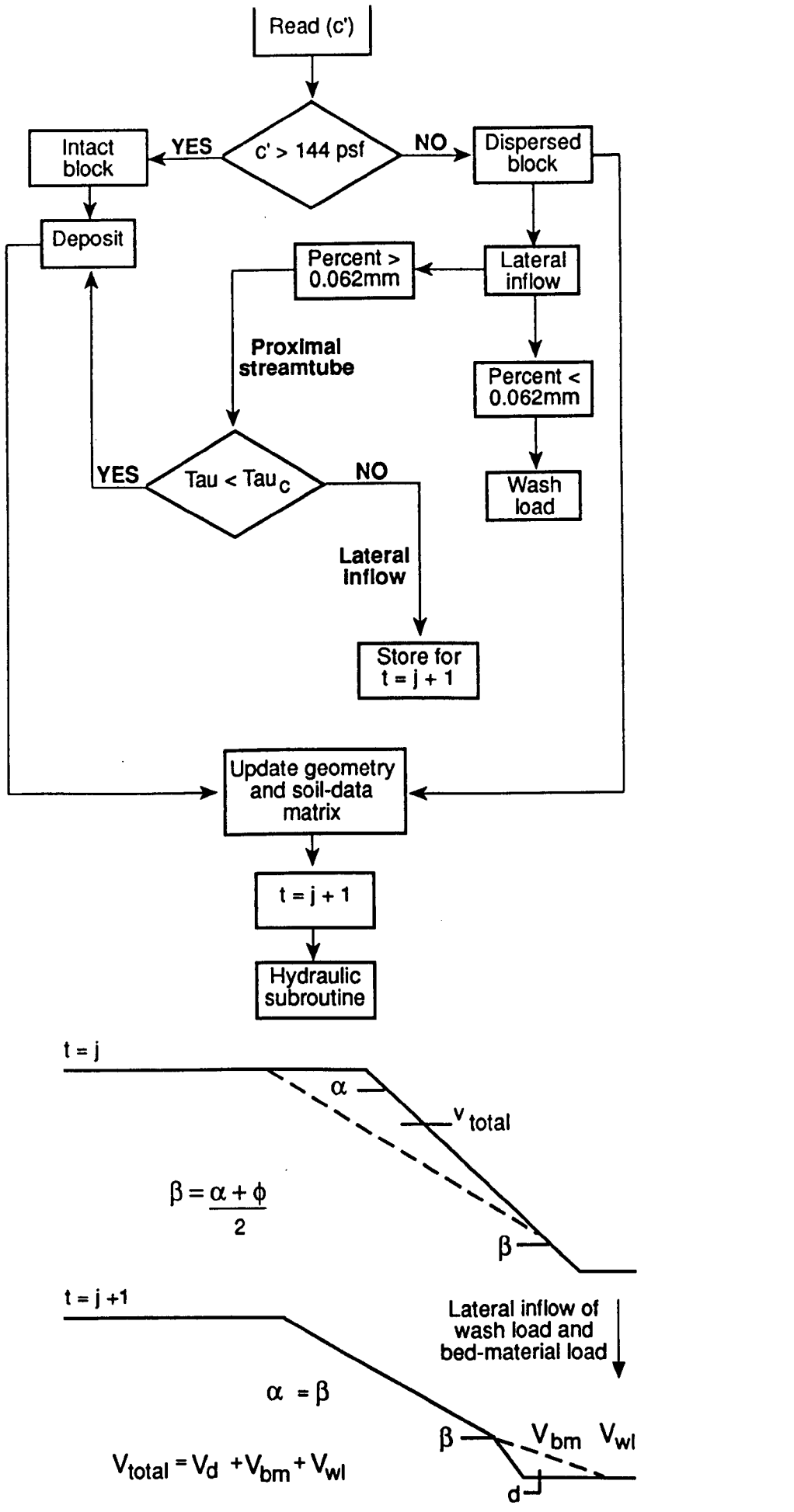

Figure 3.10 Conceptual Model of Simon *et al.* for Maintaining Continuity of Failed Bank Materials (after Simon *et al.*, 1991)

maintaining the continuity of the failed bank material as the pivotal link in coupling bank stability and bed evolution models. However, in order to develop physically-based models of channel width adjustment based on basal endpoint control, more rigorous criteria than they used are required to discriminate between the various transport modes for the failed bank material. In this section an improved physical basis for the conceptual framework outlined by Simon *et al.* (1991) is developed. This framework is applicable to the bank materials which fail by mass wasting. The continuity of any products of direct lateral fluvial erosion of cohesive bank materials may be maintained by simply updating any fraction of the bank material that is finer than the finest sand (0.062 mm) directly to wash load, while the coarser sediment fractions are transferred directly to bed material and/or bed material load.

3.5.1 Physical Properties of Failed Bank Materials

The conceptual model presented by Simon *et al.* (1991) recognises the importance of the interaction between the physical properties of the failed bank materials and the hydraulic and sedimentological conditions in the near bank zone in controlling the way in which the bank material is transferred from mass-wasting to sediment transport algorithms. In order to apply this framework within a physically-based, deterministic widening model, it is clear that a fundamental precursor is the ability to predict the physical properties of the failed bank materials. With respect to fluvial transport and basal cleanout of the failed bank materials, the important physical properties are the gradation of failed bank material particles, their density (specific gravity), cohesion and the overall composition of the bank material (gravel, sand, silt, clay fractions). During mass failure, bank material accelerates downslope and is translated down the failure plane before coming to rest. The failure block is subject to a disturbance during failure, which may significantly impact the physical properties of the bank material. It is the aim of this sub-section to develop a framework for predicting the physical properties, particularly the gradation, density and cohesion, of the bank materials following the disturbance of a mass failure.

Since the primary disturbance to the bank material contained in the failure block is caused by the mass failure itself, it can be hypothesized that the failure mechanism and failure geometry exert the primary controls on the physical properties of the bank material products following failure. Physically, cohesive, undisturbed bank material may disperse into a range of aggregates if the resisting forces binding the soil together (the soil cohesion) are overcome by external forces applied to the bank material during mass failure. Simon *et al.* (1991) suggested that the cohesion of the bank material

controlled the dispersion of the failure block. However, they used a threshold cohesion criterion alone to control the dispersion of bank material in their mass-wasting algorithm (Figure 3.10). In fact it is possible to formulate a dimensionless dispersion parameter, analogous to the stability number, where:

$$DP = \frac{\gamma H_v}{C} \tag{3.49}$$

where DP = dimensionless dispersion criterion and H_v = a length scale, equal to the *effective* vertical "drop" through which the block falls during failure (m). On this basis, the bank material is predicted to disperse into aggregates if the numerical value of the dispersion criterion exceeds unity (DP > 1). This suggests that the primary control on bank material dispersion (if the effects of soil property variation are held constant) will be the influence of the vertical drop height parameter, H_v. The product γH_v may be interpreted as an energy term. If the available energy converted during mass failure from the total potential energy of the failure block is sufficient to overcome the internal resistance of the soil (the cohesion), dispersion results. The total potential energy of the incipient failure block is equal to the product:

$$PE = \gamma \Delta H \tag{3.50}$$

where PE = potential energy of the failure block (J) and ΔH = the difference in elevation of the failure block before and after mass failure (m) (Figure 3.11). During failure, the dissipated potential energy of the block can be assumed to comprise two main components:

$$PE = E_f + E_v \tag{3.51}$$

where E_f = energy dissipated in overcoming the frictional resistance of the failure plane (J) and E_v = kinetic energy converted to dispersive force on impact at the base of the slope (J). It is reasonable to assume that it is the latter component that is relevant with respect to the dispersion process, as it is a measure of the magnitude of the impact between the failure block and the slope base. Hence, the magnitude of this impact shock is taken to be the primary factor controlling dispersion of the bank material.

By dividing equation (3.51) through by the soil unit weight, it is possible to divide the resulting length scales into their equivalent components to clarify the definition of H_v:

$$\Delta H = H_f + H_v \qquad (3.52)$$

where, the length H_f = fraction of the "drop" height, ΔH, that supplies the potential energy dissipated in overcoming frictional resistance (m) and H_v = fraction of the "drop" height that supplies the potential energy that is dissipated by the impact of the failure block at the base of the slope (m). While it is a complicated task to formulate H_f it is possible to hypothesize that the magnitude of the term is controlled primarily by the shape and geometry of the failure surface. This interpretation is consistent with observations that, holding the effects of soil property variation constant, the primary control on the dispersion of failed bank materials is the mechanism of mass failure. This is illustrated in Figure 3.11.

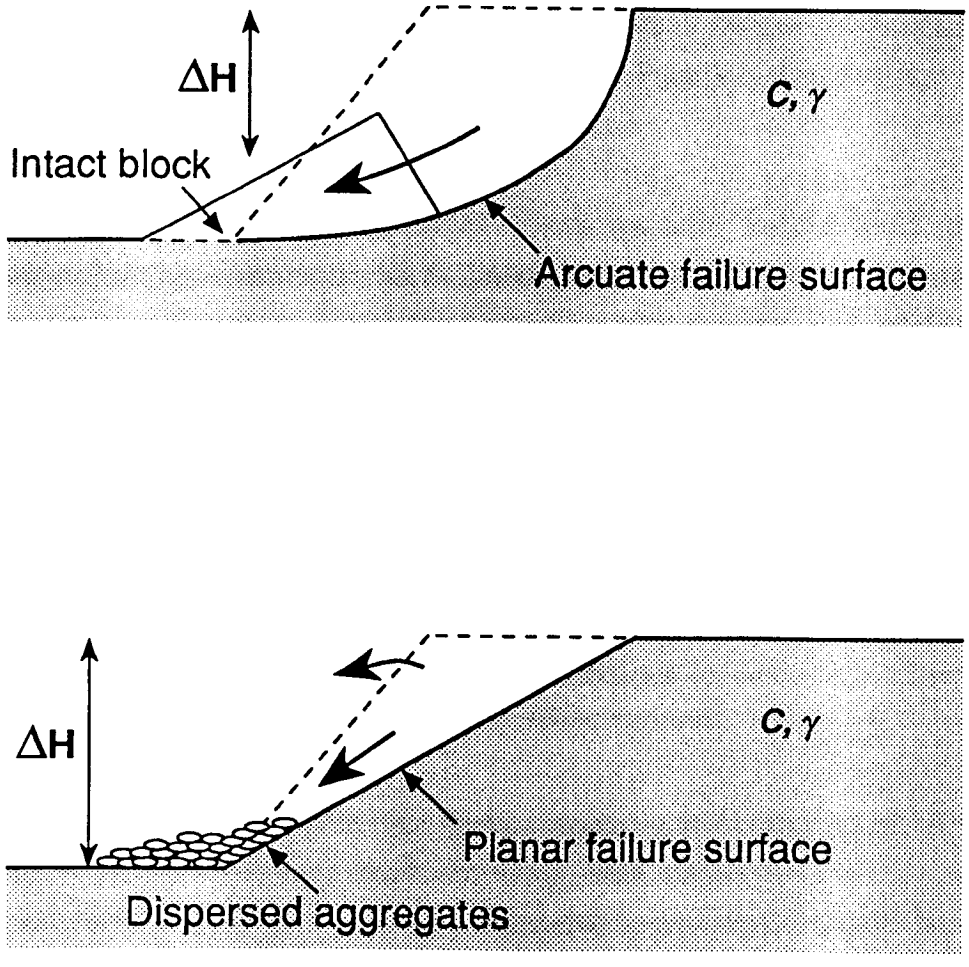

Figure 3.11 Definition Diagram for Rotational Slip versus Planar Failure Dispersion Criterion

Rotational slip type failures are characterised by a translation of the failure block around a relatively long and approximately circular failure surface. The block may even be raised up the failure plane in the basal region (Figure 3.11). The length ΔH is, therefore, relatively small. The potential energy associated with the failing block also tends to be dissipated primarily by frictional contact with the long, arcuate failure plane. The magnitude of the term H_f is, therefore, relatively large. Not only is the overall vertical height through which the block fails less than the overall bank height, but the potential energy associated with this drop height is dissipated largely in overcoming frictional resistance with the failure plane. Consequently, during mass failure by rotational slip, the failure block is usually not subject to major disturbance. The overall magnitude of the term H_v is, therefore, small, so that the chance of the critical dispersion criterion, DP, being exceeded is also small. Observations of natural rotational slips support this interpretation. Typically, such failure blocks retain their cohesion and remain largely intact (see failure block in Plate 3.1). Only a small amount of bank material will be disaggregated during the failure.

Under these circumstances, the entire bank material failure block may be conceptually updated as bank material. In effect, there is no influx of bank material, so that the primary impact of a rotational slip failure is on the geometry and stability of the slope with respect to mass failure, due to the sudden decrease in both slope and bank height. Bank material properties are, therefore, assumed here to remain largely the same following mass failure by rotational slip. Dispersion of significant fractions of the failure block bank material during mass failure by rotational slip is probably restricted to exceptional cases where the bank material is saturated and almost liquifies during mass failure (Simon & Hupp, 1992). This is consistent with the above interpretation, so that in these exceptional circumstances, C is reduced to levels that allow DP to exceed 1, even though the term H_v may be still relatively small.

In the case of slab type failures the failure surface is in contrast short, steep and planar and the failure block may topple violently, slide rapidly or otherwise collapse into the channel through an almost vertical fall which approximates closely the overall height of the bank (Figure 3.11). Not only is the term ΔH larger than the equivalent rotational slip case, but the frictional resistance term H_f is smaller. Consequently, the terms H_v and DP are relatively large in the case of the planar failure. While the potential energy associated with the failure block in the case of rotational slip is dissipated largely in overcoming the frictional resistance of the long, shallow failure plane; the potential energy of the block failing by a slab type mechanism will be dissipated mainly in the impact of the failure block with the base of the slope (the channel bed). Consequently,

Plate 3.4 Disaggregated Blocks of Cohesive Bank Materials Following Mass Failure of IJssel River Banks, The Netherlands

Plate 3.5 Disaggregated Blocks of Cohesive Bank Materials Following Mass Failure of IJssel River Banks, The Netherlands

there is a much higher chance that the planar type failure will result in dispersion, relative to the rotational slip case.

Field observations support this interpretation. The failure block associated with planar type failures often loses cohesion and internal structure during the shock of this impact, resulting in the dispersion of the failure block into a mass of bank material aggregates (Plates 3.4, 3.5), these aggregates come to rest at their angle of repose at the foot of the slope, where they are highly susceptible to entrainment by the flow. Again, exceptions to this rule may be explained within the framework of equation (3.49). Bank material that remains intact following mass wasting by slab type failure mechanisms is frequently observed to be bound together by roots, so that C is large enough to prevent DP exceeding unity, despite the relative high value of H_v.

Qualitative observations of the dispersion of blocks of cohesive bank material cut from natural river banks and dropped vertically in order to simulate the toppling type "failure block-drop" suggest that these aggregates are usually well graded. An explanation for this is that the size of the dispersed clasts may often be controlled by any internal aggregate or crumb structures (see Thorne, 1978) present in the cohesive soil (Plates 3.6, 3.7). The important point is that these observations suggest that it may be possible to characterize the size of the dispersed bank material aggregates using a single representative particle size. If this clast size is in fact scaled on the soil crumb structure, it may also be possible to predict the size of the bank material aggregates following failure. However, this is a topic that needs to be addressed by future research. In the meantime, the observation that the bank material tends to be well graded is used to justify the use of a single value to represent the size of the dispersed bank material aggregates in the bank material sediment transport computations (section 3.5.2). In the absence of field data, this value may be specified by the user as a calibration coefficient.

The simple model developed here is applicable to the idealized case in which only gravitational forces act on the dispersing failure block, so that all of the bank material mass is assumed (initially) to come to rest at the base of the bank. In natural river channels, however, the failure products may fall into the channel and be subjected to fluid forces before coming to rest. The magnitude of this effect is unknown at present. However, in situations where flows are of sufficient magnitude to directly entrain failing bank material, failed bank materials updated initially as bed material are anyway likely to be predicted to be entrained in the next computational time step, so that errors introduced as a consequence of this assumption may not be significant.

Plate 3.6 Crumb Structure of Intact Cohesive Bank Material, River Severn, UK

Plate 3.7 Non-Cohesive Aggregates of Cohesive Bank Materials

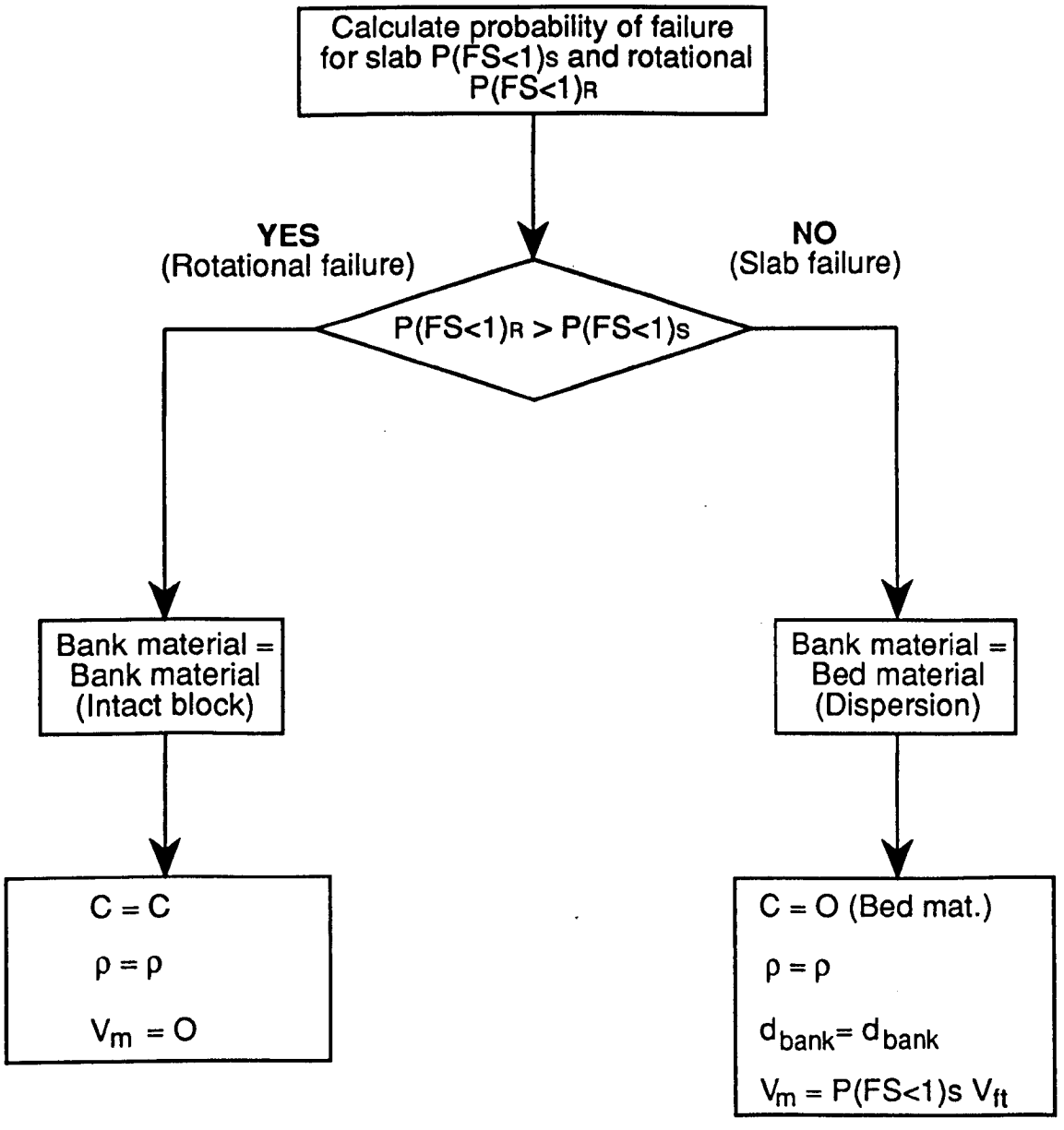

Figure 3.12 Algorithm for Determining Physical Properties of Failed Bank Material

While bank material which fails by rotational slip tends to remain intact and retain its cohesion, the dispersion of bank material into aggregates following slab type mass failures alters significantly the cohesive properties of the bank material. Observations of both real and simulated mass failures in the field suggest that while the dispersed bank material aggregates characteristic of wedge type failures are composed of cohesive bank material, the aggregates themselves are large enough to behave as non-cohesive sediment clasts. They are also large enough that the density of these clasts is similar to the original density of the bank material, and the size range of particles contained within the clasts can also be assumed identical to the original bank material. This is a very important assumption, since it implies that, following dispersion of the bank material during slab type failures, the cohesive bank material is transformed conceptually into clasts of relatively low density, non-cohesive sediment, allowing the application of conventional sediment transport theory to the problem of the transport of both the bed material and failed bank material mixture away from the near bank zone. This point is developed further in section 3.5.2. The method of predicting the physical properties of the failed bank materials is summarised in Figure 3.12.

3.5.2 Transport of Bed and Bank Material Mixtures

Following mass failure, the classification of eroded bank material must be updated as either bank material, bed material, bed material load or wash load, to enable a channel widening model to transfer the failed bank material between the mass-wasting and sediment transport algorithms, and thereby achieve coupling between mass-wasting and sediment transport mechanisms. In section 3.5.1 it was shown that the failure mechanism determines the physical properties of the bank material immediately following failure. The conceptual framework proposed by Simon *et al.* represents an improvement over existing models of meander migration (*e.g.* Crosato (1990)) and width adjustment (Osman (1985); Alonso & Combs (1986); Borah & Bordoloi (1989)), which simply assume that the cohesive bank material is directly transferred to wash load following failure. However, only broad, qualitative criteria are suggested by Simon *et al.* to govern the transfer of the failed bank material to the various sediment transport modes in the time steps after mass failure and following its deposition onto the bed in the near bank zone. Yet basal endpoint control shows that it is the transport of the the failed bank material and bed material mixture away from the near bank basal area that is the link in maintaining the continuity of the bank material which ensures that channel widening can be simulated deterministically. It is, therefore, vital to take explicit account of the impact of mixtures of bed and bank material with widely varying physical properties on the near bank sediment transport fluxes, if the goal of a

deterministic channel widening model is to be achieved. Consequently, the aim of this section is to provide an improved mechanistic basis to the framework proposed by Simon *et al.* (1991), in order that the critical interaction between bank material supply and bed material transport that is the primary control on the basal endpoint status and the rate of bank retreat can be more rigorously modelled.

The problem of the mechanics of transport of mixtures of sediments with widely varying physical properties (cohesion, size, density) can be treated using a mixed, or "active", layer theory. A number of schemes have been developed by a variety of authors (*e.g.* Bennett & Nordin, 1977; Thomas, 1982; Karim & Kennedy, 1981; Borah *et al.*, 1982; Holly & Karim, 1986; Karim & Holly, 1986; Rahuel *et al.*, 1989; Holly & Rahuel, 1990; Niekerk *et al.*, 1992). The motivation for these studies has usually been to predict the transport of widely graded sediments, but also to predict the transport of mixtures of sediment of different densities. Since the properties of the bank materials delivered to the bed region in the near bank zone may be predicted using the methods presented in section 3.5.1 such schemes may be applied directly to calculate the transport of bed and bank material mixtures in the channel widening model developed here. Only minor modifications are required in order to apply these theories to the special conditions of the near bank environment.

Essentially, the method of handling the sediment mixture is to assume firstly that the sediment mixture can be discretized into a finite number of size-density classes, with a single size-density value representing that class (Figure 3.13). It is then assumed that, during any given time increment, the flow is capable of transporting the bed material only in a layer of a finite depth below the surface of the bed so that a control volume of sediment, termed the mixed or "active" layer, can be established at each model computational node. A physical-numerical interpretation of the mixed layer has been given Bennett & Nordin (1977) and Rahuel *et al.* (1989). Rahuel *et al.* (1989) stress that this interpretation cannot be disassociated from the time-scale under consideration. Over very short time-scales, the mixed layer can be considered as a thin surface layer containing particles that are susceptible to entrainment by the flow. Over medium time-scales, such as the order of time it takes for a bedform (ripple or dune) to traverse its own wavelength, the mixed layer can be envisaged as occupying the vertical space traversed by these bedforms in their downstream movement (Rahuel *et al.*, 1989). Over longer time-scales, in which the bed elevation may change significantly, the mixed layer can be thought of as the thickness of the layer of material eroded or deposited. However, even in this case, if the bed elevation changes are small, the mixed layer can still be thought of as the zone of bedform movement (Rahuel *et al.*,

1989) (Figure 3.14). Since the depth of the mixed layer is linked to the time-scale under consideration, for numerical modelling one cannot choose the computational time step and mixed layer thickness entirely independently. Consequently, the choice of computational time step length is limited by the requirement that changes in bed elevation be small.

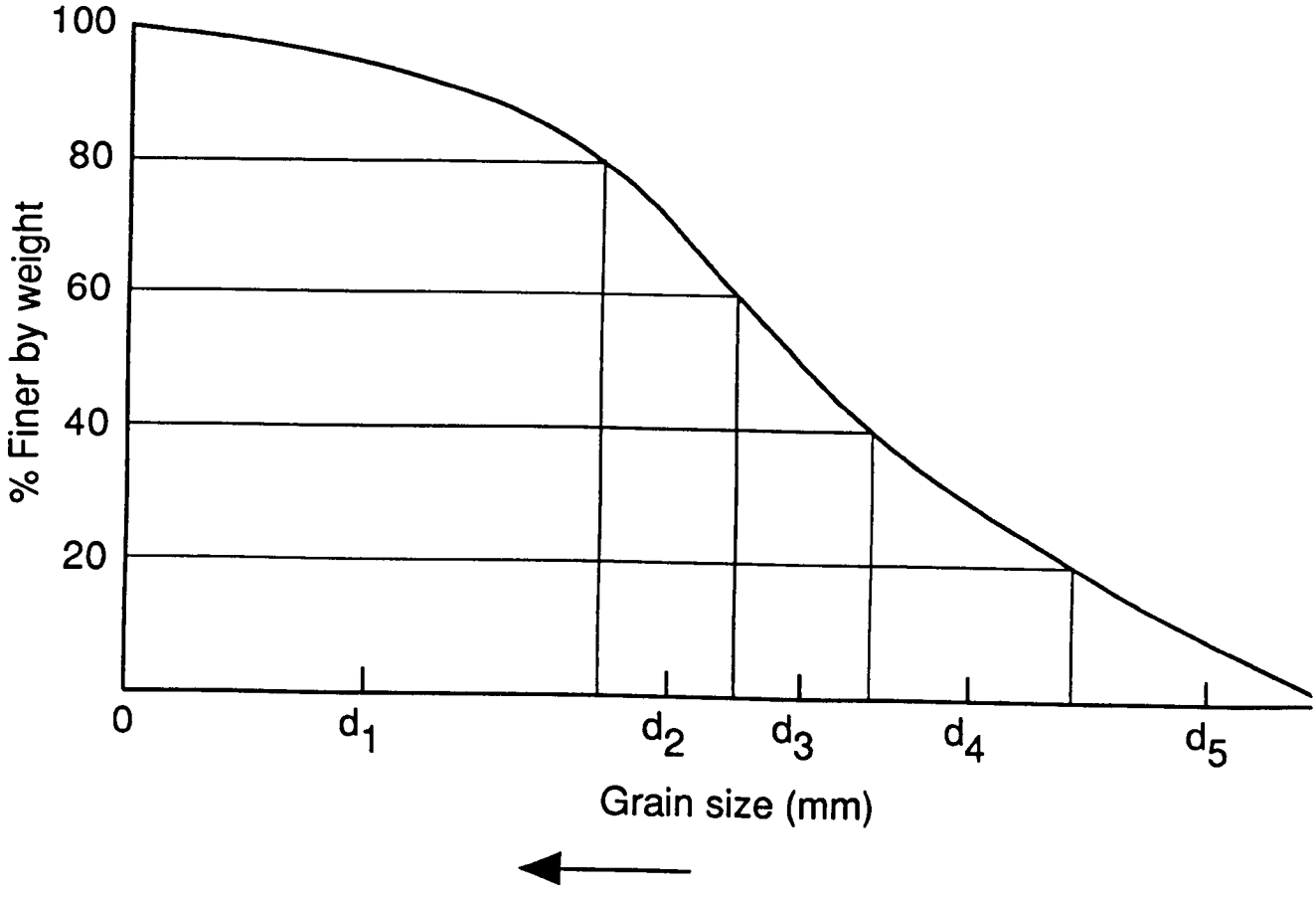

Figure 3.13 Division of Bed Material Gradation Curve into Representative Size Classes

Regardless of the precise depth of the mixed layer, the mixed layer concept allows the assumption to be made that each sediment size-density class distributed throughout the mixed layer (*i.e.* all of the bed material contained in the control volume) is equally susceptible to entrainment by the flow (Figure 3.14) within a computational time step. Various formulations have been used to relate the mixed layer depth to some measure of flow intensity. A simple model is presented by Karim & Kennedy (1981), who relate the mixed layer depth to the flow depth. This model is plausible physically because it is generally true that the maximum height of dunes relative to the flow depth is more or less constant from river to river (Rahuel *et al.*, 1989), so that:

$$D_{mix} = a_2 D \qquad (3.53)$$

where D_{mix} = mixed layer depth (m), D = flow depth (m) and a_2 = calibration coefficient (Karim & Kennedy suggest $a_2 = 0.15$, the value adopted here). This formulation was selected for its simplicity, physical plausibility, dimensional consistency and the potential flexibility offered by using a method with an empirical calibration coefficient. Moreover, the formulation remains valid even in channels with no bedform movement, since the layer can still reasonably be expected to be some calibrated function of water depth (Rahuel *et al.*, 1989).

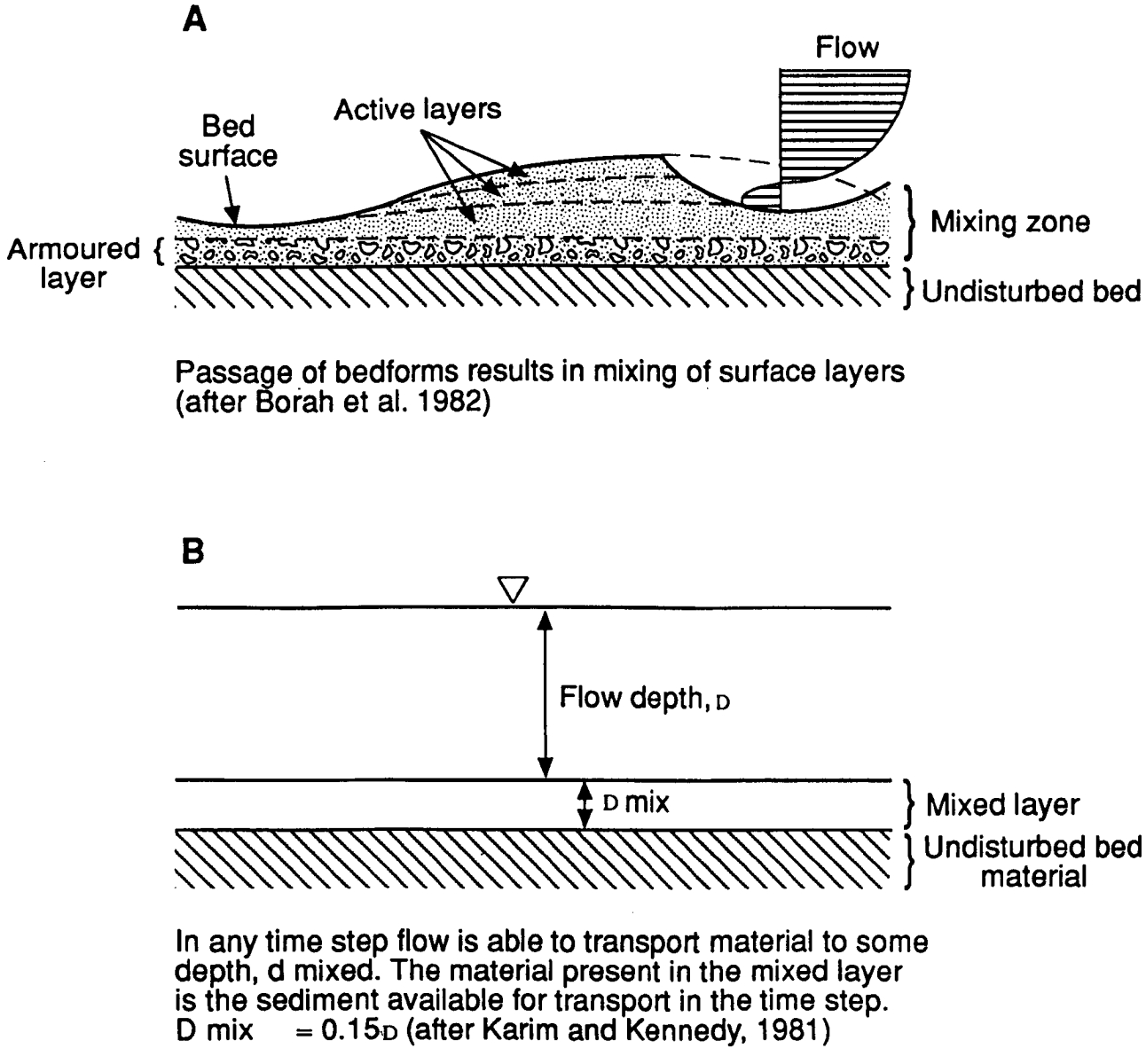

Figure 3.14 Diagrams Showing Physical Interpretation of Mixed Layer Concept

Regardless of the precise formulation of the mixed layer depth, the important point is that the mixing hypothesis allows the transport of each individual size-density class of sediment to be treated independently. The total transport rate of the sediment mixture can, therefore, be expressed in the form:

$$q_s = \sum_{i=1}^{i=i} q_{si}^* \tag{3.54}$$

where q_s = total transport rate per unit channel width (m^2s^{-1}) and q_{si}^* = actual transport rate per unit channel width of the i th bed material class (m^2s^{-1}). In equation (3.54), the total sediment discharge is expressed as the sum of all the actual sediment transport rates of each of the i independent size-density sediment classes. The *actual* transport rate of each bed material size-density class must be modified from its *potential* value determined using the sediment transport equations previously presented in section 3.3. This is because the potential rate refers to the sediment transport rate that would occur in the idealized case of a uniform, well-graded sediment, with no supply limitation. Remembering that the mixed layer is assumed to have a finite depth in each time step, it is necessary to take into account the limited availability for transport of the individual sediment classes present in the mixed layer. The actual transport rate, therefore, must be reduced from the potential value by a factor depending on the availability of sediment in each class present in the mixed layer, so that:

$$q_{si}^* = q_{si}\ \beta_i \tag{3.55}$$

where β_i = fraction of sediment in the ith sediment size-density class present in the mixed layer and q_{si} = potential transport rate per unit channel width for ith sediment size-density class (m^2s^{-1}), determined using the equations presented in section 3.3.

In addition to supply limitation, an additional physical process needs to be accounted for when dealing with the transport of sediment mixtures. This is the influence of the variation in sediment sizes and consequent particle interactions on the process of entrainment. In sediment mixtures, the particles interact such that small grains tend to fall into the voids between large grains, creating a "hiding" effect, while the larger grains tend to protrude into the flow, so that the drag force on these grains is preferentially increased, tending to compensate for the greater submerged weight of these particles. The overall effect is that the critical stress for entrainment ("mobility") of the large and small grains tends to "equalize" (Parker *et al.*, 1982; Andrews, 1983), although completely "equal mobility" probably does not occur. It is necessary to build a

"hiding" factor into equation (3.55) to express this effect. The actual sediment transport rate of each individual size-density sediment class is, therefore, related to the potential rate for that size-density class using (Rahuel *et al.*, 1989):

$$q_{si}^{*} = q_{si}\ \beta_i \left(\frac{d_i}{d_{50}}\right)^{0.85} \tag{3.56}$$

where d_i = the median sediment diameter (mm) of the ith sediment class and d_{50} = the median diameter (mm) of the bed material mixture. The value of the exponent on the hiding factor $\frac{d_i}{d_{50}}$ expresses the degree of "equal mobility" (unity for "equal mobility") observed in the sediment entrainment process and its value has been a subject of intense and, with the benefit of hindsight, somewhat pointless debate (Parker *et al.*, 1982; Andrews, 1983; Komar, 1987, 1989; Ashworth & Ferguson, 1989). Presumably, the tendency to either size selective transport or true "equal mobility" as evidenced by the value of the exponent on the hiding factor is dependent on local conditions (Richards, 1990) and is perhaps influenced by a variety of local, site-specific sedimentological and hydraulic properties. Indeed Richards (1990) suggests that the controversy over selective entrainment versus "equal mobility" is somewhat artificial for precisely this reason; first, because the hiding factor does not explicitly take into account the influence of grain size on packing and pivoting angles and second, because the value of the exponent determined by the various authors is anyway masked by the empirical vagaries of individual data sets. Rahuel *et al.* (1989) suggest that the exponent takes a value of 0.85, the value adopted by Karim & Kennedy (1981). This appears to be a reasonable compromise of values from the literature, which range between about 0.65 and about 0.95 (Richards, 1990) and is, therefore, adopted here as a baseline value, while leaving scope for varying its value for purposes of calibration, to express the tendency of the degree of equal mobility to be dependent upon local conditions (Richards, 1990).

In order to apply equation (3.56) it is necessary to determine the value of β_i, the fractional composition of the mixed layer. This parameter may be calculated using a budgeting approach for each of the fractions within the mixed layer. Since the composition of the bed material mixture is known at the start of the model simulation (from the sediment gradation curve), it is possible to apply the sediment continuity equation to each of the individual size-density classes in each time step, in order to determine the depth of scour or deposition for each individual size-density class. Summation gives the total scour or deposition at that cross-section. Note that the depth of scour of each size-density class is limited in each time step to a maximum value equal

to the depth of material in the size class that is available in the mixed layer during that time step. This information, together with the mixed layer depth during that time step (found from equation (3.53)), allows the fractional compositions of the sediment classes to be updated at the end of each time step. This also allows re-calculation of the median sediment size in the mixture, which is required as input to equation (3.56). At the start of the next time step, a new mixed layer depth is inserted according to the flow conditions in the new time step. The mixed layer composition is updated accordingly, following insertion of the new active layer allows the new fractional compositions to be calculated, and the calculations are repeated. This procedure for calculating the fractional composition of the sediment size-density classes is illustrated in Figure 3.15.

The updating scheme employed here and illustrated in Figure 3.15 is distinct from many other mixed layer schemes. Such schemes commonly only use two bed material horizons - the original bed material and the mixed layer - to characterise the variation of sediment horizons with depth (*e.g.* Bennett & Nordin, 1977; Karim & Holly, 1986). In most applications of mixed layer theory, this is a satisfactory representation of the full depth of bed material since usually one of *either* degradation *or* aggradation is simulated, but *cycles* of scour and deposition are not. Such cycles are responsible for the creation and destruction of a variety of sediment horizons throughout the depth of the bed material mixture.

This minor distinction is quite important with regard to the applications of mixed layer theory within the near bank zone. The scheme used here allows for the tracking of any new stratigraphic layer created following deposition. This is important in the near bank zone, since cycles of aggradation and degradation may be expected to occur in response to rapid fluctuations in bank material inflow rates as the stability of the banks varies. This, in turn, can potentially result in cycles of creation and destruction of stratigraphic layers at various depths in the bed material. Large variations in mixed layer depth as a consequence of rapid stage variations between model time steps may also contribute to situations where the mixed layer depth may potentially extend into several distinct stratigraphic layers at varying depths over even short time periods. If proper account of the historical composition of stratigraphic layers throughout the entire depth of the bed material is not made, there is increased potential for errors in determining the fractional composition of the sediment classes in the current mixed layer.

Although the bank material clasts in the near bank basal sediment mixture behave as cohesionless aggregates of bank material, these clasts nevertheless are made up of cohesive bank material particles, and tend to be much less dense and also softer than

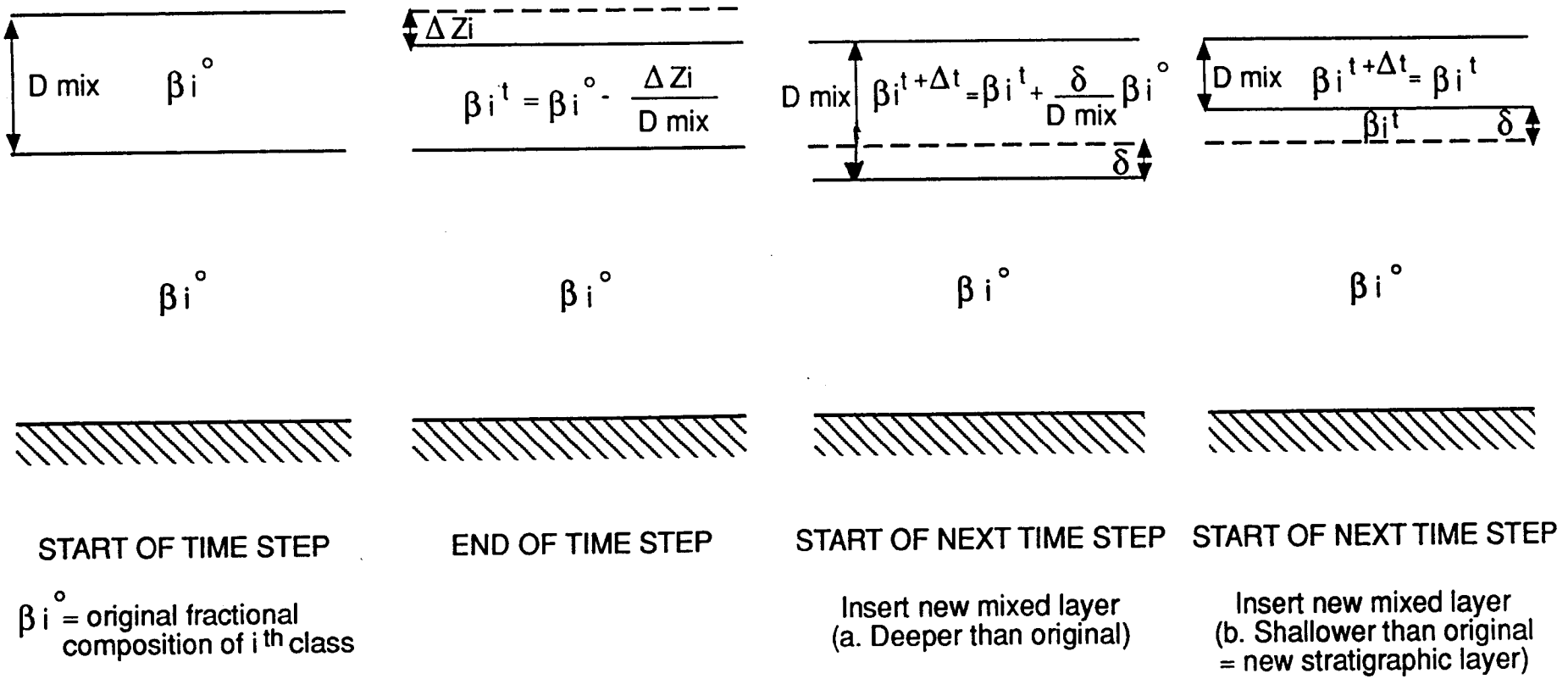

Figure 3.15 Diagram Showing Mixed Layer Updating Scheme

bed material. Although cohesive bank material usually is composed of predominantly very fine-grained materials, sand fractions may also be included. It may be assumed that following entrainment, the (relatively soft) clasts of bank material very rapidly break down to their constituent particles by the process of attrition. It will, therefore, be necessary to track these particles, since once broken down the very fine particles will become suspended load, whilst the sand fraction of the bank material may be added to either the bed material or the bed material load. In fact, by assuming that the rapid breakdown of the bank material clasts occurs immediately following entrainment and by specifying the fraction of the bank material that is coarser than very fine sand as input data, it is possible to track these constituents as sediment classes in the mixed layer compositions, and so maintain the continuity of all the bank and bed material sediments, as envisaged by Simon *et al.* (1991). In effect, rather than simply updating the bank material to wash load or bed material fractions immediately following failure, it is the assumptions that the bank material disperses into clasts following mass failure, and that these clasts then attrit instantaneously on entrainment, that allow this scheme to take into account the effect of storing the wash load fraction in the bank material clasts at the base of the bank on the transport of the bed and bank material mixture from the near bank basal zone. The complete framework for maintaining the continuity of bank material following mass failure, based on that originally proposed by Simon *et al.* (1991) and revised and extended here, is summarised in Figure 3.16.

3.6 NUMERICAL SOLUTION STRATEGY

The individual hydraulics, sediment transport and bank stability algorithms developed in the previous sections may be combined in order to simulate channel widening through time in response to imposed discharges and sediment loads, given the physical properties of the channel boundary materials. The aim of this section is to detail the procedure used to combine these individual algorithms into a numerical channel widening model which is based on the concept of basal endpoint control and to explain the numerical solution strategy. It is important to draw attention to the assumptions and limitations used to combine these algorithms into a channel adjustment model, because these obviously influence the predictive ability of the model, and the temporal and spatial scales over which the model may be applied successfully (Holly & Rahuel, 1990). The channel widening algorithm is summarised in Figure 3.17. This algorithm was coded into FORTRAN and loaded onto a Digital Equipment Corporation VAX mainframe computer. Due to RAM quota limitations, model simulations were limited to a maximum period of 3500 computational time steps, requiring about 12 hours processing time to execute. The corresponding length of simulated real time is

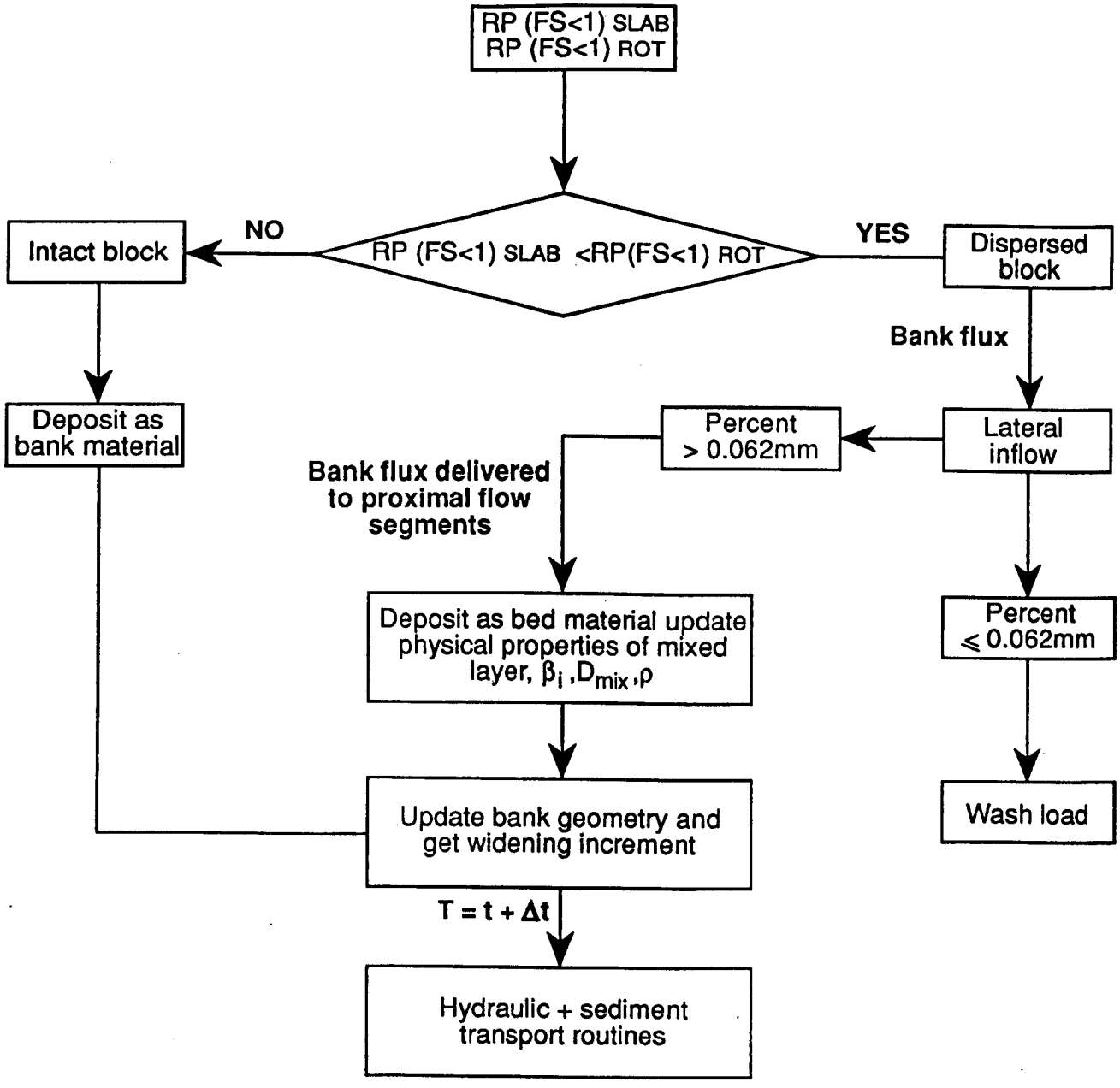

Figure 3.16 Diagram Showing Framework for Maintaining Continuity of Bank Sediments

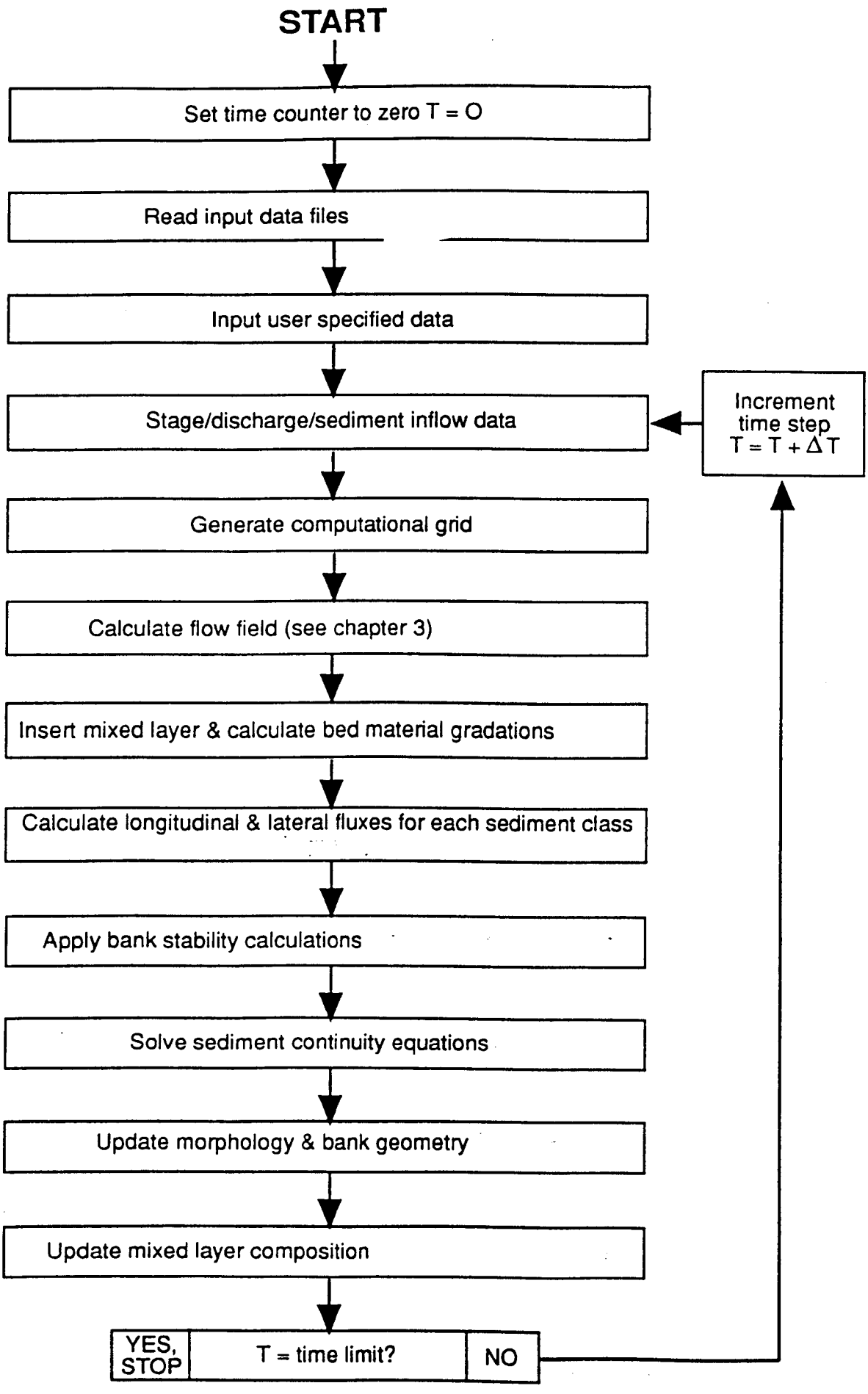

Figure 3.17 Numerical Channel Evolution Model Algorithm

constrained by the length of an individual time step, which is limited by numerical stability considerations. This is discussed below.

Having selected a prototype reach to be modelled, the first step is to compile the necessary data required as input. Details of the model data requirements, which are quite large, are summarised in Table 4.1. A computational grid is fitted to the prototype channel by dividing it into a finite number of cross-sections. Up to a maximum of 20 cross-sections are allowed in the present version of the code. Ideally, the choice of model cross-sections should be made on the basis that these cross-sections should adequately reflect the morphology along the reaches making up the length of the prototype channel (Cunge *et al.*, 1980). In practice, the choice of cross-section location is usually constrained by the data availability. In order to represent the lateral distributions of flow and sediment transport which influence the stability of the banks, each cross-section is divided into 3, one-dimensional flow segments, 2 near bank and one central flow zone (Figure 3.18). It would be possible to modify the code to include more flow segments, if required. However, this was considered unnecessary for the purposes of this research. This quasi two-dimensional approach is an improvement over existing methods which assume the entire cross-section may successfully be modelled using a one-dimensional approach. The width of the near bank zones is defined as extending a distance of two bank heights from the base of the bank. Observations suggest that this is a reasonable approximation of the width of the bank boundary layer. This definition is further justified by the observation that all bank material entering into the channel is likely to be delivered within these segments. Having fitted this grid to the prototype channel, the procedure is then to solve the flow, sediment transport and bank stability (not applicable in the central flow segment) equations in each of the segments in order to solve equation (3.8) and update the geometry of each segment at each cross-section at the end of the time step. Once a computational grid is fitted to the prototype channel, input data files are read, the time step length and length of time of simulation are specified and computations proceed.

The distribution of flow across each model cross-section is determined using the hydraulics algorithm presented in section 3.2. First, the backwater equation is solved using the standard step method in order to provide the water surface elevation and water surface slope at each model cross-section. The bisection method is used to solve the backwater equation iteratively. In order to solve the backwater equation, the water surface elevation for the specified discharge (stage-discharge curve) is required at the downstream boundary. In each time step, the flow is assumed to be steady. However,

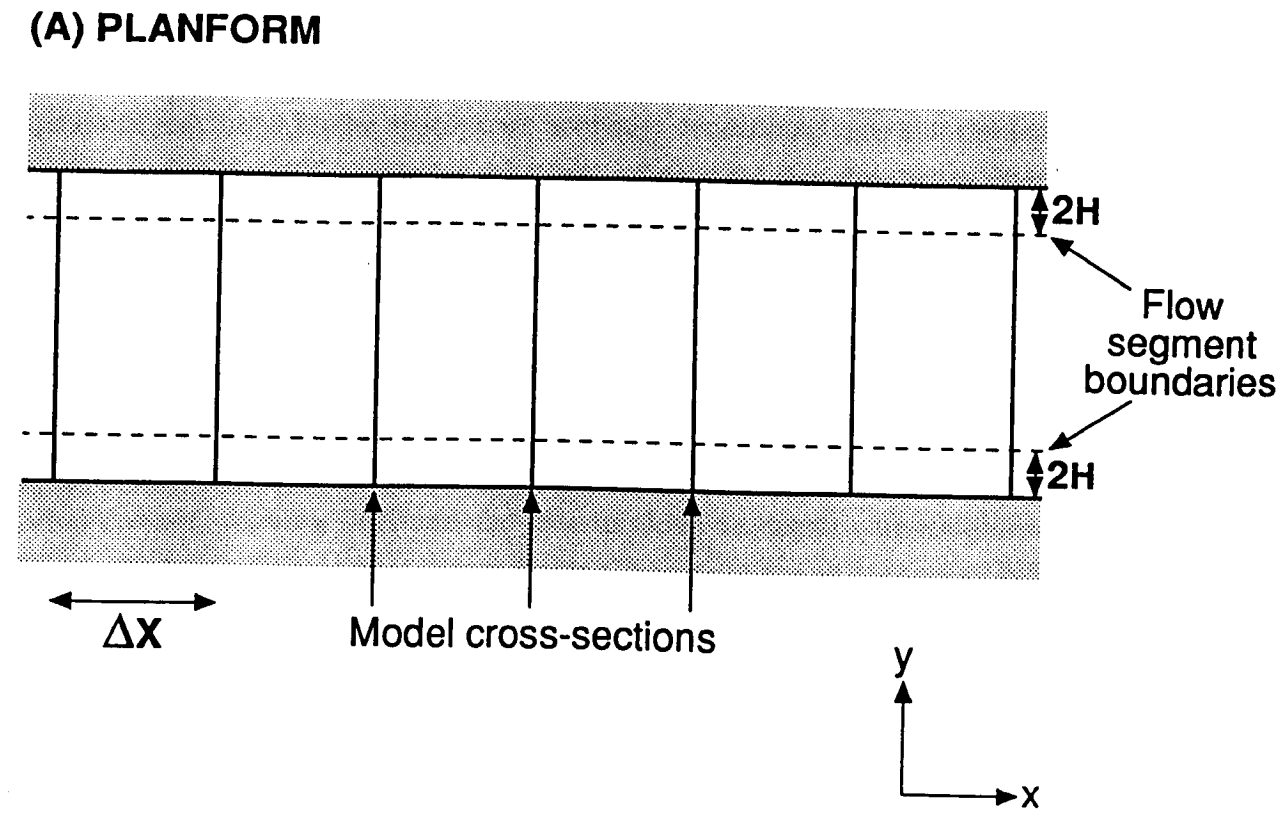

Figure 3.18 Diagram Showing Computational Grid Scheme

it is possible to represent varying flows over time through use of a stepped hydrograph, in which constant values of discharge are specified within each time step.

Having determined the water surface elevation and slope at each cross-section, the lateral distribution of flow at each cross-section is then calculated by solving (3.2) using a finite difference algorithm and Newton's method for simultaneous non-linear equations, together with the appropriate boundary conditions (zero unit discharge at the channel boundaries). The code for this part of the model was supplied by James Wark and obtained from the code written to support the LDM of Wark *et al.* (1990). At each section it is assumed that the water surface elevation, determined from the backwater equation, is constant across the full width of each cross-section: that is the water surface is assumed to be planar and horizontal in the lateral direction. A finite difference grid is set up across each model cross-section using a user-supplied number of computational points. About 200 to 300 points have been found to be adequate for most in-bank flows. Having obtained the distributions of depth and roughness, initial estimates of unit flow at each computational point are found by setting NEV = 0.0. Newton's method is then applied to iterate until the method converges to a final solution. The total discharge obtained using the LDM is usually not identical to that used to generate the backwater curve, but these differences have been found to be minor for typical channel shapes (width-depth ratios of at least 10) and in-bank flows. The LDM developed by Wark *et al.* assumes uniform flow and, therefore, uses the longitudinal bed slope as input to equation (3.2). However, the backwater routine solves the water surface profile for gradually varied flow. In these circumstances the longitudinal water surface slope determined from the backwater calculations is used as input to equation (3.2), though the bed slope must still be used to calculate the B_s factor (J. B. Wark, personal communication, 1991). Having determined the lateral distribution of flow, the mean unit discharge and mean flow depth in each of the flow segments at each cross-section are calculated by lateral integration. Together with the energy slope found from the solution of the backwater curve, these are the input data required for the sediment transport calculations.

Following determination of the hydraulics along each of the flow segments, calculations move onto the sediment sorting and transport algorithms. First, the mixed layer depths are calculated in each flow segment according to equation (3.53). This allows the varying composition of the mixed layer to be determined over both the lateral and longitudinal directions. Sediment transport rates in both the longitudinal and lateral directions are then calculated for each of the flow segments using the sediment transport algorithms detailed in section 3.3. Lateral sediment transport fluxes (including the bank

material fluxes) are positive in sign when directed towards the right bank, otherwise they are negative. Potential sediment transport rates are calculated for each of the sediment size-density classes at every grid point, wether those individual classes are present in the mixed layer or not. Actual sediment transport rates are determined through use of equation (3.56), so that accurate tracking of the fractional composition of each of the size-density classes present in the mixed layer is vital.

However, a difficulty in applying the mixed layer concept arises when the cross-section of a widening channel is divided into flow segments in this way. The aim of the mixed layer concept is to establish a fixed unit control volume of sediment, the composition of which may then be tracked by budgeting for sediment removed or deposited by sediment transfer processes operating in the vertical dimension. But, since the width of the mixed layer in each flow segment may vary in response to changes in the width of the channel or bank heights (since the widths of the near bank flow segments are defined by the height of the banks), the mixed layer control volumes in each of the segments are not fixed. Furthermore, the composition of the mixed layer in any one flow segment will be influenced by the composition of sediment in the adjacent flow segment mixed layer, as the flow segment boundaries migrate laterally. So, the control volume of sediment stored in an individual flow segment mixed layer may be influenced not only by vertical adjustment (aggradation or degradation), but also by lateral adjustment as adjacent segment boundaries migrate in to each other between different time steps. Yet the effect of such lateral adjustments on the composition of the mixed layer are not accounted for. This may potentially lead to errors in tracking the composition of each of the mixed layers, but this effect will be small if the change in the width of the segments during any one time step is small in relation to the width of the mixed layers (that is, the change in unit volume of the mixed layer due to unaccounted for lateral adjustment is small in comparison to the overall magnitude of the unit volume of the mixed layer). For this reason, applications using the code based on the algorithms developed here are limited to cases where changes in width or depth in any time step are small in comparison to the overall width and depth of the prototype channel. This is not a significant limitation for many natural channels and, in practice, the effects of this constraint can also be minimised by using relatively short time steps.

A further difficulty is that in natural river channels, both the width of the stream and the height of the banks are frequently variable in the longitudinal direction. However, since these variables define the flow segments at each cross-section, this may lead to cases where the flow segment boundaries are not parallel to the mean streamwise direction. It is, therefore, possible that longitudinally transported sediment in an

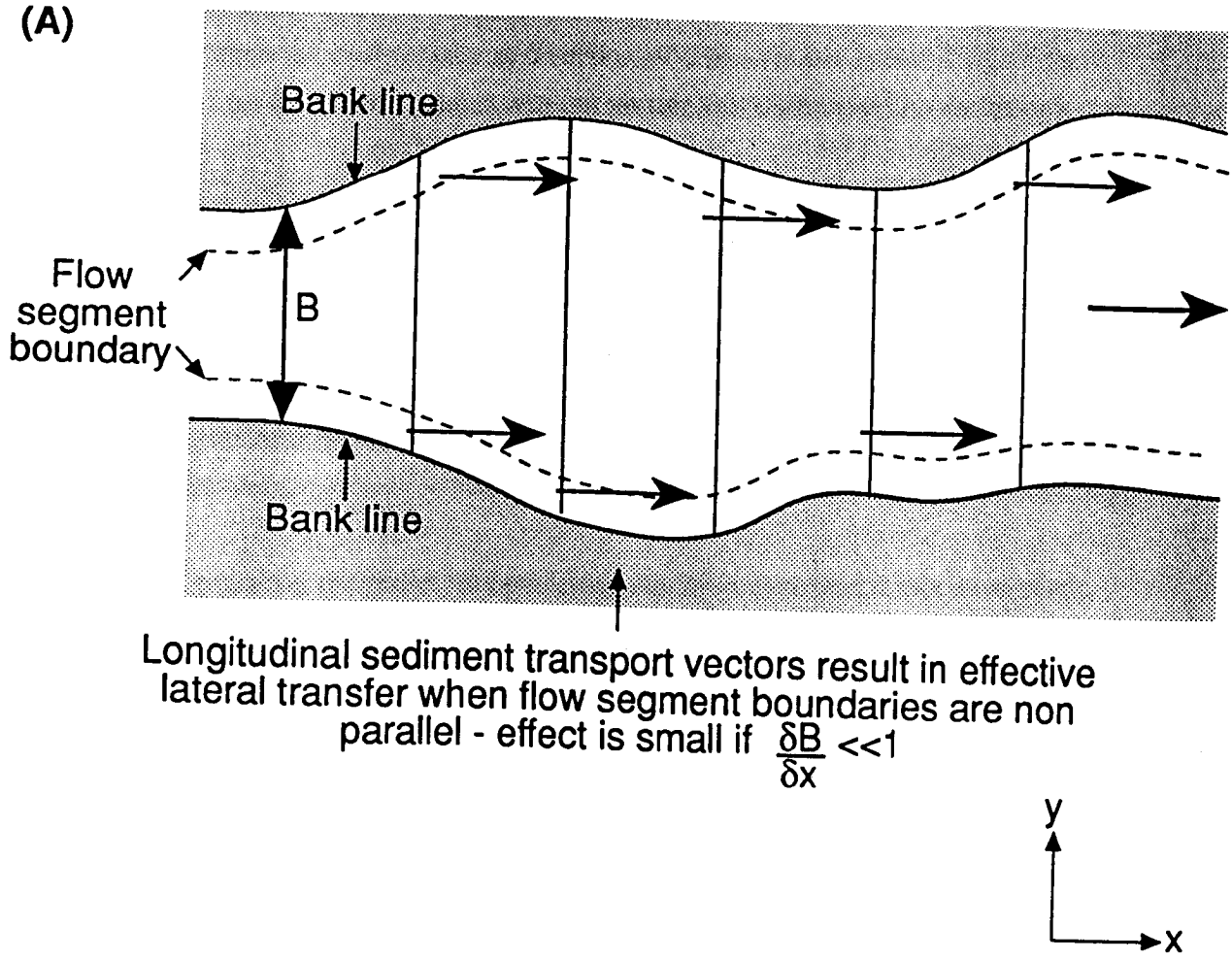

Figure 3.19 Diagram Showing Effects of Longitudinal Change in Width on Predicted Lateral Sediment Exchanges

individual flow segment may be directed into an adjacent flow segment further downstream, leading to an apparent and erroneous lateral transfer of sediment between flow segments over and above that calculated previously in the lateral sediment transport flux algorithm (Figure 3.19). This effect can be neglected if the rate of change of width with distance is small (Darby & Thorne, 1992b) and this is not a significant limitation for most natural river channels without abrupt longitudinal width variations.

Bank stability and lateral erosion on both the left and right banks are calculated separately using the methods outlined in section 3.4. For each bank, the bank material flux is computed and the bank geometry and bankfull and bed widths updated according to the predicted flood plain widening and lateral erosion. The bank material fluxes provide the final fluxes required to apply the sediment continuity equation in order to update the morphology in each of the flow segments at the end of each computational time step.

In each flow segment, the sediment continuity equation is solved using an explicit, uncoupled finite difference technique. The sediment continuity equation can be written in finite difference form:

$$\Delta Z = \frac{\Delta t}{1 - \lambda}\left(\frac{\Delta q_x}{\Delta x} + \frac{\Delta q_y}{\Delta y}\right) \tag{3.57}$$

where ΔZ = depth of degradation (m) (negative values imply aggradation). The longitudinal sediment flux divergence term was presented in central difference form because this form is preferable than either forward or backward differences, since the former have truncation errors of order $(\Delta x)^3$ while the latter have truncation errors of order $(\Delta x)^2$ (Osman, 1985). The lateral sediment flux divergence term is calculated by dividing the difference between the fluxes calculated at the two lateral boundaries of each flow segment by the width of that flow segment. The bed material porosity, λ, is estimated from the empirical relation (Komura & Simons, 1967):

$$\lambda = 0.245 + \frac{0.0864}{d_{50}^{0.21}} \tag{3.58}$$

The use of an explicit, uncoupled finite difference solution constrains the choice of length of time step used in the simulation, due to potential problems with numerical instability (Cunge *et al.*, 1980). For explicit, uncoupled finite difference schemes, numerical stability is conditionally dependent on the Courant condition, which is a function of the spatial scale, time step and celerity of the bed disturbance:

$$Cr \frac{\Delta t}{\Delta x} \leq 1 \qquad (3.59)$$

where Cr = celerity of bed disturbance (ms^{-1}), Δt = time step length (s) and Δx = length of model reach (m). The time step must be constrained below some upper limit for numerical stability, for given model reach lengths and boundary conditions. However, this constrains the length of real time simulation to an amount set by the rule:

$$\text{Simulation Time} = \Delta t_{max} * \text{LIM} \qquad (3.60)$$

where Δt_{max} = maximum time step length for numerical stability (s) and LIM = maximum allowable number of time steps, set by the RAM limitation on the size of the output arrays. This constraint on time step length is not a major additional problem, since the length of time step should anyway be "small", as discussed previously. In the simulations of the South Fork of the Forked Deer River used to validate the model (see Chapter 4), time steps of half a day were found to be an upper limit for stability. This limited the use of the model to maximum real time simulations of about 5 years duration.

The sediment continuity equation is solved at each model cross-section and segment for each of the sediment size-density classes. This information allows the bed elevations and fractional composition of the mixed layers in each segments to be updated at the end of each time step, together with any detected widening increments. The cross-sectional coordinates are then updated using this information and the time step is incremented. If the number of time steps has not reached the user specified limit, computations are directed back to the hydraulics algorithm (with discharge values appropriate for the time step) and the sequence is repeated. Otherwise, the required output data is directed to output files and the model computations stop.

CHAPTER FOUR

A PHYSICALLY-BASED NUMERICAL MODEL OF CHANNEL EVOLUTION II: ASSESSMENT OF PREDICTIVE ABILITY

4.1 MODEL VALIDATION

In order to apply the numerical widening model developed in chapter 3 with any degree of confidence, it is necessary to test the predictive ability of the model against independent observations. By comparing model predictions against observed data, it is possible to establish the accuracy of the model.

Two distinct, but mutually complementary, approaches to testing the channel widening model developed in the previous chapter were undertaken. First, a "dynamic" validation of the model was performed in which the results of a model simulation, through time, of a reach of unstable channel were compared to repeated observations of the actual morphology of the adjusting stream throughout the period of adjustment. Second, a "regime", or "steady-state", validation of the model was performed by using the model to generate stable channel forms for a given combination of input variables under conditions of steady flow. The stable channel morphologies predicted by the model were then compared to stable channel morphologies predicted from an empirical regime type equation derived from real world observations of stable channel geometries. Use of these two separate approaches, which are outlined in more detail in the relevant sections below, allows the ability of the model to predict both transient channel adjustments and equilibrium ("end point") channel geometries to be established. These distinct approaches are complimentary in that they allow the predictive ability of the model to be assessed more fully along the length of the entire adjustment curve (Figure 1.1), than would be possible if either approach had been used in isolation.

A second benefit of using the "regime" type validation approach in tandem with the "dynamic" validation approach lies in the wider availability of regime data across a range of environments. A great deal of accurate data are required in order to test the model using the dynamic approach and great difficulty was experienced in finding a temporally-based data set appropriate for testing the model. In fact, only one comprehensive data set was found to be suitable for the dynamic testing of the model (see below). Inevitably, conclusions about the predictive ability of the model based on only one data set are limited both in statistical and geographical senses. The wide availability of regime data for alluvial channels from all over the world adds statistical

weight to conclusions drawn from the results of the temporally-based, dynamic model validation and questions of the wider validity of the model can also be at least partly addressed.

4.2 DYNAMIC VALIDATION

In any assessment of the predictive ability of a model based on comparing model predictions with observed prototype behaviour, uncertainty is introduced into the comparative analysis from a number of sources. There are two main sources of uncertainty in analyses of this type, which make it difficult to establish the true predictive ability of the model. First, observations of prototype behaviour are themselves subject to measurement error and uncertainty and in some instances it is not always possible to measure the complete range of data required as input to the model. Problems with data influence the ability to analyse the predictive ability of a model in direct and indirect ways. Measurement error or uncertainty leads to direct problems in analysing the predictive ability of a model since it is not possible to tell if discrepancies between observed and model data are due to inaccuracies in the model or in the data. Indirect problems also arise if there is missing data, or if data is subject to measurement error or uncertainty, as it is not possible to tell if the initial conditions programmed into the model exactly match the initial prototype conditions. However, if the model prediction is sensitive to the initial conditions, and in dynamical systems this may frequently be the case (*e.g.* Lorenz, 1963), subsequent model predictions may not match the observed data, even if the model in fact has perfect, or even adequate, predictive ability.

A second problem in comparing model predictions and observations is associated with the choice of the numerical values of empirical exponents and coefficients in the model equation set. The inevitable introduction of empirical coefficients and exponents into the turbulence closure, flow resistance and sediment transport equations can reduce the physical basis of the model if these values are varied from their standard, accepted, values in order to reduce any discrepancy between model predictions and prototype observations. Furthermore, since these coefficients and exponents have been determined using data sets gathered in particular environments, there is also uncertainty in choosing the numerical values of the empirical coefficients and exponents that should be used when they are applied to cases in which the environmental boundary conditions differ from those under which they were originally determined.

Where uncertainties of the type described above exist, it is not possible to tell if discrepancies or coincidences between observation and prediction are due to error and uncertainty in the observed data, error and uncertainty in the choice of the numerical values of empirical coefficients and exponents in the model itself, or simply due to the inability or ability of the model to simulate prototype behaviour correctly. Great care must, therefore, be taken to eliminate as much of this uncertainty from the comparison between observed and predicted data as possible. By reducing uncertainty associated with the observed data set, or taking it explicitly into account, it becomes easier to interpret the true meaning of any discrepancies - or agreement - between observed and predicted data. The approach taken in both the selection of the data set and the procedure used to perform the dynamic validation of the channel widening model were designed to take account of these problems. These approaches are now outlined.

4.2.1 Dynamic Validation: Data Selection and Quality Control

Temporally-based channel geometry data from the South Fork Forked Deer River (SFFDR) in West Tennessee, USA, which were originally collected by researchers with the United States Geological Survey (USGS), were used in an attempt to test model predictions of channel morphology through time. The study site is located in the Forked Deer River basin, which drains westwards to the Mississippi River (Figure 4.1). The South Fork Forked Deer flows through loess derived alluvium. There is a complete lack of bedrock control of local base level, allowing virtually unrestricted channel adjustment (Simon & Hupp, 1992). Prior to major deforestation in West Tennessee after the American Civil War, the undisturbed rivers of this region "flowed with good depths year round" (Ashley, 1910). Following deforestation, intense upland erosion and agricultural field gullying led to deposition of sediment on flood plains and in stream channels, resulting in loss of channel capacity, increases in sinuosity and increased flooding potential (Simon & Hupp, 1992). To reduce flood risk, most stream channels in West Tennessee had been dredged and straightened by 1926. However, these channelization works resulted in destabilization of river banks, bank erosion and sedimentation, as well as accumulation of organic debris from failed river banks (Simon & Hupp, 1992). As a consequence, from the late 1950s through to the 1970s, a variety of channelization projects were again undertaken in the West Tennessee drainage basins. These projects again destabilized many of the West Tennessee creeks, including the South Fork Forked Deer River (Simon & Hupp, 1992). The response of the streams of West Tennessee has followed an essentially similar pattern to that which followed the earlier phase of channelization, and this cycle of adjustment has been described and explained in considerable detail by the United States Geological Survey

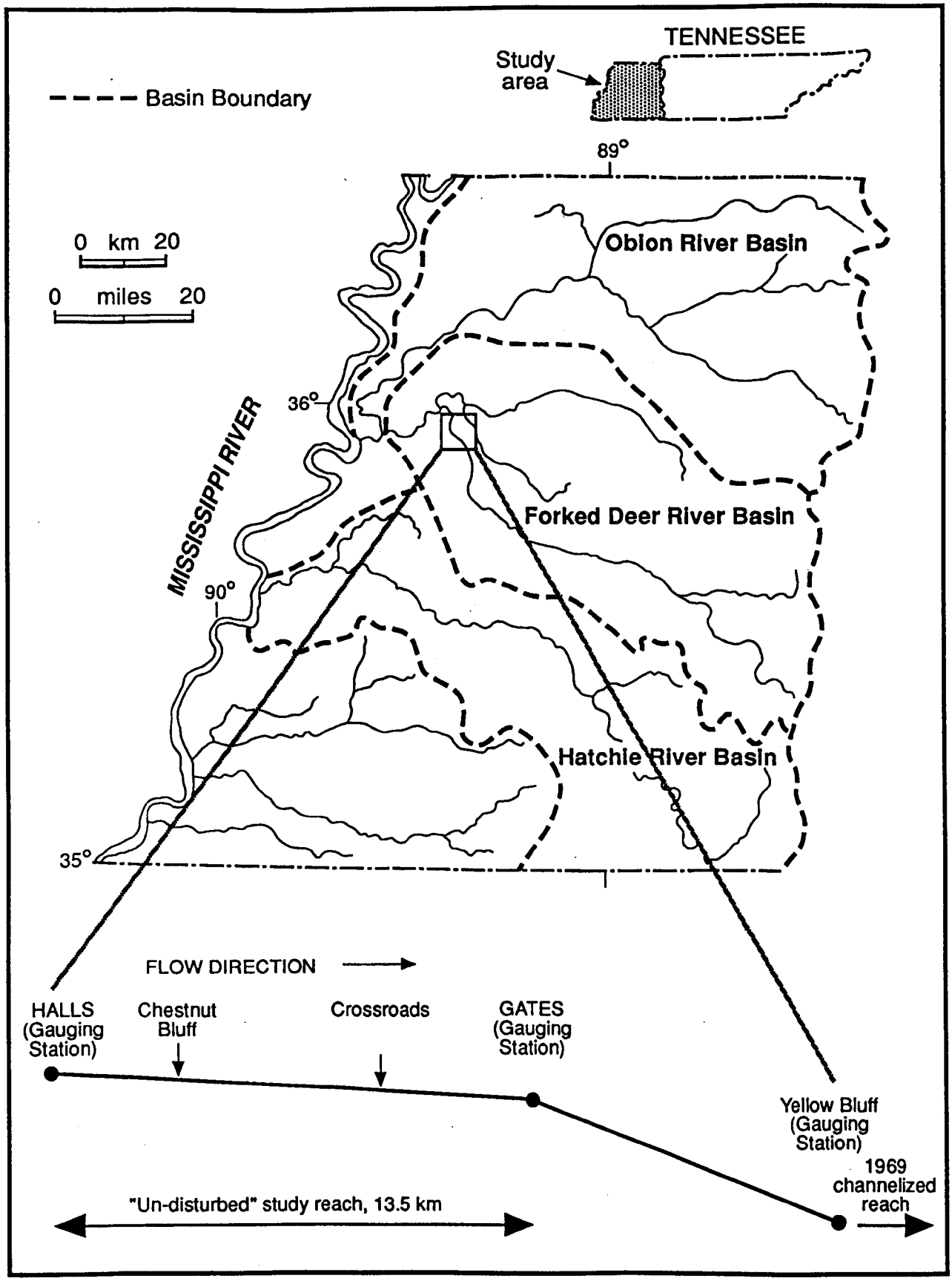

Figure 4.1 Diagram Showing Location of South Fork Forked Deer River Study Sites

(USGS) researchers (Simon & Hupp (1992, 1987, 1986ab), Hupp & Simon (1986, 1991), Simon (1989), Robbins & Simon (1983), Simon & Robbins (1987)).

Data collected in the course of the USGS studies of the geomorphic response of the destabilized West Tennessee streams formed the basis of the comprehensive set of data which describes channel adjustment of the South Fork Forked Deer River over the period 1969-1987. Measurements of bed and bank material properties, sediment discharges and repeated cross-section surveys were made during the course of this work, which was initiated in 1983. These data were supplemented with daily stage and discharge data from US Army Corps of Engineers gauging stations located in the study basin. Construction plans and surveys made by various groups were used to augment the USGS field measurements made during 1983-1987 over the entire West Tennessee region, to collate observations of channel change for the period 1969-1987. This foundation data set was further supplemented by additional fieldwork concentrated on the South Fork Forked Deer study sites. This latest phase of fieldwork was conducted in cooperation with the USGS in the summer of 1993 to produce an extensive set of data documenting the geomorphic response of the SFFDR at two study sites (Figure 4.1), Chestnut Bluff (RM 13.3) and Crossroads (RM 11.9), throughout the period 1969-1993. Observations throughout this period of channel adjustment at these two sites have been used to test the predictive ability of the numerical channel widening model.

The study reach (Figure 4.1) comprises a 13.5 km reach with an average channel gradient of 0.00016 and bounded at its upstream and downstream ends by the Corps of Engineers gauging stations. The reach is located just upstream of a 325m transition channel that was constructed in 1969 with a gradient of 0.0012 to connect the "undisturbed" reach to the downstream channelized reach. The simulated reach was extended downstream to the transition channel. Four cross-sections with known initial geometry were used in addition to the downstream boundary cross-section at the transition channel. Morphologic data were available throughout the period 1969-1993 for two cross-sections, Crossroads and Chestnut Bluff.

The West Tennessee data was selected for use in testing the channel widening model for a number of reasons. First, this data set contains a large amount of the high quality input data required to run the channel widening model. Second, the model was designed to be applied to rivers such as those found in West Tennessee: destabilized, sand-bed, cohesive-bank channels which are widening at relatively rapid rates. An important point is that relatively free adjustment of channel morphology has, in the

West Tennessee streams, continued at measurable rates over a relatively long period of time. Moreover, the various data have been collected at sufficiently short time intervals to allow a detailed picture of the adjustment process to be drawn. This is an important point - very few suitable data sets of channel adjustment exist, because channel surveys are usually conducted at long intervals, so missing the important details of the rapidly adjusting system. The West Tennessee streams are ideal, since adjustment has not been so rapid that all detail has been lost between surveys, but has not been so slow or small as to be undetectable. The final advantage of the West Tennessee streams is that they have tended to maintain a relatively straight planform throughout much of the period following the initial disturbance of the stream by channelization. This last point is clearly of fundamental importance in this study, since the model is applicable to straight channels.

Overall the SFFDR data set represents a data set of rare quality and quantity that is suitable for testing a channel adjustment model of the type developed in this research. No other data sets of comparable quality and scope, and which are applicable for straight channels with sand-bed and cohesive banks, are known to the writer. As such the SFFDR data set is the best, perhaps the only, set of data available for testing the channel widening model developed in this research.

Although the data are comprehensive, the channel widening model is complex and has heavy data requirements. The complete input data required by the channel widening model are summarised in Table 4.1. It is apparent that not all of the data required to run the widening model are available at the study reach. Furthermore, it is also possible that the data obtained at the study site are subject to measurement uncertainty or inaccuracy. Subjective estimates of the reliability of each item of data used in testing the model are also summarised in Table 4.1. Data were considered to be unreliable if measurement error or uncertainty exceeded ±20%.

For the variables in Table 4.1 which are either unknown, or judged as subject to enough uncertainty to warrant not being fixed at a single, baseline, numerical value, it is necessary to estimate the range of values which are thought most likely to safely represent that variable in the study reach of the South Fork Forked Deer River. The estimates of the range of these variables made for the purposes of the dynamic validation are summarised in Table 4.2. For each of these variables, sensitivity tests were conducted in order to account for the influence of uncertainty in the input variable on the model output. In this way the highest possible quality data were selected, but

Table 4.1 Estimated Reliability and Availability of Channel Evolution Model Input Data Used in Dynamic Validation

Variable	Symbol	Description	Reliability Estimate
Discharge	Q	Daily discharge data	Reliable
Stage	h	Stage at downstream boundary	Reliable
Sediment Inflow	Qs	Sediment discharge at upstream boundary	Reliable
Channel Gradient	S		Reliable
Channel Cross-Section Coordinates	x, y	Cross-section geometry	Reliable
Bank Height	H		Reliable
Bank Angle	α		Reliable
Bed Material Gradation	d_{50}	Median bed sediment diameter	Reliable
Bed Material Specific Gravity	SG		Missing
Bed Material Coulomb Friction Coefficient	μ		Missing
Bed Material Porosity	λ		Missing
Bank Material Geotechnical Characteristics	C, ϕ, γ	Cohesion, friction angle and unit weight soil frequency distributions	Reliable
Intact Bank Material Gradation	SAND d_{sand}	Percent sand content of bank material; size of sand	Reliable
Failed Bank Material Gradation	d_{bank}		Missing

where gaps in the quality were located, provision was made to determine the effect of the uncertainty so introduced.

It should be noted that the Manning's n hydraulic roughness is listed in Table 4.2 as an unknown or unreliable input variable. Strictly speaking, n is not an input variable, but is in fact estimated using the Strickler equation (equation 3.7), which relates the bed sediment diameter to Manning's n via an empirical coefficient. This coefficient may be interpreted as a "catch-all" coefficient representing the influence of channel shape, bedforms, vegetation characteristics and various other factors on the hydraulic roughness. In fact, it is the estimation of this coefficient that is subject to considerable uncertainty. However, since variation in Manning's n is easier to interpret physically, the uncertainty in estimating the correct value of the Strickler coefficient for the study site is presented throughout this chapter in terms of variation in the global Manning's n value. In each case, the prescribed range of Manning's n thought likely to safely cover the range of values in the study site was estimated, then the Strickler coefficient was varied to achieve this range for the given bed material diameter.

Table 4.2 Estimated Range of Unknown or Unreliable Input Variables in the SFFDR Data Set

Variable	Symbol	Estimated Likely Maximum Range
Bank Aggregate Diameter	d_{bank}	0.0001 - 0.01m
Manning's n	n	0.012 - 0.036
Bed Material Specific Gravity	SG	2.50 - 2.80
Bed Material Coulomb Friction Coefficient	μ	0.45 - 0.85

Care was taken to ensure that uncertainty arising from the use of other empirical coefficients and exponents in the model equations was reduced or taken account of in the assessment of the predictive ability of the model. First, as discussed previously, the observed data set was chosen to match as far as possible the conditions and constraints imposed in the model development. This also ensured that there was the best possible chance that comparisons between predictions and observations would represent a fair

trial of the channel widening model's accuracy, within the limitations set by the assumptions used to derive the model. Second, the influence of uncertainty in specifying the precise value of each of the model empirical coefficients and exponents for application of these equations in the study site was quantified in a series of sensitivity tests. The results of these sensitivity analyses are reported fully in chapter 5. For the moment it is sufficient to summarise by stating that predictions of channel morphology were in most cases found to be insensitive to variation in the numerical values of the empirical coefficients and exponents used in the model development. Hence, uncertainty over the accuracy of the specified values of the empirical coefficients and exponents for the special case of the study site environment appears in general to have a minimal effect on the model predictions. The exception to this rule is that the model output was found to be sensitive to variation in values of Manning's n, determined using the Strickler equation (equation 3.7), indicating that care must be taken in the selection of the value of this coefficient. The effect of variation in values of empirical coefficients and exponents on model predictions in the dynamic validation were, therefore, ignored in all cases with the exception of the Manning's n. In this case, sensitivity tests were undertaken in order to determine explicitly the influence of this uncertainty on the model predictions.

4.2.2 Dynamic Validation: Procedure

Having established the likely maximum range of the unreliable input data the known, or "reliable", input data were then used together with these best estimates of the unknown or "unreliable" input variables - the median values of the estimated range - to establish a set of baseline, numerical, input data. The output of the channel widening model obtained using this set of baseline input data was then compared to the observed data in order to assess the predictive ability of the model. Moreover, sensitivity tests were conducted for each of the unknown or "unreliable" input variables in order to establish the influence of varying an individual unknown or "unreliable" parameter over its estimated range on the model predictions. For each of the four variables outlined in Table 4.2, model runs were conducted for input data files representing both the upper and lower end of the prescribed variable ranges so that a total of 8 runs, in addition to the baseline run, were made. In this way the validity of the channel widening model was established, even taking account of the uncertainty associated with the estimated range of the unknown or uncertain input data.

Each of the total of 9 model runs conducted for the dynamic validation was conducted in the same way, with the aim of comparing the observations of channel

morphology made at the study sites with the model predictions. Observations of channel widening at the study sites were made at various intervals during a 24 year period between 1969 and 1993, but, due to the RAM limitations described in chapter 3, the numerical model developed in this research is able only to produce output for individual simulations over spans of approximately five years. In order to utilise the full set of observations, the 24 year observation period was broken down into five periods, each of approximately 5 years length. Simulations were then carried out over each period of these individual components. The procedure was to start the model run with the initial (1969) observed data. At the end of the first five year simulation period, the arrays containing the model output were directed to the model input files for the commencement of the second simulation period, as well as being directed to output files for storage. This procedure was repeated until the end of the 24 year simulation period had been reached. In this way, the model was able to simulate channel adjustment over the full 24 year observation period, instead of being limited to a 5 year simulation period as a consequence of the RAM constraint. It is stressed that the output arrays were not in any way corrected using observed data before being redirected to the input arrays for the start of subsequent simulations. Model predictions were then compared with the observed data in order to assess the predictive ability of the model.

It is important to stress once again that the assessment of the predictive ability of the channel widening model presented below takes account of the limitations of the observed data set. Furthermore, with the exception of the Manning's n (Strickler coefficient) the numerical values of empirical exponents and coefficients contained in the model have not in any way been manipulated or modified from their values presented in the equation sets in chapter 3, in order to calibrate the model during the testing process. Not only is the physical basis of the model thus retained, but the results of the comparison between observed data and model predictions presented below can, therefore, be reasonably assumed to adequately represent the true predictive ability of the (physically-based) model. Any agreement between observed and predicted data may reliably and justifiably be used to accept the validity of the channel widening model, just as any disagreement may reliably and justifiably be used to refute its validity. The overall accuracy of the model may, therefore, be quantified with a high degree of certainty.

4.2.3 Dynamic Validation: Results

Figures 4.2 and 4.3 show comparisons between the predicted and observed trends of channel morphology at the two study sections for which data are available

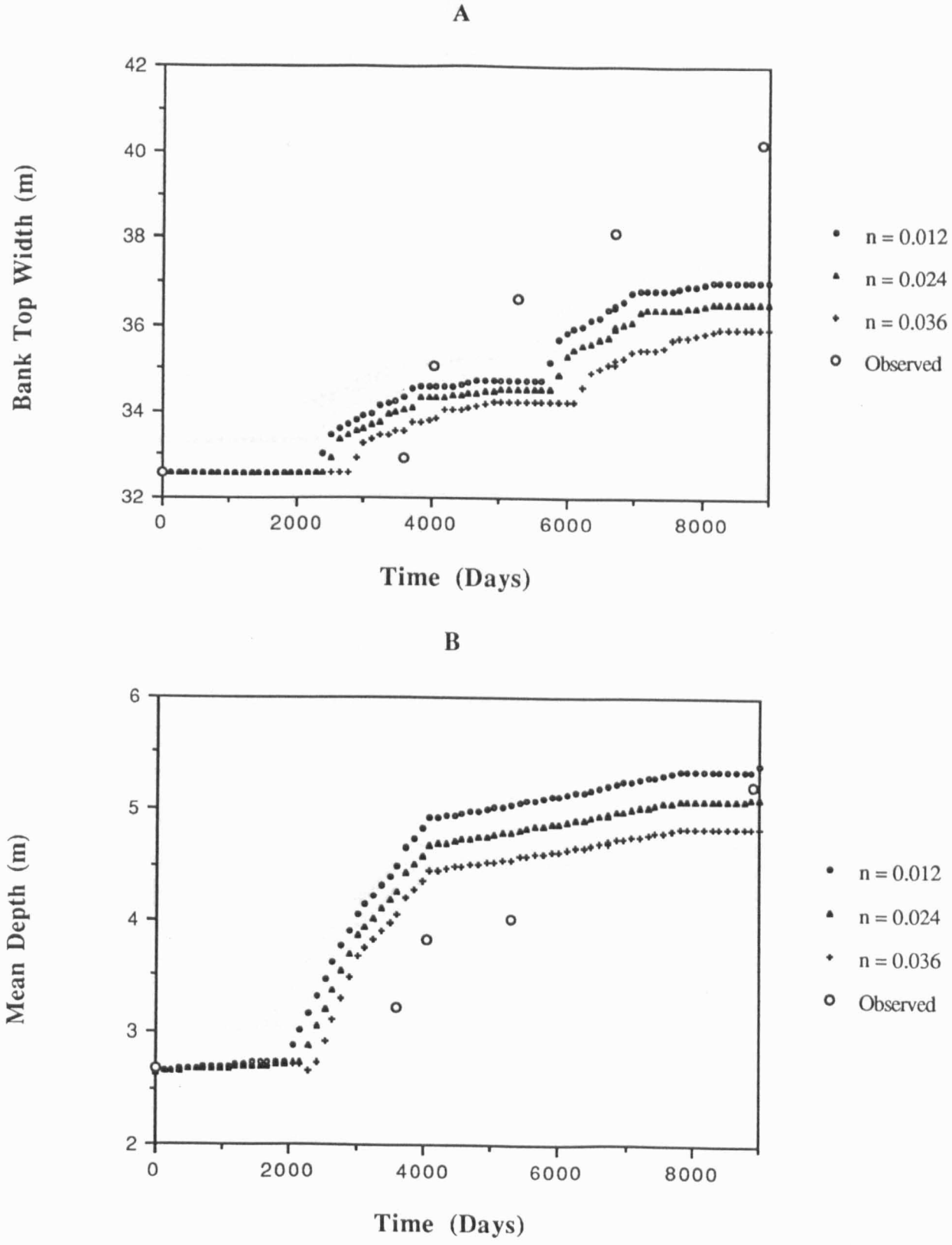

Figure 4.2 Predicted and Observed Temporal Trends of (A) Bank Top Width and (B) Mean Channel Depth at Chestnut Bluff

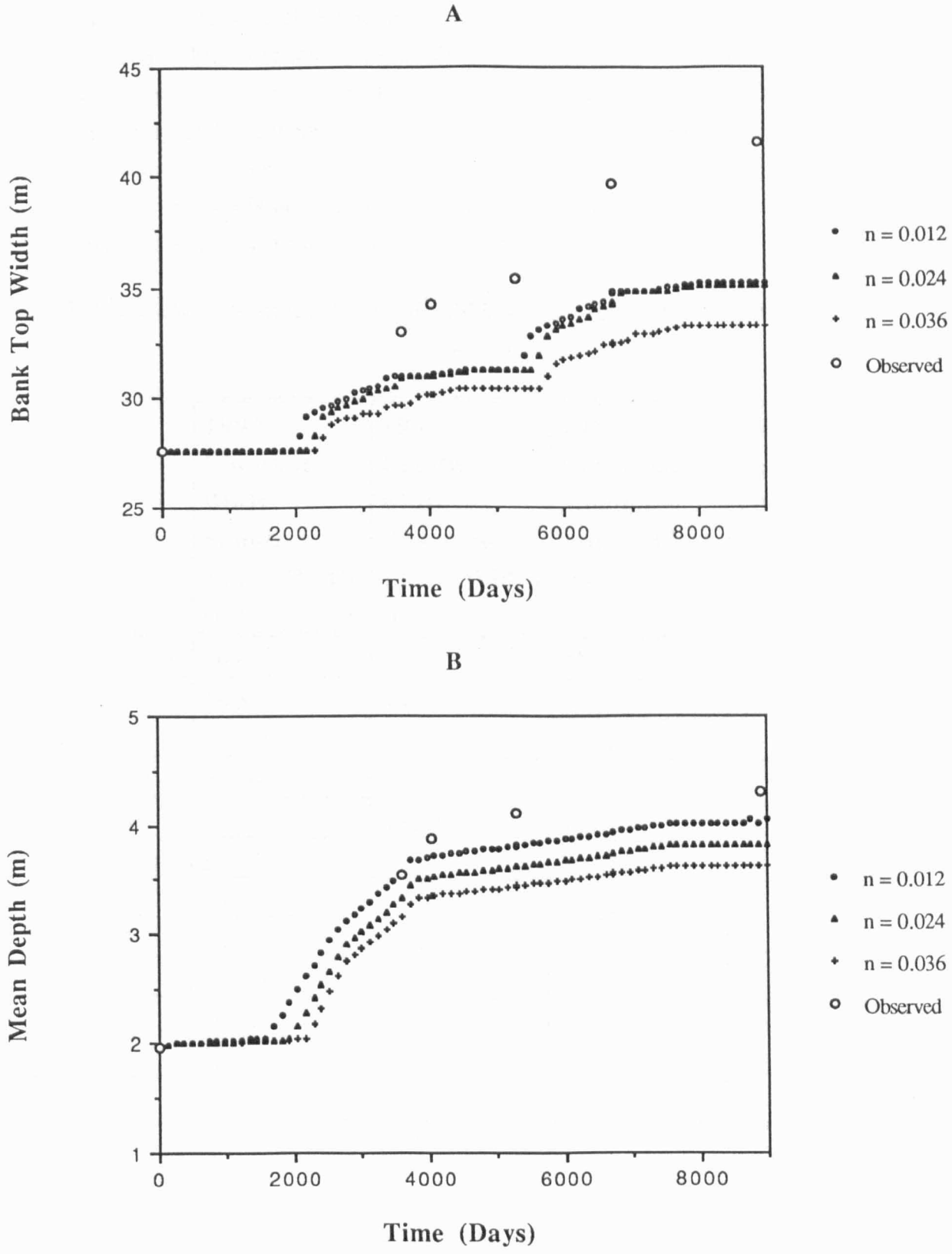

Figure 4.3 Predicted and Observed Temporal Trends of (A) Bank Top Width and (B) Mean Channel Depth at Crossroads

throughout the period 1969-1993. These figures illustrate the predictions for the baseline run (Manning's n = 0.024), together with runs representing the upper (n = 0.036) and lower (n = 0.012) bounds of the estimated likely maximum range of Manning's n (Strickler coefficient) values (Table 4.2). Only the sensitivity analyses for the Manning's n are presented here. Plots for the other three variables in Table 4.2 for which sensitivity analyses were conducted in the dynamic validation model runs are not presented because the model output is so insensitive to changes in these variables that the predicted variation is not easily seen in graphical form. Instead, the results from these remaining analyses are summarised in Table 4.3.

Table 4.3 Comparison of Observed and Predicted Bank Top Widths (Dynamic Validation)

Variable	1993 Chestnut Bluff Simulated Top Width (m)	1993 Chestnut Bluff Observed Top Width (m)	1993 Crossroads Simulated Top Width (m)	1993 Crossroads Observed Top Width (m)
$\mu = 0.50$	36.613	40.20	35.216	41.57
$\mu = 0.65$	36.532		35.051	
$\mu = 0.80$	36.426		34.921	
$d_{bank} = 0.1mm$	36.493	40.20	35.007	41.57
$d_{bank} = 1cm$	36.532		35.026	
$d_{bank} = 1.5mm$	36.507		35.051	
SG = 2.50	36.393	40.20	34.981	41.57
SG = 2.65	36.532		35.051	
SG = 2.80	36.728		35.208	
n = 0.012	36.997	40.20	35.100	41.57
n = 0.024	36.532		35.051	
n = 0.036	35.912		33.215	

Prior to discussing the predicted sequences of channel adjustment at the Forked Deer study sections illustrated in Figures 4.2 and 4.3, it is appropriate to briefly summarise the observed sequences of channel adjustment to which the predictions must be compared. Figures 4.2a and 4.3a show changes of observed bank top widths

between 1969 and 1993 at Chestnut Bluff and Crossroads, respectively. In both cases, the general pattern of width adjustment is similar. Initially, widths are stable, then they rapidly increase before the rate of widening slows as the system tends towards equilibrium. The initial, rapid widening phase occurs first at Crossroads (approximately day 2500) and then Chestnut Bluff (approximately day 3500). At the Crossroads site, there appear to be two distinct phases of widening, the first at day 2500, the second starting at about day 5500.

The observed sequences of widening appear, as expected, to be related to the sequences of depth adjustment, as evidenced from the observed changes in depth illustrated in Figures 4.2b and 4.3b. Initially, mean depths at both sites increase slowly and are relatively stable, but this relative stability is followed by rapid increases in mean depth. This rate of increase then appears to slow at both Chestnut Bluff and Crossroads. The rapid increase in mean depth appears to be related to a major phase of knickpoint degradation which migrates upstream through the study reaches from the area of maximum disturbance (AMD) associated with the 1969 channelization and dredging works downstream of Crossroads (Figure 4.1; Simon & Hupp, 1992). The degradation phase therefore reaches Crossroads prior to reaching Chestnut Bluff. Hence, widening appears to be in response to destabilization of the river banks as a result of bed degradation caused by knickpoint migration upstream from the AMD through the study reach. This explains why the observed widening is delayed until day 2500 at Crossroads and day 3500 at Chestnut Bluff. Following the initial rapid increase of depth as a result of this degradation, the rate of increase of channel depth slows as the channel tends towards some degree of stability.

Figures 4.2 and 4.3 show that the channel widening model predicts the trends and sequences of channel adjustments outlined above quite well. Initially, no widening is correctly predicted at both Chestnut Bluff and Crossroads. The predicted timing of the onset of widening at Chestnut Bluff and Crossroads appears, in both cases, to be earlier than that actually observed. Nevertheless, the model correctly predicts that widening is initiated at Crossroads prior to Chestnut Bluff, for the entire range of Manning's n values used in these tests. At both sites the model correctly predicts that widening rates are relatively rapid, then slow and become almost negligible. However, the model clearly underpredicts the magnitude of these initial widening rates at both Chestnut Bluff and Crossroads, leading to an increasingly large divergence between observed and predicted widths with time. However, the absolute magnitude of even the largest discrepancy is within about 15% of the total channel width, indicating that overall agreement between predicted and observed widths is generally acceptable. In

fact, this largest discrepancy corresponds with what is considered to be an anomalous observation at Crossroads in 1993, because of local channel re-alignment associated with the construction of a new bridge in the Crossroads reach during 1992.

The model also predicts a second phase of widening followed by restabilization at both Chestnut Bluff and Crossroads. Again, the second phase of predicted widening occurs first at Crossroads. However, while the predicted onset of this second phase (approximately day 5500) appears to be very close to the observed timing of the onset of the second widening phase at Crossroads (approximately day 5500), no such second widening phase was observed at Chestnut Bluff. Hence, predicted and observed widths again begin to converge at the Chestnut Bluff site after about day 5700, but for apparently the wrong reason, while predicted and observed widths continue to disagree at Crossroads despite the success of the model in predicting the onset of a second phase of widening at this site!

Model predictions of mean channel depth also are qualitatively similar to the observed sequences of depth adjustment, though in detail and in quantitative terms there are discrepancies between predicted and observed adjustment sequences. At both sites, depths are initially relatively stable, before degradation passes through each site, resulting in rapid increases of mean depth. The model correctly predicts that major degradation, in response to upstream knickpoint migration, is experienced first at Crossroads, then at Chestnut Bluff, but the time lag between the onset of degradation at the two sites appears to be small (about 300 days). However, this represents a headward migration rate of about 2.7 km/y. This predicted rate of knickpoint migration is the same as that observed between these two sites by Simon & Hupp (1992), although this agreement may be fortuitous. The lag in the onset of widening associated with bank destabilization as a consequence of this deepening phase also appears to be correctly predicted by the model at both sites.

Despite almost contemperaneous widening associated with this degradation phase, which results in considerable quantities of bank materials being delivered to the channel, depths continue to increase between about days 2000 and 4000 at both sites, indicating that deepening is predicted to continue throughout the initial width adjustment period. Quantitative agreement between predicted and observed depths is excellent throughout the model simulation at Crossroads, with a slight tendency for underprediction of depth at this site. However, at Chestnut Bluff predicted depths are somewhat larger than observed depths, except in 1993 (about day 9000). After day 4000, depths are predicted to increase much less rapidly at both sites. Indeed, the

predicted depths are almost stable from this point in time. This corresponds with the tendency for channel depths to recover as the channel widens and sediment is supplied to the widening reaches from bank failures and bed degradation at upstream sites.

The sensitivity analyses for the 4 uncertain variables, Manning's n (Strickler coefficient), bed material specific gravity, bank material aggregate diameter and Coulomb friction coefficient all show that, with the exception of the Manning's n (Strickler coefficient), varying the value of the variable over even its entire estimated range has little effect on the predicted bank top width. Although Table 4.3 and Figures 4.2 and 4.3 clearly indicate that the predicted morphology is sensitive to variation in the Manning's n, this sensitivity is not large enough to reduce significantly the predicted underprediction of bank top width by the model, for even the lowest value of 'n' (0.012). In any case, the use of this low value results in a yet more rapid onset of widening, *increasing* the error in the predicted date of the onset of widening. It follows that uncertainty in specifying the values of the unreliable data is insufficient to effect significantly the agreement between predicted and observed data. Adjustment of the model input data to account for potential uncertainty in these variables does not, therefore, either significantly increase or decrease the apparent predictive ability of the model. In summarising the predictive ability of the model, therefore, it is appropriate to consider only the baseline run, because the impact of uncertainty associated with unreliable or missing data on model predictions of channel morphology appears to be small.

The ability of the model to predict adjustment of channel morphology using the baseline run data is summarised in Figures 4.4a and 4.4b, which show comparisons between observed and predicted widths and depths, respectively, at observational points throughout the adjustment sequence at Chestnut Bluff and Crossroads. Figure 4.4a suggests that overall agreement between predicted and observed bank top widths is good, though predicted widths are, for the most part, smaller than observed widths. It appears that underprediction of channel width is greater at the Crossroads site than at Chestnut Bluff. Figure 4.4b shows that agreement between observed and predicted depths is good, though the results are somewhat more variable for channel depths than channel widths. Channel depth is overpredicted at Chestnut Bluff, but underpredicted at Crossroads. Overall, channel depths appear to be slightly overpredicted by the model.

To determine the performance of the channel widening model objectively, the mean of the discrepancy ratio (Me): a measure of the deviation between predicted and observed values for the data set as a whole; and the mean absolute deviation of the

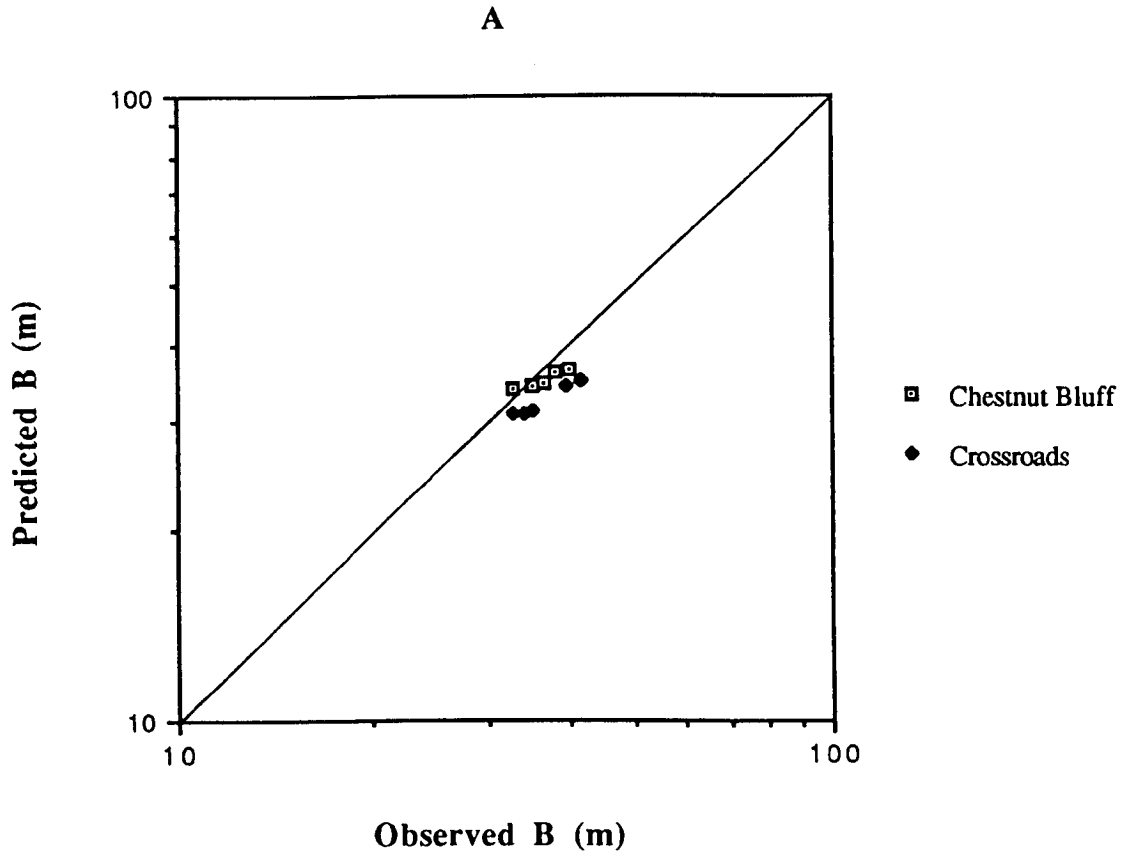

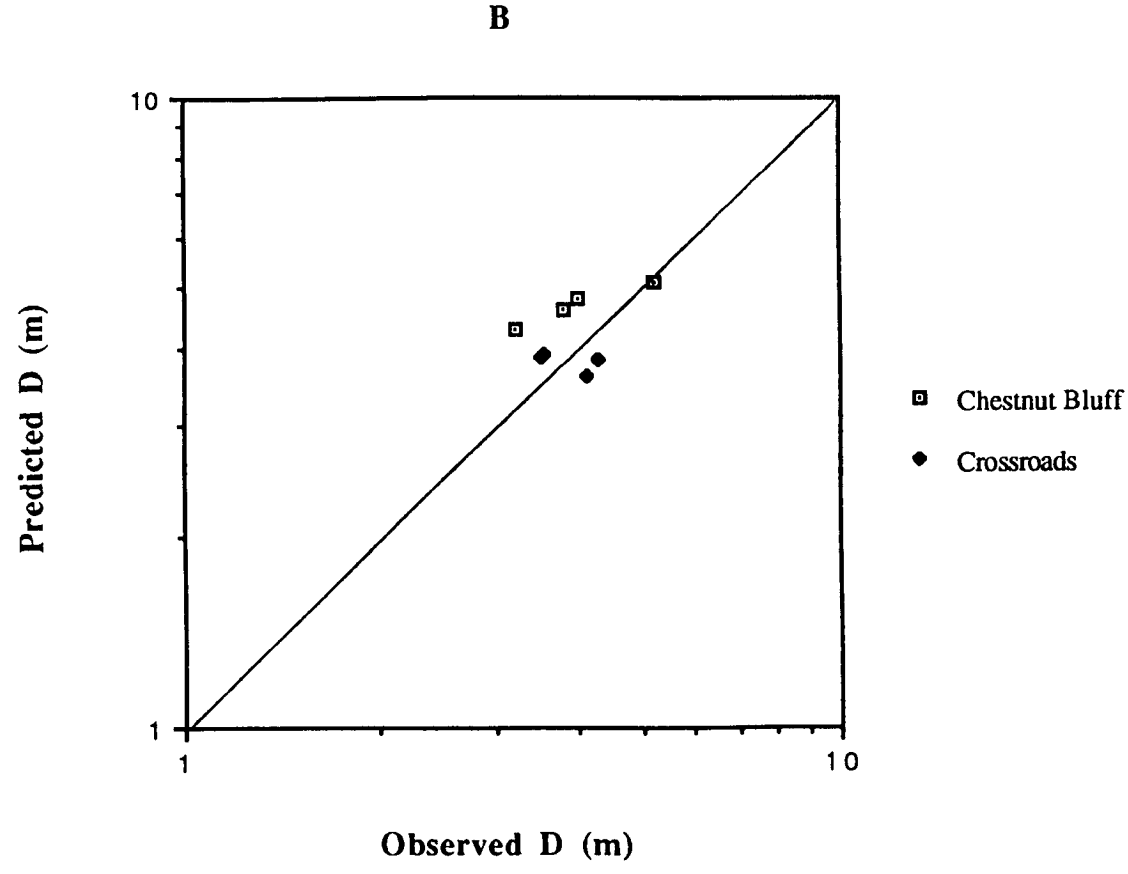

Figure 4.4 Summary Comparison of Predicted and Observed (A) Widths and (B) Depths

discrepancy ratio (Ad): a measure of the degree of scatter, were used to quantify the predictive ability of the model:

$$Me = \frac{1}{n} \sum_{i=0}^{n} \left(\frac{B_p}{B_o} \right) \tag{4.1}$$

$$Ad = \frac{1}{n} \sum_{i=0}^{n} \left| \left(\frac{B_p}{B_o} - Me \right) \right| \tag{4.2}$$

where n = number of data points, B_p = predicted channel width (or predicted aspect ratio or channel depth) (m) and B_o = observed channel width (or observed aspect ratio or channel depth) (m). It follows that perfect agreement is indicated when Me = 1 and Ad = 1.

Table 4.4 Summary of Calculated Me for Channel Morphology Variables (Dynamic Validation)

Variable	Chestnut Bluff	Crossroads	Overall
Width	0.962	0.887	0.925
Depth	1.176	0.990	1.040
Aspect Ratio	0.822	0.985	0.903

The calculated mean discrepancy ratios for the various channel morphology variables at Chestnut Bluff and Crossroads are summarised in Table 4.4. The calculated overall mean discrepancy ratio of 0.925 for the baseline channel width run confirms the impression gained from Table 4.3 and Figures 4.2, 4.3 and 4.4 that the agreement between predicted and observed bank top widths is good, though the model underpredicts the bank top width. The calculated mean absolute deviation of the discrepancy ratio of 1.059 also indicates a relatively low level of scatter. The calculated overall mean discrepancy ratio of 0.903 for the baseline channel aspect ratio indicates that the overall agreement between predicted and observed aspect ratios is also good, though the model again underpredicts this variable. There is also more scatter in this variable (Ad = 1.199). The similarity of the underprediction of widths and aspect ratios indicates that most of the error in B/D ratio is probably due to the underprediction of

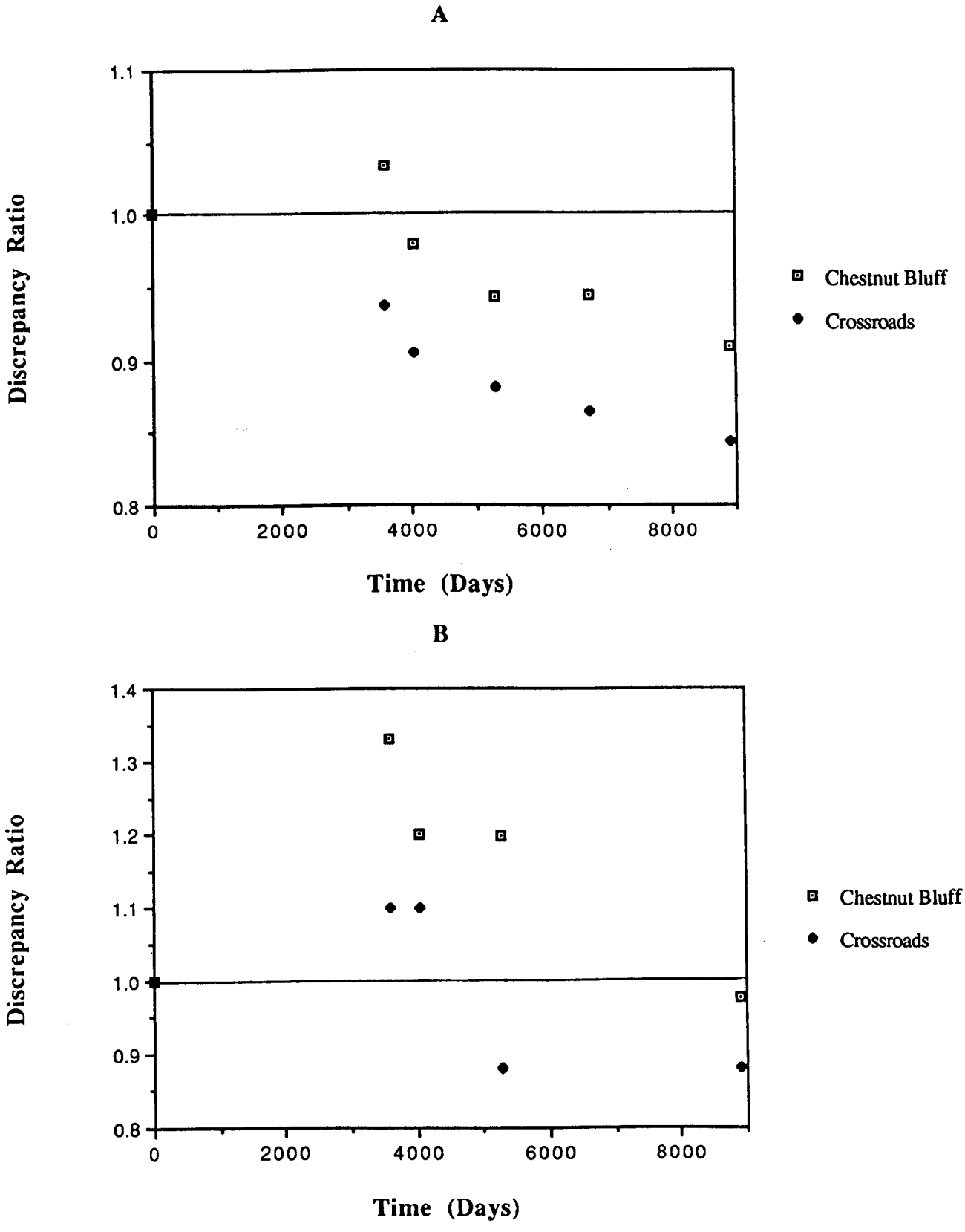

Figure 4.5 Temporal Trends of Discrepancy Ratios for (A) Width and (B) Depth

channel width. This is confirmed by the calculated overall mean discrepancy ratio of 1.04 for channel depth (Ad = 1.38), indicating slight overprediction of this variable.

In fact, it can be shown that discrepancies between predicted and observed bank top widths and depths vary systematically through time at both Chestnut Bluff and Crossroads. Figure 4.5 shows discrepancy ratios (the ratio between predicted and observed bank top width) plotted versus time at each study site. Agreement between predicted and observed widths (Figure 4.5a) is good in the initial stages of the simulation, then rapidly falls after about 2-3000 days of simulation time, as the model begin to systematically underpredict the initial phase of widening (Figures 4.2 and 4.3). The magnitude of the underprediction continues to grow (discrepancy ratio continues to decrease below unity) for the rest of the simulation as the predicted and observed widths continue to diverge. It appears that the divergence through time between predicted and observed widths ultimately stabilises at a constant value, when both observed and predicted widening rates fall to negligible values: that is at the point when both model and prototype widths are "stable". An important point is that even the worst discrepancy ratio of about 0.84 at the Crossroads site in 1993 still represents acceptable agreement between predicted and observed widths, and recall that this is also considered to be an anomalous observation. There does not appear to be a simple temporal trend of discrepancy ratio for channel depth (Figure 4.5b).

Overall, the dynamic validation analysis indicates that the numerical model is able to qualitatively simulate the observed *sequence* of events in this reach of the South Fork Forked Deer River very well. Errors in predicting observed channel widths and depths are generally small, even though there is divergence between observed and predicted widths through time. Since adjustments to channel depth are predicted reasonably well as in the case of Crossroads, or are overpredicted as is the case with Chestnut Bluff, it appears that width underprediction (which is greatest at the Crossroads site) may not be related to underpredictions of bank height and factor of safety of the channel banks. Indeed, the fact that widening trends are correctly predicted is evidence that factor of safety trends are also correctly predicted. Instead, while the timing and onset of bank instability appears to be correctly predicted by the model, two factors seem likely to have caused the underprediction of width:

1. Failure block widths (which determine the widening rate) may be systematically underpredicted by the bank stability algorithm, and
2. By forcing simulated failures through the toe of the bank, the entire bank is continually flattened with each successive failure, leading to more stable conditions.

Darby & Thorne (in press) have recently highlighted some of the problems of accurately predicting failure block width using the Osman-Thorne analysis, which was used as the foundation analysis for the basic stability algorithm used in this model. These problems have also been discussed in this thesis (see chapter 3). They illustrated that the Osman-Thorne analysis does indeed tend to underpredict failure block widths and went on to present a method that resulted in improved predictions of failure block geometry. It may be the case that channel widening predictions could be improved by using a more sophisticated bank failure geometry model, such as that developed by Darby & Thorne (in press) rather than the original Osman & Thorne (1988) analysis. However, no attempt was made to incorporate the Darby-Thorne analysis into this model, due to difficulties in applying the new model within a probabilistic framework (see Chapter 3).Similarly, the Osman-Thorne analyses constrain the failure surface to pass through the toe of the bank, negating the possibility of slope failures occuring in conjunction with the toe failures accounted for by their model (Simon *et al.*, 1991). It is recommended that these deficiencies should be rectified in future research.

4.3 REGIME VALIDATION

4.3.1 Regime Validation: Data Selection

There is a wide range of existing empirical regime data that could potentially have been used to test the ability of the model to predict stable channel geometries. As discussed in section 4.2.1 it is important to select a data set that contains as much of the detailed information required by the model as possible (Table 4.1), in order to reduce uncertainty associated with missing or unreliable data. However, the very nature of regime equations, which are intended to be simple relations between one or two independent variables (usually discharge and/or sediment characteristics) and channel geometry variables (width, depth, slope) means that their associated data bases frequently do not contain all of this required data. In this study, the regime relations presented by Simons & Albertson (1963), based on data from Indian and US canals, were used in an attempt to test the ability of the model to predict stable channel geometries. The Simons & Albertson regime equations were selected for use in this study because the classificatory approach used by them explicitly includes a regime relation for the general type of river channel for which the channel widening model has been developed (sand-bed and cohesive banks). In any case, the regime relations presented by Simons & Albertson are quite similar in form to many other regime and hydraulic geometry studies (see chapter 2), in which the exponent on the discharge in

the width equation tends to vary in a narrow range between about 0.45 and 0.52 (Table 2.1). This compares well with the value of 0.493 in the Simons & Albertson equation (equation 4.10, below). The main aim of the regime validation experiments was to attempt to replicate the value of this exponent using model simulations, as evidence of the model's ability to replicate successfully the tendency of many natural river channels, as evidenced by the empirical regime relations, to have stable widths that are proportional to approximately the square root of the channel forming discharge.

4.3.2 Regime Validation: Procedure

The procedure was as follows. Having selected the regime equation for the type of channel of interest, this equation was used to back calculate the "observed" stable channel geometries for a range of specified discharges. In this case, the Simons & Albertson (1963) regime equations applicable to "Type 2" channels - sand bed with slightly cohesive to moderately cohesive bank materials, were selected. The Simons & Albertson equations summarise observed stable channel data from Indian and US canals in the form of the following regression equations which were developed in US Customery units:

$$P = 2.6\, Q^{0.5} \tag{4.3}$$

$$B_b = 0.9\, P \tag{4.4}$$

$$B_b = 0.92\, B - 2.0 \tag{4.5}$$

$$R = 0.44\, Q^{0.36} \tag{4.6}$$

$$D = 1.21\, R \qquad (R \leq 7 \text{ ft}) \tag{4.7}$$

$$D = 2 + 0.93\, R \qquad (R \geq 7 \text{ ft}) \tag{4.8}$$

$$V = 16.0\, (R^2\, S)^{0.33} \tag{4.9}$$

where P = wetted perimeter (ft), R = hydraulic radius (ft), S = channel gradient, Q = discharge (cfs), B_b = bed width (ft), B = top width (ft) and D = flow depth (ft). In SI units, the equation for the bank top width is written:

$$B = 4.842\ Q^{0.493} \qquad (4.10)$$

For any specified discharge, the input data modules were then programmed with the calculated initial values of channel morphology, roughness and bed and bank boundary material properties, together with any required boundary conditions (stage-discharge relationship at the downstream boundary; sediment load at the upstream boundary) and the model run, in an attempt to match the model predictions with these "observed" regime channels at the appropriate value of the discharge. One problem with this approach is that although the regime equations give information about the gross stable channel geometry (width, depth, slope), there is no data available explicitly for the bank morphology, hydraulic roughness, bed and bank boundary material properties, sediment loads or stage-discharge curves at the sites of interest.

To overcome these data limitation problems it is necessary first to make an assumption about the cross-section shape of the regime channels in the Simons & Albertson data set. In this study, following the explanation of the Simons & Albertson design method reported by Henderson (1966), the stable channel cross-sections were assumed to be trapezoidal. This allows the "observed" bank angles to be calculated directly from equations (4.4) and (4.10) for the bed width and top width, respectively. Since the regime channels are, by definition, stable over moderate time scales, upstream boundary sediment loads were set equal to the transport capacity at the first model cross-section, in order to be consistent with the regime concept that the channel on average neither scours nor fills. Since regime equations are commonly developed for a channel forming "dominant" discharge flow which is frequently assumed to be close to the bankfull stage (Wolman & Leopold, 1957; Dury, 1961; Hey, 1975), the specified discharge may be assumed to occur at approximately the bankfull stage. This assumption allows the downstream stage-discharge boundary condition to be estimated. The assumption that the channel forming discharge is close to the bankfull stage is probably reasonable for the regulated canals studied by Simons & Albertson (Inglis, 1963). Having constructed the regime cross-sectional geometry and flow stage, the hydraulic roughness was calculated for the imposed discharge using Manning's equation. To reflect the nature of the applicability of both the channel widening model and the regime equations, which were derived using data from canals, the planform was assumed to be straight and the geometry of each model cross-section was assumed uniform. Four model cross-sections were used in each simulation. Output data was found to be consistent at the two sections located in the mid part of the hypothetical channel. Data from these sections were used to construct the model generated regime relations. The initial model channel bed and top widths were both set equal to 0.75 of

the regime width as determined from the Simons & Albertson equations, in order to simulate the adjustment (widening) of a channel towards a width in equilibrium with the imposed flow from an initial condition where the width is "too narrow" for the imposed discharge (Figure 4.6).

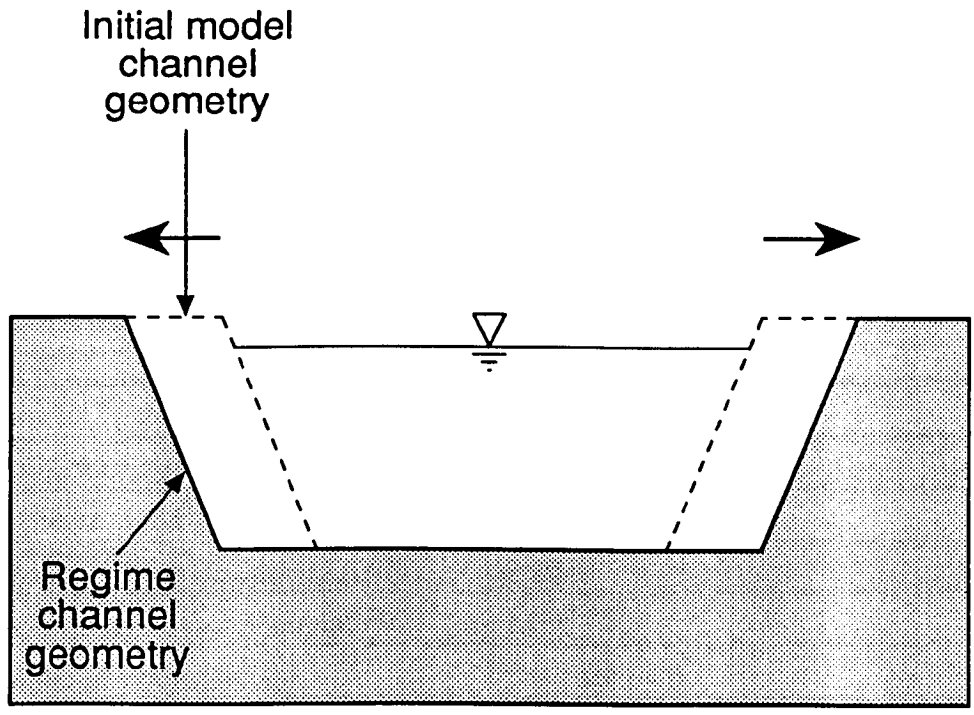

Figure 4.6 Diagram of Initial Cross-Section Geometry Used in Regime Validation Analyses

The remaining input variables to be estimated describe the physical properties of the bed and bank boundary materials. These are the gradation of bed and bank materials; cohesion, friction angle and unit weight of the bank materials; specific gravity, porosity and Coulomb roughness coefficients of the bed material. The classificatory approach used by Simons & Albertson means that the precise numerical values of these parameters are unknown, but must nevertheless be estimated for programming into the model input data modules. However, since the aim is to replicate the general form of an equation derived from empirical data summarising a range of sites, with different boundary material properties at each individual site, the uncertainty introduced by this "missing" data is not a significant limitation for the purposes of this analysis. Instead, it is acceptable to use values which reflect generalised properties of a sand-bed stream with moderately cohesive bank material, in an attempt to replicate the empirically-derived *general* channel geometry trends as a function of discharge, rather than attempting to predict the stable channel geometry of the *individual* sites that were used to derive the Simons & Albertson regime equations. This approach contrasts with the

much more detailed analysis of the ability of the model to predict channel widening through time on individual cross-sections of the South Fork Forked Deer River (see section 4.2). However, the more detailed, but statistically limited, dynamic validation analyses are nevertheless complemented by these less detailed analyses of stable channel geometries because they are based on a much more extensive body of data. The values of the bed and bank boundary material properties used in the regime validations are summarised in Table 4.5. These values were selected to be representative of sand-bed streams with moderately cohesive bank materials.

Table 4.5 Summary of Boundary Material Characteristics Used in Regime Validation

Variable	Estimated Value
Bed Material Diameter (d_{50})	1mm
Bank Material Aggregate Size (d_{bank})	10mm
Bank Material Sand Size (d_{sand})	1mm
Bank Material Sand Fraction (SAND)	0.20
Specific Gravity of Bed Material (SG)	2.65
Bank Material Cohesion (C)	See Table 4.6
Bank Material Friction Angle (ϕ)	See Table 4.6
Bank Material Unit Weight (γ)	See Table 4.6
Bed Material Coulomb Friction Coefficient (μ)	0.65

The estimates of the values of the boundary material properties made in Table 4.5 are probably reasonable for sand-bed streams with cohesive bank materials. In any case, with the exception of the intact bank material geotechnical properties, the results of sensitivity tests conducted in Chapter 5 indicate that predictions of channel morphology are for the most part relatively insensitive to the variables in Table 4.5. In order to account for potential uncertainty in specifying the exact characteristics of the bank material geotechnical properties, an attempt was also made to account explicitly for the influence of varying the bank material characteristics within the general Simons & Albertson category of "moderately cohesive to cohesive bank materials" on the simulated results. One problem with this is that, for the channel widening model developed here, the bank material properties of cohesion, friction angle and unit weight must be specified as frequency distributions. To overcome the problem of not being able to specify either absolute values of geotechnical parameters or their frequency

distributions, the soil frequency distributions from the West Tennessee streams used in the dynamic validation were used as a baseline bank material that fits into the Simons & Albertson category (see Appendix B). This baseline soil frequency distribution has relatively low cohesion values, but high friction angle values, tending to give moderate to high shear strength values that are probably in the mid to upper range of the Simons & Albertson category. By holding the unit weight and cohesion frequency distributions constant and progressively reducing the positive skew in the friction angle distribution, two more model bank material categories (in addition to the baseline data) were derived in order to represent the possible range of soil shear strength values within the Simons & Albertson category more realistically. The modal values of each of the geotechnical properties for the three bank material categories used in the regime validation are summarised in Table 4.6, while the complete frequency distributions are presented in Appendix B. It is apparent that the geotechnical resistance of the bank material is progressively, but moderately, reduced from category BM1 to BM3.

Table 4.6 Summary of Geotechnical Characteristics of Bank Material Categories Used in Regime Validation

Bank Material	Unit Weight (kNm^{-3})	Cohesion (kPa)	Friction Angle (Degrees)
BM1	19.0	7.5	32.5
BM2	19.0	7.5	22.5
BM3	19.0	7.5	17.5

Having determined the stable channel morphology for the specified discharge from the regime equations and set the model input data files to match this initial morphology in all respects apart from the reduced channel width, the specified discharge was run through the model. In effect the simulated channel was designed to represent a channel stable in all respects apart from the channel being too narrow for the imposed, steady discharge. The model was allowed to simulate the consequent tendency of the narrow channel to adjust to a wider, stable channel form in equilibrium with the imposed discharge (Figure 4.6). These experiments were repeated for a range of discharges in order that a model generated regime equation could be constructed and compared to the relevant empirically-derived ("observed") Simons & Albertson regime equation. In this way predicted stable channel widths were compared to the corresponding "observed" stable channel widths determined from the empirically-derived Simons & Albertson

regime data in order to assess the ability of the model to predict stable channel geometries.

It is important to stress that the procedure used here to obtain simulated stable channel geometries is not a definitive assessment of the ability of the channel widening model to simulate the adjustment of a river channel from any arbitrary initial point that is out of regime for the specified discharge to a form that more closely reflects the channel form predicted by the empirically-derived regime equation. Rather, this study is intended to be a more limited analysis designed to demonstrate the ability of the physically-based model to predict correctly adjustment of form from an initially narrow channel to a more stable width, by processes of fluvial erosion, sediment transport and mass wasting, over a range of values of discharge. It might otherwise be argued that the procedure used to predict regime widths is limited conceptually, since two of the three degrees of freedom of channel adjustment (slope and depth) are set equal to their regime values for the prescribed discharge. Therefore, it could be argued, it is not surprising if the model does predict stable channel widths, since most of the answer is already given as the initial condition. Why not, then, set an initial channel that is also out of regime with respect to depth and slope for the specified discharge, in order to "more fairly" test the ability of the model to adjust to a stable channel geometry?

However, an argument of this type is not justified in the context of this study. First, while the channel is indeed initially set to be out of regime with respect to width only, this condition still represents an arbitrary initial condition from which all of the degrees of freedom (including the depth and slope) are free to adjust to a new channel in equilibrium with the imposed flow. That is, although the initial values of channel depth and slope are prescribed as regime values, these variables are still free to change during the simulation as the width changes to a condition closer to its regime value. Second, a more detailed analysis of the ability of the model to adjust to regime depths and slopes, in addition to widths, from a wider range of out of equilibrium initial conditions is not warranted for the purposes of this study, where the aim is to determine the ability of the model to predict the exponent in the various empirically-derived regime width equations. The emphasis on the width equation alone not only serves to highlight this neglected dimension of adjustment, but the value of the exponent in empirically-derived regime width equations is anyway more consistent, and more widely agreed upon, than either of the depth or slope regime equations. This implies that comparisons between simulated and empirically-derived slope and depth equations would in any case be more difficult to interpret than comparisons between predicted and empirically-derived width equations.

4.3.3 Regime Validation: Results

The results of the regime validation are summarised in Figure 4.7. This plot shows the model generated regime width relationships for each of the bank material categories. The Simons & Albertson Type 2 channel regime relationship is also shown for comparative purposes. It can be seen that the model generated and empirically-derived curves are similar in form, with near equal gradients on the log-log plot. This is confirmed by the similarity of the value of the exponents on the discharge for the empirically-derived and model generated curves (Table 4.7). Furthermore, the values of the simulated exponents all fall within the range of empirically-derived exponents summarised in Table 2.1.

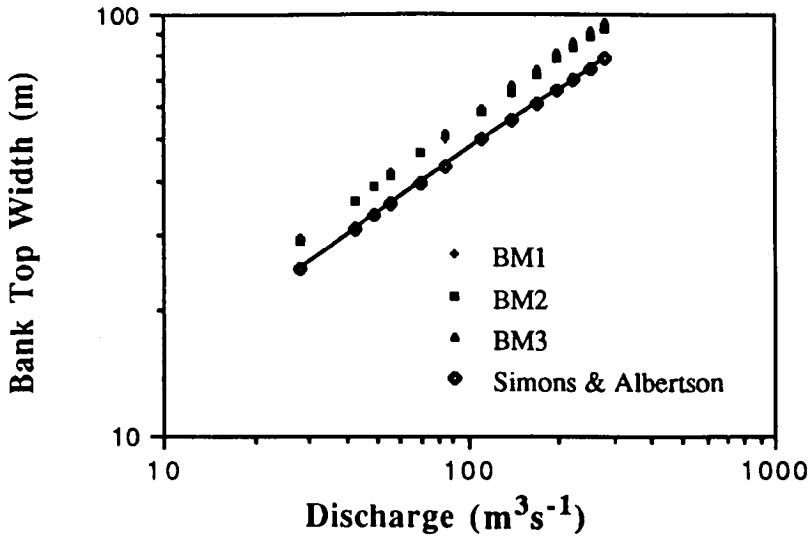

Figure 4.7 Comparison of Model-Generated and Simons & Albertson (1963) Regime Width Equations

However, while the gradients of the model and empirically-derived curves are similar for all the model simulations, indicating the empirically-derived and model generated hydraulic geometry relationships are broadly similar in form, the intercepts are quite distinct (Table 4.7), so that quantitative agreement is less good. It appears that although the model generated regime equations are correct in form, the model overpredicts channel width when compared with Simons & Albertson's empirically-derived regime curve, even for the most resistant bank material category, BM1. The exponent values and intercept values both vary systematically with bank material category. As bank strength is reduced, the exponent increases while the value of the intercept decreases. The increase in exponent value offsets the decrease in the intercept

value such that, as expected, the model predicted widths progressively increase as bank material strength is reduced.

Table 4.7 Model Generated and Empirically-Derived Regime Width Equations

Source	Regime Width Equation
Simons & Albertson (1963)	$B = 4.842\ Q^{0.493}$
Model Simulation BM1	$B = 5.439\ Q^{0.503}$
Model Simulation BM2	$B = 5.411\ Q^{0.504}$
Model Simulation BM3	$B = 5.213\ Q^{0.516}$

Although the model overpredicts the width relative to the Simons & Albertson regime equation, for all the modelled bank material categories, overall agreement between empirically-derived and model predicted channel geometries is good, with mean discrepancy ratios (Me) of the order of 1.18 (Table 4.8). Calculated mean absolute deviations of the discrepancy ratio (Ad) of the order of unity also indicate that there is little scatter in the calculated discrepancy ratios, indicating that the overprediction error is systematic over the range of simulated discharges. Moreover, Table 4.8 also shows that, while agreement between "observed" and predicted data is improved by decreasing bank material strengths, this improvement is not particularly significant, since predicted widths appear to be insensitive to the range of bank material properties used in this analysis. Attempts to improve the agreement between the model generated and the empirically-derived Simons & Albertson regime equations by calibrating the soils properties within the range described by the Simons & Albertson category were not, therefore, particularly successful.

The apparent insensitivity of channel width to the bank material categories chosen in this analysis is an intriguing result. Recent analyses of empirical data have suggested that the bank material properties and vegetation characteristics have a significant influence on the establishment of the stable channel width (*e.g.* Charlton *et al.*, 1978; Andrews, 1984; Hey & Thorne, 1986; Thorne & Osman, 1988a). The influence of bank material properties on the regime widths had, therefore, been expected to be greater. The apparent predicted insensitivity of the width to bank material characteristics is more in line with the type of opinion expressed by Bettess and White (1987b). They argue that, "The very success of regime theories in predicting channel width when such theories have in the past completely ignored both the composition of the banks and the

method of bank erosion must suggest that such factors are only secondary in the determination of width". However, in the tests conducted in this analysis, this apparent insensitivity may only occur because the bank material properties were varied only over a relatively narrow range (Table 4.5), in order to maintain approximate correspondence with the "weakly cohesive" bank material category of Simons & Albertson. In light of the possibility of highly non-linear response to changes in control variables, conclusions about the role of bank materials in influencing channel morphology are reserved until the results of more detailed sensitivity tests are presented below (chapter 5).

Table 4.8 Me and Ad for Various Bank Materials Used in Regime Validation

Bank Material Category	Me	Ad
BM1	1.199	1.008
BM2	1.180	1.009
BM3	1.179	1.017

4.4 OVERVIEW OF MODEL PREDICTIVE ABILITY

The results of both the "dynamic" validation and the "regime" validation indicate that the channel widening model has reasonably good predictive ability. In both instances, the model appears to produce qualitatively correct responses and quantitative agreement between predicted and observed or empirically-derived data is also good. Mean discrepancy ratios of approximately 0.93 and 1.18 for the dynamic and regime validations, respectively, are evidence of the accuracy of the model predictions for channel width. Overall, these results indicate that the channel widening model is capable of accurately simulating width adjustment dynamics and final, stable channel morphologies in straight river channels with a sand-bed and cohesive bank materials.

CHAPTER FIVE

SENSITIVITY ANALYSES: IMPACTS OF CHANGES IN CONTROL VARIABLES ON CHANNEL EVOLUTION

5.1 INFLUENCE OF FLUVIAL SYSTEM VARIABLES ON CHANNEL ADJUSTMENT DYNAMICS

A programme of sensitivity analyses was undertaken to establish the relative importance of individual variables and empirical coefficients and exponents in controlling channel adjustment. Such information is not only useful in analysing the relative importance of factors and controls on processes of natural river channel adjustment, but it can also be used to assess the uncertainty associated with using unreliable or missing data, or empirically chosen exponents and coefficients in the validation of the channel widening model.

5.1.1 Definition of Sensitivity Parameters

The aim of the sensitivity analyses was to establish the sensitivity of channel morphology variables to changes in the controlling variables and boundary conditions. This was done to simulate the influence of varying a range of fluvial environments on predicted temporal trends of channel morphology. A number of aspects of channel morphology sensitivity are of interest in a study of adjustment dynamics and these are illustrated in Figure 5.1. This figure illustrates a typical adjustment sequence in a hypothetical channel disturbed by starvation of sediment from the upstream boundary. Following the reduction of sediment input, the bed degrades. A wave of degradation moves through the system, starting at the upstream boundary and progressing downstream. After some time, degradation may be sufficiently severe that the banks at a section are destabilized. This initiates widening and the thrust of instability switches from the vertical to the lateral dimension. The time between the initial disturbance to the system (or the start of the model simulation) and the onset of channel widening at a study location can be termed the width adjustment *reaction time* (see Figure 5.1). It is of great interest to determine the sensitivity of the width adjustment reaction time to change in the various control variables. Once adjustment of width at the study site commences, the channel tends to evolve towards a more stable form (Figure 5.1). The magnitude of the overall change in width (stable width minus initial width) is clearly also of great interest. But the rate at which this change occurs, or the length of time taken for the stable channel width to be attained following the onset of widening, is also fundamentally important to channel dynamics. For the purposes of this study, this time scale is termed the width adjustment *recovery time* (Figure 5.1). Furthermore, it is

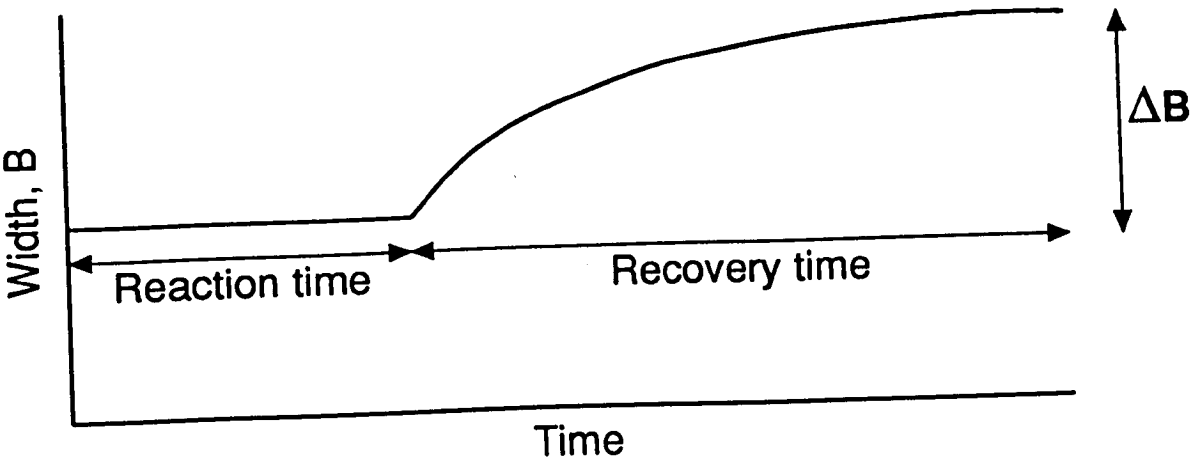

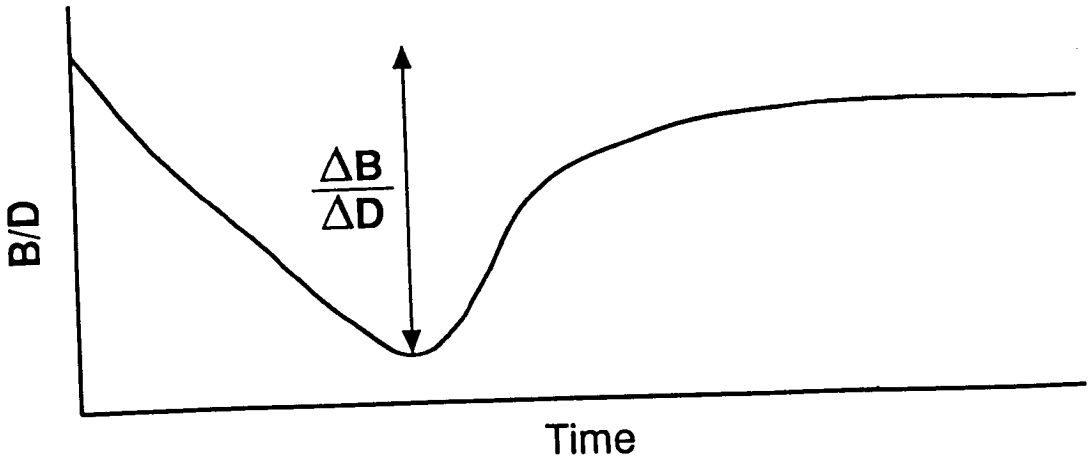

Figure 5.1 Conceptual Sequence of Channel Adjustment and Definition of Terms

likely that the sensitivity to change of a control variable may not be the same for both width and depth changes. It is, therefore, necessary to quantify the sensitivity of both width and depth changes to changes in the magnitude of the control variable. Finally, Figure 5.1 indicates that during the interval between the start of the simulation and the onset of channel widening (the reaction time) channel adjustment is primarily through bed level changes which have the effect of changing the stability of the banks with respect to mass failure. The sensitivity of the magnitude of this initial degradational change, as evidenced through the initial change in B/D ratio (Figure 5.1), to changes in the magnitude of the control variables, was also determined in this study.

To account for the influence of change in the various control variables and empirical exponents and coefficients on all of the above aspects of the channel adjustment dynamics, sensitivity parameters were formulated for each of these facets of channel evolution. First, for assessing the sensitivity of the *magnitude* of changes in width or depth to changes in the magnitude of the various control variables, a sensitivity parameter was defined as:

$$\chi_{\Delta y} = \frac{\Delta y}{\Delta x} \tag{5.1}$$

where $\chi_{\Delta y}$ = dimensionless sensitivity coefficient for change in the overall magnitude of a dependent variable (width or depth) and Δx and Δy = dimensionless parameters representing change in the independent and dependent variables, respectively, so that:

$$\Delta x = \frac{x_i - x_b}{x_b} \tag{5.2}$$

$$\Delta y = \frac{y_i - y_b}{y_b} \tag{5.3}$$

where y = dependent variable of interest (width or depth) and x = independent control variable. The subscript, b, denotes the baseline value of the variable and the subscript, i, denotes that the variable has some value varied from the baseline. It follows that increases in the magnitude of $\chi_{\Delta y}$ represent increasing sensitivity of a dependent variable to changes in a control variable, while the sign of $\chi_{\Delta y}$ indicates the direction of the predicted change. Negative values indicate that the dependent variable changes in the opposite direction to the control variable (*e.g.* decreases in control variable result in increases in the dependent variable and *vice versa*).

To assess the impact of changes in the *rate* at which the adjustment of channel width occurs, a parameter $T_{0.5}$ is defined as the time taken for one half of the overall change in the channel width to occur, starting from the time of the onset of channel widening (Figure 5.1). This parameter is a measure of the "recovery time" defined in Figure 5.1. A dimensionless, temporal sensitivity coefficient for adjustment of channel width can then be calculated using:

$$\chi_t = \frac{\Delta T_{0.5}}{\Delta x} \tag{5.4}$$

where, $\Delta T_{0.5}$ is defined by:

$$\Delta T_{0.5} = \frac{T_{0.5b} - T_{0.5i}}{T_{0.5b}} \tag{5.5}$$

where the subscripts and Δx are as defined previously. It again follows that increases in the magnitude of χ_t imply an increased impact on the rate of adjustment for a given change in the magnitude of a control variable and that positive values of χ_t imply that increases in the control variable result in increased rates of response of the channel width.

To assess the impact of change in the magnitude of control variables on the time taken for the onset of width adjustment, T, (the "reaction" time in Figure 5.1), another dimensionless temporal sensitivity coefficient for the onset of channel widening can be defined by:

$$\chi_T = \frac{\Delta T}{\Delta x} \tag{5.6}$$

where χ_T = "reaction" time sensitivity coefficient. In equation (5.6) ΔT is defined by:

$$\Delta T = \frac{T_b - T_i}{T_b} \tag{5.7}$$

where the subscripts and Δx are as defined previously. The magnitude of χ_T indicates the degree to which the reaction time, T, is sensitive to changes in the magnitude of the control variable. Negative values of χ_T indicate that the direction of change of the reaction time is opposite to the direction of change (increasing/decreasing) of the control variable.

Finally, in order to assess the sensitivity of the initial depth change, a sensitivity parameter is defined by the relation:

$$\chi_{Do} = \frac{\Delta B/D_o}{\Delta x} \qquad (5.8)$$

where $\Delta B/D_o$ = initial change in B/D ratio (Figure 5.1) and Δx is as defined previously.

5.1.2 Method

A programme of numerical experiments was devised to calculate the sensitivity parameters formulated in section 5.1.1 for a range of controlling variables, boundary conditions and empirically derived exponents and coefficients. The broad principle of each experiment was to allow a single control variable to be varied over a prescribed range, while holding all the other model variables constant at pre-determined "baseline" values. The output data was used in equations (5.1) through (5.8) to calculate sensitivity parameters for each of the control variables of interest. Each of the five sensitivity parameters describing the influence of change in control variables on initial depth changes, overall changes in width and depth, changes in reaction time and changes in rate of width adjustment was calculated for a range of control variables and model empirical coefficients and exponents.

Each of the numerical experiments involved two main components. First, it was necessary to establish an appropriate set of baseline data about which to vary each of the control variables. Second, it was necessary to determine which control variables should be analysed and what range of values should be used to characterise the range of the variable about its specified baseline value. For each of the sensitivity tests, a set of hypothetical baseline input data was, therefore, chosen. Although the specified data were hypothetical, the aim was that this baseline data should be realistic, corresponding to values associated with typical river environments. In specifying the hypothetical data, it was also the aim to define values such that each control variable could be varied above and below that baseline value to characterise the influence on the predicted channel adjustment of a wide a range of each control variable as possible. In this way the influence of varying the model boundary conditions over a wide range of various fluvial environments was analysed. However, in interpreting the results of sensitivity analyses conducted in this way, it must be borne in mind that the sensitivity parameters calculated apply only to the environment specified by the baseline data set. It may not,

therefore, be possible to extrapolate the results determined from the sensitivity analyses conducted for the particular set of baseline data used in these tests over a wider range of natural environments. Nevertheless, the sensitivity analyses do still allow the relative importance of individual variables on various aspects of channel adjustment dynamics to be assessed, within the limits of the particular environment defined by the hypothetical baseline data.

In fact the hypothetical baseline input data were selected to correspond to a moderately steep, straight, uniform channel with sand-bed and cohesive bank materials (Table 5.1). The baseline data were selected in order that the baseline channel would represent a channel out of equilibrium with the constraints of the imposed discharge, sediment load, boundary material properties and specified initial channel morphology, such that the channel response was to initially degrade and destabilize the banks, resulting in a channel adjustment sequence involving deepening followed by widening, until a more stable form was attained. The emphasis in the sensitivity analyses was, therefore, to determine the influence of the control variables and model exponents or coefficients (which together define the fluvial environment) on the processes of adjustments of the channel bed and banks (depth and width) from an arbitrarily specified initial condition, towards an equilibrium condition.

In each experiment, the influence of flow variability on channel morphology was isolated by running a constant, steady, near bankfull discharge (at the downstream boundary) through the model channel for the entire length of the simulation. Upstream boundary sediment loads (Qs) were prescribed as fractions of the transport capacity at the first (upstream) model cross-section, to facilitate analysis of the impact of changing the sediment load in generating aggradational ($Qs > 1$) or degradational ($Qs < 1$) environments. Baseline sediment loads were set equal to half the transport capacity at the first model section, so that instability was generated in the baseline run by degrading the channel bed. Bed material was sand with a median diameter of 1mm. Simulations were run for real time periods of 300 days. Usually, the model channel adjusted to a stable width within this period. The model channel was designed to be straight and initially uniform in geometry (same channel gradient and cross-section shape at each model cross-section). Numerical cross-sectional geometry data for each of the model cross-sections were calculated using the prescribed values of bank height (equal to bankfull depth), bank angle and width-depth ratios, together with the the assumption of initially trapezoidal cross-section shape. Model output data were used to calculate each of the sensitivity parameters defined in section 5.1.1. Data were calculated at two locations in the hypothetical model channel, at "upstream" and

Table 5.1 Summary of Hypothetical Baseline Data Set and Variable Ranges Used in Sensitivity Analyses

Variable Description	Symbol	Baseline Value	Variable Range
Discharge	Q	$100 m^3 s^{-1}$	Not Tested
Upstream sediment inflow as percent of transport capacity	Q_S	0.5	0 - 2.0
Downstream boundary stage as percent of bank height	h	0.95	Not Tested
Width-Depth Ratio	B/D	10	Not Tested
Channel Gradient	S	0.001	0.0001 - 0.001
Bank Height	H	3.60m	2.70 - 3.60
Bank Angle	α	60 degrees	Not Tested
Manning n	n	0.025	0.015 - 0.035
Bed Material Diameter	d_{50}	1mm	0.025 - 2.0
Bed Material Specific Gravity	SG	2.65	2.20 - 3.00
Critical Shear stress for bank material entrainment	τ_c	99 dynes/cm^2	14.6 - 99.0
Bank Material Cohesion	C	10.0 kPa	2 - 40
Bank Material Friction Angle	ϕ	32.5 degrees	Not Varied
Bank Material Unit Weight	γ	19.0 kNm^{-3}	Not Varied
Tension Crack Index	K	0.0	0 - 0.4
Bank Material Sand Content	SAND	0.2	0 - 0.4
Bank Material Sand Size	d_{sand}	1mm	0.25 - 4
Bank Material Aggregate Size	d_{bank}	10mm	1.25 - 80
Bank Material Specific Gravity	SG_{bank}	1.79	1.10 - 2.00
Bed Material Porosity	λ	0.40	0.30 - 0.50
Coulomb Friction Coefficient	μ	0.65	0.45 - 0.85

Table 5.2 Summary of Model Empirical Coefficients and Exponent Sensitivity Analyses

Description of Empirical Coefficient or Exponent	Appears in Equation	Baseline Value	Variable Range
Non-dimensional Eddy Viscosity Coefficient	3.6	0.16	0.08 - 0.24
Strickler coefficient	3.7	0.025	0.015 - 0.035
Lateral Erosion Coefficient	3.23	0.0223	0.0200 - 0.0246
Hiding Factor exponent	3.56	0.85	0.75 - 0.95
Mixed Layer Depth Coefficient	3.53	0.10	0.05 - 0.15
Engelund-Hansen Sediment Transport Coefficient	3.9	65	45 - 85
Reference Concentration coefficient	3.17	$3.2474 * 10^{-4}$	$3.24 * 10^{-5}$ - $3.24 * 10^{-3}$
Lateral Eddy Diffusivity Coefficient	3.11	0.16	0.08-0.24 (varied with NEV)
Vertical Eddy Diffusivity coefficient	3.15	0.077	0.0424 - 0.77

"downstream" cross-section sites (Figure 5.2). Tables 5.1 and 5.2 summarise the details of the sensitivity analyses conducted in this study. Table 5.1 summarises the baseline values and range of values over which model control variable were changed, while Table 5.2 summarises the details of sensitivity analyses conducted for the empirically derived coefficients and exponents used in the model equations.

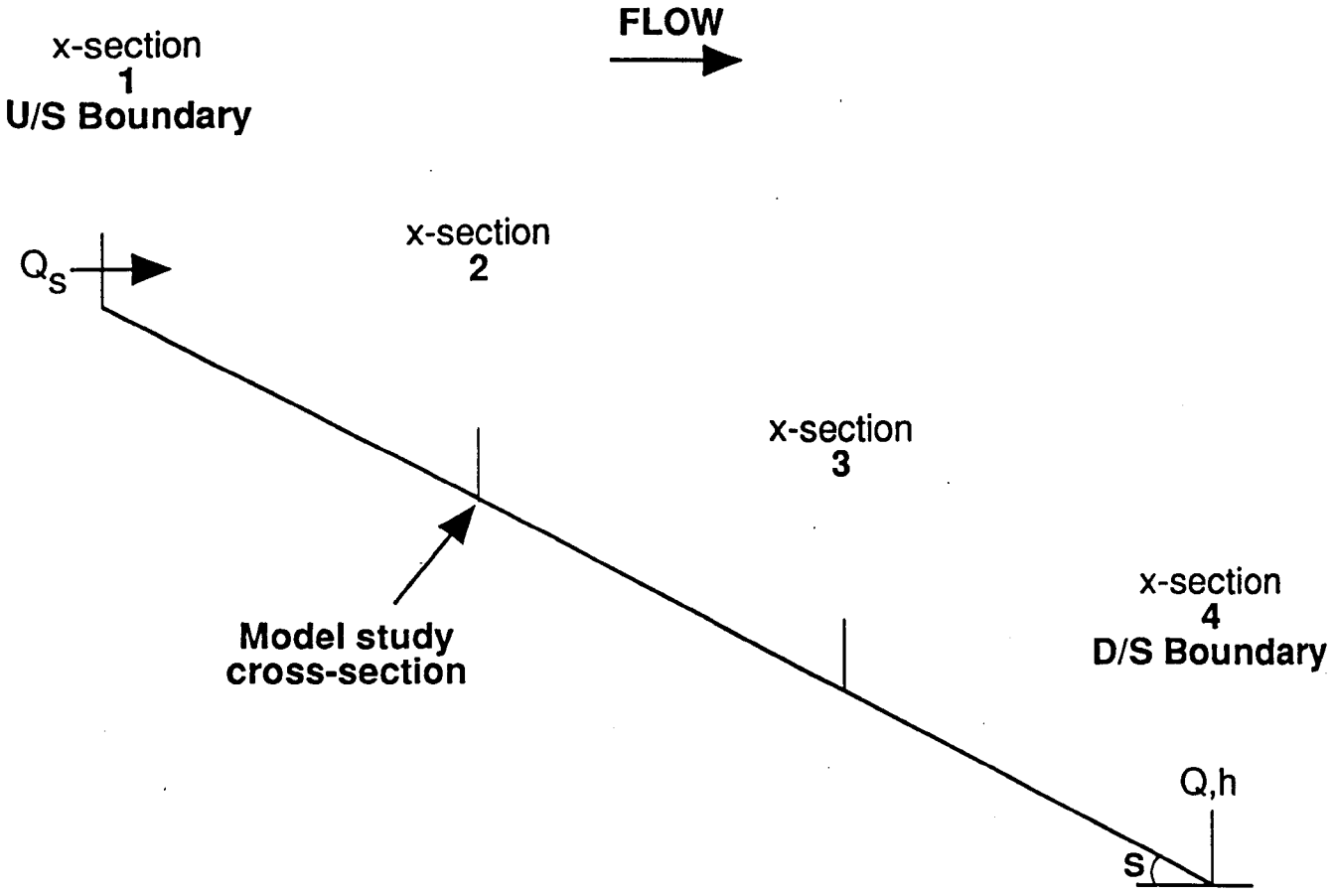

Figure 5.2 Hypothetical Channel Model Domain

As in the "regime validation" analyses reported in chapter 4, a problem in specifying baseline values of soil cohesion, friction angle and unit weight is that these geotechnical characteristics must be specified as frequency distributions for input to the numerical channel evolution model. A similar approach to that used in the regime validation analysis was, therefore, used to characterise the influence of varying soil cohesion in the sensitivity analyses reported here. By holding the baseline unit weight and friction angle soil frequency distributions constant in each model run, bank material characteristics were varied by varying the modal value of cohesion in the cohesion frequency distribution. In this way three soil cohesion frequency distributions were formulated to represent a wide range of soil strength characteristics, ranging from an almost cohesionless soil, to one with a very high cohesion. In Table 5.1, it should be noted that the quoted cohesion values correspond to these modal values. A complete summary of the soil frequency distributions used in the sensitivity analyses is found in Appendix C.

5.1.3 Results

The results of the sensitivity analyses conducted in this research are now discussed. Results of the sensitivity tests for each of the control variables and model coefficients and exponents are first presented in Figures 5.3 through 5.16. The calculated values of the sensitivity parameters are discussed in section 5.2. Each of the Figures illustrates simulated temporal trends of dimensionless bank top width, B*, and ratio of bank top width to mean depth (B/D) for the range of values of the various control variables tested in this study. Plots of B/D were preferred to plots of dimensionless channel depth as it allows overall changes in channel morphology to be quantified and it is easy to establish if width or depth adjustments are dominating at any moment in time. In any case, the depth adjustment sequence is also determined when the results for both B* and B/D are presented. In each case the channel width is non-dimensionalized by dividing the bank top width by the initial bank top width. In each of Figures 5.4 through 5.16, curves are always shown for the baseline run and the runs corresponding to the maximum and minimum of the control variable range. In some cases, curves for runs corresponding to intermediate values of the control variables are also shown on these plots. It should be noted that the same number of runs (4) were conducted for each of the control variables listed in Tables 5.1 and 5.2, but in some instances the model output is insensitive to changes in the value of the control variables. In these cases, only the maximum and minimum values are shown with the baseline run in order to clarify the diagram. In some cases where model output is very insensitive to changes in the control variable, plots are not presented at all, as it is impossible to distinguish

visually individual simulated results on the graph. In these cases, reference should be made to Tables 5.3 and 5.4 (discussed in section 5.2) which summarise all of the various numerical sensitivity parameters calculated for each of the control variables listed in Tables 5.1 and 5.2. In effect, these diagrams illustrate the influence of each of the control variables on the dynamics of channel adjustment.

It should also be noted that Figures 5.4 through 5.16 illustrate simulated temporal trends of channel width and width/depth ratio at only one of the model cross-sections, which is located in the upstream portion of the model domain (Figure 5.2), for reasons of clarity. Trends of response to changes in control variables were found to be consistent at cross-sections throughout the model channel, so this is not a major limitation. It is true, however, that the numerical values of sensitivity parameters were found to vary systematically with spatial location in the hypothetical channel reach, so that in section 5.2 calculated sensitivity parameters are presented for both "upstream" and "downstream" model locations in Tables 5.3 and 5.4. Similarly, since the reaction times of the channel width response are dependent on location with respect to the disturbance, temporal trends of B* and B/D at both upstream and downstream locations are presented for the baseline run in Figure 5.3.

5.1.3.1 Baseline Run

Before describing the impact of changing the various control variables on the simulated channel morphology dynamics, it is appropriate to describe the channel adjustments simulated during the baseline run (Figure 5.3). In the baseline run at the upstream section, B* is initially constant through time indicating that the river banks are stable with respect to mass failure, while B/D ratio declines at a relatively rapid rate, to a minimum value of about 9 at day 65. This indicates that the initial response of the system is a relatively rapid increase in mean depth as a consequence of the deficit between sediment supply (Qs = 0.5) and sediment transport capacity. The initial deepening phase eventually destabilizes the river banks with respect to mass failure and the channel begins to rapidly widen at about day 65. As a consequence of this widening, B/D ratio also increases after this time. The rapid increases in B* and B/D ratio occurs during the time period between about day 65 and 120. After this time, B* and B/D both continue to increase, but at much lower rates; after day 200, B* and B/D are relatively constant. At this point in time, the "stable" channel width is about 10% larger than the initial width, while B/D ratio is similar to its approximate starting value, indicating that the "stable" mean channel depth is also greater than the initial mean depth. Qualitatively, the sequence of temporal trends of adjustment of B* and B/D

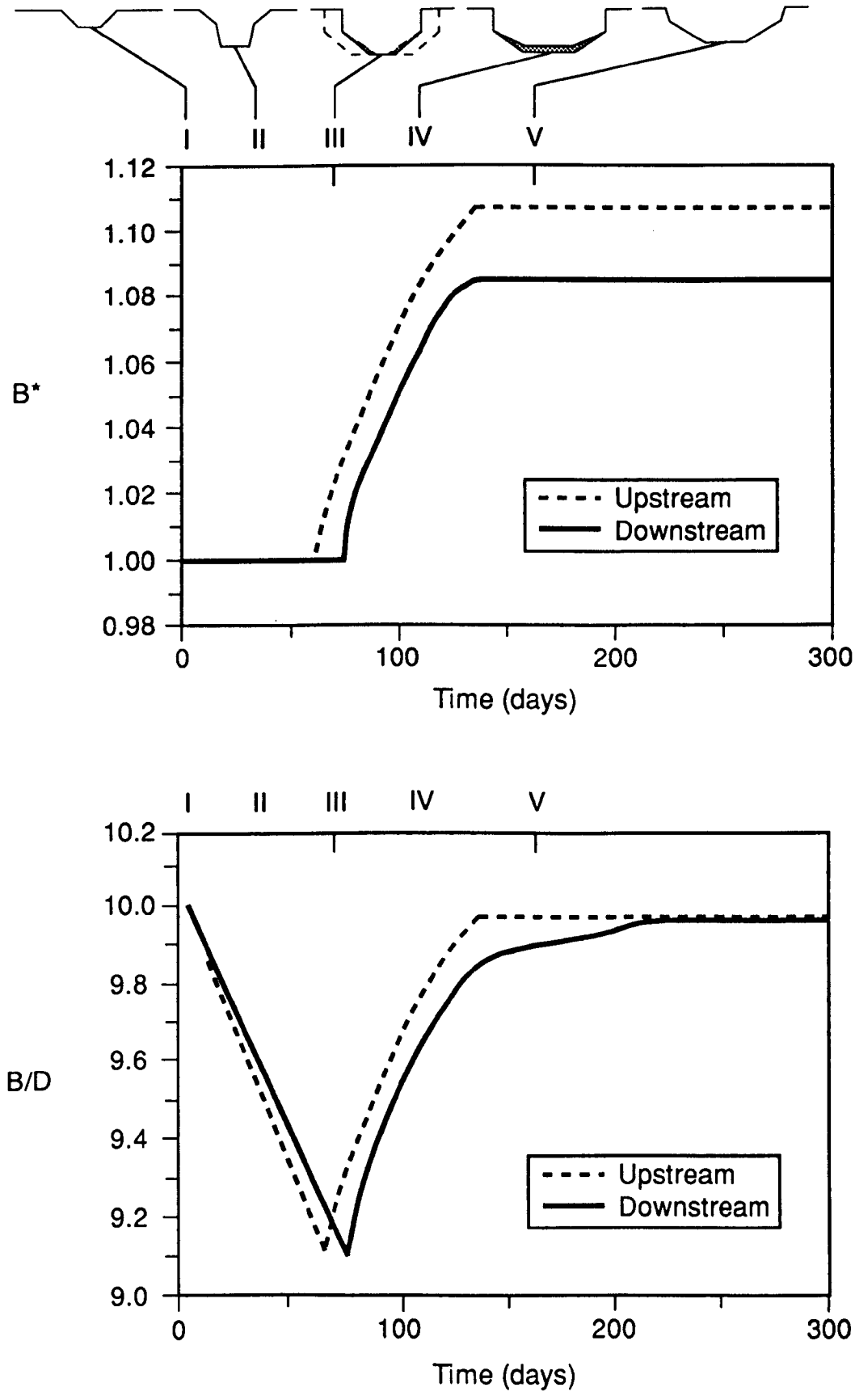

Figure 5.3 Comparison of Simulated Temporal Trends of Channel Morphology and Thorne & Osman Conceptual Model of Channel Evolution

appear similar at both the upstream and downstream sites, but there are important quantitative differences in the response of the system at the two locations, reflecting the significance of spatial location on the response of the fluvial system to a disturbance. First, the onset of widening is delayed at the downstream location. This is a result of the extra time taken for bed degradation to migrate to downstream sections from the upstream disturbance and, consequently, destabilize the banks to initiate widening. Second, the simulated "stable" B* is smaller at the downstream section than at the upstream section. This is because additional sediment is supplied to the downstream reaches from upstream bed degradation and bank failures, resulting in a situation where less channel widening is required at these sections to bring sediment transport capacity to levels where capacity is equalled or exceeded by sediment supply. This damping of response with increasing distance from the channel disturbance, as a result of sediment supply processes varying through time and space, is the reason for systematic differences in the values of calculated sensitivity parameters between the upstream and downstream locations (Tables 5.3 and 5.4). Nevertheless, the relative rankings of these variables appears mostly to be independent of location within the fluvial system (see section 5.2).

It is an interesting and useful exercise to compare the model output for the baseline run to conceptual models of channel evolution applicable to channels with non-cohesive sediment beds and cohesive banks that are destabilized by bed degradation. Such conceptual models have been presented by Schumm *et al.* (1984), Thorne & Osman (1988a) and Simon (1989). These models are based on combinations of physical reasoning and geomorphic concepts, as well as direct observations of destabilized fluvial systems. Comparisons between model predictions of channel adjustment and those made by the conceptual models not only provides another dimension to the testing and assessment of the model, but also provide a powerful conceptual framework for explaining and analysing the predicted sequences of channel morphology and process-form interactions during these stages of channel evolution.

The Thorne & Osman (1988a) conceptual model was selected for comparison with model predictions of channel evolution, because it is more generalised than either of the Schumm *et al.* (1984) or Simon (1989) models. The Thorne & Osman (1988a) model also includes non-cohesive bank materials as well as cohesive bank materials. In any case, the sequence of events predicted by each of the conceptual models is broadly similar. Predictions of channel adjustment obtained in the baseline simulation and predictions of channel adjustment from the Thorne & Osman (1988a) conceptual model (for cohesive banks) are compared in Figure 5.3. In both cases the initial channel

(Stage 1 of the Thorne & Osman evolution model) is a trapezoidal, straight channel with non-cohesive bed and cohesive banks which are destabilized by bed degradation (Stage 2). Thorne & Osman (1988a) use the concept of basal endpoint control to describe the basal endpoint status during each of the stages of adjustment. Thus, in Stage 2, there is a state of *Excess Basal Capacity* and the channel incises with little or no widening to produce a narrow, deep channel. This is reflected in the model simulations, in which B/D rapidly decreases, but B* remains constant, indicating increases in channel depth but stable widths. Thorne & Osman (1988a) note that if the bed is formed in gravel, degradation may be limited by bed armouring at this stage, so that the banks may never reach the critical height for mass failure. In this case, if the bank material is highly resistant to erosion, Stage 2 may terminate channel adjustment (Thorne & Osman, 1988a).

However, if degradation continues, the banks eventually reach the critical height for mass failure. Slab or rotational failures occur, initiating rapid widening which supplies large volumes of bank material to the basal areas (Thorne & Osman, 1988a). The state of endpoint control switches to *Unimpeded Removal* and degradation ceases. This "threshold stage" (Simon, 1989) is Stage 3 of the Thorne-Osman model. The numerical model correctly appears to predict the onset of the Stage 3 channel following the degradation phase. Simulated B/D values fall to a minimum and then begin to rise rapidly contemporaneously with a rapid increase in B*. The simulated output is consistent with attainment of the critical bank geometry and the onset of rapid widening, which limits channel incision to about the critical bank height value.

Stage 4 channels are attained when the channel is sufficiently wide that the flow at the banks is no longer able to remove the sediment supplied to the near bank zones from upstream transport and bank failures (*Impeded Removal*). Eventually, as berms begin to be deposited, bank heights and angles are reduced and a re-stabilisation of the bank is achieved. Bank erosion is slowed and eventually ceases, resulting in a Stage 5 channel which is characterised by a stable width and depth (Thorne & Osman, 1988a). Again, the numerical model appears to be capable of correctly simulating this sequence of adjustment, with rates of widening slowing (Stage 4) then ceasing altogether (Stage 5). In this simulation, the model appears to predict the true attainment of a stage 5 channel, since both the B* and B/D curves stabilise at constant values. It appears that the numerical model is capable of simulating the sequences of adjustment predicted by the channel evolution model of Thorne & Osman (1988a). Not only is this further evidence of the ability of the model to simulate trends of channel adjustment accurately, but it also means that the model can be used to diagnose the various stages of

adjustment, based on the simulated trends of B* and B/D at any moment in time. This then enables the basal endpoint status to be diagnosed, so that the dominant processes at any time in the adjustment sequence may be identified. This provides a powerful conceptual tool for analysing the sensitivity tests which are now reported in more detail.

5.1.3.2 Upstream Boundary Sediment Load (Qs)

Figure 5.4 illustrates the influence of the upstream boundary sediment load on the simulated temporal trends of B* and B/D. The sediment load, Qs, is prescribed as a fraction of the sediment transport capacity at the first model cross-section, and has a value of 0.5 in the baseline run. Figure 5.4a shows that reductions in sediment load are predicted to result in increased channel widths, when the sediment load is less than or equal to 1.0 (degradational environments), but in aggradational environments (Qs > 1.0) there appears to be no impact of variation in Qs on channel width. Predicted B/D ratios progressively increase as sediment load is increased; but the sensitivity of B/D to changes in Qs appears to be greater in aggradational environments. This is because in degradational environments, predicted increases in mean depth result in destabilization of river banks and predicted increases in channel width, so that the overall impact on B/D ratios is small. However, in aggradational environments, mean depths are predicted to decrease so that bank heights are reduced and the banks remain stable with respect to mass failure under gravity. There is, therefore, no change in width to offset the predicted decrease in mean depth, so that B/D ratios increase with increases in Qs.

While simulated widths are sensitive to gross changes in aggradational or degradational environments, it is apparent that within these environments simulated widths do not appear to be overly sensitive to changes in Qs. Indeed, as mentioned previously, widths are not predicted to change at all over the spectrum of aggradational environments tested in this analysis ($1.0 < Qs \leq 2.0$). However, predicted impacts of changes in Qs on the temporal aspects of width adjustment appear to be much more profound.

It is clear that the reaction time with respect to width adjustment is quite sensitive to the value of Qs. Reductions in Qs result in progressive reductions in the reaction time. However, following the onset of widening, the rate of adjustment to a more stable width (recovery time) appears to be similar in all cases. The sensitivity of the widening reaction time to Qs is a function of the influence of Qs on depth adjustments in the early stages of the simulation. Variations in Qs have a significant impact on the rate of reduction of B/D ratio, as reductions in Qs result in progressive increases in the rate of

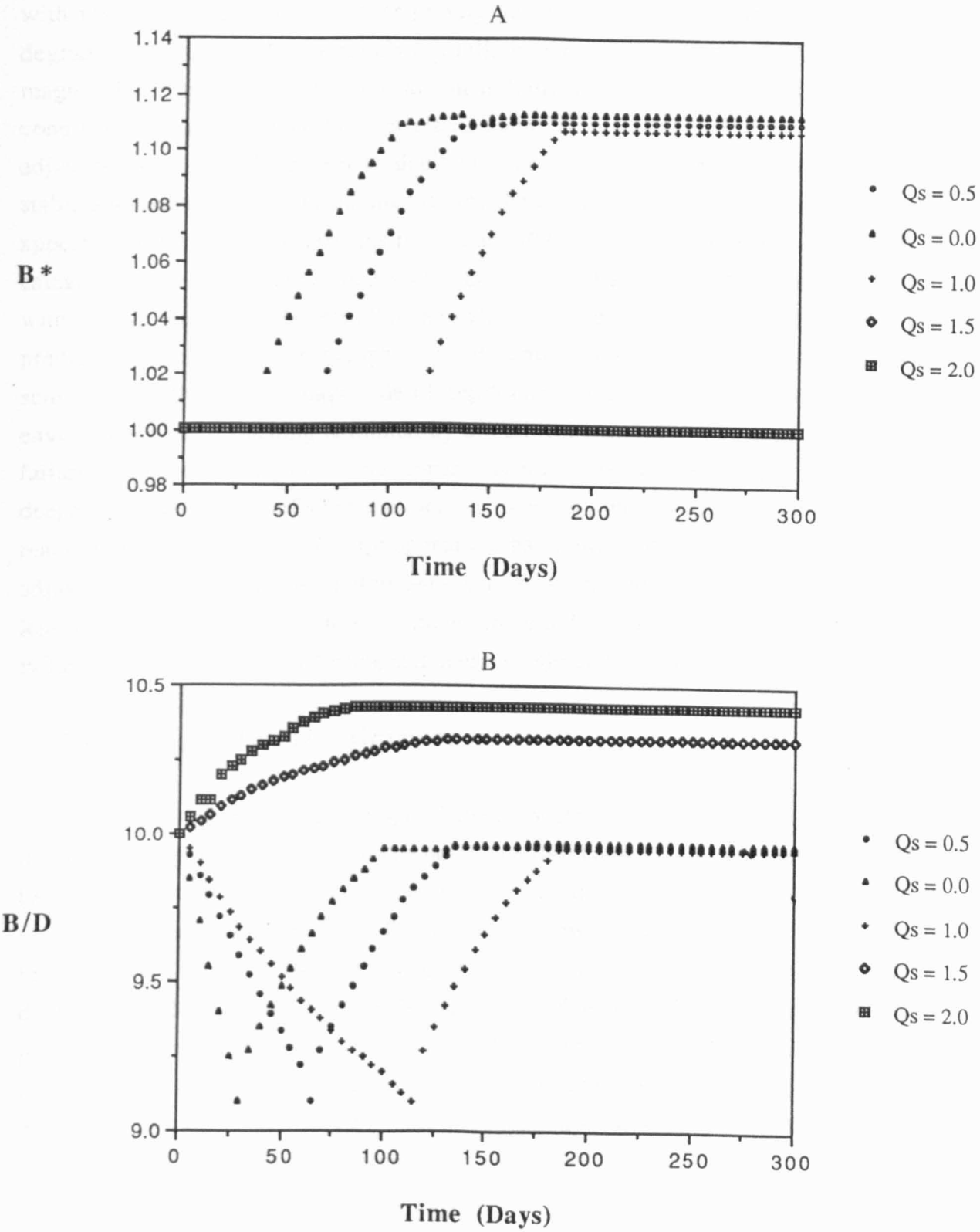

Figure 5.4 Simulated Temporal Trends of (A) Non-Dimensional Bank Top Width and (B) Aspect Ratio for Varying Qs

initial downcutting. The rate of deepening then controls the time required to degrade the channel and increase the height of the banks to the point at which they become unstable with respect to mass failure under gravity and begin to fail and retreat. In each degradational run, the B/D ratio always falls to about 9, indicating that the overall magnitude of the initial depth adjustment is limited by the critical bank geometry conditions. This highlights the interrelated nature of the predicted depth and width adjustments. In aggradational runs, depth decreases, B/D increases, the banks remain stable and widening is never initiated during the course of the simulation. Overall, it appears that the predicted changes in B* and B/D are sensitive to broad changes in category of sediment supply - degradational versus aggradational environments - but within these conditions, the overall magnitude of changes in B* and mean depth is not predicted to be very large, though rates of depth change are sensitive to Qs. The sensitivity of the overall magnitude of depth changes is not great in degradational environments, as deepening is limited by the critical bank geometry to initiate mass failure and widening. However, the apparently relatively large sensitivity of rates of deepening to Qs has the effect of significantly impacting the sensitivity of the widening reaction time to changes in Qs. Qs appears to have little impact on the rate of width adjustment following the onset of widening, as the simulated curves of B* are more or less parallel. Qs is not, therefore, predicted to be a dominant variable in terms of its influence of channel width adjustment dynamics following the onset of widening.

5.1.3.3 Initial Channel Gradient (S)

Figure 5.5 shows predicted temporal trends of B* and B/D for various values of initial channel gradient, S. It should be noted that the channel gradient is initially equal to the valley gradient, but is subsequently free to adjust in response to the imposed water and sediment discharges. The diagram shows that an order of magnitude reduction in S from its baseline value of 0.001 results, as expected, in somewhat decreased predicted stable B* and B/D ratio. The channel widening reaction time is progressively reduced with increases in S, reflecting the impact of increased channel gradient on increased rates of initial channel deepening. The magnitude of the initial deepening, as evidenced through the initial reduction in B/D ratio, is again limited by the onset of bank instability and channel widening, with B/D ratios initially declining to values of about 9 in all of the channel gradient sensitivity runs. Channel widening reaction times and rates of initial deepening do not appear to be as sensitive to changes in S as they are to changes in Qs. However, as in the Qs sensitivity tests, rates of channel widening following the onset of bank instability appear to be largely unaffected

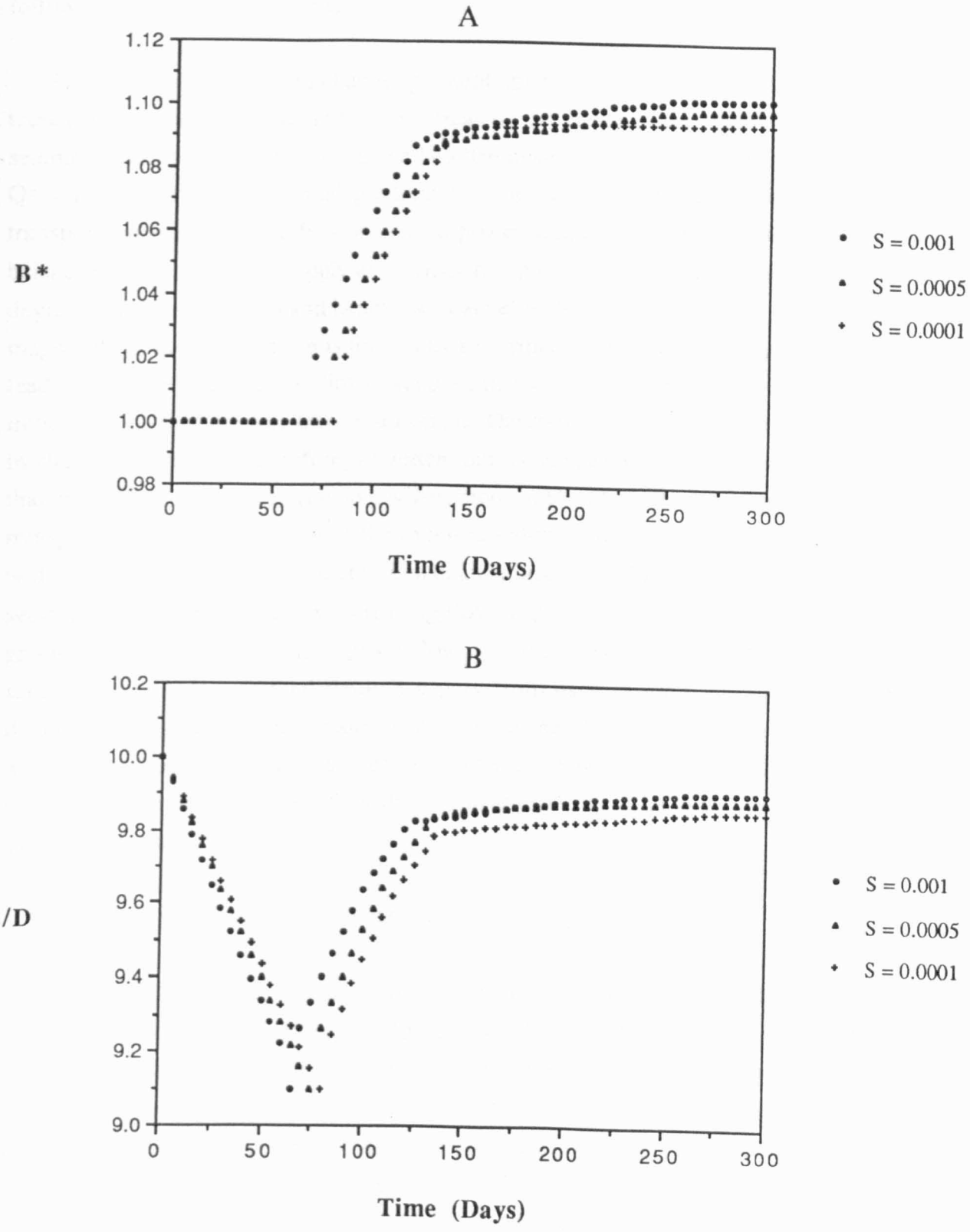

Figure 5.5 Simulated Temporal Trends of (A) Non-Dimensional Bank Top Width and (B) Aspect Ratio for Varying S

by changes in S, as evidenced by the parallel nature of the B* and B/D curves following the onset of widening.

The impact of changes in channel gradient appears to be related to the effect that increasing the channel gradient has on increasing the stream power, flow velocity and sediment transport capacity. For a given baseline upstream sediment inflow (in this case Qs = 0.5) variation in channel gradient has the effect of impacting the sediment transport capacity via its effect on stream power and, consequently, influencing the balance between sediment supply and transport capacity that determines the rate of bed degradation (equation 3.8) and hence the channel widening reaction time. The overall magnitude of bed degradation is limited by the critical bank height. Increases in slope lead in this case to a larger sediment supply : transport deficit, effectively moving the initial channel further away from equilibrium. The response of the channel to increases in channel gradient is, therefore, to widen, but by greater amounts and more rapidly than the equivalent baseline run, to a wider, more stable, channel which has a sediment transport capacity in balance with the imposed sediment supply. In effect, the channel widening offsets the imposed increase in channel gradient. Channel widening reduces sediment transport capacity by increasing flow resistance as flow depths and channel gradient are reduced (at constant Q) and flow velocities are decreased. At the same time, sediment supply is increased through supply from bank failures and upstream bed degradation. As the sediment supply eventually exceeds the sediment transport capacity and the banks begin to be restabilized as sediment is deposited in the basal zone, bank heights and angles are reduced to the extent that the bank is stable and widening eventually ceases.

5.1.3.4 Hydraulic Roughness (n)

The sensitivity of temporal trends of B* and B/D to changes in Manning's n roughness (Strickler coefficient) are illustrated in Figure 5.6. Increases in 'n' result in decreases of predicted stable B* and B/D, with increased hydraulic roughness also slowing the rate of initial degradation and, therefore, leading to increases in the channel widening reaction time. The magnitude of the initial downcutting phase again appears to be independent of changes in Manning's n and the extent of the initial degradation is limited by the amount required to destabilize the banks and cause widening. Rates of width adjustment following the onset of bank instability are related in a weak, though complex, way to the hydraulic roughness. Increases in hydraulic roughness reduce the length of time for which the banks are unstable, so that the magnitude of widening is inversely proportional to increases in Manning's n. Increases in Manning's n result in

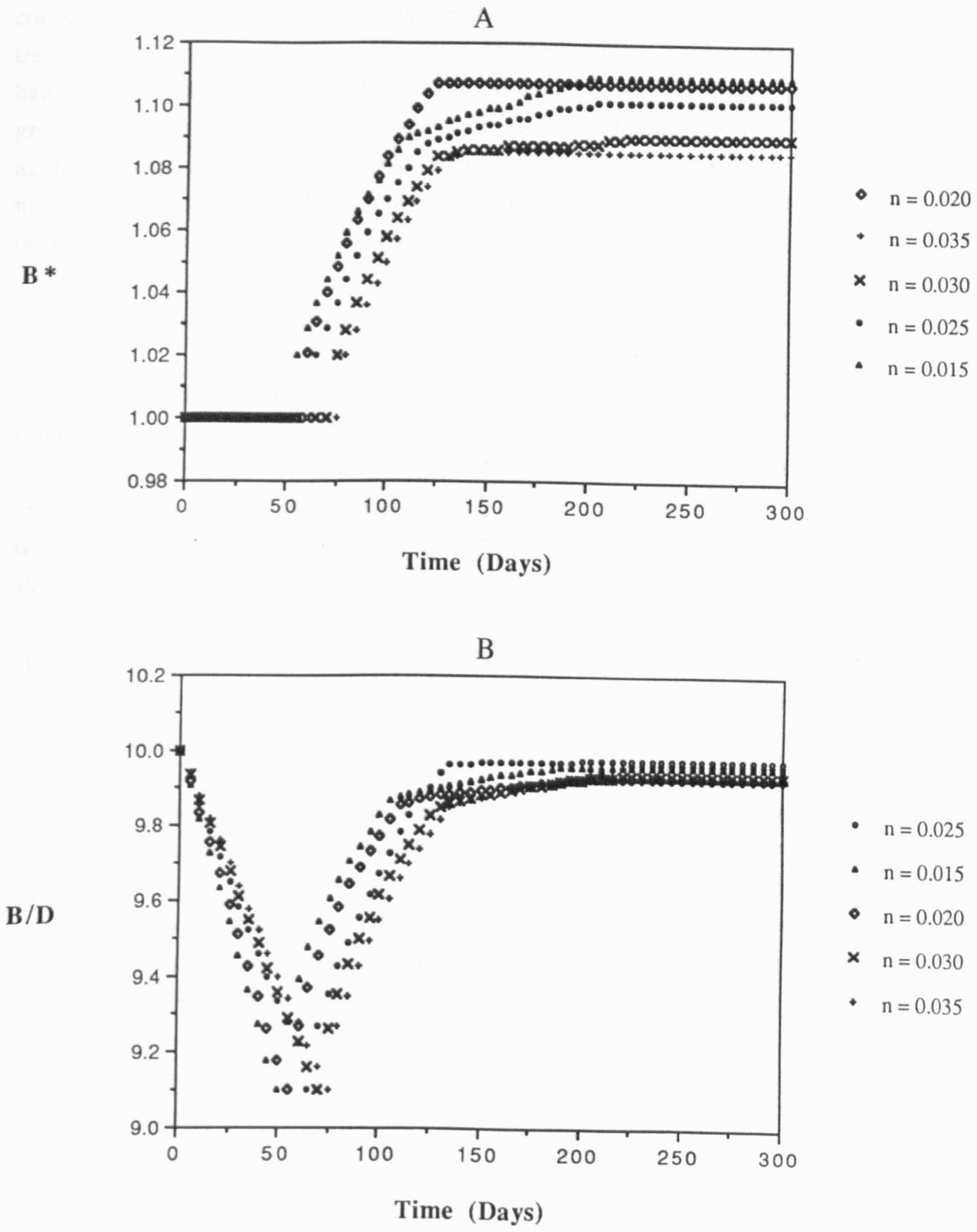

Figure 5.6 Simulated Temporal Trends of (A) Non-Dimensional Bank Top Width and (B) Aspect Ratio for Varying n

decreases in flow velocity and stream power, reducing sediment transport rates and consequently reducing the deficit between sediment supply (Qs = 0.5) and sediment transport rate. Thus, as the channel widens, increasing the supply of sediment from bank failures and causing a reduction in transport capacity as flow depths and channel gradient decrease, the supply of sediments will exceed the transport capacity (and hence aggrade the bed and stabilize the banks) sooner in rougher channels. Higher Manning's n values also reduce rates of initial deepening resulting in the simulated delays in the onset of channel widening with increasing 'n'.

5.1.3.5 Bank Material Cohesion (C)

Simulated temporal trends of B* and B/D as a function of the intact bank material shear resistance, as described by changes in the modal value of the cohesion, are shown in Figure 5.7. Predicted trends of B* and B/D are non-linearly sensitive to changes in bank material cohesion. In general, increases in the value of the intact bank material cohesion result in a reduction of the predicted stable values of both B* and B/D, together with an increase in the channel widening reaction time. The bank material cohesion has no impact on the initial *rate* of deepening, as evidenced by the fact that the B/D curves for C = 10 kPa and C = 40 kPa follow identical paths prior to the onset of widening. This is because this parameter has no influence on the dynamics of channel sediment transport.

However, there are considerable impacts on the channel widening reaction time as a consequence of changes in bank material cohesion. Indeed, widening begins immediately at low values of cohesion, but does not commence at all during the course of the simulation at the highest values of bank material cohesion. The effect of increases of bank material cohesion is to lead to increases in initial bank stability so that greater *amounts* of degradation (relative to the baseline run) and, therefore, increased widening reaction times, are required to destabilize the banks and lead to widening. This contrasts with the results above, in which the tested control variables impacted *rates* of channel deepening, leading to variation in the simulated reaction times. So, when C = 40 kPa, there is no predicted widening and B/D is predicted to fall throughout most of the simulation, to a minimum value of about 8 at day 250. After this time depths begin to recover as the supply of sediment is increased from upstream degradation, and local sediment transport capacity is reduced by decreases in channel gradient as a consequence of bed degradation. Even the maximum amount of deepening is insufficient to destabilize banks of such high shear resistance. Conversely, at the lowest cohesion value, the banks are erodible and unstable even at the initial bank height, so

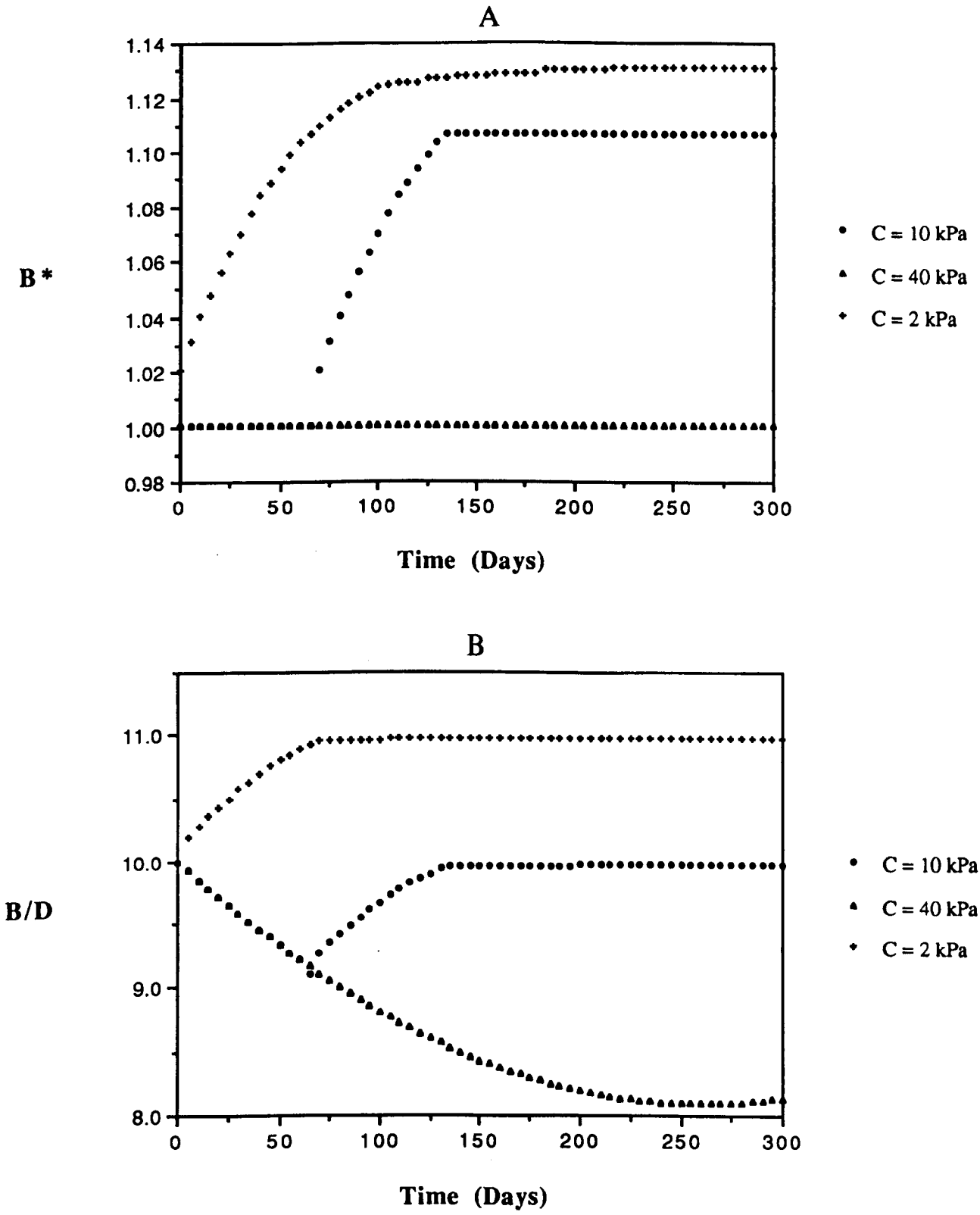

Figure 5.7 Simulated Temporal Trends of (A) Non-Dimensional Bank Top Width and (B) Aspect Ratio for Varying C

that no degradation is required to destabilize them. Rapid widening begins immediately and B/D ratio is also, therefore, predicted to increase at once, despite the general degradational tendency (Qs = 0.5) of these simulations.

5.1.3.6 Initial Bank Height (H)

Simulated temporal trends of B* and B/D for a range of initial bank heights (Figure 5.8) are similar to the cohesion plots as variation in H also has the effect of changing the initial factor of safety of the river banks. Figure 5.8 shows that by progressively reducing the initial bank height from its baseline value (H = 3.6m), factor of safety is increased so that the onset of widening is progressively delayed as greater amounts of deepening are required to bring the banks to their critical geometry. The magnitude of the initial deepening phase is, therefore, quite sensitive to changes in H. The magnitude and rate of width adjustment following the onset of bank instability and channel widening is also sensitive to the initial bank height, with decreases in initial bank height resulting in reductions of simulated channel widening.

The explanation for the apparent sensitivity of the overall magnitude of channel width to *initial* bank height appears to be related to the relative difference in channel *depths*, as evidenced by the variation in simulated B/D ratio, that the model channels have at the onset of widening, as a consequence of the variation in initial bank height. As initial bank height is decreased, the onset of widening is progressively delayed as channels respond by degrading their beds until the critical bank geometry conditions are reached. The prolonged degradation phase appears to result in a situation where sediment transport capacities are significantly reduced by channel gradient reduction prior to the onset of widening. In these cases, only a small amount of bank retreat is required to input sufficient volumes of bank material to the channel to establish an excess or approximate equilibrium between sediment supply and transport capacity and restabilize the banks through combinations of bank angle reduction and bank height reduction as berms are deposited at the base of the bank. This contrasts with the previous simulations in which equilibrium was re-established primarily through reduction in transport capacity by shallowing as a consequence of widening, together with inputs of bank material increasing sediment supply.

5.1.3.7 Tension Crack Index (K)

Results of the tension crack index (K) sensitivity tests illustrated in Figure 5.9 are also similar to those from the bank material cohesion analysis described previously and

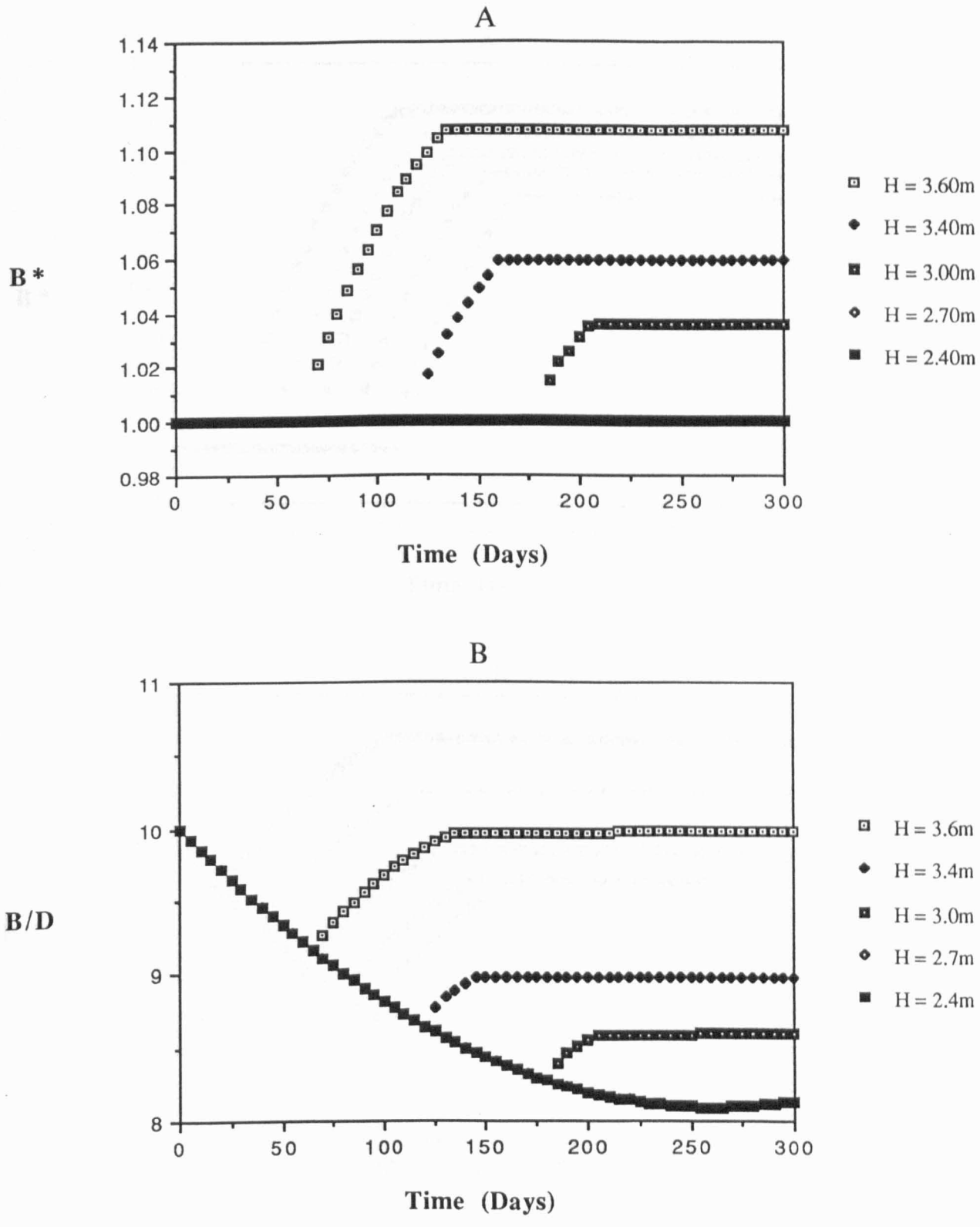

Figure 5.8 Simulated Temporal Trends of (A) Non-Dimensional Bank Top Width and (B) Aspect Ratio for Varying H

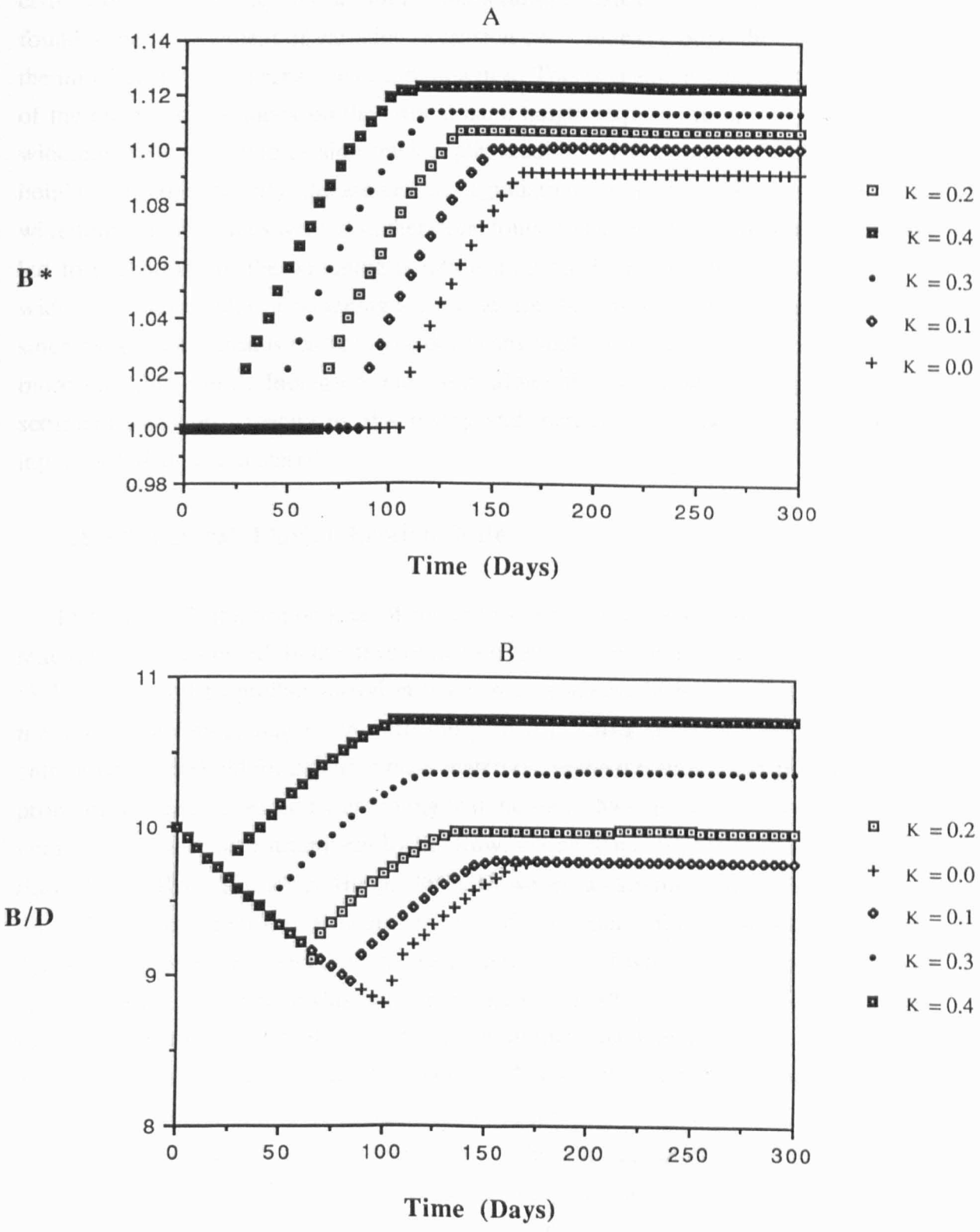

Figure 5.9 Simulated Temporal Trends of (A) Non-Dimensional Bank Top Width and (B) Aspect Ratio for Varying K

illustrated in Figure 5.7. This is not surprising, since the effect of increasing the tension crack index is also to destabilize the banks with respect to mass failure, reducing the critical bank height required to initiate mass failure. Rates of initial deepening were found to be independent of variation in tension crack index, though the magnitude of the initial deepening is sensitive to variation in K. This is again because of the influence of the tension crack index on the critical bank height required to initiate failure and widening, with increased tension crack depths leading to reductions in the critical bank height and, consequently, the amount of degradation required to initiate failure. The widening reaction times were also, therefore, found to be sensitive to K. Increases in K led to reductions in the widening reaction time but increases in the magnitude of widening. Magnitudes of widening are greater for the less stable banks (increased K) since more bank retreat is required to reduce bank angles sufficiently to restabilize these more unstable banks. Increased widening allows this to happen through reducing sediment transport capacity by shallowing and increasing sediment supply through inputs of failed bank material.

5.1.3.8 Lateral Fluvial Erosion Rate

In Chapter 3, the importance of modelling the lateral erosion of cohesive bank materials was discussed. In the development of the channel evolution model, equation (3.22) was used to predict lateral erosion, but problems in the application of this method were noted, due to the difficulty in predicting the value of the critical entrainment threshold for cohesive bank materials. In the dynamic validation runs, this problem was circumvented by assuming that the intact bank material was nonerodible with respect to direct entrainment by the flow, which is reasonable in the South Fork Forked Deer River (Simon & Hupp, 1992). However, an attempt was made to analyse the influence of direct fluvial lateral erosion of bank material on channel adjustment dynamics, through two sensitivity analyses, the results of which are shown in Figures 5.10 and 5.11. Figure 5.10 shows temporal trends of B* and B/D for two groups of values of the critical threshold for entrainment of intact bank material (τ_c). The first of these groups is for values of τ_c which never fall below the shear stress applied by the flow on the banks: that is nonerodible banks (τ_c = 99, 25 dynes/cm^2). The second group is for values of τ_c in which there is lateral erosion (τ_c = 14.60, 14.63 dynes/cm^2). It is clear that when the banks are nonerodible, changing the value of τ_c has no impact on the simulated trends of B* and B/D. However, when the applied fluid shear is greater than τ_c it appears that simulated trends of B* and B/D are very sensitive to even small changes in τ_c. Indeed, the simulations are so sensitive that even variations

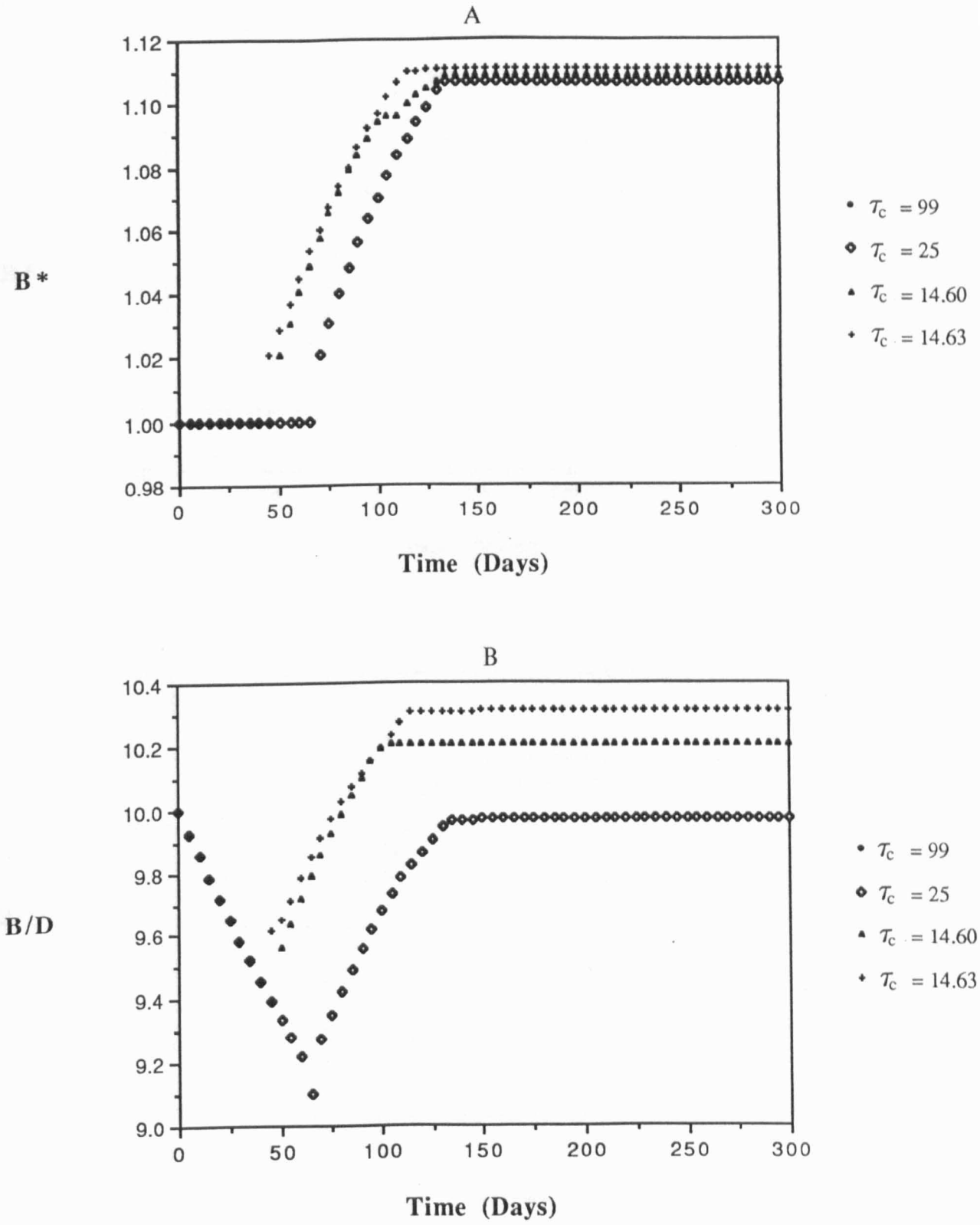

Figure 5.10 Simulated Temporal Trends of (A) Non-Dimensional Bank Top Width and (B) Aspect Ratio for Varying τ_c

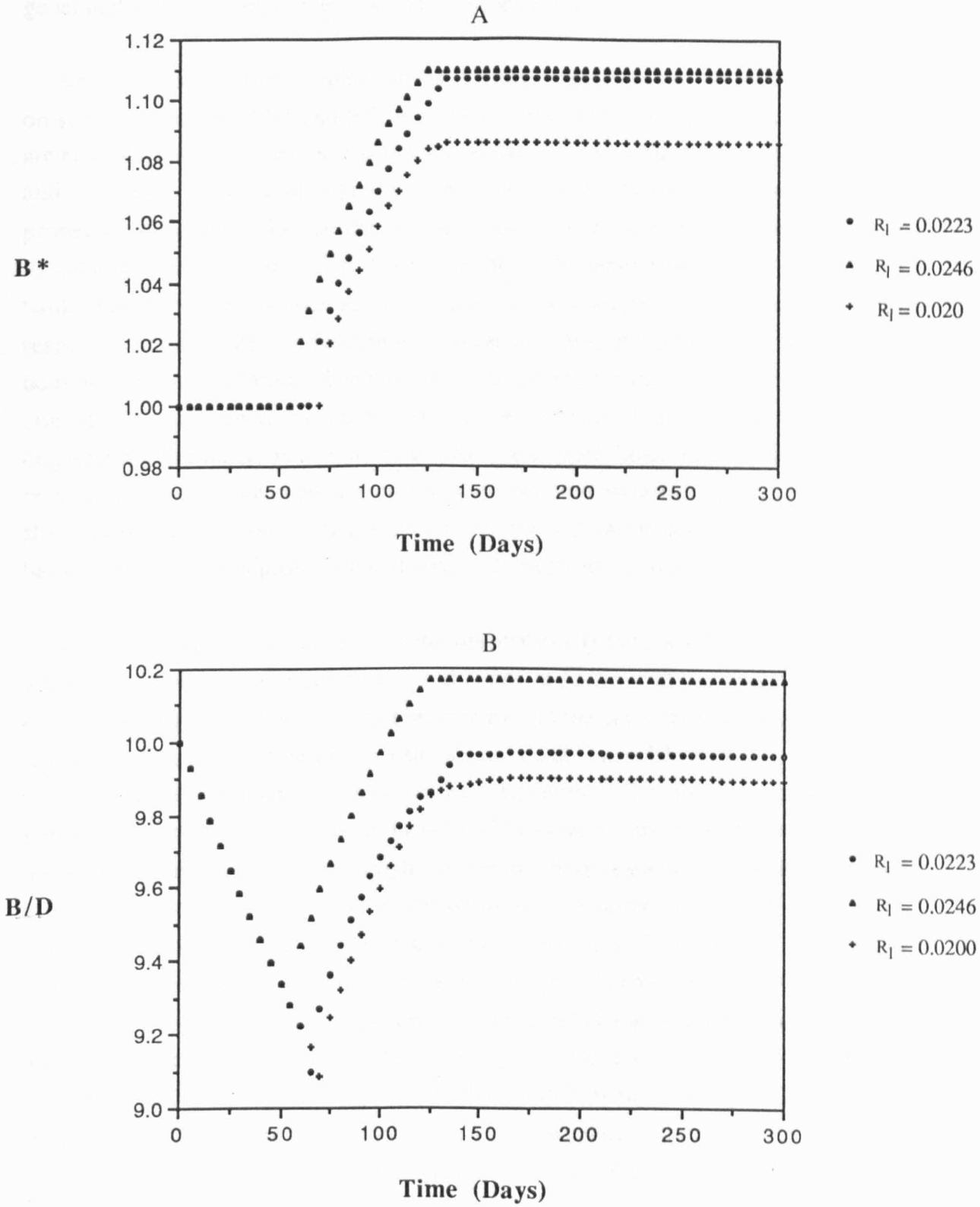

Figure 5.11 Simulated Temporal Trends of (A) Non-Dimensional Bank Top Width and (B) Aspect Ratio for Varying R_l

of τ_c to the first decimal place were often enough to result in numerical instability being generated by the model, as the flow undercut the bank generating overhangs.

Despite such practical problems in the sensitivity tests, the impacts of changes in τ_c on simulated trends of B* and B/D is still clear from these analyses. When the banks are erodible, overall increases in τ_c result in increases in simulated stable channel width and the onset of widening is predicted to occur earlier. While τ_c - a bank material property - does not influence the rate of initial deepening, the magnitude of initial deepening is sensitive to τ_c. This is because although lateral erosion has no impact on bank height changes, it does act to steepen the bank angle, reducing stability with respect to mass failure and reducing the amount of degradation required to bring the bank to the point of failure. The onset of bank instability and widening is, therefore, considerably hastened by lateral erosion occurring in combination with bed degradation. Similarly, as lateral erosion continues after the onset of widening, but at reduced rates as the channel widens and becomes shallower (reducing the boundary shear stress), factors of safety continue to be lower than the equivalent nonerodible bank case, resulting in prolonged widening and, therefore, increased widths.

An interesting point that arises from this analysis is that, when τ_c is less than the applied fluid shear, increases in τ_c - and hence *reductions* in the magnitude of the excess shear stress -apparently result in *increases* in the amount of lateral erosion. Yet equation 3.22 suggests that the opposite should be the case. This apparent paradox is resolved by realising that the coefficient R_l in equation 3.22 is also a function of τ_c. It seems that increases in τ_c result in increases in R_l that in turn result in predictions of increased lateral erosion, even though the surplus shear stress is reduced by increases in τ_c. It is apparent that the lateral erosion model formulated by Arulanandan *et al.* (1980) (equation 3.22) requires revision to correct this error. Nevertheless, this is not a significant limitation for this study, since it is still possible to show unequivocally the impact of increases of lateral erosion rate on the simulated trends of B* and B/D. This was done by varying the value of the coefficient R_l in equation 3.22 while holding τ_c constant at an "erodible" value (τ_c = 14.60 dynes/cm^2). In this way R_l can be used as a surrogate variable for the rate of lateral erosion. The results of this analysis are shown in Figure 5.11, which confirms the explanation of the influence of lateral erosion on trends of B* and B/D given above. Increases in lateral erosion rate result in increased rapidity of the onset of bank top widening, as well as increases in the magnitude of bank top widening.

5.1.3.9 Failed Bank Material Properties

Figures 5.12 and 5.13 illustrate the role of the failed bank material products in influencing the sequence of simulated channel adjustments. Figure 5.12 illustrates temporal trends of B* and B/D for a range of values of failed bank material aggregate diameters, while Figure 5.13 shows these trends for a range of values of failed bank material aggregate specific gravities. Both variables are, in effect, measures of the transportability of the failed bank material deposited in the near bank zone at the base of the bank following mass failure and, therefore, show similar trends. In each case, these variables of course have no impact on the initial deepening phase or the onset of channel widening. However, once widening is initiated, the input of the failed bank material aggregates to the near bank zones means that these variables begin to have some effect on the channel adjustment dynamics. During the rapid widening phase immediately following the onset of bank instability, there is little impact on the trends of either B* or B/D, but in both cases increasing transportability (decreasing d_{bank} or SG_{bank}) of the bank sediments results in marginally increased values of both B* and B/D. However, this impact on B* and B/D becomes more marked as the widening rates begin to slow. It appears that during the initial stages of rapid widening, bank retreat is dominated by the constraints set by the critical failure geometry and geotechnical properties, so that the impact of less sensitive variables is dwarfed. But, once the rates of widening begin to slow and these impacts diminish, the impact of changes in the transportability of failed bank materials becomes progressively more marked. Increases in transportability mean the failed bank materials are removed more rapidly by the flow, reducing the near bank sediment store, thereby prolonging instability until the channel widens to offset the flows increased ability to entrain the more transportable bank sediments. Figures 5.12 and 5.13 illustrate that the properties of the failed bank materials do play a role in influencing the adjustment of channel morphology through their influence on the transportability of the mixture of sediments in the near bank zone. It is the transportability of these sediments, together with the conditions of hydraulics and sediment supply to the near bank zone that controls the length of time required to remove the failed bank materials from the near bank zone, destabilize the banks and once again initiate bank failure and channel widening, as envisaged in the "basal clear out" phase of the concept of basal endpoint control (Figure 2.7) (Thorne, 1978; Thorne & Osman, 1988a).

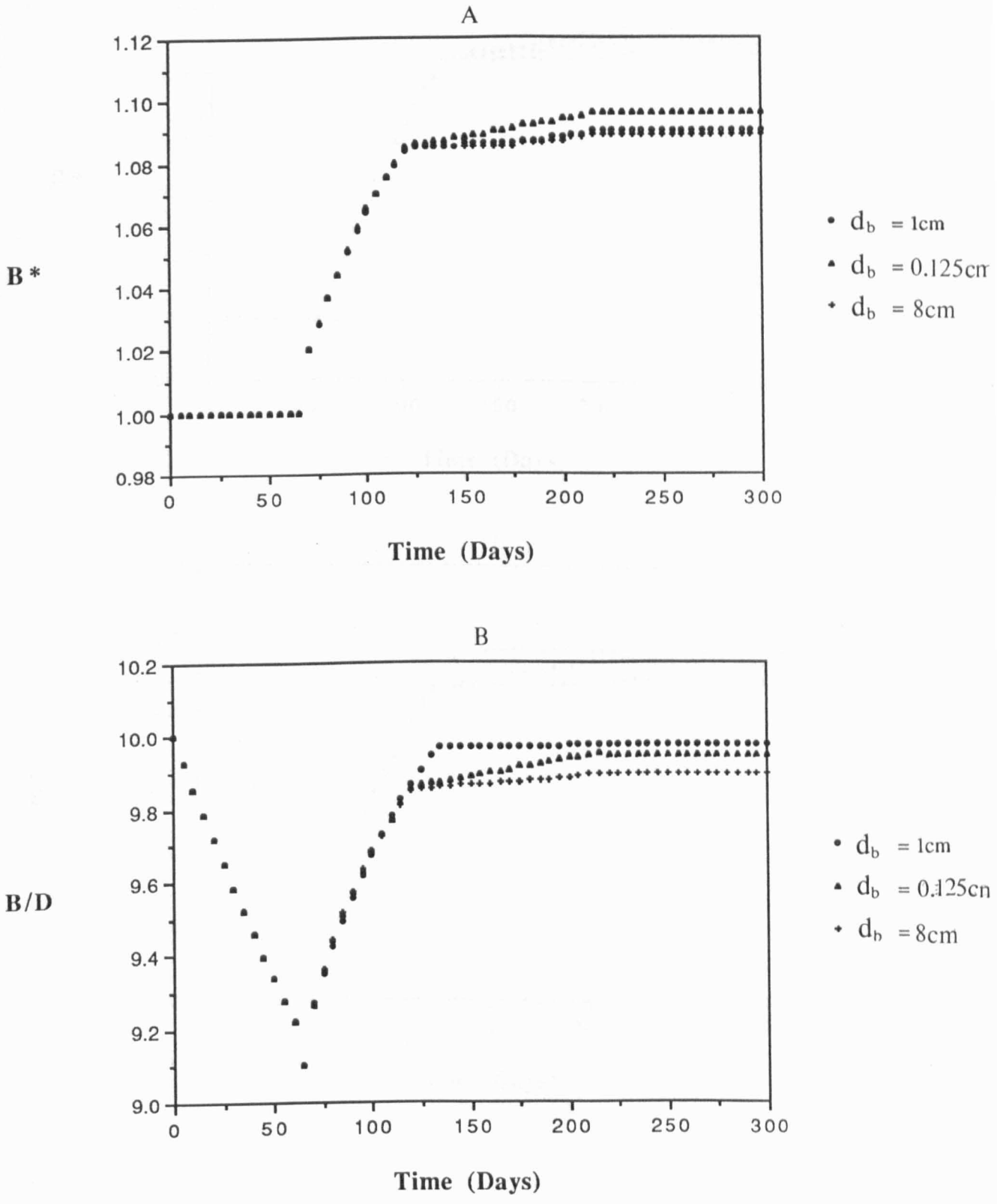

Figure 5.12 Simulated Temporal Trends of (A) Non-Dimensional Bank Top Width and (B) Aspect Ratio for Varying d_{bank}

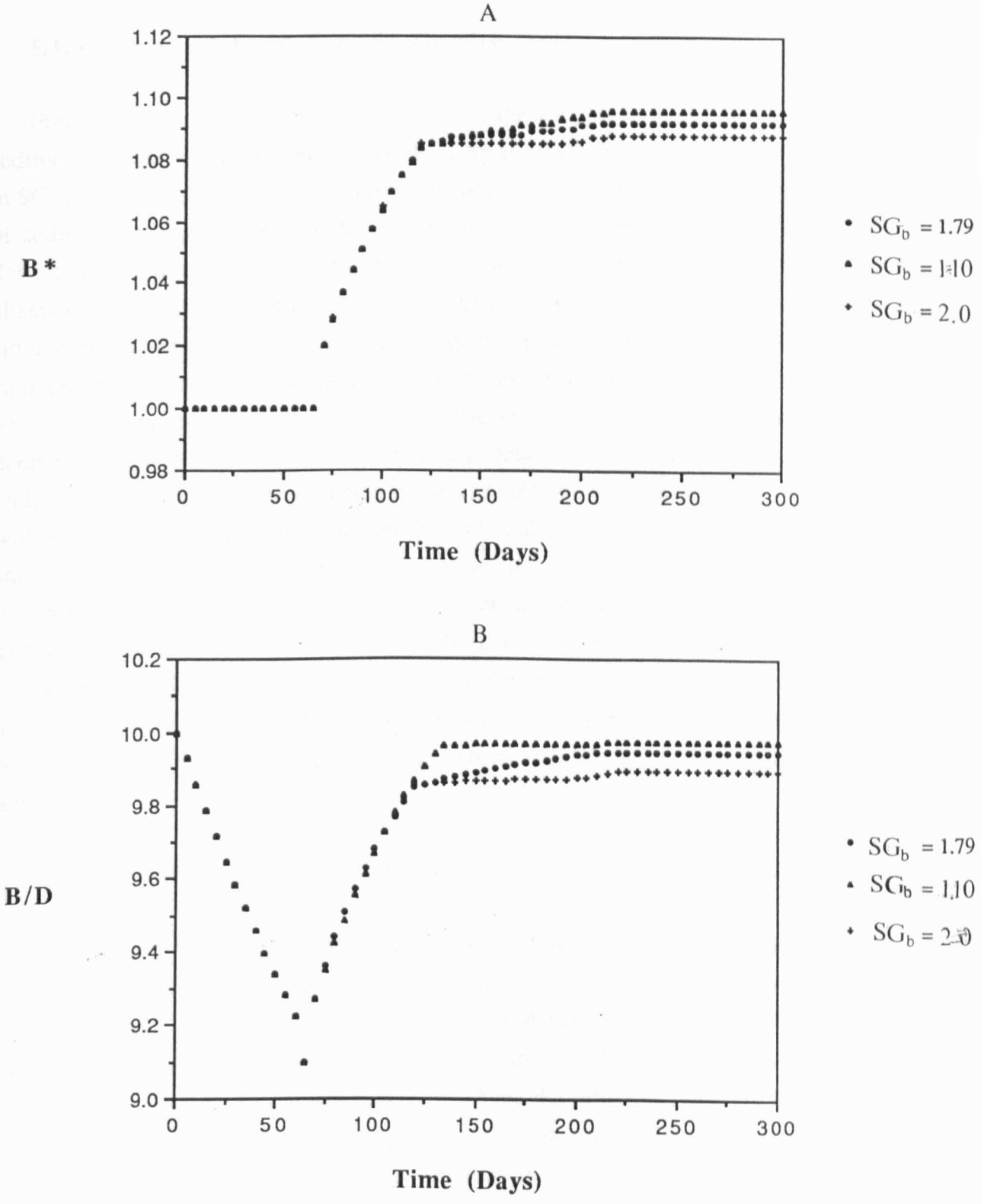

Figure 5.13 Simulated Temporal Trends of (A) Non-Dimensional Bank Top Width and (B) Aspect Ratio for Varying SG_{bank}

5.1.3.10 Bed Material Specific Gravity (SG)

Figure 5.14 shows the impact of changes in the specific gravity (SG) of the bed sediments on the simulated temporal trends of B* and B/D. It is apparent that increases in SG make the bed sediments less transportable by the flow. This results in a reduction of sediment transport rates, a reduction in the sediment supply : transport capacity deficit and reduced rates of initial bed degradation. Degradation continues in the absence of channel widening until the critical bank geometry is attained in all simulations. The magnitude of the initial deepening phase is, therefore, independent of changes in SG, but is instead determined by the constraints of the bank geometry and geotechnical properties of the bank soils. The impact of SG on the initial rate of deepening is such that the onset of widening is delayed by increases in SG. Rates of width adjustment during the widening phase appear to be moderately sensitive to SG, with increases in SG resulting in the more rapid establishment of a relatively reduced, stable channel width. These reduced stable widths are attained more rapidly as a consequence of the decreased transportability of the bed sediments as SG increases. The reduction in transport rates reduces the deficit between sediment supply and transport capacity so that less widening is required to reduce the transport capacity to levels at which there is a surplus of sediment supply relative to the transport capacity, resulting in basal deposition and an increase in bank stability as bank heights and angles are reduced.

5.1.3.11 Bed Material Porosity (λ)

Figure 5.15 shows temporal trends of B* and B/D for various values of bed material porosity. The sediment continuity equation (3.8) indicates that increases in porosity result in reduced increments of aggradation or degradation for given combinations of sediment supply and transport conditions. In the simulations shown in Figure 5.15, increases in porosity, therefore, have the effect of reducing the rate of initial deepening and delaying the onset of channel widening. The overall magnitude of change in channel width appears to be moderately sensitive to porosity, with increases in porosity leading to reductions in the predicted stable channel widths. Stable widths are predicted to become relatively smaller as porosity is increased, since relatively reduced amounts of widening are required to reduce sediment transport capacity (by shallowing) to levels at which the bank stability is able to recover through aggradation as sediment supply, from bank failures and upstream bed degradation, begins to exceed sediment removal. The influence of increasing porosity is to reduce the initial degradational deficit, so that relatively smaller changes in sediment supply and transport

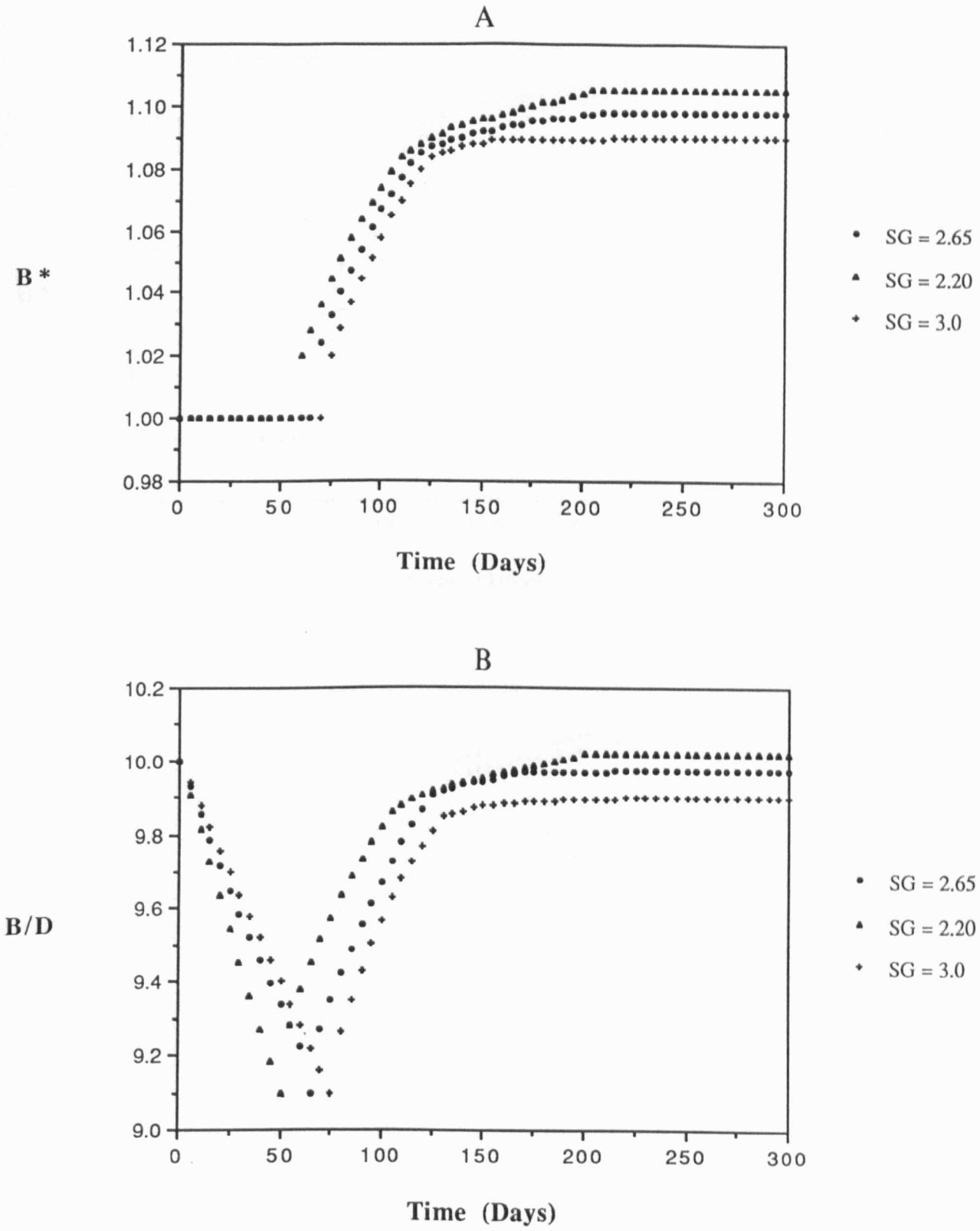

Figure 5.14 Simulated Temporal Trends of (A) Non-Dimensional Bank Top Width and (B) Aspect Ratio for Varying SG

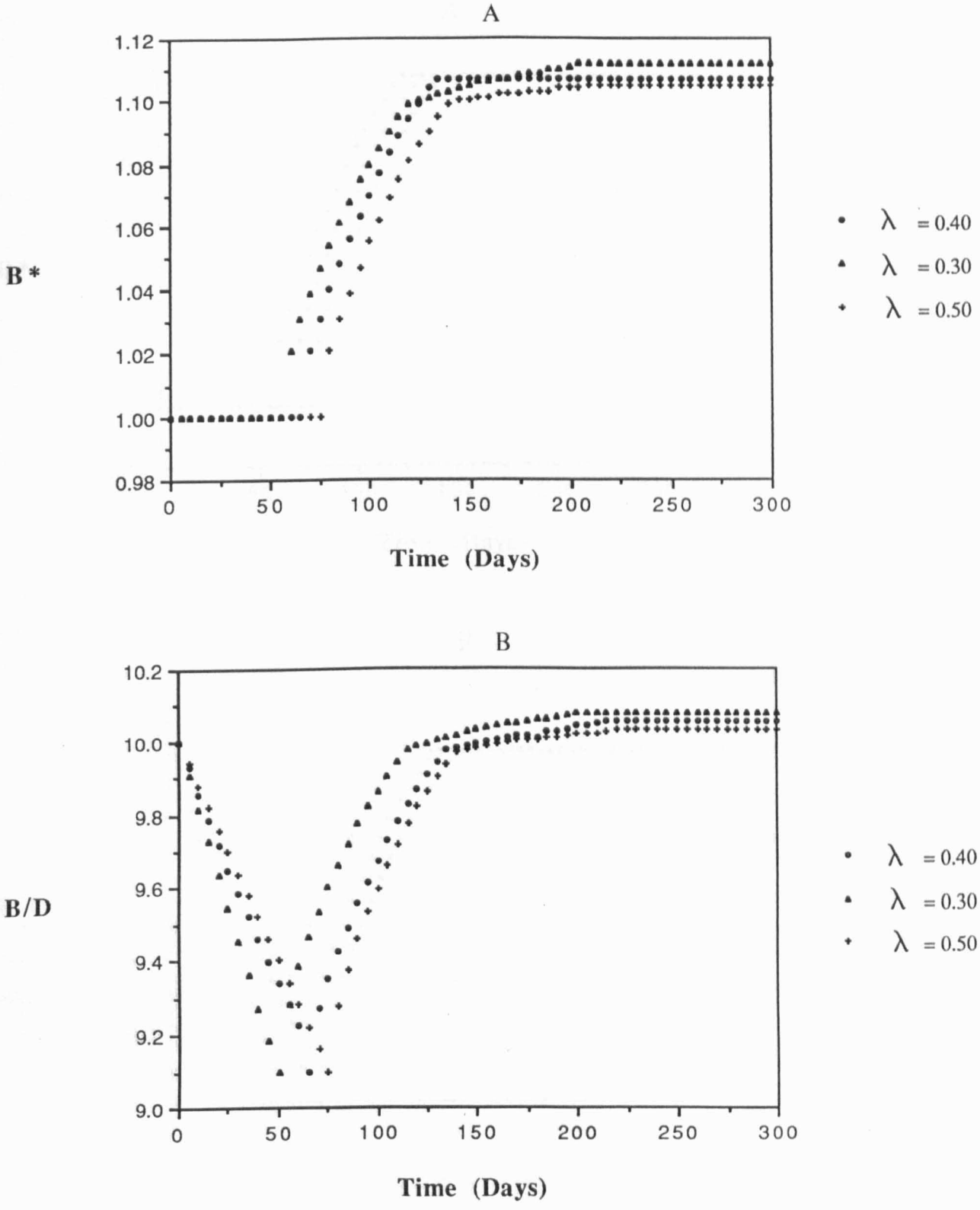

Figure 5.15 Simulated Temporal Trends of (A) Non-Dimensional Bank Top Width and (B) Aspect Ratio for Varying λ

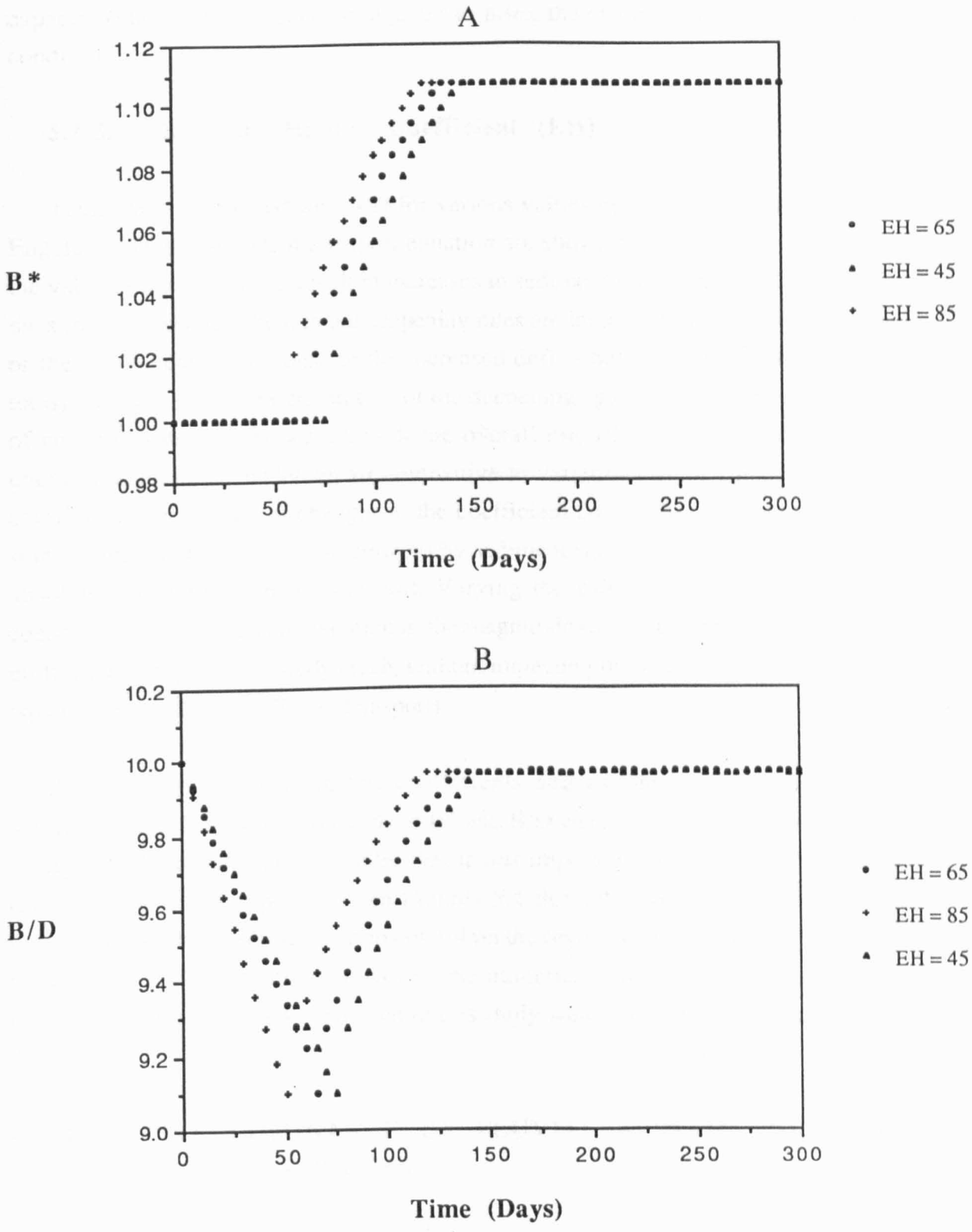

Figure 5.16 Simulated Temporal Trends of (A) Non-Dimensional Bank Top Width and (B) Aspect Ratio for Varying EH

capacity (via width changes) are required to bring the channel back to a more stable condition.

5.1.3.12 Engelund-Hansen Coefficient (EH)

Temporal trends of B* and B/D for various values of the coefficient used in the Engelund-Hansen sediment transport equation are shown in Figure 5.16. Increases in the value of the coefficient result in increases in sediment transport rate. This explains the simulated results, where initial deepening rates are increased by increasing the value of the coefficient, in response to the increased deficit between sediment supply and transport capacity. Increased rapidity of the deepening again results in an earlier onset of channel widening. However, both the overall rate of width adjustment and the overall magnitude of widening are insensitive to variations in the Engelund-Hansen coefficient. The impact of changes in the coefficient on channel adjustment is small since channel deformation is determined by sediment flux divergences, rather than by absolute values of sediment transport. Varying the value of the Engelund-Hansen coefficient simply results in variation in the magnitude of the sediment transport fluxes uniformly throughout the study reach, without impacting the sediment flux divergences (spatial distribution of sediment transport).

A number of other variables, coefficients and exponents were subjected to sensitivity tests, but simulated trends of B* and B/D were found to be so insensitive to changes in these remaining variables that it was impossible to distinguish individual runs on plots of the type shown in Figures 5.4 through 5.16 by inspection. These remaining variables exert little or no control on the response of channel morphology to an unstable initial condition. However, the numerical values of various sensitivity parameters for all the tests conducted in this study were calculated and these are now discussed.

5.2 RELATIVE DOMINANCE OF FLUVIAL SYSTEM VARIABLES DURING CHANNEL EVOLUTION

The results of the sensitivity tests illustrated in Figures 5.4 to 5.16 are useful in determining the impact changes to individual fluvial system variables have on channel adjustment dynamics, and how changes in the variables control the adjustments of channel morphology at different times during the response sequence. However, it is also interesting to compare the relative sensitivity of channel morphology to changes in each of the control variables, to determine the relative importance of those variables in

controlling the various aspects of the dynamics of channel adjustment. Establishing the relative importance of individual variables is not only interesting from the point of view of analysis of the fluvial system, but also has important practical implications. Modification of dominant variables, perhaps as a result of river engineering projects, may result in changes in channel morphology. Identification of sensitive variables could help to improve our ability to predict such changes and make due allowance for them in engineering design.

However, it is not always sufficient to determine the relative dominance of individual variables in controlling the overall magnitude of changes in channel geometry variables from an initial, disturbed, state to a final, more stable equilibrium form. As the channel adjusts through the various phases of channel evolution (Schumm *et al.*, 1984; Thorne & Osman, 1988a, Simon, 1989), different processes may dominate adjustment and different variables may shift in dominance and dependence and may even become extraneous during different phases of adjustment (Simon & Darby, in preparation). It is, therefore, necessary to analyse the relative dominance of individual fluvial system variables in a dynamically based framework in addition to establishing the relative dominance of these variables in influencing overall changes in form. Simon (1992) used empirical data of channel adjustment to establish the dominance of different processes and forms in two diverse fluvial systems by analysing temporal trends of components of flow-energy variables. This work was further extended by Simon & Darby (in preparation), who used the physically-based numerical model developed in this research to similarly establish the dominance of processes and forms through temporally based analysis of flow-energy variables. The analyses reported here complement these studies by directly quantifying the sensitivity of channel morphology to changes in a much wider range of individual fluvial system variables than previously attempted, in order to rank the relative dominance of fluvial system variables influencing form throughout the various stages of channel adjustment.

To achieve this, the numerical values of each of the sensitivity parameters formulated in section 5.1.1 (sensitivity of the overall change in the channel width ($\chi_{\Delta B}$), overall change in the channel depth ($\chi_{\Delta D}$), initial change in channel depth ($\chi_{\Delta Do}$), widening rate (χ_t) and time to onset of widening (χ_T) to changes in control variables) were calculated for each of the variables subjected to sensitivity tests. Calculated mean values at both upstream and downstream locations in the model channel are shown in Tables 5.3 and 5.4. In calculating each of the sensitivity parameters, the model output data from each of the runs for each of the control variables were used in equations 5.1 to 5.8. Four runs were made for each variable, in

Table 5.3 Mean Sensitivity Parameters (Upstream Location)

Variable	$\chi_{\Delta B}$	$\chi_{\Delta D}$	$\chi_{\Delta D_0}$	χ_T	χ_t
Q	0.4535	0.3143			
Qs	-0.412	-0.0286	0.207 or 0	1.003	-0.0347
S	0.0146	0.0491	0	-0.308	0.619
n	-0.035	0.0247	0	0.5288	0.208
C	-0.00427	0.0618	-0.146	13.636	Unavailable
H	0.407	-0.640	0.554	-12.788	3.661
K	-0.0129	-0.0392	0.047	-0.638	0.122
τ_c	6.211 or 0	0.0638 or 0	0.0868 or 0	60.836 or 0	97.33 or 0
D_{mix}	0	-0.000245	0	0	0
R_l	0.0263 or 0	-0.135 or 0	0.102 or 0	-1.231 or 0	0 or 0
d_{bank}	0.00873	0.00423	0	0	0.0532
SG_{bank}	-0.0689	-0.00314	0	0	0.196
SG	-0.0855	0.0275	0	0.746	-0.554
λ	0.0108	0.0200	0	-0.635	0.400
EH	0	0.0219	0	-0.500	0
μ	0	0	0	0	0
NEV	0	0	0	0	0
ε_z	0	0	0	0	0
E	0	0	0	0	0
d_{sand}	0	0	0	0	0
d_{50}	-0.00360	0.00813	0	0.333	0
SAND	0	0	0	0	0
HF	0	0.000347	0	0	0

Table 5.4 Mean Sensitivity Parameters (Downstream Location)

Variable	$\chi_{\Delta B}$	$\chi_{\Delta D}$	$\chi_{\Delta D_0}$	χ_T	χ_t
Q	0.4535	0.3143			
Qs	-0.136	-0.0317	0.214 or 0	0.917	-0.0347
S	0.040	0.0532	0	-0.308	0.25
n	-0.057	0.0263	0	0.357	0.208
C	-0.00427	0.0613	-0.133	13.636	Unavailable
H	0.407	-0.593	0.509	-11.321	3.661
K	-0.0131	-0.0382	0.0392	-0.571	0.122
τ_c	2.200 or 0	0.0609 or 0	0.0803	60.836 or 0	24.333 or 0
D_{mix}	0	0.00115	0	0	0
R_l	0.0263 or 0	-0.133 or 0	0.101	-1.231 or 0	0 or 0
d_{bank}	0.00349	0.00409	0	0	0.149
SG_{bank}	-0.0951	-0.00320	0	0	0.196
SG	-0.0840	0.0276	0	1.406	-0.554
λ	0.0208	0.0200	0	-0.571	0.311
EH	0	0.0209	0	-0.371	0
μ	0	0	0	0	0
NEV	0	0	0	0	0
ε_z	0	0	0	0	0
E	0	0	0	0	0
d_{sand}	0	0	0	0	0
d_{50}	-0.0110	0.0180	0	0.123	4
SAND	0	0	0	0	0
HF	0.00576	0.00802	0	0	0

addition to the baseline run. Values for each of the sensitivity parameters were calculated for each of the four values of the control variables used in the sensitivity tests. In each case some variation in calculated sensitivity as a function of the magnitude of the control variable was found. A mean sensitivity parameter was, therefore, calculated on the basis of the four results. The mean sensitivity parameter was found in all cases to be reasonably representative of the range in calculated sensitivity parameters. The variation of the various sensitivity parameters as a function of control variables indicates that overall channel response (*e.g.* width versus depth response), is a function of environmental boundary conditions. This is explored further in section 5.3.

Tables 5.3 and 5.4 indicate that there is a wide range of calculated mean sensitivity parameters for each of the five categories of sensitivity parameter. In each case, the sensitivity parameter represents a quantitative estimate of the amount of dimensionless change in the output variable of interest (either width, depth, initial decrease in B/D, widening reaction time or rate of widening) per unit dimensionless change in the control variable of interest. Negative values of the mean sensitivity parameters indicate that the direction of change (increase or decrease) of the output variable is opposite to the direction of change in the control variable. In each case the maximum range and mean values of the sensitivity parameters are located at the upstream cross-section, indicating that the morphological response to changes in the control system variables is relatively greater and more variable at the upstream location than the downstream location.

However, when ranking fluvial system variables to determine the dominant controls on natural channel adjustment, the use of mean sensitivity parameters can be misleading. This is because mean sensitivity parameters summarise predicted change in output variables per unit change in control variables. Sensitivity parameters calculated in this way do not take account of the magnitude of the variation of the control variable likely to be experienced in nature. This may be illustrated using an example.

The mean channel width sensitivity parameters at the upstream model location for specific gravity (SG) and bank material cohesion (C) have values of -0.0855 and -0.00427, respectively (Table 5.3). This suggests that channel width is much more sensitive to unit changes in specific gravity of bed material than to bank material cohesion. However, this conclusion ignores the fact that the range of values of SG found in nature is quite small relative to the range of possible values of bank material cohesion. Despite the lower sensitivity of channel width to *unit* changes in cohesion, relative to *unit* changes in bed material specific gravity, it is likely that variations in

channel width in nature are controlled more by variation in cohesion than variation in bed material specific gravity, because of the much wider range of cohesion values relative to specific gravity values. This would be in contrast to the conclusion drawn from the use of the mean sensitivity parameters that specific gravity is predicted to be a more significant control on channel width than cohesion.

To overcome this problem, the mean sensitivity parameters were adjusted using a weighting coefficient. The effect of the weighting coefficient is to reduce the influence of control variables on channel morphology when those control variables have only a small natural variation, but to increase the significance of control variables with a large natural variation. Weighted mean sensitivity parameters were estimated from the product of the mean sensitivity parameters presented in Tables 5.3 and 5.4 and a maximum weighting coefficient. The weighting coefficient was estimated from the estimated likely range of the control variable (Table 5.5). The dimensionless weighting coefficient, WC, is, therefore, defined by:

$$WC = \frac{x_i - x_b}{x_b} \qquad (5.9)$$

where x_b = baseline value of a control variable and x_i = value of the variable that gives the largest difference between the baseline value and that value. By estimating the likely maximum naturally occuring range of the various control variables, the weighting coefficient at the extremes of the range may be determined using equation (5.9). The maximum weighting coefficient in this range was then used to determine the weighted sensitivity parameters. Estimates of the likely maximum naturally occuring range of control variables and corresponding range of weighting coefficients used in this study are summarised in Table 5.5.

Although the method used to obtain the precise *magnitudes* of the weighted sensitivity parameters is subject to some uncertainty as a consequence of the limitations of the sensitivity tests, accuracy of the model and the reliability of the estimates of the variable ranges made in Table 5.5, the *relative* rankings of the various control variables can be established with a reasonable degree of confidence using this procedure. The control variable rankings for each of the weighted mean sensitivity parameters are summarised in Tables 5.6 and 5.7, which report the relative rankings by location in the modelled channel, and Table 5.8, which summarises the ranked means of each variable for the two locations. The relative rankings of each variable are relatively independent of location in the modelled reach, though the values of the sensitivity parameters are influenced by location in the hypothetical channel. In effect, these tables are "league

Table 5.5 Dimensionless Weighting Coefficients for Control Variables Used in Sensitivity Analyses

Variable	Baseline value	Estimated Range	Reference	Range of Dimensionless Weighting Coefficients
Q	100 m^3s^{-1}	0 to 1000		1 to 9.0
Qs	0.5	0.0 to 2.0		-1.0 to 3.0
S	0.001	0.01 to 0.00001		-0.99 to 9.0
n	0.025	0.015 to 0.075	Barnes, 1967	-0.6 to 2.0
C	10.0 kPa	0 to 40 kPa		-7.0 to 7.0
H	3.60 m	0 to 7.2 m		-1.0 to 1.0
K	0.2	0 to 0.5	Taylor, 1948	-1.0 to 1.5
τ_c	14.0 dynes/cm^2	0 to 14.0		-1.0 to 1.0
D_{mix}	0.10	0.05 to 0.15		-0.5 to 0.5
R_l	0.023	0 to 0.046		-1.0 to 1.0
d_{bank}	1 cm	1mm to 1 m	Thorne, 1978	-0.9 to 49.0
SG_{bank}	1.79	1.1 to 3.0		-0.385 to 0.676
SG	2.65	2.3 to 3.0		-0.132 to 0.132
λ	0.40	0.3 to 0.5		-0.25 to 0.25
EH	65	45 to 85		-0.308 to 0.308
μ	0.65	0.45 to 0.85		-0.308 to 0.308
NEV	0.16	0.08 to 0.24	Wark *et al.* 1990	-1.0 to 1.0
ε_z	0.077	0 to 0.154		-1.0 to 1.0
E	$3.2474 * 10^{-4}$	$3*10^{-4}$ to $3*10^{-1}$	Garcia & Parker, 1991	-0.08 to 922.0
d_{sand}	1 mm	0.063 to 2 mm		-0.937 to 1.0
d_{50}	1 mm	0.063 to 2 mm		-0.937 to 1.0
SAND	0.2	0 to 1.0		-1.0 to 4.0
HF	0.85	0.65 to 1.0	Richards, 1990	-0.235 to 0.176

Table 5.6 Ranked Weighted Mean Sensitivity Parameters (Upstream Location)

$\chi_{\Delta B}$	$\chi_{\Delta D}$	$\chi_{\Delta Do}$	χ_T	χ_t
τ_c (6.211)	Q (2.829)	C (1.023)	C (95.452)	τ_c (97.33)
Q (4.081)	H (-0.639)	Qs (0.621)	τ_c (60.836)	S (5.571)
d_{bank} (0.428)	S (0.442)	H (0.554)	H (-12.788)	H (3.661)
Qs (-0.426)	C (0.432)	R_l (0.102)	Qs (3.010)	d_{bank} (2.606)
H (0.407)	d_{bank} (0.207)	τ_c (0.087)	S (-2.772)	n (0.417)
S (0.132)	R_l (-0.135)	K (0.071)	R_l (-1.231)	K (0.183)
n (-0.070)	Qs (-0.086)	NEV	n (1.058)	SG_{bank} (0.133)
SG_{bank} (-0.047)	τ_c (0.064)	μ	K (-0.958)	Qs (-0.104)
C (-0.030)	K (-0.059)	ε_z	d_{50} (0.333)	λ (0.100)
R_l (0.026)	n (0.049)	E	λ (–0.159)	SG (-0.073)
K (-0.019)	SAND (0.020)	d_{sand}	EH (-0.154)	NEV
SG (-0.011)	d_{50} (0.008)	SAND	SG (0.098)	μ
d_{50} (-0.004)	EH (0.007)	HF	NEV	ε_z
λ (0.003)	λ (0.005)	D_{mix}	μ	E
NEV	SG (0.004)	EH	ε_z	d_{sand}
μ	SG_{bank} (-0.002)	d_{bank}	E	SAND
ε_z	D_{mix} (-0.0001)	SG_{bank}	d_{sand}	HF
E	HF	n	SAND	D_{mix}
d_{sand}	d_{sand}	λ	HF	EH
SAND	NEV	SG	D_{mix}	R_l
HF	μ	d_{50}	d_{bank}	d_{50}
D_{mix}	ε_z	S	SG_{bank}	(C not available)
EH	E			

Table 5.7 Ranked Weighted Mean Sensitivity Parameters (Downstream Location)

$\chi_{\Delta B}$	$\chi_{\Delta D}$	$\chi_{\Delta D_0}$	χ_T	χ_t
Q (4.081)	Q (2.829)	C (0.929)	C (95.452)	τ_c (24.333)
τ_c (2.200)	H (-0.593)	Qs (0.641)	τ_c (60.836)	d_{bank} (7.324)
Qs (-0.408)	S (0.479)	H (0.509)	H (-11.321)	H (3.661)
H (0.407)	C (0.429)	R_l (0.101)	S (-2.772)	S (2.250)
S (0.36)	d_{bank} (0.200)	τ_c (0.080)	Qs (2.750)	n (0.417)
d_{bank} (0.171)	R_l (-0.133)	K (0.059)	R_l (-1.231)	K (0.183)
n (-0.070)	Qs (-0.095)	NEV	K (-0.857)	SG_{bank} (0.133)
SG_{bank} (-0.064)	SAND (0.088)	μ	n (0.714)	Qs (-0.104)
C (-0.030)	τ_c (0.061)	ε_z	SG (0.186)	λ (0.078)
R_l (0.026)	K (-0.057)	E	λ (–0.143)	SG (-0.073)
K (-0.020)	n (0.053)	d_{bank}	d_{50} (0.123)	d_{50} (0.123)
SG (-0.011)	d_{50} (0.018)	SG_{bank}	EH (-0.114)	NEV
d_{50} (-0.011)	EH (0.006)	d_{sand}	NEV	μ
λ (0.005)	λ (0.005)	SAND	μ	ε_z
NEV	SG (0.004)	HF	ε_z	E
μ	SG_{bank} (-0.002)	D_{mix}	E	d_{sand}
ε_z	HF (0.002)	n	d_{bank}	SAND
E	D_{mix} (0.001)	λ	SG_{bank}	HF
d_{sand}	d_{sand}	SG	d_{sand}	D_{mix}
SAND	NEV	EH	SAND	EH
HF	μ	d_{50}	HF	R_l
D_{mix}	ε_z	S	D_{mix}	(C not available)
EH	E			

Table 5.8 Ranked Weighted Mean Sensitivity Parameters (Mean of Locations)

$\chi_{\Delta B}$	$\chi_{\Delta D}$	$\chi_{\Delta Do}$	χ_T	χ_t
τ_c (4.206)	Q (2.829)	C (0.976)	C (95.452)	τ_c (60.83)
Q (4.081)	H (-0.616)	Qs (0.631)	τ_c (60.836)	d_{bank} (4.965)
Qs (-0.417)	S (0.461)	H (0.532)	H (-12.055)	S (3.911)
H (0.407)	C (0.430)	R_l (0.102)	Qs (2.880)	H (3.661)
d_{bank} (0.300)	d_{bank} (0.207)	τ_c (0.083)	S (-2.772)	n (0.417)
S (0.246)	R_l (-0.134)	K (0.065)	n (1.772)	K (0.183)
n (-0.070)	Qs (-0.091)	NEV	R_l (-1.231)	SG_{bank} (0.133)
SG_{bank} (-0.056)	τ_c (0.063)	μ	K (-0.908)	Qs (-0.104)
C (-0.030)	K (-0.058)	ε_z	d_{50} (0.456)	λ (–0.089)
R_l (0.026)	n (-0.051)	E	λ (–0.151)	SG (-0.073)
K (-0.020)	SAND (0.054)	d_{bank}	SG (0.142)	d_{50}
SG (-0.011)	d_{50} (0.013)	SG_{bank}	EH (-0.134)	NEV
d_{50} (-0.008)	EH (0.007)	d_{sand}	NEV	μ
λ (0.004)	λ (0.005)	SAND	μ	ε_z
NEV	SG (0.004)	HF	ε_z	E
μ	SG_{bank} (-0.002)	D_{mix}	E	d_{sand}
ε_z	HF (0.001)	n	d_{bank}	SAND
E	D_{mix} (0.0006)	λ	SG_{bank}	HF
d_{sand}	d_{sand}	SG	d_{sand}	D_{mix}
SAND	NEV	EH	SAND	EH
HF	μ	d_{50}	HF	R_l
D_{mix}	ε_z	S	D_{mix}	(C not available)
EH	E			

tables" establishing the relative importance of the individual control variables on the various facets of channel adjustment dynamics. It should be noted that each league table has arbitrary groupings of parameters which correspond to "divisions" of equal orders of magnitude of the numerical value of the sensitivity parameters. In each table, the lowest "division" is composed of variables with calculated weighted mean sensitivity parameters equal to zero. The highest "division" of channel adjustment variables is at the top of each table. These variables are predicted to be among the most significant in controlling the various aspects of channel adjustment.

5.2.1 Relative Dominance of Variables Controlling Stable Channel Geometry

The sensitivity parameters which describe overall change in channel morphology between initial and final "stable" states are those for overall change in channel width and depth; $\chi_{\Delta B}$ and $\chi_{\Delta D}$, respectively. Tables 5.6 to 5.8 indicate that the most sensitive variables in determining overall change in channel width and depth appear to be the discharge (Q) and the critical threshold for entrainment of the bank material (τ_c) in the case of channel width, and discharge in the case of channel depth. At both the upstream and downstream locations in the modelled reach these "first division" variables have estimated sensitivity parameters approximately an order of magnitude higher than their closest "rivals" in the league tables. However, in light of the uncertainty concerning the status of τ_c, this variable is excluded from the analysis. According to these results, the single most dominant variable in controlling overall change in channel width and depth in these simulations is, therefore, the discharge. This result is consistent with the traditional use of bivariate relationships in hydraulic geometry analyses, in which channel morphology variables are related to "channel-forming" discharge alone. It appears from the results of the sensitivity tests conducted here that, insofar as discharge is the dominant variable, the use of such bivariate relationships is justified.

A particular question concerning the sensitivity of channel morphology to the discharge has been the relative roles of the channel discharge and bank material characteristics in establishing the stable channel morphology, especially the channel width. Bank material characteristics include the bank material cohesion (C), initial bank height (H), tension crack index (K) and parameters representing the resistance of the bank material to lateral erosion (τ_c and R_l). Calculated sensitivity parameters for width and depth for each of these bank material characteristic variables are at least an order of magnitude smaller than the corresponding sensitivity parameters for discharge, confirming that discharge is indeed the dominant variable in terms of its influence on

both stable channel widths and depths. This supports the argument of Bettess and White (1987b) that, "The very success of regime theories in predicting channel width when such theories have in the past completely ignored both the composition of the banks and the method of bank erosion must suggest that such factors are only secondary in the determination of width", though admittedly this conclusion is based on (sensibly) discounting the calculated sensitivity parameters for τ_c.

However, it appears that the difference in the magnitude of channel depth sensitivity parameters for discharge and bank material cohesion is much less than the difference in the channel width sensitivity parameters for these variables. This suggests that, although discharge is clearly the dominant variable for both width and depth, discharge is less important in establishing the channel depth relative to the bank material characteristics than it is in establishing the channel width. This is equivalent to saying that bank material characteristics appear to be more important in establishing *depth* than in establishing *width*, despite empirical studies of hydraulic geometry which have emphasised the role of bank material characteristics on the stable channel width (Charlton *et al.*, 1978; Andrews, 1984; Hey & Thorne, 1986). Intuitively, this also appears a surprising result, as bank properties should exert a direct control on width adjustment.

Resolution of this apparent paradox lies in recognition of the role that the bank material characteristics play in controlling both the channel depth and width, but at different times in the adjustment sequence. The bank material cohesion partially determines the factor of safety of the banks and the critical geometry required to initiate mass failure and rapid widening. Assuming that the initial condition is stable relative to the critical bank geometry, then prior to the onset of bank instability, depth is free to adjust, while the width is constrained by the stability of the banks. But, once the critical bank height for generating instability with respect to mass failure is reached, bank retreat and widening is initiated, sediment is supplied to the channel from bank failures, boundary shear is reduced as the channel widens and the rate of degradation slows and ceases. This process threshold limits further degradation and so geotechnical characteristics control depth adjustment as well as width adjustment. Further evidence of the important control that the bank material characteristics exert on depth adjustment is supplied from the values calculated for the sensitivity parameter representing initial change in width-depth ratio, which is a measure of the magnitude of the initial deepening phase. From Tables 5.6 to 5.8 it is seen that, apart from the sediment load supplied from the upstream boundary of the modelled reach, the only significant

controls on the magnitude of the initial deepening phase of channel adjustment are the variables which represent bank material characteristics.

In light of the strong influence of the bank material characteristics on the establishment of the stable hydraulic geometry predicted by these model simulations, it is perhaps surprising that more emphasis has not been placed on empirical analyses of the effects of bank material characteristics on depth as well as width. Data from 62 gravel-bed rivers in the United Kingdom presented by Hey & Thorne (1986) are suitable for the analysis of the effects of bank material characteristics on stable channel geometry. In this data set, an index of bank vegetation density was determined at each site. The vegetation index is based on dividing the density of bank vegetation into categories, with Category I the least dense vegetation cover and Category IV the highest density. Increased vegetation density is supposed to represent increasing bank material resistance to erosion. Values of channel depth against bankfull discharge were then plotted against each other, but with each point classified by the vegetation indices. In this way it is possible to see if there is a systematic impact of vegetation density on observed depths as a function of discharge (Figure 5.17). It appears that, in fact the data do reveal a trend for depth to increase as the density of bank vegetation increases, providing empirical support for the simulated results obtained above. However, there are two main reasons why this supporting evidence must be regarded as very tentative. First, bank vegetation impacts are complex (Thorne, 1990) and the vegetation density index is possibly not, therefore, a good surrogate for bank material strength. Second, the Hey & Thorne data is for gravel-bed streams which may behave in ways distinct from the sand-bed streams modelled in this study. It is recommended that future hydraulic geometry analyses should include observations of bank material shear strength in the analyses of trends of channel depth, slope and width against discharge so that these effects may further be analysed in a wide variety of streams.

The predicted dominance of the discharge in establishing stable channel geometry, in line with the arguments of Bettess & White, is apparently in contradiction with Thorne & Osman (1988a), who emphasise the influence of bank material characteristics on the stable channel geometry. In fact it seems that while the discharge clearly is the dominant variable in these simulations, bank material characteristics are also predicted to have moderately high sensitivity parameters for channel width and depth, suggesting that although the primary constraint is set by the magnitude of the flow in the channel, the width and depth are free to adjust according to the constraints set by the interactions among the remaining relatively sensitive variables, which include the bank material properties. The role of bank material characteristics, therefore, appears to be in

influencing the detailed form of the channel within the broad constraints set by the flow characteristics.

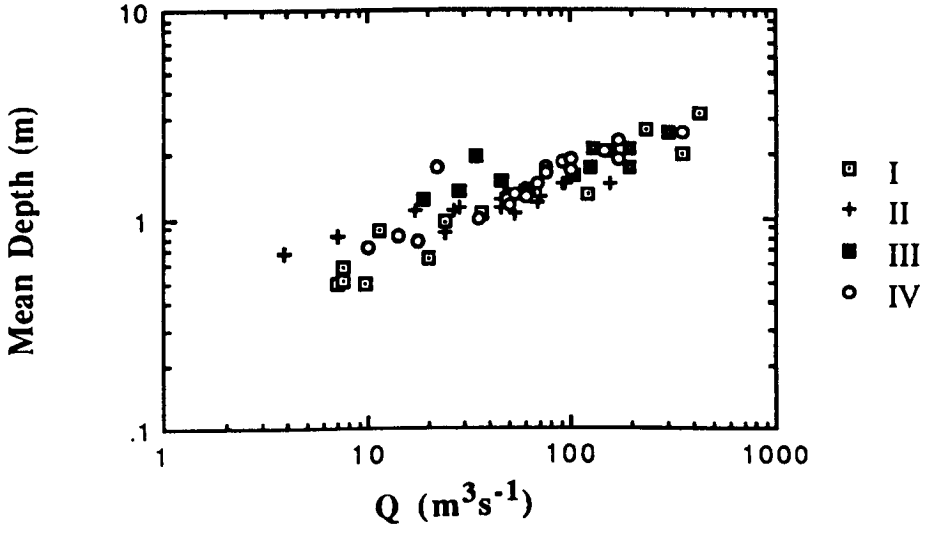

Figure 5.17 Channel Depth Versus Discharge for Various Bank Vegetation Categories for the British Gravel-Bed River Data of Hey & Thorne (1986)

There are a number of other variables of interest in Tables 5.6 to 5.8, which have sensitivity parameters approximately one order of magnitude smaller than for the discharge. Although not as significant as discharge, these variables also influence the channel morphology within the constraints set by flow regime determined by catchment hydrology.

The sediment load supplied from the upstream boundary of the model (Qs) is, as a major independent variable, expected to have a significant influence on channel geometry. This is partially confirmed from the sensitivity parameter league tables. For channel width the simulations show that the sediment load is predicted to be the next most significant variable after the discharge, above channel gradient (S), hydraulic roughness (n) and the various bank material characteristics. From Table 5.8, the sensitivity of overall change in channel width to sediment load ($\chi_{\Delta B}$ = -0.417) appears to be much larger than the sensitivity of channel depth ($\chi_{\Delta D}$ = -0.091). This is an apparently confusing result, as the sediment load supplied from the catchment would normally be expected to have a direct impact on bed elevation changes through its influence on aggradation and degradation, while the impact of Qs on width is less direct, influencing bank processes as a result of the impact of these bed elevation changes on the stability of the river banks. However, the depth sensitivity parameter in Tables 5.6 to 5.8 merely reflects the overall predicted change in channel depth. Channel

response in these simulations is characterised by an initial degradational phase, then widening and reduction of depth so that the final depth happens, in this case, to be similar to its initial value. Nevertheless, the role of Qs in influencing bed elevation changes is clearly shown from the magnitude of the $\chi_{\Delta Do}$ sensitivity parameter for this variable (0.631). This indicates that Qs has a more significant impact on depth adjustment at this stage of channel evolution than it does on the overall change in either channel width or depth.

The initial channel gradient (S), which in these simulations is equal to the valley gradient, is another major boundary condition which is expected to have a significant impact on the evolution of channel morphology, through its influence on the available stream power. Calculated sensitivity parameters indicate that the channel gradient is the third most dominant variable (after discharge and initial bank height and ahead of sediment load and various bank material and channel roughness variables) in terms of its influence on overall change in channel depth ($\chi_{\Delta D} = 0.461$). Channel gradient is ranked 6th in terms of overall dominance in the channel width league table ($\chi_{\Delta B} = 0.246$), following discharge, sediment load, some bank characteristics variables, but ahead of channel roughness, and various other bank material characteristic variables.

In both cases, increases in channel gradient lead, as expected, to increases in width and depth. It seems that channel gradient is significant in determining the stable channel morphology. As expected, channel gradient has no impact on the *magnitude* of the initial deepening phase ($\chi_{\Delta Do} = 0$), which is determined only by the constraints of the sediment load and bank material characteristics, though channel gradient does have an impact on the *rate* at which this deepening is accomplished (see below). The result that channel depth appears to be more sensitive to S than channel width is a little surprising in light of studies which emphasise the role of channel gradient in the meandering-braided river transition (Leopold & Wolman, 1957), but may merely reflect the fact that the channels simulated in these tests are below the "threshold" channel gradient required to initiate rapid widening and braiding. The sensitivity of depth to changes in channel gradient, relative to width, reflects the direct impact on stream power and sediment transfer processes (bed processes) of changes in channel gradient.

Interestingly, the size of the failed bank material aggregates (d_{bank}) is a "second division" variable for the sensitivity parameters corresponding to overall changes in width and depth. The magnitudes of the calculated sensitivity parameters ($\chi_{\Delta B} = 0.300$; $\chi_{\Delta D} = 0.207$) are similar, indicating that the size of the failed bank material influences change in width and depth by approximately equal magnitudes. This variable

is predicted to have no impact on the magnitude of the initial deepening phase ($\chi_{\Delta Do}$ = 0). This is logical since there are no failed bank materials delivered to the channel during this phase of channel evolution, when the banks are stable. In terms of the relative dominance of this variable, it is located within the second division of fluvial system variables, for both channel width and depth.

For channel width, the size of the failed bank material aggregates ranks below discharge, sediment load and initial bank height, but is apparently more important than channel gradient, hydraulic roughness and geotechnical bank material characteristics. For channel depth, only the discharge, initial bank height, channel gradient and bank material cohesion are more significant than the size of the failed bank material aggregates. This emphasises the significance of the role of the failed bank materials as a control on the evolution of channel geometry to a stable state. In particular, the size of the failed bank material aggregates is a surrogate for the "transportability" of the failed bank material aggregates. Similarly, the specific gravity of the failed bank material aggregates (SG_{bank}) is also a surrogate variable for the transportability of the failed bank materials. While this variable lies in the third division of fluvial system variables for both width and depth changes ($\chi_{\Delta B}$ = -0.0555, $\chi_{\Delta D}$ = 0.002), for channel width, SG_{bank} is still a mid-table parameter overall, though its relative significance with respect to other variables does diminish in the channel depth league table of sensitivity parameters. This is explained by the dominance of the size of the failed blocks, particularly for large blocks, on the influence of failed bank material aggregate transportability, relative to the density of the failed materials.

The hydraulic roughness (Manning's n) coefficient appears to have a relatively low significance, at least with respect to the other fluvial system variables. It is ranked 7th in the league table of channel width sensitivity parameters ($\chi_{\Delta B}$ = -0.070) and 10th in the channel depth league ($\chi_{\Delta D}$ = 0.051), though it is, significantly, by far the highest ranked empirical coefficient in the league tables (see section 5.2.3 for implications of this result). Hydraulic roughness has no impact on the magnitude of the initial deepening phase ($\chi_{\Delta Do}$ = 0), as it only impacts the rate of bed adjustment during this phase. The calculated values of the sensitivity parameters indicate that channel width is more sensitive to changes in hydraulic roughness than is channel depth, which is surprising as the hydraulic roughness directly affects flow velocities and sediment transport processes, which in turn would be expected to first impact bed, rather than bank, processes. One possibility is that changes in roughness may tend to have a relatively greater impact on the sediment transport dynamics in the near bank zone, which is subject to both bed and bank friction effects. Impacts felt in this zone would

tend to influence bank processes more than processes acting across the full width of the bed zone so that this explanation is, therefore, consistent with the simulated results.

Surprisingly, bed material property variables (specific gravity, median diameter and porosity) are amongst the lowest ranked non-zero valued fluvial system variables in the league tables for width and depth. Indeed, the values of the calculated sensitivity parameters are so low as to suggest that they have a negligible effect on the establishment of stable channel cross-section in these simulations. One reason for this may be related to the use of a hypothetical sand-bed channel with uniformly graded materials in these simulations. Variations of bed material size within the sand size range are not particularly large and increased sensitivity may have been predicted if a wider range of bed materials had been used, by including gravel-bed materials, for example. This is a limitation of the present model, but the inclusion of gravel-bed materials in future versions of the code is planned. However, in the case of these simulations, it appears that the sand-bed material characteristics are of negligible significance compared to discharge, slope, sediment load and bank material characteristics in establishing the stable channel geometry.

The remaining variables in the channel width and depth league tables all have calculated sensitivity parameters equal to zero, indicating that these variables are predicted to have no impact on channel morphology in these simulations. These parameters are composed primarily of the empirical coefficients and exponents used in the model equations. This is an encouraging result, because it means that the uncertainty introduced through the use of empirical approximations (*e.g.* for the eddy viscosity, bed roughness coefficient, hiding factor exponent, mixed layer depth and sediment transport rate equation coefficient) appears to have no impact on predictions of stable channel geometry.

5.2.2 Shifting Dominance of Variables Through Adjustment Cycle

This discussion has concentrated on the sensitivity parameters which describe overall changes in channel width and depth. However, the sensitivity of temporal aspects of the channel width adjustment sequence to changes in the various fluvial system variables are also of interest. In this study, these temporal aspects are quantified using the reaction (χ_T) and recovery (χ_t) time sensitivity parameters (which both apply to channel width). It should be noted that, for these parameters, the sensitivity of the discharge was not quantified in these instances. However, for the remaining variables, the bank material cohesion appears to be the dominant variable in terms of its influence

on channel widening reaction time (χ_T = 95.452). For given sediment load and hydraulic conditions, this clearly shows the dominant influence of the geotechnical properties of the bank materials in controlling the time taken for the channel to degrade sufficiently to reach the critical bank height required to initiate mass-failures, bank retreat and widening. This is also reflected in the high sensitivity of the reaction time to the critical entrainment threshold (χ_T = 60.836) and initial bank height (χ_T = -12.788). These parameters also describe aspects of the stability of the banks with respect to mass failure and appear to be dominant relative to the remaining fluvial system variables.

Of the remaining variables, sediment load unsurprisingly has a relatively major impact (χ_T = 3.010), followed in order by the channel gradient, lateral erosion coefficient and hydraulic roughness. Of these groups of parameters, the bank material cohesion, bank height and lateral erosion coefficients between them determine the amount of degradation required to reach the critical condition from the initial condition, which in turn determines the reaction time for a given set of hydraulic variables that control the rate of bed degradation. Of moderately low sensitivity are the various bed material parameters (median diameter, porosity, specific gravity), which have relatively little effect on the channel widening reaction time, for the reasons discussed previously. All of the remaining variables are predicted to have no impact on widening reaction time. These variables are the various empirical coefficients and exponents and, as expected, the variables which describe the properties of the failed bank materials .

The channel recovery time is equal to the time period between the onset of widening and the establishment of half the overall change in channel width. The bank material critical entrainment threshold is predicted to be the most sensitive parameter (χ_t = 60.83) but, as discussed previously, this may be a spurious result. This is particularly the case in this example as the impact of varying the lateral erosion coefficient is predicted to be zero. This conflicting result again highlights the potential uncertainty involving the interpretation of lateral erosion in this model. It is clear that, in applications where lateral erosion is significant, it is necessary to have a method of determining the lateral erosion which has an improved physical basis and increased predictive ability. Discarding this result, the channel gradient appears to be the dominant variable in terms of impact on the rate of channel width adjustment (χ_t = 3.911). This reflects the role of channel gradient in influencing the available stream power and sediment transport rate and, therefore, the basal endpoint status. Intriguingly, the initial bank height is the next most dominant variable (χ_t = 3.661). This is interesting, as the *initial* bank height should not affect the retreat rate directly, as this is governed by the *critical* bank geometry conditions. In fact the initial bank height

does set a major control on the evolution of the bed prior to onset of widening. Lower initial bank heights imply that more degradation is required to attain the critical condition and initiate widening, but this means that once the channel does widen, it is subject to the constraint of a reduced channel gradient so that deposition of sediment, recovery of channel depth and stabilisation of channel banks are attained more rapidly. This explains why increases in bank height lead to increases in recovery time (decreases in rate of attainment of stable width) (positive values of χ_t).

Unsurprisingly, the transportability of the failed bank materials is predicted to be a significant control on the recovery of channel width. Both the size and specific gravity of the failed bank material aggregates have reasonably high rankings in this league table (d_{bank} is 4th, SG_{bank} is 8th).

Although the league tables of the sensitivity parameters give useful information about the relative dominance of individual fluvial system variables at various "snapshot" moments during channel evolution, they do not provide direct information about how the dominance of these variables shifts as process-form interactions evolve during the various phases of channel adjustment. To quantify shifting dominance of the fluvial system variables, weighted sensitivity parameters for channel width and depth for a range of independent fluvial system variables were calculated at each time step of the model simulation so that temporal plots for each of the sensitivity parameters could be obtained. The relative magnitudes of the sensitivity parameters at any time in the simulation then provides a direct measure of the relative dominance of the control variables at that point in the simulation. Variables selected for analysis were the sediment load at the upstream boundary (Qs), the channel gradient (S), the bank material cohesion (C) and the size of the failed bank material aggregates (d_{bank}). With the exception of the imposed discharge and the bed material size, these variables between them cover the primary independent variables - sediment load, channel gradient and boundary bank material characteristics. Since the bed material is restricted to sand fractions, the explicit omission of this variable is not a significant limitation, as variation of sediment diameter within this size range was previously found to have little effect on channel morphology. Similarly, it has already been established that discharge dominates the control variables throughout the adjustment cycle, by at least an order of magnitude (section 5.2.1). Omission of discharge from this analysis allows more subtle variations in dominance of control variables to be analysed. Of the two bank material variables, the cohesion is effectively a measure of the "erodibility" of the bank material and the size of the failed bank material aggregates is a measure of the "transportability" of the failed bank material.

Temporal plots of width and depth sensitivity parameters for the selected fluvial system variables are shown in Figures 5.18 and 5.19, respectively. Also shown on these diagrams are the various corresponding stages of channel evolution (Thorne & Osman, 1988a), as diagnosed during the sensitivity tests conducted in section 5.1. By comparing the relative dominance of fluvial system variables in terms of the influence they have on channel depth and width at the various stages of adjustment, it is possible to place these results within the context of the shifting process-form interactions identified by Thorne & Osman (1988a) in their conceptual model.

Stage 1 of the channel evolution model represents the initial condition of the channel. Each of the variables in Figures 5.18 and 5.19 is predicted to have sensitivity parameters equal to zero for both depth and width adjustment at this initial condition. This is logical given the stability of the bed and banks at this point. Once the channel adjustment sequence is initiated (the simulation started), the channel is in Stage 2 of the channel evolution sequence. This corresponds to a phase in which the banks remain stable, but sediment transport processes act to drive morphological response of the channel through degradation of the bed. Stage 2 is terminated by the onset of channel widening, which is caused by the onset of instability of the banks with respect to mass failure, as the channel eventually deepens to produce over-heightened and over-steepened banks. In these simulations, Stage 2 lasts up until approximately day 65 of the simulation, though the precise duration of the Stage 2 channel is dependent on the variable of interest, indicating the influence that these variables have on the temporal aspects of the channel evolution sequence. During this time, Figure 5.18 illustrates that none of the variables has any impact on the width sensitivity parameter ($\chi_{\Delta B} = 0$ for all variables). This is as expected, for at this stage of channel adjustment the channel is degrading, the banks are stable with respect to mass failure and there is, therefore, no channel widening. The width sensitivity parameters are equal to zero at this stage because bank processes are effectively inoperative during this stage of channel adjustment.

While the independent variables have no impact on the widening during this stage, they do partially control the length of time at which the channel remains in Stage 2 status, through the impact that these variables have both on the magnitude of degradation required to initiate mass failure and widening and the rate at which this degradation occurs. This is reflected in Figure 5.18 by the different points in time at which the independent variables are predicted to have non-zero width sensitivity parameters. The precise time of the onset of widening corresponds to the moment at

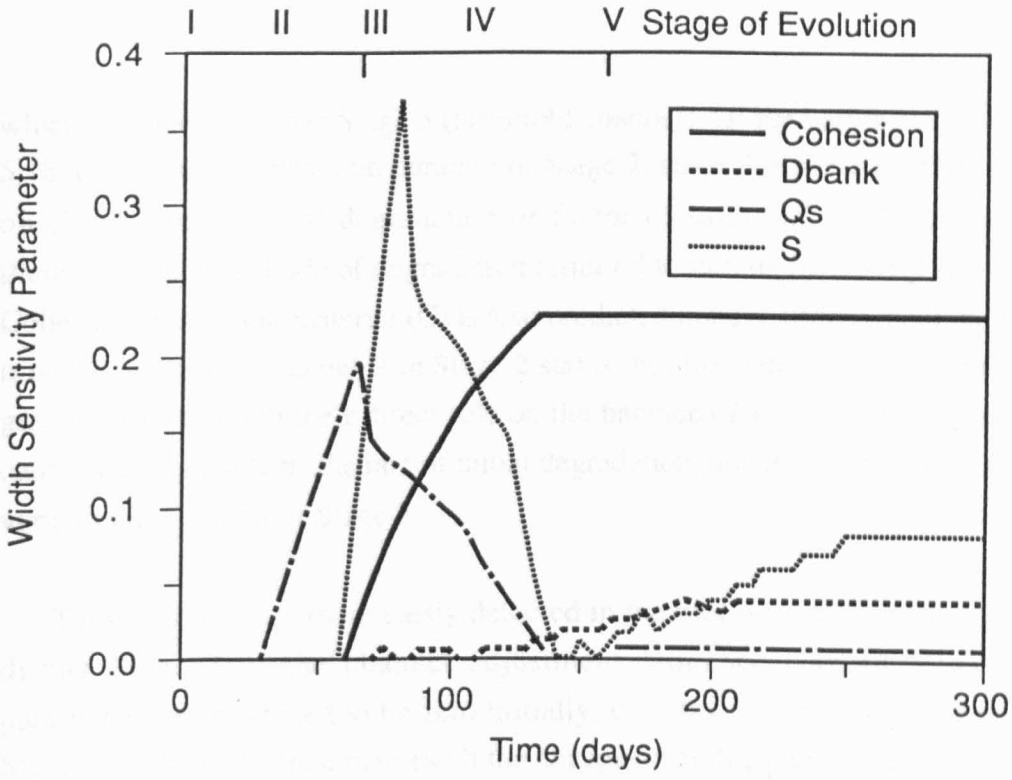

Figure 5.18 Shifting Dominance of Variables Controlling Width

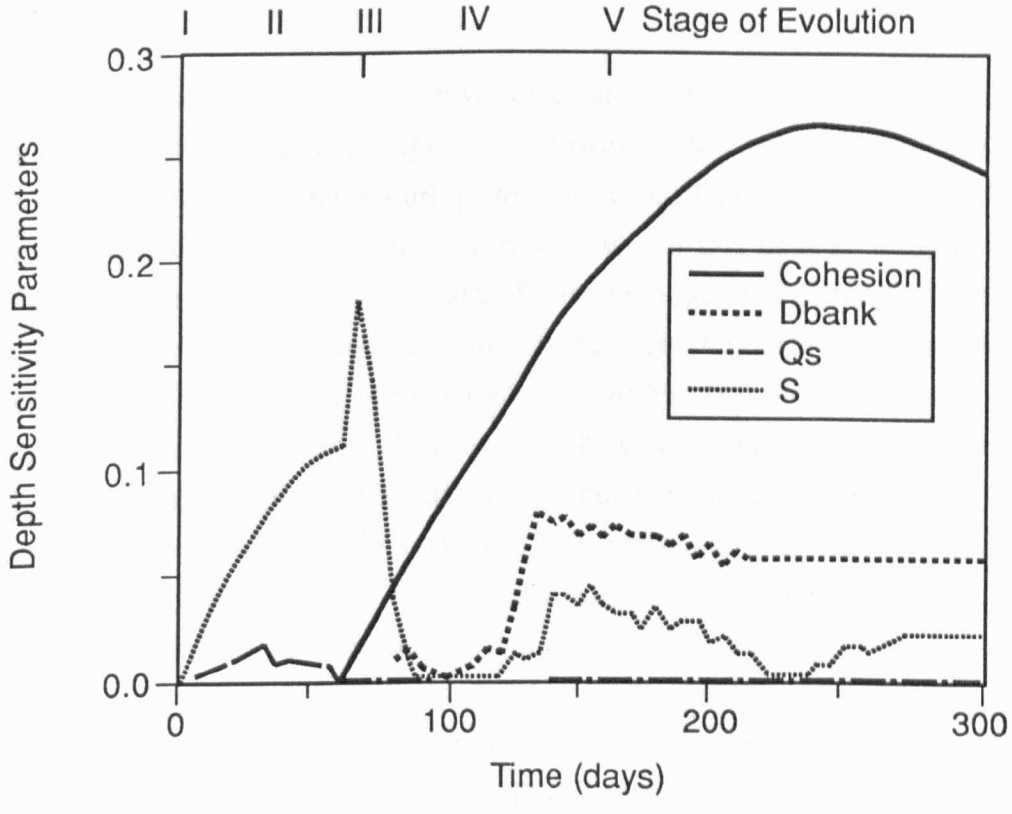

Figure 5.19 Shifting Dominance of Variables Controlling Depth

which the channel enters Stage 3 (threshold channel). Of the variables shown on Figure 5.18, d_{bank} has no impact on duration of Stage 2, since this parameter has no influence on either rate of initial degradation or factor of safety of the bank materials and, therefore, the magnitude of degradation required to initiate instability and bank retreat. Cohesion of the bank material (C) is also predicted to have little impact on the length of time for which the channel is in Stage 2 status, but the sediment load (Qs) and channel gradient (S), through their direct role on the balance of sediment supply and transport capacity and, therefore, the rate of initial degradation, apparently may lead to significant variation in duration of Stage 2.

These impacts are more easily detected in the plot of depth sensitivity parameters during Stage 2 of the channel adjustment sequence (Figure 5.19). Sensitivity parameters are predicted to be zero initially, but they rise at varying rates throughout Stage 2 of channel adjustment (with the exception of d_{bank} which retains a zero value). For these variables, this indicates that there is an increased impact on depth, for given change in each of the independent variables, as time progresses throughout Stage 2. Figure 5.19 shows that the gradients of the temporal plots of depth sensitivity parameters are highest for bank material cohesion, decreasing to channel gradient, and then sediment load.

During Stage 2 fluvial system variables all have zero impact on channel widening, as widening processes are inoperative. However, the independent variables do affect channel depth adjustments during this phase of channel evolution, influencing the magnitude of change in depth, the rate at which this change in depth occurs and, therefore, the duration of this phase of channel adjustment. During Stage 2 variables which control the bed processes, therefore, exert the dominant controls on channel response. Cohesion is the dominant variable with respect to the control it exerts on the *magnitude* of depth change, followed by the channel gradient and the sediment load supplied from the upstream boundary. But channel gradient and Qs exert more control on the *rate* of adjustment than cohesion. This leads to an overall situation where channel gradient and sediment load influence the duration for which the channel is in stage 2 more than cohesion of the bank material.

Stage 3 represents a point in time, rather than a period of time, at which a major process threshold occurs in the channel evolution cycle. Immediately prior to this time, depth adjustment is the dominant process and mass-wasting processes are inoperative. Immediately following the onset of critical conditions for bank instability, widening commences, so that both bed and bank processes are active. It is, therefore, reasonable

to expect a major shift in the dominance of the controlling fluvial system independent variables in terms of the influence they have on channel morphology, corresponding to this shift in process dominance.

In fact this is precisely what occurs in the simulated results. Figure 5.18 shows that at the point when the channel switches to Stage 3, there is a rapid increase in the width sensitivity parameters for cohesion, sediment load and channel gradient, together with a slower rate of increase for the size of the failed bank material aggregates. Then, immediately following this rapid increase during Stage 4, there is a systematic decrease in the widening sensitivity parameters for both channel gradient and sediment load, but a continuing increase in the bank material parameters, C and d_{bank}. During this time, the increase in the width sensitivity parameter for cohesion exceeds the increase in the d_{bank} width sensitivity parameter, which is small, so that the bank "erodibility" parameters appear to be the dominant control on widening, relative to the "transportability" parameters, throughout this stage of channel evolution.

The increasing significance of the bank material characteristics (d_{bank}, C) with respect to channel widening during stages 3 and 4, contemporaneously with decreases in the significance with respect to channel widening of the "bed process" variables (channel gradient and sediment load) is an indication of the dominance of bank processes over bed processes in terms of their influence on channel form in these stages of channel evolution. Moreover, this switch in dominance of the controlling variables also occurs for the controls on depth adjustment. Figure 5.19 indicates that, for the channel depth sensitivity parameters, the bed process variables (Qs, S) also decline in significance during stages 3 and 4, while the bank process variables (C, d_{bank}) increase in significance. It is clear that the attainment of threshold conditions and resulting switch to widening rather than deepening results in a situation where the controls exerted by the independent variables on fluvial system response also change dramatically. Prior to Stage 3 deepening without widening is the dominant process, so that variables related to bed processes exert the dominant control on all modes of channel response. But, in the widening phase the variables controlling bank processes dominate channel response for both the width and the depth dimensions. It seems that the widening phase also appears to have a dramatic influence on depth adjustment, so that the influence of bed process variables on depth adjustment is swamped by the dominant influence of the variables controlling widening. This is consistent with the hypothesis that the critical bank geometry limits further depth adjustments (Thorne & Osman, 1988a), and stresses the interdependent nature of the morphological response of natural river channels.

As Stage 4 progresses, the supply of sediment from bank failures and upstream bed degradation increases, boundary shear stress is reduced as the channel depth and gradient decrease, basal deposition begins to occur and the rate of widening diminishes. Figures 5.18 and 5.19 indicate that this sequence of events is also reflected in simulated shifts in the relative dominance of the fluvial system variables. In the case of the channel width sensitivity parameters (Figure 5.18), it is seen that as widening begins to diminish in significance the bed process variables (channel gradient, sediment load) begin again to increase with time, while bank process variables (C, d_{bank}) apparently remain at a more or less constant levels of sensitivity. Although the bank material cohesion is clearly the dominant variable throughout Stages 4 and 5, as the channel widening rate reduces and the channel tends towards dynamic equilibrium, bed process variables increases in significance and reduce the level of the relative dominance of the cohesion. However, this trend is not clear cut and there appears to be some complexity in the temporal trends of the independent variables during these later stages of channel adjustment. This is evidenced by the complex shape of the temporal plots of the depth sensitivity parameters in these later stages (Figure 5.19). The rate of increase of the bank material cohesion depth sensitivity parameter slows and eventually decreases during these late stages of adjustment, but remains dominant throughout Stage 4. However, each of the remaining variables, including the bed process variables (Qs, S), decrease in significance for depth changes throughout stage 4.

Stage 5 channels represent the final stage of channel adjustment, the attainment of a stable channel in dynamic equilibrium. In this stage of channel adjustment, the sensitivity parameters attain constant, but non-zero values, reflecting the overall stability of the system. For channel width, the cohesion (bank material "erodibility") is the dominant factor in influencing channel width, followed by channel gradient, size of failed bank material aggregates (bank material "transportability") and, finally, the sediment load. For channel depth, the bank material parameters (cohesion and failed aggregate size) are also the dominant control at this stage, followed by channel gradient and sediment load.

5.2.3 Discussion

The results shown in Figures 5.18 and 5.19 complement the rankings of the fluvial system variables summarised in Tables 5.5 to 5.8 and also have practical implications concerning the potential use of the model in engineering applications. These implications are concerned with the uncertainty that is introduced to model predictions

as a result of the sensitivity of model output to the variable and the ability to measure or predict the variable with any degree of accuracy. For example, if a variable exerts a dominant control on channel adjustment, but it is difficult to estimate the value of the variable, then large uncertainty will be introduced into the model predictions of channel morphology, limiting the utility of the model in a variety of applications. Conversely, variables which have little impact on model predictions may be irrelevant, so that it may be possible to exclude these variables from the analysis thereby simplifying the model code and input data requirements.

Table 5.9 Summary of Measurable/Predictable Variables

Measurable Variables	Immeasurable Variables
Q	n
H	NEV
S	μ
SG	HF
SG_{bank}	EH
C,γ,ϕ	D_{mix}
d_{50}	E
λ	ε_z
SAND	ε_y
d_{sand}	K
	d_{bank}
	R_l
	τ_c
	Qs

Several of the variables tested in this study are, fortunately, either easily and accurately measurable, or readily predictable. However, the remaining variables are either difficult to predict or measure. Table 5.9 summarises the variables falling into either of these two categories. It is these uncertain variables that may influence the predictability of the model output and limit the utility of the model in a variety of applications.

In fact, most of this latter group of variables were shown to have little impact on model output, at least in the sensitivity tests conducted in this study. Of the empirical coefficients and exponents, only the Manning's n was found to have any significant impact on channel morphology (Tables 5.5 to 5.8). However, the bank material variables K, R_l, τ_c and d_{bank} may all have significant impacts on the channel morphology predictions. It seems that these variables may result in the predictive ability of the model being reduced in circumstances where these variables are significant or

cannot accurately be determined. Similarly, measurement errors may often lead to uncertainty in specification of the sediment load at the upstream boundary and this source of error may also lead to the introduction of serious error and uncertainty into the model output. This emphasises the need for care to be taken in calculation of the sediment rating curve at the upstream boundary when using the model to obtain predictions of channel morphology. To reduce uncertainty associated with the other variables, it is recommended that research is required into three aspects of river bank erosion processes and mechanisms:

1. Research is required into the prediction of the physical properties of the failed bank materials, perhaps using the ideas outlined in section 3.5.1 as a framework for predicting the size of the failed bank materials;
2. The development of a physically-based method of predicting lateral fluvial erosion of cohesive bank materials is urgently required;
3. Refined methods of predicting the depth of tension cracks are required. An improved method of predicting tension crack formation and failure block geometry has recently been presented by Darby & Thorne (in press). This new method should now be modified for inclusion in the probabilistic mass-wasting algorithm developed in this research.

The fact that a number of variables tested in the sensitivity analyses were found to have little impact on channel morphology also suggests that a number of simplifications could potentially be made, or gross approximations retained. In particular, on the basis of these results, there appears to be little reason to include more complex formulations for eddy viscosity, mixed layer depth, and the transport of graded sediments. However, this conclusion is tentative, as this result may not be valid in fluvial environments, such as gravel-bed systems, which are unlike those considered in this study.

5.3 RELATIVE DOMINANCE OF WIDTH VERSUS DEPTH RESPONSE IN UNSTABLE CHANNELS

Although the analysis of sensitivity parameters conducted in the previous section provides useful information about the temporal response of channel width and B/D ratio to changes in the individual control variables tested, this analysis does not provide any direct information concerning the overall response of channel form to changes in control variables. This is a particularly interesting question in fluvial systems, which are characterised by their ability to mutually adjust interdependent system variables as

the channel tends towards equilibrium. Significantly, many of the presently available models of channel morphology obtain simplified solutions by constraining the response of one or more dimensions of channel response by specifying, or holding constant, one or more of the dependent channel geometry variables (usually width) that make up the interdependent fluvial system.

Against this background, analysis of the relative sensitivity of width versus depth response to changes in fluvial system control variables not only provides further useful insight into river channel evolution, but also highlights potential problems in the application of many of the existing models of channel morphology - including those which are used as standard tools in river engineering practice - which constrain various dimensions of channel adjustment in the way described. Specifically, if it is shown that the dimensions of response constrained in these models (usually width) are as important as the dimensions that are free to adjust (usually depth and slope), then the predictive ability of these models must become questionable.

The relative sensitivity of width versus depth adjustment can be quantified by a form adjustment parameter defined by the simple relation:

$$F = \frac{\Delta B^*}{\Delta D^*} \tag{5.10}$$

where F = dimensionless form adjustment parameter, ΔB^* = overall change in the magnitude of dimensionless channel width and ΔD^* = overall change in the magnitude of dimensionless channel depth. In each case the width and depth are normalized through dividing by the initial width and depth, respectively. Overall changes in magnitude are determined by subtracting the initial values from the final simulated values. Since the value of F is determined by overall change in the magnitude of the width and depth between the start and end of the simulations, it is clear that the form adjustment parameter is not at all temporally based. In fact the parameter is simply a measure of the relative magnitudes of width versus depth changes and, therefore, provides a simple answer to the question, "Is channel response characterised primarily by width adjustment, or primarily by depth adjustment ?".

Care is required in the interpretation of F as a consequence of the possibility that the numerical value of ΔD^* can be either positive or negative, while ΔB^* can only be positive. This is because the model cannot simulate channel narrowing. Shallowing is indicated by negative values of ΔD^* and, therefore, F. However, in these simulations,

shallowing channels always result in stable banks and no change in width, so that F is always equal to zero. Values of F equal to unity always indicate that channel response is characterised equally by width and depth adjustments and values of F less than unity, but greater than zero, indicate that the channel response is characterised more by deepening, relative to widening. In contrast, values of F equal to zero indicate no change in width, but provide no information on the direction of depth response. The range of modes of channel response and their corresponding F values are summarised in Table 5.10.

Table 5.10 Summary of F Values and Corresponding Modes of Response

F Value	Channel Response	Dominant Response
$F < 0$	Widening and shallowing	Unknown
$F = 0$	1. No change in morphology 2. No Widening with depth increase or decrease	Non-specific depth adjustment
$0 < F < 1$	Deepening with widening	Deepening
$F = 1$	Deepening with widening	Widening and deepening equally significant
$F > 1$	Widening with deepening	Widening
$F = \infty$	Widening with no change in depth	Widening

F values were calculated for each of the runs conducted in the sensitivity tests. To establish the relative sensitivity of width versus depth response over a range of each of the control variables, F values were plotted against the values of a range of control variables. This enabled the changing morphological response of the channel as a function of the various control variables, which represent changing fluvial environmental conditions, to be determined. In this way it is possible to predict how variation in environmental conditions leads to changing dominance of width versus depth adjustment in channel response. It should be noted that this exercise was conducted for a selection of the most sensitive variables, as determined from the analysis in the previous section. This filters out the control variables which give F values equal to zero (no morphological change) across their entire range. The results are shown in Figures 5.20 to 5.29.

Interpretations based on these diagrams are subject to the same limitations as the sensitivity tests reported in the previous section. In scope, the baseline test is applicable to sand-bed channels with cohesive bank materials and moderate channel gradient (S = 0.001) which are destabilized by sediment starvation. Perhaps the most significant way in which the baseline characteristics influence the results is that the selection of moderately cohesive bank materials will influence the ability of the channel to respond by widening. These limitations should be considered when interpreting the results.

Figure 5.20 shows F values plotted against upstream boundary sediment loads (Qs). At values of Qs less than or greater than unity, F values show little or no variation with Qs, indicating that within degradational or aggradational environments there is little variation in the response of channel morphology as a function of changing sediment load. However, there is a marked discontinuity in the relationship at Qs values close to one, indicating that small changes between aggradational or degradational environments can have significant impacts on the morphological response of the channel in these simulations.

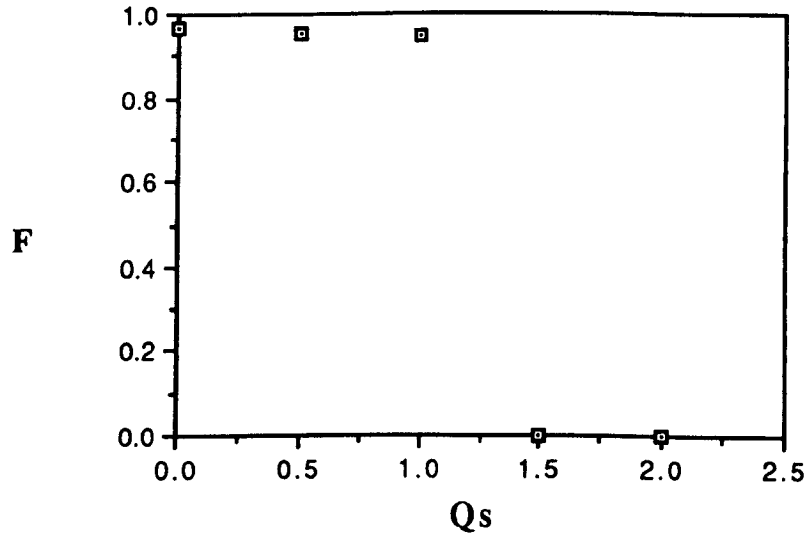

Figure 5.20 Form Adjustment Parameter Versus Qs

In degradational environments, F values of about 0.98 indicate that deepening is marginally more significant than widening in characterising the overall response of the channel. However, the closeness to F = 1 indicates that width and depth adjustments are both fundamental facets of channel adjustment in these environments. In these cases, constraining one or other dimension of channel response would be expected to have a significant impact on the other dimensions of channel response.

In aggradational environments F values are always equal to zero. In this example, this indicates that the simulated channel response is dominated entirely by channel shallowing (since Qs > 1); banks remain stable and there is no widening. In these instances constraining the width dimension of channel response would have no impact on the accuracy of depth dimension predictions obtained using the methods described above.

The impact of changes in channel gradient (S) on the overall morphological response of the channel is summarised in Figure 5.21. Increases of S result in non-linear increases in the F values between a minimum of 0.855 and a maximum of about 0.91. This indicates that increasing channel gradient results in a morphological response to a (degradational) disturbance being characterised increasingly by widening rather than deepening. This result is consistent with empirical analysis of the transition between meandering and braided rivers (Leopold & Wolman, 1957), which show that increasing gradient ultimately leads to a braided planform. However, for the range of channel gradients tested in this study, F values are always between 0.85 and 0.91. This indicates that, in this example, channel deepening is always more significant relative to channel widening, but this dominance is not sufficient to warrant neglecting the width adjustment dimension when considering morphological change.

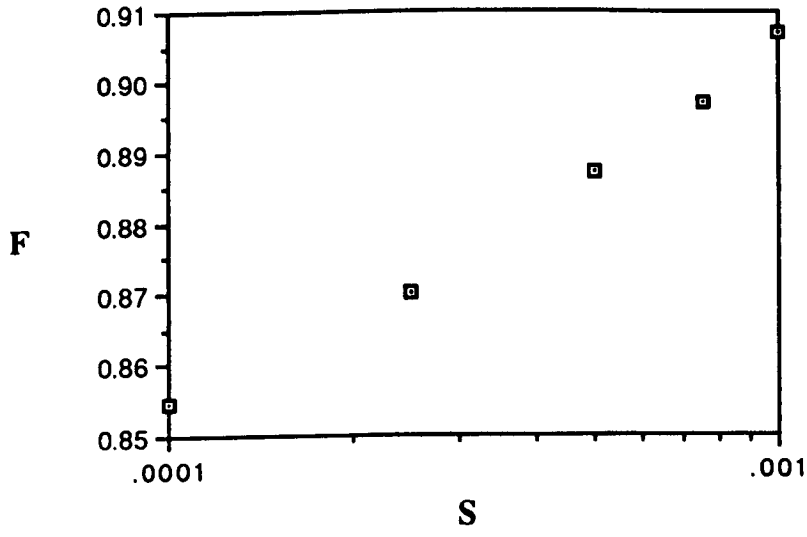

Figure 5.21 Form Adjustment Parameter Versus S

Figures 5.22 to 5.24 illustrate the relationships between the F parameter and variables which influence the initial factor of safety of the river banks: initial bank height (H); bank material cohesion (C); and, tension crack index (K). The relationships between morphological response and control variables are qualitatively similar in each

case. Each plot is characterised by non-linear relationships between the form adjustment parameter and the initial factor of safety. As factor of safety is increased, a progressive and asymptotic decrease in the value of the F parameter occurs, so that, as expected, widening becomes progressively more significant, relative to depth adjustment, as the initial factor of safety of the river banks is decreased.

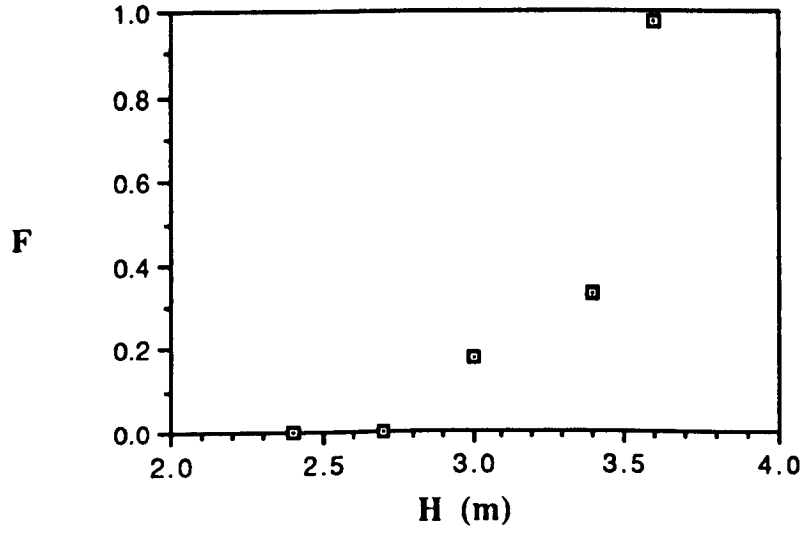

Figure 5.22 Form Adjustment Parameter Versus H

The relationship between bank height and F value is shown in Figure 5.22. For the range of bank heights tested, F value increases non-linearly with bank height up to a maximum of about 1.0. Minimum values of F, equal to zero, occur at bank heights less than about 2.7m. Below these bank height values, banks remain so stable that the morphological response of the channel is attained entirely by depth adjustment. However, above this critical bank height, the highly non-linear relationship between F and H indicates that, although deepening is more significant relative to widening over the entire range of bank heights tested in this example, the dominance of deepening over widening is rapidly diminished as bank heights are increased above the critical value of about 2.7m. In this example, then, the morphological response of the channel is quite distinct above and below the critical bank height value. This result is consistent with the hypothesis that the critical bank height for instability with respect to mass failure is a significant geomorphic threshold (Thorne & Osman, 1988a; Schumm & Thorne, 1989). The results suggest that the width dimension can only be safely neglected if bank heights are sufficiently low that the critical value to initiate mass failure and widening is never exceeded by the deepening of the channel.

Similar results are shown in Figure 5.23, which illustrates the impact of varying bank material cohesion on the form adjustment parameter. Again, there is a highly non-linear relationship between F and cohesion, with increases in cohesion leading to reductions in the value of the form adjustment parameter. In these simulations, the F value becomes zero at values of cohesion of about 25 kPa or greater. For these strongly cohesive banks, width is constrained by the high shear resistance of the bank materials, so that morphological response is characterised by depth adjustment alone. However, once the cohesion falls below this limiting value, the response of the system changes markedly as F increases rapidly. Between about 10 and 25 kPa F remains less than or equal to unity, indicating width and depth adjustments are both significant, but with a tendency for deepening to dominate the response. However, below about 10 kPa, further reductions in cohesion rapidly lead to large increases in F, so that widening dominates the morphological response of the system. There appear to be 3 distinguishable morphological response domains corresponding to transitions in bank material characteristics. Again, this indicates a discontinuity in the response of the channel associated with a threshold condition for the stability of the bank.

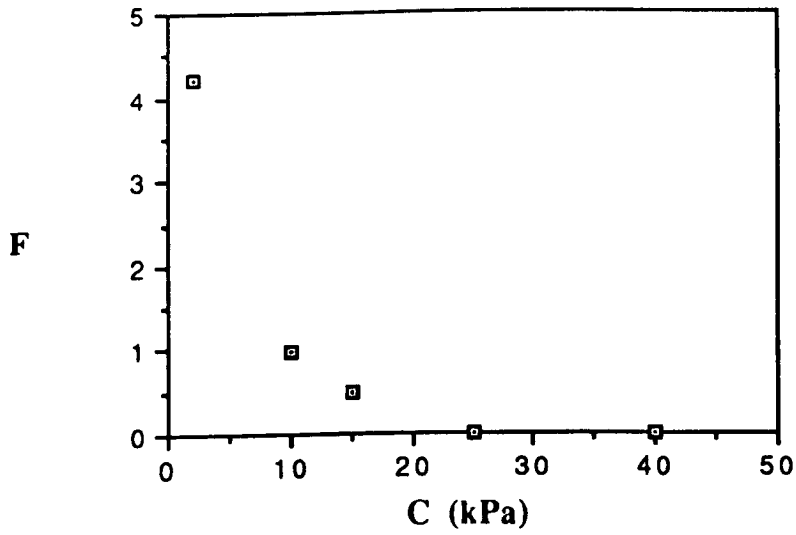

Figure 5.23 Form Adjustment Parameter Versus C

For banks of low cohesion, widening is the dominant response (to the extent that perhaps *depth* adjustments could safely be neglected in the case of non-cohesive bank materials). For moderately cohesive bank materials, deepening dominates widening, though widening is still significant and cannot be neglected. Finally, for banks of very high cohesion, depth adjustment is dominant, so that widening could safely be neglected. These results indicate that the morphological response of the channel, holding all other factors constant, is likely to be quite distinct in fluvial environments

with non-cohesive and cohesive bank materials. This further indicates that large-scale variations in bank material characteristics, for a given discharge, exert a significant control on the evolution of destabilized river channels, as suggested in the previous section and by Thorne & Osman (1988a).

The relationship between Tension Crack Index (K) and form adjustment parameter is shown in Figure 5.24. Increases in Tension Crack Index result in a non-linear increase in F, from a minimum value of about 0.8 at K = 0.0, up to a maximum of about 2.5 at K = 0.4. In this example, increasing tension crack index results in a progressive dominance of channel widening over channel deepening. At the lowest value of tension crack index, deepening just dominates widening, but this dominance is not sufficiently large to warrant neglecting the width dimension.

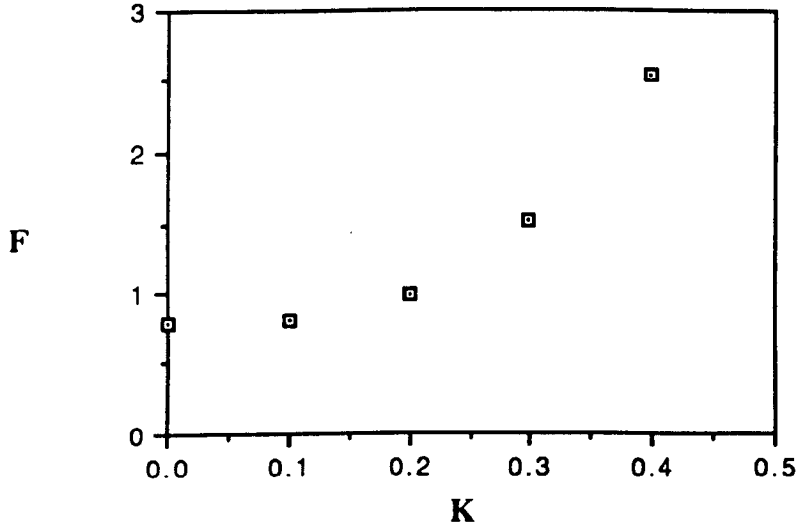

Figure 5.24 Form Adjustment Parameter Versus K

Figure 5.25 illustrates the relationship between form adjustment parameter and lateral erosion coefficient, which controls the lateral erosion rate. In this section, this coefficient is preferred to the critical entrainment threshold (τ_c) for direct lateral erosion of the bank materials as a measure of lateral erosion rate, due to the uncertainty concerning the role of τ_c in determining lateral erosion rate, as discussed previously. The results show that increases in lateral erosion coefficient (rate) result in progressive and moderately non-linear increases in form adjustment parameter. In this example, the values of the form adjustment parameters only vary between about 0.9 and 1.2, indicating that widening and deepening are approximately equally significant over the range of lateral erosion coefficients tested in this example. However, the non-linear

form of this plot suggests that by extrapolating the lateral erosion rates beyond the range of those tested in this study, increases in lateral erosion rate would soon lead to a dominance of channel widening over deepening. Such instances would occur in streams with high boundary shear stresses relative to the shear resistance of the bank materials and is also consistent with observations of the occurrence of braided rivers. The development of braided rivers is apparently facilitated in high gradient, high shear stress environments which encounter weakly cohesive or non-cohesive boundary materials (Leopold & Wolman, 1957).

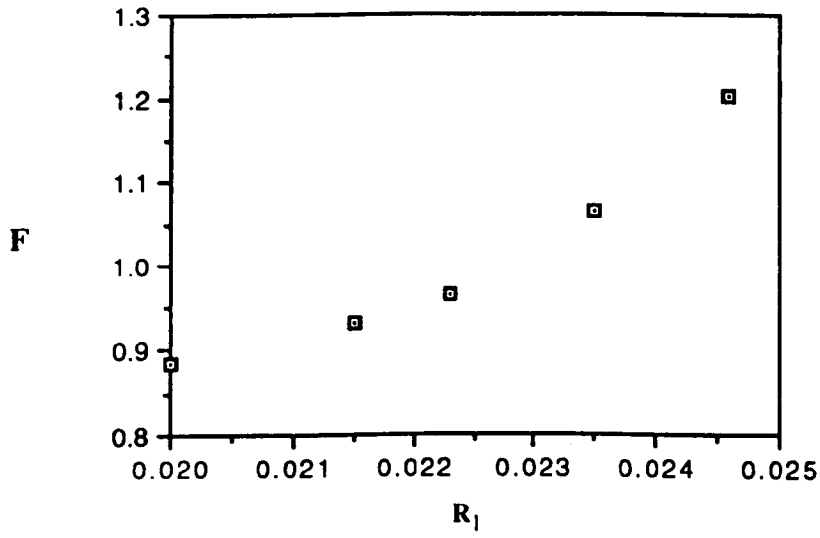

Figure 5.25 Form Adjustment Parameter Versus R_l

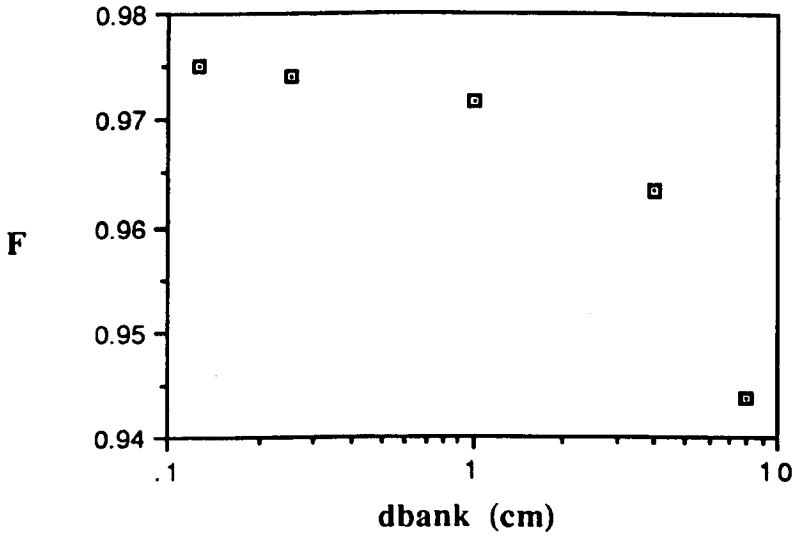

Figure 5.26 Form Adjustment Parameter Versus d_{bank}

The relationship between form adjustment parameter and transportability of the failed bank material aggregates is shown in Figure 5.26, which uses the diameter of the failed bank material aggregates as a surrogate for the transportability of the failed bank material aggregates. Increases of d_{bank}, therefore, represent decreases in transportability. Figure 5.26 shows that there is a non-linear relationship between F and d_{bank}, indicating that decreases in transportability of the failed bank material aggregates result in progressive, but non-linear, decreases in F. In this example, F values only range between about 0.975 and 0.94 over two orders of magnitude of change in the size of the failed bank material aggregates. This indicates that although deepening becomes more significant as the size of the failed bank material aggregates increases (transportability decreases), deepening and widening are more or less equally significant over the entire range of d_{bank} tested. However, extrapolation of the relation shown in Figure 5.26 suggests that values of d_{bank} greater than 10cm would result in an increasing dominance of deepening over widening. The non-linear nature of the relationship also indicates that small changes in d_{bank} could lead to large changes in the morphological response of the channel above this value. It may be that the deposition of *large* strongly bound blocks of intact failed bank material at the base of the bank following mass failure may have a significant impact on the morphological evolution of river channels. There are some field observations that support this idea. For example, observations indicate that deposition of large failed blocks at the base of the banks of the Allt Dubhaig, a relatively small stream in Scotland, following mass failure may provide effective protection of the bank from further erosion by the flow, as well as concentrating low stage flows into the main bed region of the channel, perhaps resulting in enhanced deepening (Simon, personal communication, 1993). This is also similar to a sequence of events described by Leopold *et al.* (1964). However, it appears that the magnitude of the river channel and occurrence of flood flows will significantly modify this relation. In large flows, the blocks may become entrained, and once entrained have been observed to rapidly break down into constituent particles (Thorne, 1978). In any case, it has already been argued that the principal control on whether or not a block disperses or remains intact is perhaps the failure mechanism (see section 3.5.1). The potential importance of the deposition of intact bank material blocks on the evolution of small rivers highlights the urgent need to advance our ability to predict the physical properties of failed bank materials, and this should be addressed as a topic for future research.

Figure 5.27 illustrates the relationship between form adjustment parameter and bed material specific gravity, which represents the transportability of the bed material. The results show a tendency for form adjustment parameter to decrease with increasing bed

material specific gravity (*i.e.* decreasing transportability). However, the range in predicted F values is not large, varying only between about 1.03 and 0.9. This indicates that increasing bed material transportability tends to increase the significance of widening relative to deepening, but only by a small amount. In all instances shown in this example, widening and deepening are approximately equally significant.

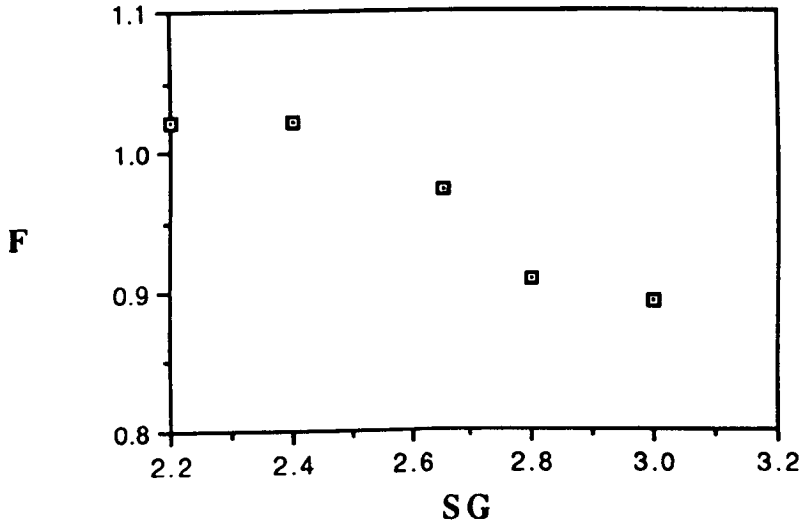

Figure 5.27 Form Adjustment Parameter Versus SG

The role of bed material porosity on the overall morphological response of the channel is summarised in Figure 5.28. Increases in bed material porosity result in a linear decrease in form adjustment parameter, though once again the range of F values is small and close to unity, indicating widening and deepening dominate the response of the channel equally in these simulations. In this example, increases in porosity lead to decreases in F as increases in porosity result in progressively larger increments of degradation (recall that the disturbance to the channel is a deficit of sediment supply relative to transport capacity). Apparently the increase in predicted degradation leads to an increasing dominance of deepening relative to widening, even though widening should also be enhanced as banks are increasingly destabilized by bed degradation.

Figure 5.29 shows the relationship between form adjustment parameter and Manning's n (strictly, the initial Manning's n of the simulation, as determined by the Strickler coefficient and median sediment diameter). It appears that there is no relationship between hydraulic roughness and the overall morphological response of the channel. In any case, all points on this diagram indicate that the range of predicted F values falls between about 0.92 and 0.98, so that widening and deepening are predicted to be approximately equally dominant for each of the hydraulic roughness values tested.

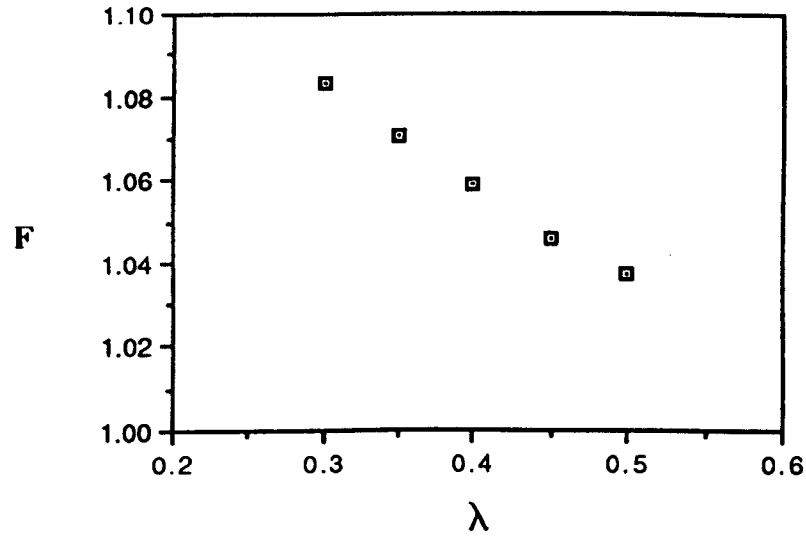

Figure 5.28 Form Adjustment Parameter Versus λ

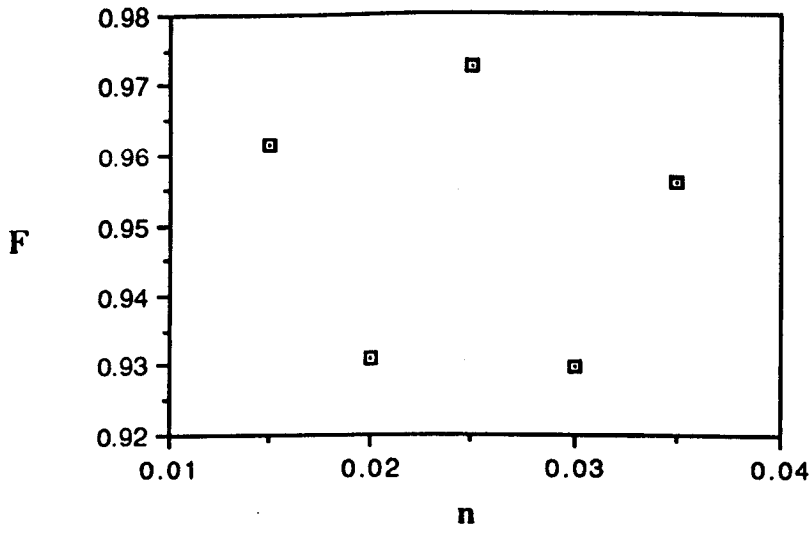

Figure 5.29 Form Adjustment Parameter Versus n

5.3.1 Implications

These results highlight, above all, the interdependent nature of the response of the channel morphology to a disturbance. Instances where one or the other of the depth or width dimensions are constrained or insignificant appear to be the exception, rather then the rule. This means that the predictive ability of models of channel morphology which constrain one or other of the degrees of freedom of channel response in order to obtain simplified solutions for the remaining dependent variables must be questionable.

Examples of such models include numerical mobile-bed (aggradation-degradation) models which specify channel width as a fixed, independent variable (*e.g.* the commercially available and widely used HEC-6, MIKE-11 and FLUMORPH codes) and kinematic models of meander migration, which also assume that the width is a specified value which remains constant through time (Ikeda *et al.*, 1981; Parker *et al.*, 1983; Odgaard, 1989). In particular, the mobile-bed models are frequently used as standard tools in engineering practice for the prediction of bed elevation changes and have also been used in applications where the aim has been analysis of sediment sorting processes (Hoey & Ferguson, 1991). However, an important implication of the results discussed above is that, in many instances where the width dimension is free to adjust, the predictions obtained from these methods are likely to be erroneous.

An example may help to reinforce this crucial point. One of the most frequent problems encountered by river engineers is the need to predict future trends of bed aggradation or degradation to help them in the safe and economic design of, for example, flood control schemes, navigable waterways and structures such as bridges or barrages. Commonly, the approach is to use mobile-bed, aggradation-degradation models which use width as a specified variable, assumed constant through time. This is the approach taken in perhaps the most widely used mathematical models of channel morphology, such as the HEC-6 code developed and used throughout the United States by the U.S. Army Corps of Engineers; the MIKE-11 code developed by the Danish Hydraulics Institute and widely used in developing countries; and the FLUMORPH code developed at Hydraulics Research Ltd, UK.

To highlight the potential deficiencies of these approaches, it is possible to compare the temporal trends of dimensionless channel depth (depth non-dimensionalized by dividing by the initial depth) obtained using the numerical channel evolution model developed in this research from various hypothetical scenarios in which the width is free to adjust and in which the width is constrained as a fixed, specified variable, which does not change through time. This is achieved by varying the cohesion of the bank material from the baseline sensitivity run in order to simulate banks with low cohesion, moderate cohesion and high cohesion. In effect, the high cohesion run represents predictions of channel depth obtained from a mobile-bed model which, like the commonly used codes mentioned above, assumes a fixed width. The moderate cohesion and low cohesion runs represent predictions of channel depth obtained from the model developed in this research, that is a code which takes into account the width adjustment dimension on the prediction of channel depth.

The results of this comparison are shown in Figure 5.30. It is clear that the predictions of channel depth obtained from the "fixed-width" and "mobile-width" models are quite distinct. As soon as widening begins in the unconstrained runs, channel depth is predicted to be limited and predictions of channel depth using the two approaches diverge as the magnitude of the widening increases. It is clear from this diagram that, in situations where the width is free to adjust, predictions of channel depth obtained from the existing mobile-bed codes are likely to be erroneous unless extensive and, therefore, expensive calibration procedures are rigorously followed. Admittedly, such models may be successfully applied in situations where the width is constrained (*e.g.* along channels with extensive "hard" bank protection). However, it is strongly recommended that future research should be directed at including a width predictor into these mobile-bed codes, in the way proposed in this research.

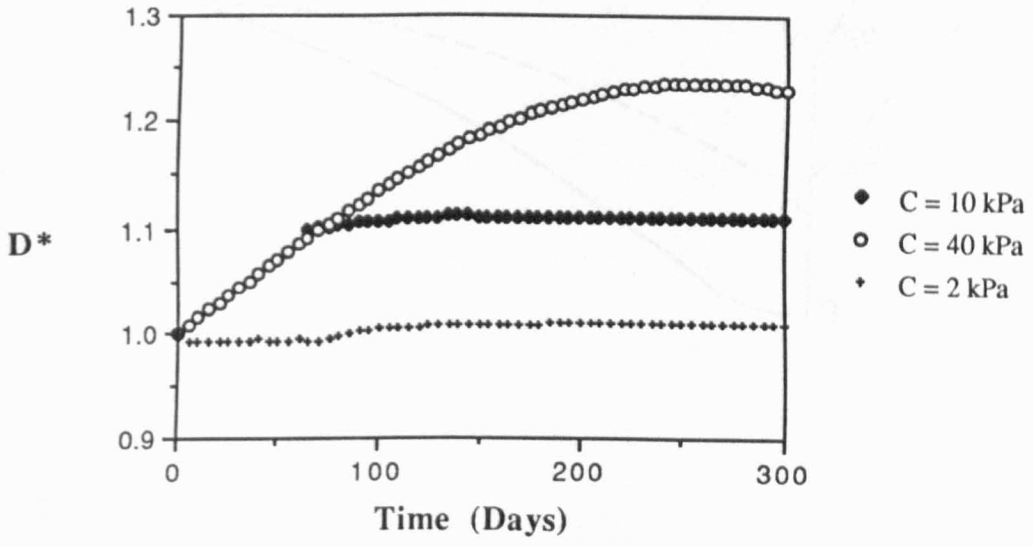

Figure 5.30 Temporal Trends of Dimensionless Depth For Varying Bank Material Strengths

A further result is apparent from Figure 5.30. Once widening is initiated, further increases in channel depth are limited. This result is also consistent with the hypothesis that the critical bank height limits the depth of degradation (Thorne & Osman, 1988a). Further degradation is limited as further increases in bank height cannot be sustained without the bank collapsing and initiating bank retreat instead of further bed degradation. Bank failures generated in this way supply sediment to the basal zone which also helps to redress the sediment supply : transport capacity deficit that generated the degradation in the first place. Thorne & Osman (1988b) argued that this result has important implications in the modelling of flow in channel bends and the prediction of the equilibrium cross-section (*e.g.* Engelund, 1974; Falcon & Kennedy,

1983; Odgaard, 1989). Existing models predict the equilibrium radial bed profile without considering whether the outer bank geometry could be stable with respect to mass failure. Thorne & Osman (1988b) showed that predictions of the transverse bed profile in bendways obtained using methods that ignore bank stability considerations can significantly overpredict the scour depth at the outer bank (Figure 5.31). This result is also expected from Figures 5.22 through 5.24 which illustrate that artificially constraining the channel width - by increasing the factor of safety of the bank - will lead to increased deepening in the channel.

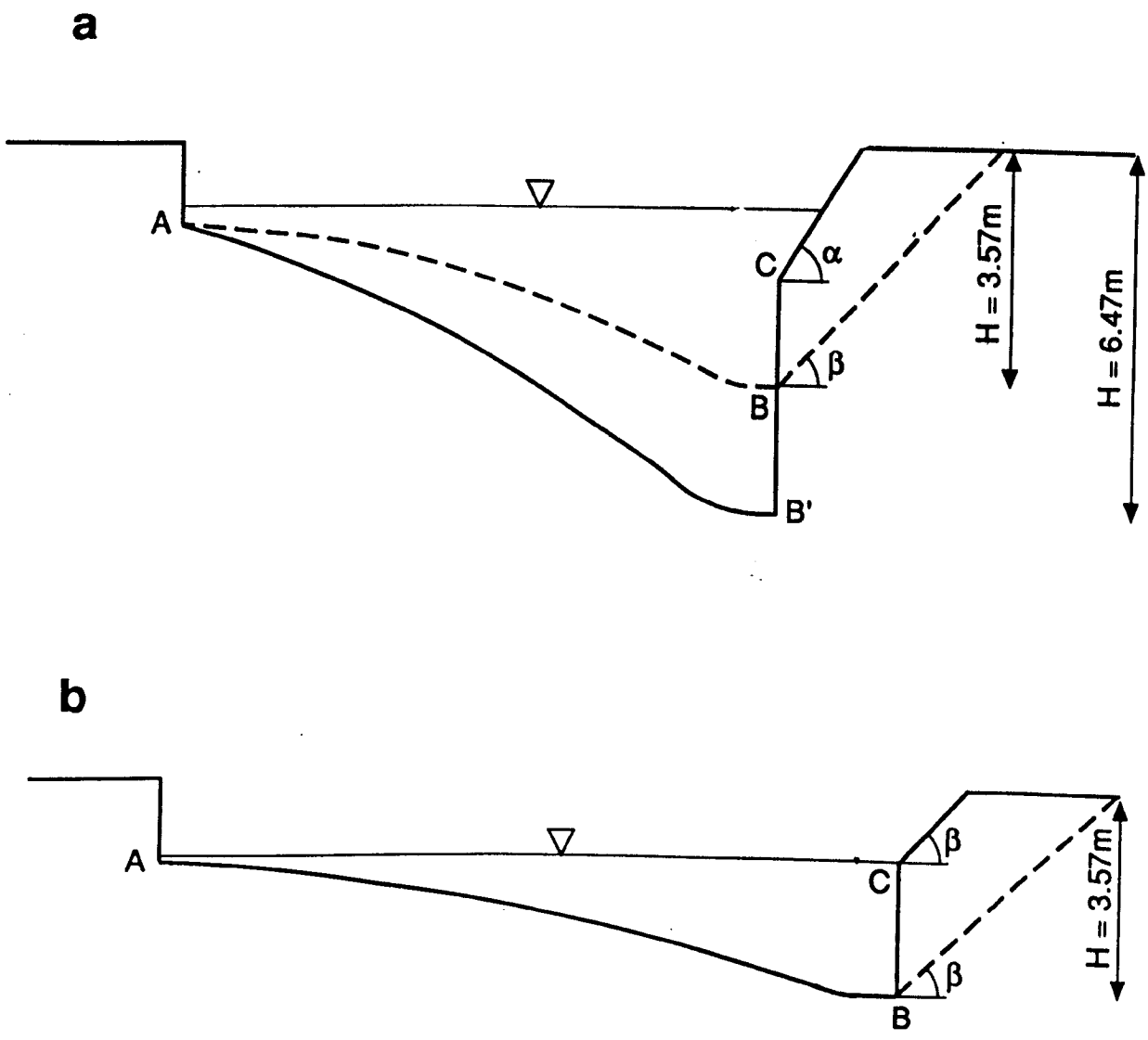

Figure 5.31 (A) Predicted Equilibrium Transverse Bed Profile in Bendway Ignoring Bank Stability Considerations (B) Predicted Equilibrium Transverse Bed Profile in Bendway Including Bank Stability Considerations (after Thorne & Osman, 1988b)

Thorne & Osman (1988b) invoked these results to explain the commonly observed phenomenon that the depth of scour in a migrating bend increases markedly either when the bend encounters a resistant bank material, or when the bend is stabilized using a revetment. The results obtained in this study support Thorne & Osman's (1988b) explanation of this behaviour - constraint of the width dimension, either in a model simulation or by using bank protection measures in real world engineering problems, cuts-off the supply of sediment to the channel from bank failures, reduces widening that would otherwise result in decreased boundary shear stresses and, therefore, enhances the potential for bed degradation in situations where transport capacity exceeds sediment supply. Thorne & Osman (1988b) stress that the implication of this result is that construction of revetments on eroding banks in bendways may result in increased bed scour which may ultimately result in failure of the revetment by undermining. If expensive mistakes such as these are to be avoided, it is recommended that bank stability analyses should be included in models of meander bend evolution. The Thorne & Osman (1988b) example represents a first step to progress in this direction. More recently, Darby & Thorne (1993) outlined a framework for including bank stability computations within a morphological model applicable to meander bends. The full scale development and testing of a numerical model of meander bend evolution which includes mass-wasting algorithms is planned as a topic of future research.

CHAPTER SIX

CONCLUSION AND RECOMMENDATIONS

6.1 SUMMARY

Existing methods of predicting channel morphology are severely limited by their inability to account for bank erosion and changing channel width through time, and their inability to account adequately for the physical processes governing the deformation of the channel boundary. In this project a physically-based, quasi two-dimensional, numerical model of channel evolution that does account for channel widening has been developed, tested and applied to analyse the influence of various fluvial system variables on channel adjustment dynamics. The application of the model developed in this research to analysis of the various controls on channel evolution represents a significant advance over previous approaches, because the numerical model is based on detailed representations of the physical processes governing channel deformation, rather than empirical approximations or unverified hypotheses, in order to obtain a solution.

Predictions of channel evolution are obtained by solving deterministically each of the governing equations of flow resistance, flow momentum and continuity, sediment transport, bank stability and conservation of sediment mass. By selecting physically-based algorithms for each of the flow, sediment transport and bank stability sub-models, the number of empirical coefficients and adjustable parameters is reduced to a minimum, so that a high degree of validity is ensured. The model is applicable to relatively straight, sand-bed streams with cohesive bank materials, and so covers a wide range of alluvial streams occurring in nature. In the numerical solution sequence, a method is first used to solve the shallow water flow equations, and to account for lateral shear stresses which significantly influence the flow in the near bank zone. The predicted distribution of flow velocity is then used to predict the sediment transport over the full width of the channel, including the near bank zones. Deformation of the bed is calculated from solution of the sediment continuity equation. Predictions of bed elevation changes obtained in the near bank zone, together with predictions of lateral fluvial erosion of the bank materials, allow the variation in bank geometry to be simulated through time. Since bank stability is determined by the limiting geometry of the bank for the given geotechnical properties of the bank material, channel widening can be simulated by combining a suitable bank stability algorithm with flow and sediment transport algorithms for the channel in the near bank zones.

In combining bank stability algorithms with flow and sediment transport algorithms, two considerations are paramount. First, the longitudinal extent of mass failures within modelled reaches must be accounted for. Second, it is necessary to maintain the sediment continuity in the time steps following mass failure, when the channel perimeter and sediment load both consist of mixtures of bed and bank materials with widely varying physical properties. In the model developed in this research, a probabilistic approach to prediction of factor of safety was used to estimate the fraction of the banks in the modelled reaches that fail during any time step. Mixed layer theory is then used to model the transport of the resulting bed and bank material mixture away from the near bank zone. The physical properties of the failed bank materials were predicted using a number of assumptions based on observations of mass failures and physical reasoning.

The predictive ability of the model was assessed in two distinct, but mutually complimentary ways. First, the ability of the model to simulate the evolution of the South Fork Forked Deer River, West Tennessee, was determined by comparing model predictions with observations of channel geometry obtained at intervals during the period 1969 to 1993. Overall agreement between predicted and observed channel geometries was found to be good, with mean discrepancy ratios of 0.93 and 1.04 for channel width and depth, respectively. The model was also found successfully to replicate the form of empirically-derived hydraulic geometry equations, indicating that the model is also able to predict ultimate, stable channel geometries after widening of an unstable channel with reasonable accuracy.

The physically-based numerical model was also applied in a series of sensitivity tests to investigate the influence of varying the independent variables and boundary conditions on channel adjustment dynamics in sand-bed streams with cohesive bank materials. Conclusions drawn from the results of the numerical experiments are based on detailed and realistic simulations of the physical processes acting in natural river channels and should, therefore, have a wide validity within the scope of the study.

A series of numerical experiments were made which elucidated the impact of changes in individual control variables on the evolution of a hypothetical channel destabilized by a reduction in sediment supply from upstream. Results obtained from these numerical experiments are useful in illustrating the dynamic behaviour of unstable river channels. In channels destabilized by sediment starvation, the initial morphological response is usually characterized by bed degradation. However, deepening is limited by the stability of the banks. The critical bank height for instability

with respect to mass failure triggers widening that limits further deepening and, once this critical value is obtained, widening dominates the continued morphological adjustment of the channel.

The data obtained from the numerical experiments were used to calculate sensitivity parameters which quantify the sensitivity of various dimensions of channel response to changes in control variables. By ranking the various sensitivity parameters, it was possible to determine which variables exert the most control on the evolution of sand-bed channels with cohesive bank materials. The results of the analysis indicate that the magnitude of the discharge is the dominant control on channel evolution. However, the sediment load, channel gradient and bank material characteristics are also significant, though much less so than discharge. Bed material characteristics do not appear to significantly influence the establishment of channel morphology in sand-bed streams.

The results of the numerical experiments were also used to establish relationships between a form adjustment parameter describing the dominant mode of channel change (the ratio of change in width to change in depth) and the control variables, to establish how changes in environmental boundary conditions impact the nature of the response of the fluvial system to a disturbance. Results show that in a wide range of environments, both width and depth adjustments are significant facets of the channel response. This implies that the applicability of models which artificially constrain any of the degrees of freedom of channel adjustment to obtain simplified solutions will be severely limited, unless sound judgement is used by the modeller to allow for the impacts of neglected processes and adjustments. Examples of such models include mobile-bed models such as HEC-6, FLUMORPH and MIKE-11, meander migration models (*e.g.* Ikeda *et al.*, 1981; Odgaard, 1989) and sediment sorting models (*e.g.* Hoey & Ferguson, 1991); all of these approaches exclude the possibility of channel width adjustment and must, therefore, be erroneous in situations where width adjustments are significant.

6.2 LIMITATIONS OF THE MODEL

The model is applicable to effectively straight, sand-bed channels with cohesive bank materials and channel gradients up to order of magnitude 0.001. Flows are assumed to be sub-critical, steady and uniform within any computational time step. Unsteady flows can still be modelled, however, through the use of a stepped hydrograph. Over-bank flows and secondary currents are neglected. The model is applicable to non-layered river banks which either remain stable with respect to mass

failure, or fail along approximately planar or circular failure surfaces which pass through the toe of the bank. The effects of vegetation on flow resistance and bank stability are neglected. The effects of pore-water and confining pressures on bank stability are not directly accounted for. It is planned to address many of these limitations in future research (see section 6.4, below).

6.3 POTENTIAL MODEL APPLICATIONS

The numerical model may potentially be applied to solve a variety of problems, both as a potential engineering prediction tool and as a scientific research tool for analysis of various aspects of fluvial system behaviour. The model is well suited as a tool for prediction of river channel response to modifications in channel geometry, sediment load or flow regime made as a consequence of a variety of river engineering projects (*e.g.* dam construction, river regulation, channelization).

The model may also prove to be a useful research tool in the analysis of a variety of problems in fluvial geomorphology. The following are just a few examples of planned or potential future applications. The model has already been used to simulate temporal sequences of channel morphology and flow-energy variables, such as energy dissipation rate, specific energy and total mechanical energy, over a range of environmental boundary conditions. This work has been useful in identifying the shifting dominance of the various process-response mechanisms in evolving channels (Simon & Darby, in preparation). This work could be extended to elucidate the validity and physical-basis of various extremal hypotheses across a range of environments. The model could also be used to investigate sediment sorting processes and trends in both downstream and lateral dimensions, again over a range of environmental boundary conditions. Finally, the influence of flow variability and flow sequencing on channel morphology and dominant discharge could be investigated using this model.

Researchers who require further information about the work reported here, or who are interested in using the model in any of the above listed, or other, potential applications, should contact the author in writing at the Department of Geography, University of Nottingham, Nottingham NG7 2RD, UK.

6.4 RECOMMENDATIONS FOR FUTURE RESEARCH

During the course of this project, a number of topics were identified for which further research is required in order to improve the description of the physical processes

controlling deformation of alluvial channel boundaries. To conclude this thesis, a variety of recommendations urging that these topics be addressed by substantial research projects are summarised below. These recommendations are aimed at highlighting areas of uncertainty concerning the physical processes controlling channel adjustment in general, rather than providing recommendations on how to improve the scope of the model or how the model might be used as a tool in future research projects. Such recommendations are implicitly suggested in sections 6.2 and 6.3 and are planned to be implemented as part of a continuing effort to improve the code developed in this research and to apply the code in the analysis of morphological problems. Areas of uncertainty which probably need to be addressed by large scale research projects are now summarised:

1. There is an urgent requirement for a reliable, physically-based method of predicting the lateral fluvial erosion rate of cohesive bank materials. Present methods (such as Arulanandan *et al.*, 1980) appear to be inadequate;

2. More research is required into the physics of near bank flows, in both straight and meandering reaches, in order to elucidate the nature of the near bank boundary layer. In particular, it is necessary to determine the relative orders of magnitude of each of the terms in the momentum equation. The relative significance of lateral shear stresses and secondary flows is at present largely unknown, especially in curved channels and during over-bank flow events. The lack of knowledge of near bank flow processes is the major obstacle to the development of a channel adjustment model applicable in curved channels (Darby & Thorne, 1993);

3. Little is known about how the flow hydraulics, bank material properties and failure mechanism interact to determine the physical properties of the failed bank materials, and the way in which these failure products are distributed across the near bank zone. Bank sediment tracing experiments would be one way of investigating these relationships;

4. The scope of the present model should be increased, in order that the model may be applied to analyse channel evolution dynamics in a wider range of environments than has been possible to date. In particular, flow resistance and sediment transport subroutines should be added that are capable of handling gravel-bed materials. A wider range of bank stability mechanisms should also be included to account for non-cohesive bank materials, and to allow for failure mechanisms with more complex geometries than accounted for by the existing code.

Although technical studies such as those described above are undoubtedly important, there now also exists a broader opportunity for significant progress to be made in the field of river modelling. By building upon the advances made in this study, as well as addressing the areas of uncertainty described above, there now exists the possibility of developing advanced physically-based numerical channel evolution models, with a minimum number of adjustable parameters, which are capable of faithfully replicating the physical processes that interact to control all dimensions of channel response in a range of fluvial environments. Such models would integrate state-of-the-art hydraulic models, applicable to natural meandering channels, with advanced flow resistance, sediment transport and river bank stability algorithms to obtain predictions of channel evolution without constraining any of the degrees of freedom of channel adjustment. This advance, which is now possible, would represent a quantum leap over the existing generation of morphological models, which give biased solutions by constraining one or more of the river system's adjustable degrees of freedom. These existing morphological models are used in standard engineering practice across the world, but are significantly restricted by this inability to account for all dimensions of channel adjustment and, therefore, often require extensive calibration and verification studies. While it is unrealistic to expect that new state-of-the-art models would immediately replace the existing commercially available codes (due to the considerable investment already made in them), the more advanced codes would certainly have considerable potential for improving predictions of channel morphology.

Moreover, such new models could also be applied as research tools in physically-based approaches aimed at addressing a number of fundamental problems in fluvial geomorphology, for example as outlined in section 6.3. Such studies, unlike most existing approaches, would be based on full, unbiased solutions of the governing equations with the number of restricting assumptions and limiting approximations kept to a minimum. A similar quantum leap in our ability to understand the processes-response dynamics in river channel evolution would, therefore, also be achievable once such models are developed.

In making progress towards these goals, three fundamental guidelines should be borne in mind. First, if channel evolution models are to include accurate representations of the processes of channel adjustment, then each sub-model of the hydraulics, flow resistance, bank stability and sediment transport must have a high physical basis and predictive ability. Individual algorithms must, therefore be thoroughly assessed and validated prior to inclusion in the model code. Of these sub-models, probably the two

most critical are the hydraulic and bank stability algorithms. This is because if truly unbiased solutions are to be obtained, then unlike existing approaches, the processes governing width adjustment must be fully accounted for. Hydraulic models must, therefore, be capable of simulating flow processes within the near bank boundary layer, where there are significant lateral momentum exchanges. Existing empirical, analytical and numerical studies have almost entirely neglected this zone, primarily because of the difficulty in obtaining reliable flow measurements close to the channel boundary. Consequently, virtually nothing is known about the flow processes operating in near bank boundary layers. The second guideline is, therefore, that this area of uncertainty must immediately be addressed and in assessing the merits of individual hydraulic sub-models, the ability of the model to predict the flow in the near bank zones must be taken into account. Finally, an accurate bank stability algorithm is required, simply because the bank flux is often the dominant term in the near bank sediment balance. Approaches to modelling channel evolution which ignore these considerations are likely to fail in their stated aim of faithfully replicating the process-form interactions that really govern channel boundary deformation in natural river channels.

BIBLIOGRAPHY

BIBLIOGRAPHY

Abrahams, A. D. 1993. "An experimental study of step-pools in stream channels: Evidence for the maximum friction factor hypothesis", *Paper Presented at the 3rd International Geomorphology Conference*, Hamilton, Ontario, August 23-28, 1993.

Ackers, P. & Charlton, F. G. 1970. "Meander geometry arising from varying flows", *Journal of Hydrology*, 11, 230-252.

Alonso, C. V. & Combs, C. T. 1986. "Channel width adjustment in straight alluvial streams", *Proceedings of the 4th Federal Interagency Sedimentation Conference, Las Vegas, Nevada, March 24-27 1986*. p5-31 - 5-40.

Alvarez, J. A. M. & Villanueva, C. C. 1973. "Stable channels in alluvium", *Sediment transportation, Vol. 1. Proceedings of the International Association for Hydraulic Research Symposium on River Mechanics, Bangkok*, p715-718.

Andrews, E. D. 1982. "Bank stability and channel width adjustment, East Fork river, Wyoming", *Water Resources Research*, 18, 1184-1192.

Andrews, E. D. 1983. "Entrainment of gravel from naturally sorted riverbed material", *Geological Society of America Bulletin*, 94, 1225-1231.

Andrews, E. D. 1984. "Bed material entrainment and hydraulic geometry of gravel-bed rivers in Colorado", *Geological Society of America Bulletin*, 95, 371-378.

Andrews, E. D. & Smith, J. D. 1992. "A theoretical model for calculating marginal bedload transport rates of gravel", in Billi, P., Hey, R. D., Thorne, C. R. & Tacconi, P. (eds) *Dynamics of Gravel-bed Rivers*, John Wiley and Sons, Chichester, p41-52.

Arulanandan, K., Gillogley, E. & Tully, R. 1980. "Development of a quantitative method to predict critical shear stress and rate of erosion of naturally undisturbed cohesive soils", Report GL-80-5, U.S Army Engineers Waterways Experiment Station, Vicksburg, Mississippi. 41p.

ASCE Task Committee on Turbulence Models in Hydraulic Computations. 1988. *Journal of Hydraulic Engineering*, 114, 970-1073.

Ashida, K. & Michiue, M. 1964. *Laboratory Study of Suspended Load Discharge in Alluvial Channels*, Disaster Prevention Research Institute, Kyoto University, Kyoto, Japan.

Ashida, K. & Okabe, T. 1982. "On the calculation of method of the concentration of suspended sediment under non-equilibrium condition", *Proceedings of the 26th Conference on Hydraulics*, Japanese Society of Civil Engineers, p153-158.

Ashley, G. H. 1910. "Drainage problems in Tennessee", *Tennessee State Geological Survey Bulletin*, 3-A, 1-15.

Ashworth, P. J. & Ferguson, R. I. 1989. "Size-selective entrainment of bedload in gravel bed streams", *Water Resources Research*, 25, 627-634.

Bagnold, R. A. 1954. "Experiments on a gravity free dispersion of large solid spheres in a Newtonian fluid under shear", *Proceedings of the Royal society of London, Series A*, 225, 49-63.

Bagnold, R. A. 1956. "The flow of cohesionless grains in fluids", *Philosophical Transactions of the Royal Society of London*, 249A, 235-297.

Bagnold, R. A. 1966. "An approach to the sediment transport problem from general physics", *United States Geological Survey Professional Paper*, 422-I, 1-37.

Bagnold, R. A. 1973. "The nature of saltation and of bed load transport in water", *Proceedings of the Royal society of London, Series A*, 340, 141-171.

Barnes, H. H. 1967. "Roughness characteristics of natural channels", *U. S. Geological Survey Water Supply Paper*, 1849, 213p.

Barton, J. R. & Lin, P. N. 1955. "A study of the sediment transport in alluvial streams", *Report 55JRB2*, Colorado A & M College, Fort Collins, Colorado.

Begin, Z. & Schumm, S. A. 1984. "Gradational thresholds and landform singularity", *Journal of Quaternary Research*, 21, 267-274.

Bennett, R. J. 1976. "Adaptive adjustment of channel geometry", *Earth Surface Processes*, 1, 131-150.

Bennett, J. P. & Nordin, C. F. 1977. "Simulation of sediment transport and armoring", *Hydrological Sciences Bulletin* , 22, 214-228.

Bettess, R. & White, W. R. 1987a. "Extremal hypotheses applied to river regime", in Thorne, C. R., Bathurst, J. C. & Hey, R. D. (eds) *Sediment Transport in Gravel-Bed Rivers*, John Wiley & Sons, Chichester. p767-789.

Bettess, R. & White, W. R. 1987b. Reply to Discussions of "Extremal hypotheses applied to river regime" by Bettess & White, in Thorne, C. R., Bathurst, J. C. & Hey, R. D. (eds) *Sediment Transport in Gravel-bed Rivers*, John Wiley & Sons, Chichester. p786-789.

Bettess, R., White, W. R. & Reeve, C. E. 1988. "On the width of regime channels", in White, W. R. (ed) *International Conference on River Regime*, Hydraulics Research/John Wiley & Sons, Chichester. p149-161.

Bird, J. F. 1980. "Geomorphological implications of flood control measures: Long Long River, Victoria", *Australian Geographical Studies*, 18, 169-183.

Bishop, A. W. 1955. "The use of the slip circle in the stability analysis of slopes", *Geotechnique*, 5, 7-17.

Blench, T. 1952. "Regime theory for self formed sediment bearing channels", *Transactions of the American Society of Civil Engineers*, 117, 383-400.

Blench, T. 1969. *Mobile bed fluviology. A regime treatment of canals and rivers for engineers and hydrologists*. University of Alberta Press, 2nd Edition, Edmonton. 168p.

Borah, D. K., Alonso, C. V. & Prasad, S. N. 1982. "Routing graded sediments in streams: Formulations", *Journal of the Hydraulics Division of the American Society of Civil Engineers*, 108, 1486-1503.

Borah, D. K. & Bordoloi, P. K. 1989. "Stream bank erosion and bed evolution model", in Wang, S. S. Y. (ed),*Sediment Transport Modelling*, Proceedings of the 1989 International Symposium of the American Society of Civil Engineers, p612-617.

Boussinesq, J. 1877. "Theorie des ondes et des remous quise propagent le long d'un canal rectangulaire horizontal, en communiquant au liquide contenu dans ce canal des vitesses sensiblement pareilles de la surface au fond", *Journal de Mathematiques Pures et Appliquees Deuzieme Serie*, 17, 55-108.

Bray, D. I. 1982. "Regime equations for gravel-bed rivers", in Hey, R. D., Bathurst, J. C. & Thorne, C. R. (eds)*Gravel-Bed Rivers: Fluvial processes, Engineering and Management*, John Wiley & Sons, Chichester. p517-552.

Bridge, J. S. 1983. "Flow and sedimentary processes in river bends; comparisons of field observations and theory", in C. M. Elliott (ed), *River Meandering: Proceedings of the Conference, Rivers '83*, American Society of Civil Engineers, New York. p857-872.

Brooks, N. H. 1954. *Laboratory studies of the mechanics of motion of streams flowing over a movable-bed of fine sand*, Thesis presented to California Institute of Technology, at Pasadena, California, in partial fulfilment of the requirements for the degree of Doctor of Philosophy.

Brundett, E. and Baines, W. D. 1964. "The production and diffusion of vorticity in duct flow", *Journal of Fluid Mechanics*, 19, 375-394.

Brunsden, D. & Kesel, R. H. 1973. "Slope development on a Mississippi River bluff in historic time", *Journal of Geology*, 81, 576-598.

Brush, L. M. 1961. "Drainage basins, channels and flow characteristics of selected streams in Central Pennsylvania", *United States Geological Survey Professional Paper*, 282-F, 145-175.

Burkham, D. E. 1972. "Channel changes of the Gila River in Safford Valley, Arizona 1846-1970", *United States Geological Survey Professional Paper*, 655G, 1-24.

Caddie, G. H. 1969. "An analysis of some data from natural alluvial channels", *United States Geological Survey Professional Paper*, 650-C, C188-C194.

Carling, P. A., Kelsey, A. & Glaister, M. S. 1992. "Effect of bed roughness, particle shape and orientation on initial motion criteria", in Billi, P., Hey, R. D., Thorne, C. R. & Tacconi, P. (eds) *Dynamics of Gravel-bed Rivers*, John Wiley and Sons, Chichester, p24-39.

Carlston, C. W. 1969. "Downstream variations in the hydraulic geometry of streams: Special emphasis on mean velocity", *American Journal of Science*, 267, 499-509.

Carson, M. A. & Kirkby, M. J. 1972. *Hillslope form and process*, Cambridge University Press, Cambridge. 475p.

Carson, M. A. & Griffiths, G. A. 1987. "Bedload transport in gravel channels", *Journal of Hydrology (New Zealand)*, 26, 1-151.

Celik, I. & Rodi, W. 1984. "A deposition entrainment model for suspended sediment transport", *Report SFB 210/T/6*, Universitat Karlsruhe, Karlsruhe, West Germany.

Chalov, R. S. 1972. "Geographic aspects of the study of channel regime of rivers", *Izvestiya Vsesoyuznogo Geograficheskogo Obshchestva*, 104, 455-461.

Chang, H. H. 1979a. "Minimum stream power and river channel patterns", *Journal of Hydrology*, 41, 303-327.

Chang, H. H. 1979b. "Geometry of rivers in regime", *Journal of the Hydraulics Division of the American Society of Civil Engineers*, 105, 691-706.

Chang, H. H. 1980a. "Stable alluvial canal design", *Journal of the Hydraulics Division of the American Society of Civil Engineers*, 106, 873-891.

Chang, H. H. 1980b. "Geometry of gravel streams", *Journal of the Hydraulics Division of the American Society of Civil Engineers*, 105, 1443-1456.

Chang, H. H. & Hill, J. C. 1977. "Minimum stream power for rivers and deltas", *Journal of the Hydraulics Division of the American Society of Civil Engineers*, 103, 1375-1389.

Charlton, F. G., Brown, P. M. & Benson, R. W. 1978. "The hydraulic geometry of some gravel rivers in Britain", *Report IT 180*, Hydraulics Research Station, Wallingford, UK.

Cheetham, G. H. 1979. "Flow competence in relation to stream channel form and braiding", *Geological Society of America Bulletin*, 90, 877-886.

Chien, N. 1957. "A concept of the regime theory", *Transactions of the American Society of Civil Engineers*, 122, 785-805.

Chong, S. E. 1969. "The width, depth and velocity of the Sungei Kinta, Perak", *Geographica*, 6, 72-83.

Chow, V. T. 1973. *Open-Channel Hydraulics*, McGraw-Hill, Singapore, 680p.

Christensen, R. W. & Das, B. M. 1973. "Hydraulic erosion of remolded cohesive soils", in *Soil Erosion: Causes and Mechanisms; Prevention and Control*, Special Report Number 135, Highway Research Board, National Academy of Science, Washington, DC. p8-19.

Coleman, N. L. 1969. "A new examination of sediment suspension in open channels", *Journal of Hydraulic Research*, 7, 67-82.

Coleman, N. L. 1981. "Velocity profiles with suspended sediment", *Journal of Hydraulic Research*, 19, 211-229.

Crosato, A. 1990. "Simulation of meandering river processes", *Communications on Hydraulic and Geotechnical Engineering*, 90-3, Delft University of Technology. 90p.

Cunge, J. A., Holly, F. M. & Verwey, A. 1980. *Practical Aspects of Computational River Hydraulics*, Pitman Advanced Publishing Program, Boston. 420p.

Darby, S. E. & Thorne, C. R. 1992a. "Impact of channelization on the Mimmshall Brook, Hertfordshire, UK", *Regulated Rivers: Research & Management*, 7, 193-204.

Darby, S. E. & Thorne, C. R. 1992b. "Simulation of near bank aggradation and degradation for width adjustment modelling", in Falconer, R. A., Shiono, K. & Matthew, R. G. S. (eds) *Hydraulic and Environmental Modelling: Estuarine and River Waters*. Proceedings of the 2nd International Conference on Hydraulic and Environmental Modelling, Vol 2, Ashgate, Aldershot. p431-442.

Darby, S. E. & Thorne, C. R. 1993. "Approaches to modelling width adjustment in curved alluvial channels", *Report to US Army European Research Office, Contract No. R&D DAJA45-92-M-0248*. 90p.

Darby, S. E. & Thorne, C. R. in press. "Prediction of tension crack location and riverbank erosion hazards along destabilised channels", *Earth Surface Processes and Landforms*.

Davies, T. R. H. 1987. "Channel boundary shape - evolution and equilibrium", in Richards, K. S. (ed) *River channels*, Basil Blackwell, IBG Special Publication, 18. p228-248.

Davies, T. R. H. & Sutherland, A. J. 1980. "Resistance to flow past deformable boundaries", *Earth Surface Processes*, 5, 175-179.

Davies, T. R. H. & Sutherland, A. J. 1983. "Extremal hypotheses for river behaviour", *Water Resources Research*, 19, 141-148.

Davy, B. W. & Davies, T. R. H. 1979. "Entropy concepts in fluvial geomorphology: a reevaluation", *Water Resources Research*, 15, 103-106.

Dietrich, W. E. & Smith, J. D. 1984. "Bedload transport in a river meander", *Water Resources Research*, 20, 1355-1380.

Dietrich, W. E. & Whiting, P. J. 1989. "Boundary shear stress and sediment transport in river meanders of sand and gravel", in Ikeda, S. & Parker, G. (eds), *River Meandering*, American Geophysical Union. p1-50.

Dury, G. H. 1961. "Bankfull discharge: an example of its statistical relationships", *Bulletin of the International Association of Scientific Hydrology*, 6, 48-55.

Einstein, H. A. 1950. "The bedload function for sediment transportation in open channel flows", *Technical Bulletin, United States Department of Agriculture*, 1026.

Einstein, H. A. 1972. "Sedimentation", in R. Oglesby (ed), *River Ecology and Man*, Academic Press, p309-318.

Elliott, S. C. A. & Sellin, R. H. J. 1990. "SERC Flood Channel Facility: Skewed flow experiments", *Journal of Hydraulic Research*, 28, 197-214.

Engelund, F. 1970. "Instability of erodible beds", *Journal of Fluid Mechanics*, 42, 225-244.

Engelund, F. 1974. "Flow and bed topography in channel bends", *Journal of the Hydraulics Division of the American Society of Civil Engineers*, 100, 1631-1648.

Engelund, F. & Hansen, E. 1967. *A Monograph on Sediment Transport in Alluvial Streams*, Teknisk Forlag, Copenhagen, 62p.

Falcon, M. A. & Kennedy, J. F. 1983. "Flow in alluvial river curves", *Journal of Fluid Mechanics*, 133, 1-16.

Ferguson, R. I. 1986. "Hydraulics and hydraulic geometry", *Progress In Physical Geography*, 10, 1-31.

Francis, J. R. D. 1973. "Experiments on the motion of solitary grains along the bed of a water stream", *Proceedings of the Royal Society of London, Series A*, 332, 443-471.

Garcia, M and Parker, G. 1991. "Entrainment of bed sediment into suspension", *Journal of Hydraulic Engineering*, 117, 414-435.

Ghosh, S. K. 1983. "A study of regime theories for an alluvial meandering channel", *Proceedings of the Second International Symposium on River Sedimentation, Nanjing, China*, p706-712.

Griffiths, G. A. 1984. "Extremal hypotheses for river regime: an illusion of progress", *Water Resources Research*, 20, 113-118.

Grissinger, E. H. 1982. "Bank erosion of cohesive materials", in Hey, R. D., Bathurst, J. C. & Thorne, C. R. (eds) *Gravel-bed rivers*, John Wiley and Sons, Chichester, p273-287.

Gulliver, J. S. & Halverson, M. J. 1987. "Measurements of large streamwise vortices in an open channel flow", *Water Resources Research*, 23, 115-123.

Hagerty, D. J. 1991. "Piping/sapping erosion I: Basic Considerations", *Journal of Hydraulic Engineering*, 117, 991-1008.

Hamlin, R. & Thornes, J. B. 1974. "Width variations in small perennial stream channels", *London School of Economics Graduate School of Geography Discussion Paper*, 51, 11p.

Harvey, M. D. & Watson, C. C. 1986. "Fluvial processes and morphological thresholds in incised channel restoration", *Water Resources Bulletin*, 22, 359-368.

Hedman, E. R. & Kastner, W. M. 1977. "Streamflow characteristics related to channel geometry in the Missouri river basin", *Journal of Research of the United States Geological Survey*, 5, 285-300.

Henderson, F. M. 1961. "Stability of alluvial channels", *Journal of the Hydraulics Division of the American Society of Civil Engineers*, 87, 109-138.

Henderson, F. M. 1966. *Open Channel Flow*, Macmillan, New York, 522p.

Henderson-Sellers, A. 1991. "Policy advice on greenhouse-induced climatic change: the scientist's dilemma", *Progress in Physical Geography*, 15, 53-70.

Hey, R. D. 1975. "Design discharges for natural channels", in Hey, R. D. & Davies, J. D. (eds) *Science and Technology in Environmental Management*, Saxon House, Farnborough. p73-88.

Hey, R. D. 1976. "Geometry of river meanders", *Nature*, 262, 482-484.

Hey, R. D. 1978. "Determinate hydraulic geometry of river channels", *Journal of the Hydraulics Division of the American Society of Civil Engineers*, 104, 869-885.

Hey, R. D. 1979. "Flow resistance in gravel-bed rivers", *Journal of the Hydraulics Division of the American Society of Civil Engineers*, 105, 365-379.

Hey, R. D. 1982. "Gravel-Bed rivers: Form & Process", in Hey, R. D., Bathurst, J. C. & Thorne, C. R.(eds), *Gravel Bed Rivers*, John Wiley and Sons, Chichester. p5-13.

Hey, R. D. & Thorne, C. R. 1986. "Stable channels with mobile gravel beds", *Journal of Hydraulic Engineering*, 112, 671-689.

Hicks, F. E., Jin, Y. C. & Steffler, P. M. 1990. "Flow near sloped bank in curved channel", *Journal of Hydraulic Engineering*, 116, 55-70.

Hirano, M. 1973. "River bed variation with bank erosion", *Proceedings of the Japanese Society of Civil Engineers*, 210, 13-20.

Hoey, T. & Ferguson, R. I. 1991. "Numerical simulation of downstream fining in a gravel-bed river", Paper presented at BGRG/COMTAG symposium on "Theory in Geomorphology", Leeds, September 19-21, 1991.

Holly, F. M. & Karim, M. F. 1986. "Simulation of Missouri river bed degradation", *Journal of Hydraulic Engineering*, 112, 497-517.

Holly, F. M. & Rahuel, J. L. 1990. "New numerical/physical framework for mobile bed modelling", *Journal of Hydraulic Research*, 28, 401-416.

Hooke, J. M. 1979. "An analysis of the processes of river bank erosion", *Journal of Hydrology*, 42, 39-62.

Hupp, C. R. & Simon, A. 1986. "Vegetation and bank-slope development", *Proceedings of the 4th Federal Interagency Sedimentation Conference, Las Vegas, Nevada, March 24-27 1986*. p5-83 - 5-92.

Hupp, C. R. & Simon, A. 1991. "Bank accretion and the development of vegetated depositional surfaces along modified alluvial channels", *Geomorphology*, 4, 111-124.

Ikeda, S. 1982a. "Incipient motion of sand particles on side slopes", *Journal of the Hydraulics Division of the American Society of Civil Engineers*, 108, 95-114.

Ikeda, S. 1982b. "Lateral bedload transport on side slopes", *Journal of the Hydraulics Division of the American Society of Civil Engineers*, 108, 1369-1373.

Ikeda, S. & Izumi, N. 1990. "Width and depth of self-formed straight gravel rivers with bank vegetation", *Water Resources Research*, 26, 2353-2364.

Ikeda, S., Parker, G. & Sawai, K. 1981. "Bend theory of river meanders, 1: Linear development", *Journal of Fluid Mechanics*, 112, 363-377.

Ikeda, S., Parker, G. & Kimura, Y. 1988. "Stable width and depth of straight gravel rivers with heterogeneous bed materials", *Water Resources Research*, 24, 713-722.

Inglis, C. C. 1949. "The behaviour and control of rivers and canals (with the aid of models)", *Central Waterpower Irrigation and Navigation Research Station, Poona, Research Publication No. 13*. Yeravda Prison Press, Poona.

Inglis, C. C. 1963. Discussion of "Uniform water conveyance channels in alluvial materials" by Simons & Albertson, *Transactions of the American Society of Civil Engineers*, 128, 129-134.

Ismail, H. M. 1951. "Turbulent transfer mechanism and suspended sediments in closed channels", *Proceedings of the American Society of Civil Engineers*, 77, 1-26.

Itakura, T. & Kishi, T. 1980. "Open channel flow with suspended sediments", *Journal of the Hydraulics Division of the American Society of Civil Engineers*, 106, 1325-1343.

Jin, Y. C., Steffler, P. M. & Hicks, F. E. 1990. "Roughness effects on flow and shear stress near outside bank of curved channel", *Journal of Hydraulic Engineering*, 116, 563-577.

Jones, M. D. H. & Henderson-Sellers, A. 1990. "History of the greenhouse effect", *Progress in Physical Geography*, 14, 1-18.

Julien, P. Y. 1988. "Downstream hydraulic geometry of noncohesive alluvial channels", in White, W. R. (ed) *International Conference on River Regime*, Hydraulics Research/John Wiley & Sons, Chichester. p9-16.

Kalinske, A. A. & Pien, C. L. 1943. "Experiments on eddy-diffusion and suspended-material transportation in open channels", *Transactions of the American Geophysical Union*, II, 530-534.

Karim, M. F. & Kennedy, J. F. 1981. "Computer based predictors for sediment discharge and friction factor of alluvial streams", IIHR Report No. 242, University of Iowa, Iowa City, Iowa.

Karim, M. F & Holly, F. M. 1986. "Armoring and sorting simulation in alluvial rivers", *Journal of Hydraulic Engineering*, 112, 705-715.

Kellerhals, R. 1967. "Stable channels with gravel paved beds", *Journal of the Waterways and Harbors Division of the American Society of Civil Engineers*, 93, 63-84.

Kennedy, R. G. 1895. "The prevention of silting in irrigation canals", *Proceedings of the Institute of Civil Engineers*, 119, 281-290.

Knight, D. W. & Sellin, R. H. J. 1987. "The SERC Flood Channel Facility", *Journal of the Institute of Water and Environmental Management*, 1, 198-204.

Knight, D. W. & Shiono, K. 1990. "Turbulence measurements in a shear layer region of a compound channel", *Journal of Hydraulic Research*, 28, 175-196.

Knighton, A. D. 1973. "River bank erosion in relation to streamflow conditions, River Bollin-Dean, Cheshire", *East Midlands Geographer*, 5, 416-426.

Knighton, A. D. 1974. "Variation in width-discharge relation and some implications for hydraulic geometry", *Geological Society of America Bulletin*, 85, 1069-1076.

Komar, P. D. 1987. "Selective grain entrainment by a current from a bed of mixed sizes: a reanalysis", *Journal of Sedimentary Petrology*, 57, 203-211.

Komar, P. D. 1989. "Flow-competence evaluation of the hydraulic parameters of floods: an assessment of the technique", in Beven, K. & Carling, P. A. (eds) *Floods: hydrological, sedimentological and geomorphological implications*, John Wiley & Sons, Chichester. p107-134.

Komura, S. & Simons, D. B. 1967. "River bed degradation below dams", *Journal of the Hydraulics Division of the American Society of Civil Engineers*, 93, 1-13.

Kovacs, A. & Parker, G. in press. "Time development of straight self-formed river channels in non-cohesive material", *Journal of Fluid Mechanics.*

Lacey, G. 1930. "Stable channels in alluvium", *Minutes of the Proceedings of the Institute of Civil Engineers*, 229, 259-292.

Lacey, G. & Pemberton, W. 1972. "A general formula for uniform flow in self formed alluvial channels", *Proceedings of the Institute of Civil Engineers*, 53, 373-381.

Lane, E. W. 1955. "Design of stable channels", *Transactions of the American Society of Civil Engineers*, 81, 1-17.

Langbein, W. B. 1965. "Geometry of river channels: Closure to discussion", *Journal of the Hydraulics Division of the American Society of Civil Engineers*, 92, 297-313.

Lamberti, A. 1988. "About extremal hypotheses and river regime", in White, W. R. (ed) *International Conference on River Regime*, Hydraulics Research/John Wiley & Sons, Chichester. p121-134.

Leopold, L. B. 1973. "River channel changes with time: an example", *Geological Society of America Bulletin*, 84, 1845-1860.

Leopold, L. B. & Maddock, T. 1953. "The hydraulic geometry of stream channels and some physiographic implications", *United States Geological Survey Professional Paper*, 252, 1-57.

Leopold, L. B. & Miller, J. P. 1956. "Ephemeral streams - hydraulic factors and their relation to the drainage net", *United States Geological Survey Professional Paper*, 282A, 37p.

Leopold, L. B. & Wolman, M. G. 1957. "River channel patterns - braided, meandering and straight", *United States Geological Survey Professional Paper*, 282B, 85p.

Leopold, L. B. & Langbein, W. B. 1962. " The concept of entropy in landscape development", *United States Geological Survey Professional Paper*, 500A, 20p.

Leopold, L. B., Wolman, M. G. & Miller, J. P. 1964. *Fluvial Processes in Geomorphology*, W. H. Freeman, San Francisco, 522p.

Lewin, J., Macklin, M. G. & Newson, M. D. 1988. "Regime theory and environmental change - irreconcilable concepts?", in White, W. R. (ed) *International Conference on River Regime*, Hydraulics Research/John Wiley & Sons, Chichester. p431-445.

Lewis, L. A. 1966. "The adjustments of some hydraulic variables at discharges less than 1 c.f.s.", *Professional Geographer*, 18, 230-234.

Lewis, L. A. 1969. "Some fluvial geomorphic characteristics of the Manati Basin, Puerto Rico", *Annals of the Association of American Geographers*, 59, 280-293.

Lindley, E. S. 1919. "Regime channels", *Proceedings of the Punjab Engineering Congress*, 7, 63-74.

Lohnes, R. & Handy, R. L. 1968. "Slope angles in friable loess", *Journal of Geology*, 76, 247-258.

Lorenz, E. 1963. "Deterministic Nonperiodic Flow", *Journal of Atmospheric Sciences*, 20, 130-141.

Lundgren, H. & Jonsson, I. G. 1964. "Shear and velocity distribution in shallow channels", *Journal of the Hydraulics Division of the American Society of Civil Engineers*, 90, 1-21.

Lyn, D. A. 1986. "Turbulence and turbulent transport in sediment-laden open channel flows", *Report KH-R-49*, W. M. Keck Laboratory of Hydraulics and Water Resources, California Institute of Technology, Pasadena, California.

Mackin, J. H. 1948. "Concept of the graded river", *Bulletin of the Geological Society of America*, 59, 463-512.

Maddock, T. 1969. "The behaviour of straight open channels with movable beds", *United States Geological Survey, Professional Paper*, 622A, 1-70.

Mahmood, K. 1974. "Variation of regime coefficients in Pakistan canals", *Journal of the Waterways, Harbors and Coastal Engineering Division of the American Society of Civil Engineers*, 100, 85-104.

Mahmood, K. & Shen, H. W. 1979. "The regime concept of sediment transporting canals and rivers", in Shen, H. W. (ed) *River Mechanics*, Water Resources Publications, Fort Collins, Colorado. p30-11 - 30-39.

Markham, A. J. 1990. *Flow and sediment processes in Gravel-Bed river bends*, Thesis submitted to the University of London in full requirements of the degree of Doctor of Philosophy. 417p.

Miller, J. P. 1958. *High mountain streams: Effects of geology on channel characteristics and bed material*, New Mexico Bureau of Mines Memoir 4. 52p.

Miller, T. K. 1984. "A system model of stream chanel shape and size", *Geological Society of America Bulletin*, 95, 237-241.

Miller, T. K. & Onesti, L. J. 1979. "The relationship between channel shape and sediment characteristics in the channel perimeter", *Geological Society of America Bulletin*, 90, 301-304.

Molinas, A., Denzel, C. W. & Yang, C. T. 1986. "Application of streamtube computer model", in *Proceedings of the 4th Federal Interagency Sedimentation Conference, Las Vegas, Nevada, March 24-27 1986*, p6-55 to 6-64.

Morgenstern, N. R. 1963. "Stability charts for earth slopes during rapid drawdown", *Geotechnique*, 13, 121-131.

Morgenstern, N. R. & Price, V. E. 1965. "The analysis of the stability of general slip surfaces", *Geotechnique*, 15, 79-93.

Myers, W. R. C. 1978. "Momentum transfer in a compound channel", *Journal of Hydraulic Research*, 16, 139-150.

Myers, W. R. C. & Brennan, E. K. 1990. "Flow resistance in compound channels", *Journal of Hydraulic Research*, 28, 141-155.

Naden, P. 1987. "An erosion criterion for gravel-bed rivers", *Earth Surface Processes and Landforms*, 12, 83-93.

Nanson, G. C. & Hickin, E. J. 1986. "A statistical analysis of bank erosion and channel migration in western Canada", *Geological Society of America Bulletin*, 97, 497-504.

Nicolis, G. & Prigogine, I. 1977. *Self organization in non equilibrium systems.* John Wiley and Sons, New York. 491p.

Niekerk, van, A., Vogel, K. R., Slingerland, R. L. & Bridge, J. S. 1992. "Routing heterogeneous sediments over mobile bed: Model development", *Journal of Hydraulic Engineering*, 118, 246-262.

Odgaard, A. J. 1987. "Streambank erosion along 2 rivers in Iowa", *Water Resources Research*, 23, 1225-1236.

Odgaard, A. J. 1989. "River meander model. I: Development", *Journal of Hydraulic Engineering*, 115, 1451-1464.

Orvis, C. J. & Randle, T. J. 1986. "Sediment transport and river simulation model", in *Proceedings of the 4th Federal Interagency Sedimentation Conference, Las Vegas, Nevada, March 24-27 1986*, p6-65 to 6-74.

Osman, A. M. 1985. *Channel width response to changes in flow hydraulics and sediment load*, Thesis submitted to Colorado State University in partial fulfilment of the requirements of the degree of Doctor of Philosophy. 169p.

Osman, A. M. & Thorne, C. R. 1988. "Riverbank stability analysis I: Theory", *Journal of Hydraulic Engineering*, 114, 134-150.

Osterkamp, W. R. 1976. "The role of sediment in determining the geometry of alluvial stream channels", *Dissertation Abstracts International*, B 77-7328, 201.

Osterkamp, W. R. 1979. "Variation of alluvial channel width with discharge and character of sediment", *United States Geological Survey, Lawrence, KS, Water Resources Division, Water Resources Investigation,* 79-15, 16p.

Osterkamp, W. R. 1980. "Sediment morphology relations of alluvial channels", *Symposium on Watershed Management (Boise, USA), volume 1,* New York, ASCE. p188-199.

Park, C. C. 1977. "World wide variations in hydraulic geometry exponents of stream channels: an analysis and some observations", *Journal of Hydrology,* 33, 133-146.

Parker, G. 1978a. "Self-formed straight rivers with equilibrium banks and mobile bed. Part 1. The sand-silt river.", *Journal of Fluid Mechanics,* 89, 109-125.

Parker, G. 1978b. "Self-formed straight rivers with equilibrium banks and mobile bed. Part 2. The gravel river.", *Journal of Fluid Mechanics,* 89, 127-146.

Parker, G. 1984. "Discussion of lateral bed load transport on side slopes by S. Ikeda", *Journal of Hydraulic Engineering,* 110, 197-203.

Parker, G., Klingeman, P. C. & McLean, D. G. 1982. "Bedload and size distribution in gravel-bed streams", *Journal of the Hydraulics Division of the American Society of Civil Engineers,* 108, 544-571.

Parker, G., Diplas, P. & Akiyama, J. 1983. "Meander bends of high amplitude", *Journal of Hydraulic Engineering,* 109, 1323-1337.

Parker, G. & Andrews, E. D. 1985. "Sorting of bed load sediment by flow in meander bends", *Water Resources Research,* 21, 1361-1373.

Partheniades, E. 1965. "Erosion and deposition of cohesive soils", *Journal of the Hydraulics Division of the American Society of Civil Engineers,* 91, 105-139.

Perkins, H. J. 1970. "The formation of streamwise vorticity in turbulent flow", *Journal of Fluid Mechanics,* 44, 721-740.

Pickup, G. & Rieger, W. A. 1979. "A conceptual model of the relationship between channel characteristics and discharge", *Earth Surface Processes and Landforms*, 4, 37-42.

Pickup, G. & Warner, R. F. 1976. "Effects of hydrologic regime on magnitude and frequency of dominant discharge", *Journal of Hydrology*, 29, 51-76.

Pizzuto, J. E. 1984. "Bank erodibility of shallow sandbed streams", *Earth Surface Processes and Landforms*, 9, 113-124.

Pizzuto, J. E. 1990. "Numerical simulation of gravel river widening", *Water Resources Research*, 26, 1971-1980.

Pizzuto, J. E. 1991. "A numerical model for calculating the distributions of velocity and boundary shear stress across irregular straight open channels", *Water Resources Research*, 27, 2457-2466.

Ponce, V. M. 1978. "Generalized stability analysis of channel banks", *Journal of the Irrigation and Drainage Division of the American Society of Civil Engineers*, 104, 343-350.

Prandtl, L. 1952. *Essentials of Fluid Dynamics*, Blackie, London, 452p.

Rahuel, J. L., Holly, F. M., Belleudy, P. J. & Yang, G. 1989. "Modelling of riverbed evolution for bedload sediment mixtures", *Journal of Hydraulic Engineering*, 115, 1521-1542.

Rais, S. 1985. "*Analysis of the flow close to the outer bank in a meander bend* ", Thesis presented to Colorado State University in partial fulfilment of the requirements of the degree of Doctor of Philosophy. 265p.

Raudkivi, A. J. 1989. *Loose Boundary Hydraulics*, (3rd edition), Pergamon Press, Oxford, 538p.

Rhoads, B. L. & Miller, M. V. 1991. "Impact of flow variability on the morphology of a low energy meandering river", *Earth Surface Processes and Landforms*, 16, 357-368.

Rhoads, B. L. 1991a. "A continuously-varying parameter model of downstream hydraulic geometry", *Water Resources Research*, 27, 1865-1872.

Rhoads, B. L. 1991b. "On the expansion method", *Professional Geographer*, 43, 525-527.

Rhoads, B. L. 1992. "Statistical models of fluvial systems", *Geomorphology*, 5, 433-455.

Rhodes, D. D. 1987. "The b-f-m diagram for downstream hydraulic geometry", *Geografiska Annaler, Series A*, 69A, 147-161.

Richards, K. S. 1977. "Channel and flow geometry: a geomorphological perspective", *Progress In Physical Geography*, 1, 65-103.

Richards, K. S. 1982. *Rivers: Form and process in alluvial channels*, Methuen, London. 361p.

Richards, K. S. 1990. "Fluvial geomorphology: initial motion of bed material in gravel-bed rivers", *Progress in Physical Geography*, 14, 395-415.

Richards, K. S. & Lorriman, N. R. 1987. "Basal erosion and mass movement", in Anderson, M. G. & Richards, K. S. (eds) *Slope Stability*, John Wiley & Sons, Chichester, p331-357.

Riley, S. J. 1976. "Variation in the hydraulic geometry of streams in northwestern NSW", *Search*, 7, 445-446.

Robbins, C. H. & Simon, A. 1983. "Man-induced channel adjustment in Tennessee streams", U.S. Geological Survey Water-Resources Investigations Report 82-4098, 129p.

Schumm, S. A. 1960. "The shape of alluvial channels in relation to sediment type", *United States Geological Survey Professional Paper*, 352B, 17-30.

Schumm, S. A. 1968. "River adjustment to altered hydrologic regimen - Murrumbidgee River and paleochannels, Australia", *United States Geological Survey Professional Paper*, 598, 68p.

Schumm, S. A. 1977. *The Fluvial System*, John Wiley & Sons, New York. 338p.

Schumm, S. A. & Lichty, R. W. 1963. "Channel widening and flood plain construction along Cimarron River in south western Kansas", *United States Geological Survey Professional Paper*, 352-D, 71-88.

Schumm, S. A. & Lichty, R. W. 1965. "Time, space and causality in geomorphology", *American Journal of Science*, 263, 110-119.

Schumm, S. A. & Thorne, C. R. 1989. "Geologic and geomorphic controls on bank erosion", *Paper presented at Third National Conference on Hydraulic Engineering and International Symposium on Sediment Transport Modelling, 14-18 August, ASCE, New Orleans, La. USA.*

Schumm, S. A., Harvey, M. D. & Watson, C. C. 1984. *"Incised channels, morphology, dynamics and control"* , Water Resources Publications, Colorado. 200p.

Sekine, M. & Kikkawa, H. 1992. "Mechanics of saltating grains II", *Journal of Hydraulic Engineering*, 118, 536-558.

Sekine, M. & Parker, G. 1992. "Bed-Load transport on transverse slope I", *Journal of Hydraulic Engineering*, 118, 513-535.

Sergutin, V. E. & Turutin, B. F. 1984. "On relative width and form of river channel", *Geomorfologiya*, 3, 77-80.

Shiono, K. & Knight, D. W. 1990. "Turbulent open-channel flows with variable depth across the channel", *Journal of Fluid Mechanics*, 222, 617-646.

Siegel, R. A. 1975. "PROGRAM STABL2", Joint Highway Research Project, Engineering Experiment Station, Purdue University.

Simon, A. 1989. "A model of channel response in disturbed alluvial channels", *Earth Surface Processes and Landforms*, 14, 11-26.

Simon, A. 1992. "Energy, time, and channel evolution in catastrophically disturbed fluvial systems", *Geomorphology*, 5, 345-372.

Simon, A. & Darby, S. E. (in preparation) "Modelling channel adjustments and flow-energy variables in destabilized sand-bed streams".

Simon, A. & Hupp, C. R. 1986a. "Channel evolution in modified Tennessee channels", *Proceedings of 4th Federal Interagency Sedimentation Conference, Las Vegas, Nevada, March 24-27 1986.* p5-71 - 5-82.

Simon, A. & Hupp, C. R. 1986b. "Channel widening characteristics and bank slope development along a reach of Cane Creek, West Tennessee", in Subitzky, Seymour (ed) *Selected papers in the hydrological sciences*, U. S Geological Survey Water-Supply Paper 2290, p113-126.

Simon, A. & Hupp, C. R. 1987. "Geomorphic and vegetative recovery processes along modified Tennessee streams: An interdisciplinary approach to disturbed fluvial systems", International Association of Scientific Hydrology, Special Publication 167, 251-262.

Simon, A. & Hupp, C. R. 1992. "Geomorphic and vegetative recovery processes along modified stream channels of West Tennessee", *U. S. Geological Survey Open-File Report 91-502.* 142p.

Simon, A. & Robbins, C. H. 1987. "Man-induced gradient adjustment of the South Fork Forked Deer River, West Tennessee", *Environmental Geology and Water Sciences*, 9, 109-118.

Simon, A., Wolfe, W. J. & Molinas, A. 1991. "Mass wasting algorithms in an alluvial channel model", *Proceedings of the 5th Federal Interagency Sedimentation Conference.* Las Vegas, Vol. 2, p.8-22 to 8-29.

Simons, D. B. & Albertson, M. L. 1963. "Uniform water conveyance channels in alluvial materials", *Transactions of the American Society of Civil Engineers*, 128, 65-106.

Smith, N. D. & Smith, D. G. 1984. "William River: an outstanding example of channel widening and braiding caused by bed-load addition", *Geology*, 12, 78-82.

Smith, T. R. 1974. "A derivation of the hydraulic geometry of steady state channels from conservation principles and sediment transport laws", *Journal of Geology*, 82, 98-104.

Smith, J. D. & McLean, S. R. 1977. "Spatially averaged flow over a wavy surface", *Journal of Geophysical Research*, 82, 1735-1746.

Song, C. C. S. & Yang, C. T. 1980. "Minimum stream power: Theory", *Journal of the Hydraulics Division of the American Society of Civil Engineers*, 106, 1477-1487.

Spangler, M. G. & Handy, R. L. 1982. *Soil Engineering*, 4th Edition, Intext Educational, New York, N. Y, 819p.

Stall, J. B. & Yang, C. T. 1970. "Hydraulic geometry of 12 selected stream systems of the United States", *Unpublished Report of the Water Resources Center, Illinois University, Urbana*. 73p.

Stevens, H. & Yang, C. T. 1989. "Summary and use of selected fluvial sediment discharge formulas", *USGS Water Resources Investigations Report 89-4026*, Denver, Colorado. 62p.

Stokes, G. G. 1851. "On the effect of internal friction of fluids on the motion of pendulums", *Transactions of the Cambridge Philosophical Society*, 9, 51-52.

Straub, L. G., Anderson, A. G. & Flammer, G. H. 1958. "Experiments on the influence of the temperature on sediment load", *MRD Sediment Series No. 10*, St. Anthony Falls Hydraulics Laboratory, University of Minnesota, Minneapolis, Minnesota.

Strickler, A. 1923. "Beitrage zur frage der geschwindigheitsformel und der rauhigkeitszahlen fur strome, kanale und geschlossene leitungen", *Mitteilungen des Eidgenossicher Amtes fur Wasserwirtscaft*, Bern, Switzerland, 16g.

Taylor, D. W. 1948. *Fundamentals of Soil Mechanics*, John Wiley & Sons, New York, N. Y. 700p.

Thomas, W. A. 1982. "Mathematical modelling of sediment movement", in Hey, R. D., Bathurst, J. C. & Thorne, C. R. (eds),*Gravel-Bed Rivers*, John Wiley & Sons, Chichester, UK. p487-508.

Thorne, C. R. 1978. *Processes of bank erosion in river channels*, Thesis submitted to the University of East Anglia fulfilling the complete requirements for the degree of Doctor of Philosophy . 448p.

Thorne, C. R. 1982. "Processes and mechanisms of river bank erosion", in Hey, R. D., Bathurst, J. C. & Thorne, C. R. (eds)*Gravel-Bed Rivers: Fluvial processes, Engineering and Management*, John Wiley & Sons, Chichester. p227-271.

Thorne, C. R. 1988. "Analysis of bank stability in the DEC watersheds, Mississippi", *Report to European Research Office, US Army contract No. DAJA45-87C-0021.* 62p.

Thorne, C. R. 1989. "Bank processes on the Red River between Index, Arkansas and Shreveport, Louisiana", *Report to European Research Office, US Army contract No. DAJA45-88C-0018.* 45p.

Thorne, C. R. 1990. "Effects of vegetation on riverbank erosion and stability", in J. B. Thornes (ed),*Vegetation and Erosion*, Wiley, Chichester, UK. p125-144.

Thorne, C. R. & Tovey, N. K. 1981. "Stability of composite river banks", *Earth Surface Processes and Landforms*, 6, 469-484.

Thorne, C. R. & Osman, M. A. 1988a. "The influence of bank stability on regime geometry of natural channels", in White, W. R. (ed) *International Conference on River Regime*, Hydraulics Research/John Wiley & Sons, Chichester. p135-147.

Thorne, C. R. & Osman, M. A. 1988b "Riverbank stability analysis II: Applications", *Journal of Hydraulic Engineering*, 114, 151-172.

Thorne, C. R., Little, W. C. & Murphey, J. B. 1981. "Bank stability and bank material properties in the Bluffline streams of northwest Mississippi", *Stream Channel Stability*, Appendix D, Section 32 Program, Work Unit 7, U. S. Army Corps of Engineers, Vicksburg District, Vicksburg, Mississippi. 258p.

Thorne, C. R., Chang, H. H. & Hey, R. D. 1988. "Prediction of the hydraulic geometry of gravel-bed streams using the minimum stream power concept", in White, W. R. (ed) *International Conference on River Regime*, Hydraulics Research/John Wiley & Sons, Chichester. p29-40.

Thornes, J. B. 1970. The hydraulic geometry of stream channels in the Xingu-Araguaia headwaters", *Geographical Journal*, 136, 376-382.

Thornes, J. B. 1977. "Hydraulic geometry and channel change", in Gregory, K. J. (ed) *River channel changes* , Wiley-Interscience. p91-100.

Twidale, C. R. 1964. "Erosion of an alluvial bank at Birdwood, South Australia", *Zeitschrift fur Geomorphologie*, NF8, 189-211.

Ullrich, C. R., Hagerty, D. J. & Holmberg, R. W. 1986. "Surficial failures of alluvial stream banks", *Canadian Geotechnical Journal*, 23, 304-316.

Van Rijn, L. C. 1984. "Sediment transport, Part 2: Suspended load transport", *Journal of Hydraulic Engineering*, 110, 1613-1641.

Vanoni, V. A. & Nomicos, G. N. 1960. "Resistance properties of sediment laden streams", *Transactions of the American Society of Civil Engineers*, 125, 1140-1175.

Wang Shiqiang, White, W. R. & Bettess, R. 1986. "A rational approach to river regime", in Wang, S. Y., Shen, H. W. & Ding, L. Z. (eds), *Proceedings of the 3rd International Symposium on River Sedimentation, University of Mississippi.* p167-176.

Wark, J. B., Samuels, P. G. & Ervine, D. A. 1990. "A practical method of estimating velocity and discharge in a compound channel", in W. R. White (ed),*Flood Hydraulics*, Wiley, Chichester, p163-172.

White, W. R., Milli, H. & Crabbe, A. D. 1975. "Sediment transport theories - a review", *Proceedings of the Institute of Civil Engineers, Part 2*, 59, 265-292.

White, W. R., Bettess, R. & Paris, E. 1982. "Analytical approach to river regime", *Journal of the Hydraulics Division of the American Society of Civil Engineers*, 108, 1179-1193.

Wiberg, P. L. & Smith, J. D. 1987. "Calculations of the critical shear stress for motion of uniform and heterogeneous sediments", *Water Resources Research*, 23, 1471-1480.

Wilcock, D. N. 1971. "Investigation into the relations between bedload transport and channel shape", *Geological Society of America Bulletin*, 82, 2159-2176.

Williams, R. P. 1987. "Unit hydraulic geometry - an indicator of channel changes", *United States Geological Survey Water Supply Paper*, 2330, 77-89.

Wolman, M. G. 1959. "Factors influencing erosion of a cohesive river bank", *American Journal of Science*, 257, 204-216.

Wolman, M. G. & Leopold, L. B. 1957. "River flood plains: some observations on their formation", *United States Geological Survey Professional Paper*, 282C, 87-107.

Wolman, M. G. & Brush, L. M. 1961. "Factors controlling the size and shape of stream channels in coarse noncohesive sands", *United States Geological Survey Professional Paper*, 282-G, 183-210.

Wormleaton, P. R., Allen, J. & Hadjipanos, P. 1982. "Discharge assessment in compound channel flow", *Journal of the Hydraulics Division of the American Society of Civil Engineers*, 108, 975-993.

Wormleaton, P. R. & Merrett, D. 1990. "An improved method of calculation for steady uniform flow in prismatic main channel/flood plain sections", *Journal of Hydraulic Research*, 28, 157-174.

Yalin, M. S. 1971. "On the formation of dunes and meanders", *Proceedings of the 14th International Congress of the Hydraulic Research Association, Paris*, 3, C13, 1-8.

Yang, C. T. 1971. "Potential energy and stream morphology", *Water Resources Research*, 7, 312-322.

Yang, C. T. & Song, C. C. S. 1979. "Theory of minimum rate of energy dissipation", *Journal of the Hydraulics Division of the American Society of Civil Engineers*, 105, 769-784.

Yang, C. T., Song, C. C. S. & Woldenberg, M. J. 1981. "Hydraulic geometry and minimum rate of energy dissipation", *Water Resources Research*, 17, 1014-1018.

Yang, C. T. & Wan, S. 1991. "Comparison of selected bed-material formulas", *Journal of Hydraulic Engineering*, 117, 973-989.

Yu, B. F. & Wolman, M. G. 1987. "Some dynamic aspects of river geometry", *Water Resources Research*, 23, 501-509.

Zimmerman, R. C., Goodlett, J. C. & Comer, G. H. 1967. "The influence of vegetation on channel form of small streams", *Publication, International Association of Scientific Hydrology*, 75, 255-275.

APPENDICES

APPENDIX A: LIST OF SYMBOLS

A = Cross-sectional area (m^2)

Ad = Mean absolute deviation of the discrepancy ratio

a = Coefficient in equation (3.17)

a_1 = Coefficient in equation (3.34)

a_2 = Coefficient in equation (3.53)

a = Coefficient in hydraulic geometry width equation

B = Bank-top width (m)

B_b = Bed width (m)

B* = Non-dimensional bank-top width

BW = Reach-averaged flood plain widening increment (m)

BW* = Potential failure block width (m)

B_s = Factor to relate stress on an inclined surface to stress on a horizontal plane

b = Rotational slip slice width (m)

b_1 = Coefficient in equation (3.34)

b = Exponent in hydraulic geometry width equation

C = Bank material cohesion (kPa)

Cr = Celerity of bed disturbance (ms^{-1})

CONC = Pore fluid salt concentration of bank material (N)

c(z) = Suspended sediment concentration at vertical coordinate, z (ppm)

c_1 = Coefficient in equation (3.34)

c = Coefficient in hydraulic geometry depth equation

$\frac{B}{D}$ = Aspect ratio

D = Depth (m)

D* = Non-dimensional mean channel depth

DP = Bank material dispersion criterion

D_c = Centre line depth (m)

D_m = Depth at foot of bank (m)

D_{mix} = Mixed layer depth (m)

d_{bank} = Representative failed bank material aggregate size (mm)

d_{50} = Median bed material particle size (mm)

d_i = Median diameter of ith bed material size-density class (mm)

d_s = Representative bed material particle size (mm)

d_{sand} = Representative size of bank material sand (mm)

d_t = Tension crack depth from previous failure (m)

E = Near-bed suspended sediment concentration (ppm)

EH = Coefficient in Engelund-Hansen equation

E_f = Energy dissipated by in overcoming frictional resistance of failure plane (J)

E_v = Energy converted in impact at base of slope (J)

ΔE = Daily reduction in water surface elevation (m)

F = Form adjustment parameter

F' = Frictional resistance of sediment in motion on side slope (N)

Fr = Froude number

FS = Factor of safety of bank with respect to mass failure

F_D = Driving force acting on incipient failure block (N)

F_R = Resisting force acting on incipient failure block (N)

F_l = Depth-integrated lateral volumetric flux of suspended sediment per unit width (m^2s^{-1})

F_b = Blench's bed sediment parameter

F_s = Blench's bank sediment parameter

f = Darcy-Weisbach friction factor

f = Exponent in hydraulic geometry depth equation

f_s = Lacey silt factor

g = Gravitational acceleration (ms^{-2})

H = Total bank height (m)

H' = Height of uneroded bank face (m)

HF = Hiding factor exponent

H_f = Fraction of drop height effective in dissipating potential energy through friction (m)

H_o = Initial bank height (m)

H_v = Effective vertical drop for failed bank material (m)

ΔH = Difference in elevation of failure block before and after failure (m)

h = Flow stage at downstream boundary (m)

h_f = Ratio of flow depth to bank height

K = Tension crack index

k = Coefficient in hydraulic geometry velocity equation

L = Length of model reach (m)

LE = Lateral erosion rate ($m\ min^{-1}$)

LIM = Maximum number of computational time steps

l = Length scale (m)

M = Channel silt-clay ratio

Me = Mean discrepancy ratio

m = Exponent in hydraulic geometry velocity equation

N' = Normal submerged weight component of sediment grain on side slope (N)

NEV = Non-dimensional eddy viscosity

n = Manning's n hydraulic roughness coefficient

n = Number of data points in data set

P = Wetted perimeter (m)

PE = Potential energy of incipient failure block (J)

p = Fluid pressure (Pa)

Q = Discharge (m^3s^{-1})

Qs = Sediment inflow at upstream boundary per unit channel width (m^2s^{-1})

Q_m = Mean annual discharge (m^3s^{-1})

Q_{ma} = Mean annual flood (m^3s^{-1})

q = Discharge per unit channel width (m^2s^{-1})

q_x = Streamwise total volumetric sediment flux per unit channel width (m^2s^{-1})

q_y = Transverse total volumetric sediment flux per unit channel width (m^2s^{-1})

q_{xb} = Streamwise bed load flux per unit channel width (m^2s^{-1})

q_{xs} = Streamwise suspended sediment flux per unit channel width

q_{yb} = Transverse bed load flux per unit channel width (m^2s^{-1})

q_s = Total bed material transport rate per unit channel width (non-specific vector) (m^2s^{-1})

q_{si} = Potential transport rate of ith size-density class of bed material per unit channel width (m^2s^{-1})

q_{si}* = Actual transport rate of ith size-density class of bed material per unit channel width (m^2s^{-1})

R = Hydraulic radius (m)

R_c = Non-dimensional centre line depth

R_f = Particle Reynolds number

R_l = Coefficient in lateral fluvial erosion equation

r = Initial rate of lateral fluvial erosion (m min^{-1})

S = Channel gradient

S_e = Energy gradient

S_w = Water surface gradient

S_x = Bed slope in x-direction

S_y = Bed slope in y-direction

SAND = Fractional sand content of bank material

SAR = Sodium adsorption ratio of bank material

SG = Specific gravity of bed material

SG_{bank} = Specific gravity of bank material

T = Reaction time (s)

$T_{0.5}$ = Recovery time (s)

T' = Downslope component of W' (N)

ΔT = Computational time step length (s)

t = Time coordinate (s)

Δt_{max} = Maximum time step length for computational stability (s)

U* = Shear velocity (ms^{-1})

u = Velocity component in x-direction (ms^{-1})

u_w = Pore water pressure at base of failure plane (Pa)

V = Mean stream velocity (ms^{-1})

V' = Velocity scale (ms^{-1})

V_o = Critical velocity for Kennedy regime channels ($ft\ s^{-1}$)

V_b = Lindley critical velocity for stable width (fts^{-1})

V_d = Lindley critical velocity for stable depth (fts^{-1})

V_f = Unit volume of failure block (m^2)

V_{ft} = Total bank material inflow flux due to mass failure (m^3s^{-1})

V_m = Total bank material flux from mass failure per unit reach length (m^2s^{-1})

v = Velocity component in y-direction (ms^{-1})

W_s = Weight of rotational slip slice (N)

W' = Submerged weight of boundary material particles (N)

WC = Non-dimensional weighting coefficient for sensitivity parameters

Wt = Weight of incipient failure block (N)

w = Velocity component in z-direction (m^2s^{-1})

x = Streamwise coordinate (m)

x_m = Maximum width of failure block (m)

y = Transverse coordinate (m)

y_d = Tension crack depth (m)

y_m = Flow depth above a point on the bed in Figure 2.3 (m)

Z = Bed elevation (m)

z = Vertical coordinate (m)

z' = Lateral coordinate in Lane's "Threshold Channel" design method (m)

α = Bank angle (degrees)

β = Failure plane angle (degrees)

β_i = Fraction of sediment in ith bed material size-density class present in mixed layer

$\chi_{\Delta y}$ = Non-dimensional sensitivity parameter for variable y

$\chi_{\Delta B}$ = Non-dimensional width sensitivity parameter

$\chi_{\Delta D}$ = Non-dimensional depth sensitivity parameter

$\chi_{\Delta D0}$ = Non-dimensional initial deepening sensitivity parameter

χ_T = Non-dimensional reaction time sensitivity parameter

χ_t = Non-dimensional recovery time sensitivity parameter

$\Delta\varepsilon$ = Dielectric dispersion of bank material

ε = Eddy viscosity (m^2s^{-1})

ε_y = Lateral eddy diffusivity (m^2s^{-1})

ε_z = Vertical eddy diffusivity (m^2s^{-1})

γ = Unit weight of bank material (kNm^{-3})

γ_w = Unit weight of water (kNm^{-3})

k = Von-Karman constant

λ = Bed material porosity

μ = Dynamic coefficient of Coulomb friction

μ_w = Fluid viscosity ($kgm^{-1}s^{-1}$)

ω = Particle fall velocity (ms^{-1})

ϕ = Boundary material internal friction angle (degrees)

ϕ_0 = Best case boundary material internal friction angle (degrees)

π = Pi (3.14)

φ = Daily drawdown parameter (m)

φ_{max} = Maximum daily drawdown parameter (m)

φ^* = Non-dimensional drawdown parameter

ρ = Density of fluid (water) (kgm^{-3})

ρ_s = Density of sediment (kgm^{-3})

τ = Fluid stress (Nm^{-2})

τ_c = Critical fluid shear stress for entrainment of boundary material (Nm^{-2})

τ_{cs} = Critical fluid shear stress for entrainment of boundary material on side slope (Nm^{-2})

υ = Molecular viscosity (m^2s^{-1})

ς = Depth-integrated suspended sediment concentration (ppm)

APPENDIX B: BANK MATERIAL CHARACTERISTICS USED IN REGIME VALIDATION

Bank Material	Cohesion (kPa)	P(C)	Unit Weight (kNm^{-3})	P(γ)	Friction Angle (Degrees)	P(ϕ)
BM1	2.5	0.188	7.0	0.0	7.5	0.0
	7.5	0.438	9.0	0.0	12.5	0.063
	12.5	0.250	11.0	0.0	17.5	0.0
	17.5	0.0	13.0	0.125	22.5	0.125
	22.5	0.0	15.0	0.063	27.5	0.125
	27.5	0.0	17.0	0.188	32.5	0.250
	32.5	0.125	19.0	0.625	37.5	0.375
	37.5	0.0	21.0	0.0	42.5	0.063
	42.5	0.0	23.0	0.0		
BM2	2.5	0.188	7.0	0.0	7.5	0.063
	7.5	0.438	9.0	0.0	12.5	0.125
	12.5	0.250	11.0	0.0	17.5	0.125
	17.5	0.0	13.0	0.125	22.5	0.250
	22.5	0.0	15.0	0.063	27.5	0.375
	27.5	0.0	17.0	0.188	32.5	0.063
	32.5	0.125	19.0	0.625	37.5	0.0
	37.5	0.0	21.0	0.0	42.5	0.0
	42.5	0.0	23.0	0.0		
BM3	2.5	0.188	7.0	0.0	7.5	0.125
	7.5	0.438	9.0	0.0	12.5	0.125
	12.5	0.250	11.0	0.0	17.5	0.250
	17.5	0.0	13.0	0.125	22.5	0.375
	22.5	0.0	15.0	0.063	27.5	0.063
	27.5	0.0	17.0	0.188	32.5	0.063
	32.5	0.125	19.0	0.625	37.5	0.0
	37.5	0.0	21.0	0.0	42.5	0.0
	42.5	0.0	23.0	0.0		

APPENDIX C: BANK MATERIAL CHARACTERISTICS USED IN SENSITIVITY TESTS

Bank Material	Cohesion (kPa)	P(C)	Unit Weight (kNm^{-3})	P(γ)	Friction Angle (Degrees)	P(ϕ)
Weak	1.0	0.188	7.0	0.0	7.5	0.0
	2.0	0.438	9.0	0.0	12.5	0.063
	3.0	0.250	11.0	0.0	17.5	0.0
	4.0	0.0	13.0	0.125	22.5	0.125
	5.0	0.0	15.0	0.063	27.5	0.125
	6.0	0.0	17.0	0.188	32.5	0.250
	7.0	0.125	19.0	0.625	37.5	0.375
	8.0	0.0	21.0	0.0	42.5	0.063
	9.0	0.0	23.0	0.0		
Moderate	8.0	0.188	7.0	0.0	7.5	0.0
	10.0	0.438	9.0	0.0	12.5	0.063
	12.0	0.250	11.0	0.0	17.5	0.0
	14.0	0.0	13.0	0.125	22.5	0.125
	16.0	0.0	15.0	0.063	27.5	0.125
	18.0	0.0	17.0	0.188	32.5	0.250
	20.0	0.125	19.0	0.625	37.5	0.375
	22.0	0.0	21.0	0.0	42.5	0.063
	24.0	0.0	23.0	0.0		
Strong	38.0	0.188	7.0	0.0	7.5	0.0
	40.0	0.438	9.0	0.0	12.5	0.063
	42.0	0.250	11.0	0.0	17.5	0.0
	44.0	0.0	13.0	0.125	22.5	0.125
	46.0	0.0	15.0	0.063	27.5	0.125
	48.0	0.0	17.0	0.188	32.5	0.250
	50.0	0.125	19.0	0.625	37.5	0.375
	52.0	0.0	21.0	0.0	42.5	0.063
	54.0	0.0	23.0	0.0		